Aus der Haut- und Poliklinik
der Universitätsmedizin der Johannes Gutenberg-Universität Mainz

Towards the Role of the Skin Microbiome in the Aetiopathogenesis of Cutaneous T-Cell Lymphoma

Dissertation
zur Erlangung des Grades
Doktor der Naturwissenschaften
(Dr. rer. nat.)

Am Fachbereich Biologie
der Johannes Gutenberg-Universität Mainz

Philipp Licht
geboren in Stade

Mainz, Juni 2025

Dekan: [redacted]

1.Berichterstatter: [redacted]

2. Berichterstatter: [redacted]

Tag der mündlichen Prüfung: 10.11.2025

For the patients and their family and friends.

Table of Contents

Eidesstattliche Erklärung / Statutory Declaration

Ich versichere hiermit an Eides statt, dass die vorgelegte Dissertation von mir selbstständig und ohne unerlaubte Hilfe angefertigt wurde. Des Weiteren erkläre ich, dass ich nicht anderweitig ohne Erfolg versucht habe, eine Dissertation einzureichen oder mich der Doktorprüfung zu unterziehen. Die folgende Dissertation liegt weder ganz, noch in wesentlichen Teilen einer anderen Prüfungskommission vor.

I declare that I have authored this thesis independently, that I have not used other than the declared sources/references. As well I declare that I have not submitted a dissertation without success and neither passed the oral exam. The present dissertation has not been presented to another examination board, neither as entire dissertation nor parts.

Mainz, den _____ _____

Philipp Licht

Publication List / Preface

The content of this cumulative dissertation is based on the following scientific publications, which I conducted during the course of my doctoral studies. From here on, these works will be referred to as **Publication 1**, **Publication 2**, and **Publication 3**, and are presented in chapters 2 – 4, respectively.

Publication 1: **Licht, P**. & Mailänder, V. Transcriptional Heterogeneity and the Microbiome of Cutaneous T-Cell Lymphoma. *Cells* **11**, 328 (2022).

Publication 2: **Licht, P**.*, Dominelli, N.*, Kleemann, J., Pastore, S., Müller, E.-S., Haist, M., Hartmann, K. S., Stege, H., Bros, M., Meissner, M., Grabbe, S., Heermann, R. & Mailänder, V. The skin microbiome stratifies patients with cutaneous T cell lymphoma and determines event-free survival. *npj Biofilms Microbiomes* **10,** 74 (2024).

Publication 3: **Licht, P**. & Mailänder, V. Multi-Omic Data Integration Suggests Putative Microbial Drivers of Aetiopathogenesis in Mycosis Fungoides. *Cancers (Basel).* **16,** 3947 (2024).

During the course of my doctoral studies, I additionally contributed as a coauthor to the following publication. However, as it does not pertain to the subject matter of this dissertation, it will not be discussed further. For the sake of completeness, the publication is included in the addendum.

Publication 4: Zimmer, N*., Trzeciak, E. R.*, Müller, A., **Licht, P**., Sprang, B., Leukel, P., Mailänder, V., Sommer, C., Ringel, F., Tuettenberg, J., Kim, E. & Tuettenberg, A. Nuclear Glycoprotein A Repetitions Predominant (GARP) Is a Common Trait of Glioblastoma Stem-like Cells and Correlates with Poor Survival in Glioblastoma Patients. *Cancers (Basel).* **15,** 5711 (2023).

* denotes shared first authorship

Contributions to Publications 1, 2, and 3

The contributions to individual publications are given in percent from all authors' contributions according to the Contributor Role Taxonomy (CRediT):

Contributor Role	Publication 1	Publication 2	Publication 3
Conceptualization Ideas; formulation or evolution of overarching research goals and aims.	75	90	90
Data curation Management activities to annotate (produce metadata), scrub data and maintain research data (including software code, where it is necessary for interpreting the data itself) for initial use and later re-use.	Not applicable	65	100
Formal analysis Application of statistical, mathematical, computational, or other formal techniques to analyse or synthesize study data.	Not applicable	90	100
Funding acquisition Acquisition of the financial support for the project leading to this publication.	0	15	10
Investigation Conducting a research and investigation process, specifically performing the experiments, or data/evidence collection.	100	75	100
Methodology Development or design of methodology; creation of models.	100	85	100
Project administration Management and coordination responsibility for the research activity planning and execution.	80	80	100
Software Programming, software development; designing computer programs; implementation of the computer code and supporting algorithms; testing of existing code components.	Not applicable	Not applicable	Not applicable

Resources Provision of study materials, reagents, materials, patients, laboratory samples, animals, instrumentation, computing resources, or other analysis tools.	0	0	0
Supervision Oversight and leadership responsibility for the research activity planning and execution, including mentorship external to the core team.	0	20	0
Validation Verification, whether as a part of the activity or separate, of the overall replication/reproducibility of results/experiments and other research outputs.	Not applicable	100	100
Visualization Preparation, creation and/or presentation of the published work, specifically visualization/data presentation.	95	85	95
Writing – original draft Preparation, creation and/or presentation of the published work, specifically writing the initial draft (including substantive translation).	100	100	100
Writing – review & editing Preparation, creation and/or presentation of the published work by those from the original research group, specifically critical review, commentary or revision – including pre- or post-publication stages.	90	85	100

Abbreviations

A Disintegrin And Metalloprotease 10	ADAM10
Actinic keratoses	AKs
Adult T-Cell Leukaemia/Lymphoma	ATLL
Angioimmunoblastic T cell Lymphoma	AITL
antimicrobial peptides	AMPs
Atopic dermatitis	AD
Candida albicans	*C. albicans*
central memory T cell	T_{CM}
Cluster of Differentiation	CD
corroborated immune checkpoint blockade	ICB
Cutibacterium acnes	*C. acnes*
Cytomegalovirus	CMV
effector memory T cell	T_{EM}
Eppstein-Barr Virus	EBV
Epstein-Barr Virus	EBV
Human Herpesvirus 6	HHV-6
Human Herpesvirus 7	HHV-7
Human Herpesvirus 8	HHV-8
Human T-Lymphotropic Virus	HTLV
Immunglobulin G	IgG
Interleukin	IL
internal transcribed spacer	ITS
iron-regulated surface determinant protein A	isdA
Janus kinase	JAK
Leukotoxin	Luk
metagenomic assembled genomes	MAGs
Methicillin-resistant *S. aureus*	MRSA
Methicillin-resistant *Staphylococcus aureus*	MRSA
mitogen-activated protein kinase	MAPK
naïve T cell	T_N

Next Generation Sequencing	NGS
Nuclear factor kappa-light-chain-enhancer of activated B cells	NF-κB
nuclear factor of activated T-cells	NFAT
Phosphoinositide 3-kinases	PI3K
Protein kinase B	AKT
regulatory T cell	Treg
Ribonucleic acid	RNA
RNA sequencing	RNAseq
signal transducer and activator of transcription	STAT
species	spp.
Squamous cell carcinoma	SCC
Staphylococcus aureus	*S. aureus*
Staphylococcus epidermidis	*S. epidermidis*
stem cell memory T cell	T_{SCM}
Streptococcus pyogenes	*S. pyogenes*
T helper 17 cell	Th
TCR sequencing	TCRseq
TNF receptor 1	TNFR1
transitional memory T cell	T_{TM}
Tumor Necrosis Factor	TNF
tumour microenvironment	TME
whole metagenome shotgun sequencing	WMS

Abstract (Deutsch)

Mycosis fungoides (MF) ist die häufigste Form des kutanen T-Zell-Lymphoms (CTCL), einer heterogenen Gruppe von non-Hodgkin-Lymphomen mit primärer Hautbeteiligung. Die Ätiopathogenese ist nur unvollständig verstanden, u. A. aufgrund ausgeprägter klinischer und transkriptioneller Heterogenität. Diese kumulative Dissertation präsentiert eine Multi-Omics-Analyse zur Rolle des Hautmikrobioms in der Pathobiologie von MF. Untersucht wurden metagenomische, transkriptomische, virologische und T-Zell-Rezeptor-(TCR)-Sequenzierungsdaten aus Proben von Patienten-gematcher läsionaler und nicht-läsionaler Haut, als auch funktionelle Tests an mikrobiellen Hautisolaten.

Publikation 1 untersucht die Wechselwirkungen zwischen transkriptioneller Heterogenität und Hautmikrobiota bei CTCL und schlägt eine wechselseitige Beziehung zwischen neoplastischem T-Zell-Signalling und mikrobieller Kolonisation vor.

Publikation 2 liefert den ersten überzeugenden Nachweis für taxonomische und funktionelle Veränderungen des MF Haut-Mikrobioms. Es wird eine Subgruppe von Patient*innen (ΔSA-positiv) identifiziert, die eine erhöhte läsionale Besiedlung mit *Staphylococcus aureus*, eine verringerte mikrobielle Diversität, ein eingeschränktes TCR-Repertoire sowie ein ungünstigeren klinischen Verlauf aufweist. Läsionale Isolate von ΔSA-positivem *S. aureus* zeigten Resistenzen gegenüber kutanen antimikrobiellen Peptiden, die ektop exprimiert waren und vermutlich zur Eradikation der kommensalen Flora beigetragen haben. Dieser Stamm trug zudem mutiertes *spa*, ein Virulenzfaktor mit bekannter Aktivierung des NF-κB-Signalwegs, was auf eine funktionelle Rolle in der Krankheitsprogression hinweist.

Publikation 3 zeigt, dass transkriptionelle Heterogenität Aktivitätsunterschiede in der T-Zell-Signalkaskade widerspiegelt. Multi-Omic Daten-Integration deckte eine durch ΔSA-positive *S. aureus*-Stämme hervorgerufene Aktivierung des nicht-kanonischen NF-κB und IL-1β Signalwegs auf, die beide mit T-Zell-Aktivierung und MF-Progression in Verbindung stehen. Darüber hinaus zeigten sich antivirale Signaturen und Epstein-Barr-Virus-Reaktivität in Blut und Haut, was ein Zwei-Treffer-Modell der MF-Ätiopathogenese mit viralen und bakteriellen Auslösern nahelegt.

Diese Arbeit positioniert das Hautmikrobiom als klinisch relevanten Modulator der MF-Biologie. Die Ergebnisse identifizieren *S. aureus* als potenziellen prognostischen Biomarker und therapeutisches Ziel und ebnen den Weg für mikrobiomgestützte Präzisionsmedizin.

Abstract

Mycosis fungoides (MF) is the most common form of cutaneous T-cell lymphoma (CTCL), a heterogeneous group of non-Hodgkin lymphomas with primary skin involvement. Its aetiopathogenesis remains incompletely understood, partly due to pronounced clinical and transcriptional heterogeneity. This cumulative dissertation presents a multi-omics investigation into the role of the skin microbiome in MF pathobiology, encompassing metagenomic, transcriptomic, virologic, and T-cell receptor (TCR) sequencing data from patient-matched lesional and nonlesional skin. In addition, functional assays were performed on patient-derived skin isolates.

Publication 1 reviews the interplay between transcriptional heterogeneity and the skin microbiota in CTCL, proposing a reciprocal relationship between neoplastic T-cell signalling and microbial colonisation.

Publication 2 provides the first conclusive evidence for taxonomic and functional microbiome shifts on MF skin. It identifies a distinct subgroup of patients (ΔSA-positive) with increased lesional abundance of *Staphylococcus aureus*, reduced microbial diversity, a restricted TCR repertoire, and inferior clinical outcome. Lesional isolates of ΔSA-positive *S. aureus* exhibited resistance to cutaneous antimicrobial peptides, which were ectopically expressed and may have contributed to commensal flora eradication. This strain also harboured mutant *spa*, a virulence factor known to activate NF-κB signalling, thereby supporting a functional role in disease progression.

Publication 3 shows that transcriptional heterogeneity may reflect differences in T-cell signalling activity. Multi-omic data integration revealed ΔSA-positive *S. aureus* strain-driven activation of non-canonical NF-κB and IL-1β signalling, both implicated in T-cell activation and MF progression. Importantly, denoising the skin transcriptome from microbial influence resolved the observed differential expression pattern. Additionally, antiviral signatures and Epstein–Barr virus reactivity in blood and skin suggest a two-hit model of MF aetiopathogenesis involving viral and bacterial triggers.

Together, this thesis positions the skin microbiome as a clinically relevant modulator of MF biology. The findings support *S. aureus* as a potential prognostic biomarker and therapeutic target and lay the groundwork for microbiome-informed precision medicine.

1 Introduction

1.1 Cutaneous T cell Lymphoma and Mycosis Fungoides

Cutaneous T-cell lymphoma (CTCL) comprises a heterogeneous group of non-Hodgkin lymphomas that primarily present with skin involvement, without evidence of extracutaneous spread at the time of diagnosis [1]. The skin-homing capability of (neoplastic) T cells is mediated by the expression of cutaneous lymphocyte antigen (CLA) and specific chemokine receptors (CCR), such as CCR4, CCR8, and CCR10, enabling respective benign T cell subsets to maintain cutaneous homeostasis [2].

CTCL encompasses more than eight distinct entities, varying widely in clinical presentation, biology, histopathology, and prognosis [3,4]. Despite an age-adjusted incidence rate of only 7.7 cases per million population [5], the prevalence is tenfold higher owing to patients who survived in early stages of the disease [3]. Notably, the incidence of CTCL has been increasing over the last decades, a trend attributed to advances in diagnostic capabilities that have reduced the misclassification of CTCL as benign inflammatory dermatoses [4,6,7].

The most prevalent entity of CTCL is the so called mycosis fungoides (MF), accounting for 39% of all CTCL cases [3]. Another important entity is the Sézary syndrome (SS), traditionally defined as the leukemic form of CTCL. Historically, it was believed that advanced stages of MF could give rise to SS. However, recent research suggests that MF and SS are distinct entities [8], although they may share some overlapping biological properties in advanced stages of MF [9].

Given that this dissertation focuses on patients with MF, the subsequent sections will delve deeper into the clinical and molecular aspects of this specific CTCL entity. Some papers did not explicitly distinguish between (advanced stage) MF and SS [10], and thus some aspects presented in the following sections may only available be on the level of CTCL.

Introduction

1.1.1 *Clinical Characteristics of MF*

The first description of mycosis fungoides was published in 1806 by the French physician Jean Louis Alibert, who named the disease after the "mushroom-like" appearance of the skin tumours. Similarly, Sézary syndrome was first described by Drs. Sézary and Bouvrain in 1938. Over time, three subtypes of “classical” MF were identified, most prominently folliculotropic MF, along with other, rarer variants [10]. Among all entities, classic MF is by far the most prevalent, accounting for 39% of all CTCL cases [3], with an age-adjusted incidence rate of 4.1 per million population [5,6].

Neoplastic cells in MF typically express surface markers CLA, CCR4, and CD4, exhibiting the phenotype of $CD4^+$ skin homing T cells [4]. However, malignant T cells may be $CD8^+$ or CD4/CD8 double-negative in a rare subset of patients [4,11].

Histologically MF is characterized by epidermotropism, i.e., the migration and accumulation of mature, neoplastic T cells in the epidermis and upper dermis. These T cells typically display irregular, cerebriform nuclei and are small to medium in size. A hallmark feature of MF is the formation of Pautrier microabscesses, which are clusters of neoplastic T cells and Langerhans cells (epidermal dendritic cells) within the epidermis [4]. Accumulation of neoplastic T cells, along with accompanying infiltrate (e.g., benign reactive T cells, other immune cell subsets), leads to the development of cutaneous lesions and associated inflammatory reddening.

Clinically, MF lesions progress through distinct stages — patch, plaque, and tumour — depending on the amount of infiltrate and degree of inflammation [3,12] (see Figure 1). This progression is reflected in the histopathology. In patches, neoplastic T cells are sparsely distributed, often aligned along the dermal-epidermal junction [13]. Plaque stages show more pronounced infiltration, with band-like lymphocytic infiltrates in the papillary dermis [14]. In tumour stages, dense infiltrates disrupt the dermal architecture, leading to the breakdown of normal skin structures, deeper tissue involvement, and in some cases, the formation of ulcers [13,14]. Lesions are mostly located on body areas which are infrequently exposed to sunlight, although any other body area may also be affected [3,4]. MF patients often present with many lesions that persist over long periods — typically months to years — and individual lesions may progress over time if not treated properly. Some patients may develop erythroderma, a systemic form of MF, that

shares clinical similarity to SS [4]. Notably, lesions are often scaly [3], which will be of significance for microbiome sampling and analysis.

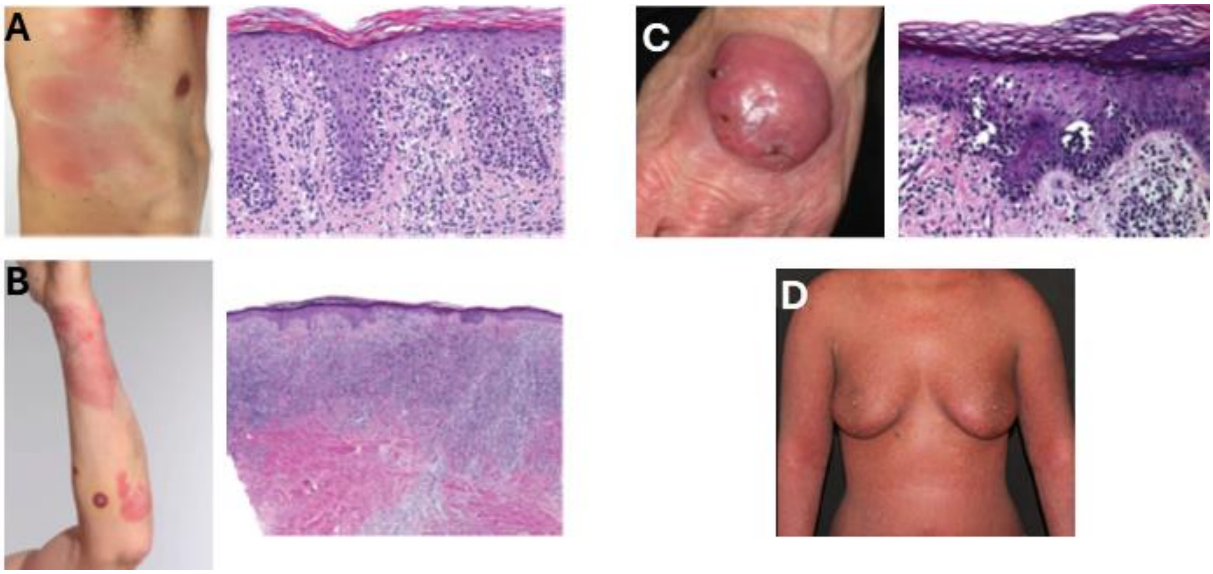

Figure 1: Overview of Lesional Stages in mycosis fundoides.
A: Patch stage, B: Patch and Plaque Stage, C: Tumour Stage, D: Erythroderma.
Reproduced and compiled from:
Kempf, W., Zimmermann, A. & Mitteldorf, C. *Hematol. Oncol.* 37, 43–47 (2019);
Whittaker, S., Hoppe, R. & Prince, H.M. *Blood* 127, 3142–3153 (2016);
Ahn, C.S., ALSayyah, A. & Sangüeza, O.P. *Am. J. Dermatopathol.* 36, 933–951 (2014);
Miyashiro, D. & Sanches, J.A. *Front. Oncol.* 13, 1–18 (2023)

To track clinical presentation over time, the modified Severity-Weighted Assessment Tool (mSWAT) was developed. The mSWAT quantifies disease burden by measuring the surface area of lesions across 12 distinct body regions and assigning a weighting factor based on the stage of the lesions [15]. In addition, the tumour-node-metastasis-blood (TNMB) classification system is widely used in clinical practice. The TNMB system assesses four key factors: i) the skin area covered by lesions and their stages (**T**umour), ii) the involvement of lymph nodes and whether dominant T cell receptor (TCR) clones of neoplastic T cells can be detected (**N**ode), iii) presence of visceral metastases (**M**etastases), and iv) the detection and amount of atypical lymphocytes, known as Sézary cells, in the peripheral blood (**B**lood). These parameters stratify MF patients into nine stages ranging from IA to IVB, with IA – IIA classified as early stage and IIB – IVB as advanced stage disease [12,16].

In early stages, MF is an indolent disease with a five-year disease-specific survival of 89%. Nevertheless, one third of patients progress into higher stages, which is associated with poor prognosis: only ~20% of MF patients in the most advanced stages survive beyond 5

years [17,18]. The clinical course of MF can be erratic, with some patients experiencing decades of indolent disease and well-controlled activity that can suddenly transition into aggressive disease [3]. Prognostic factors for aggressive disease other than clinical staging are the presence of plaques in early stages, increased age, male sex, increased lactate dehydrogenase (LDH), and the manifestations of rare MF subtypes [17].

1.1.2 *Current Treatment Options*

Treatment strategies for MF range from a "watch-and-wait" approach for very early stages to skin-directed and systemic therapies, the latter particularly in more advanced stages. The choice of treatment is guided by the patient's disease stage, prior treatments, and clinical response. To date, no truly curative treatment exists, with the exception of stem cell transplantation, which is limited to highly selected cases. Current therapies primarily aim to prolong the indolent disease course and manage symptoms [3,19–21]. An overview of treatment options is provided in Figure 2.

For early MF stages, first line therapies include topical steroids, phototherapy (UVA with psoralen, and UVB), and chlormethine gel. Second-line therapies are often employed for refractory cases and include localized radiotherapy, bexarotene gel, topical immune modulators imiquimod/resiquimod, and combination therapies like Interferon (IFN)-α with pUVA. Additional options include methotrexate, anti-CCR4 monoclonal antibody (mAb, Mogamulizumab), antibody drug conjugate (ADC) CD30-Vedotin (Brentuximab-Vedotin), and low-dosed total skin electron beam therapy.

In advanced MF stages, some second-line therapies for early-stage disease become first-line options, often in combination regimens (e.g., PUVA + IFN-α + bexarotene). Advanced-stage treatments also include ex-*vivo* UVA (extracorporeal photopheresis) and localized radiotherapy for tumours. Alternative therapies for advanced stage include systemic chemotherapy (CHOP and related schemas), and the anti-CD52 mAb Alemtuzumab [3,20]. Of note, allogenic haematopoietic stem cell transplantation has emerged as a potentially curative treatment. Albeit, patients must meet high inclusion criteria (poor prognostic factor, complete or partial remission prior to transplantation) [22].

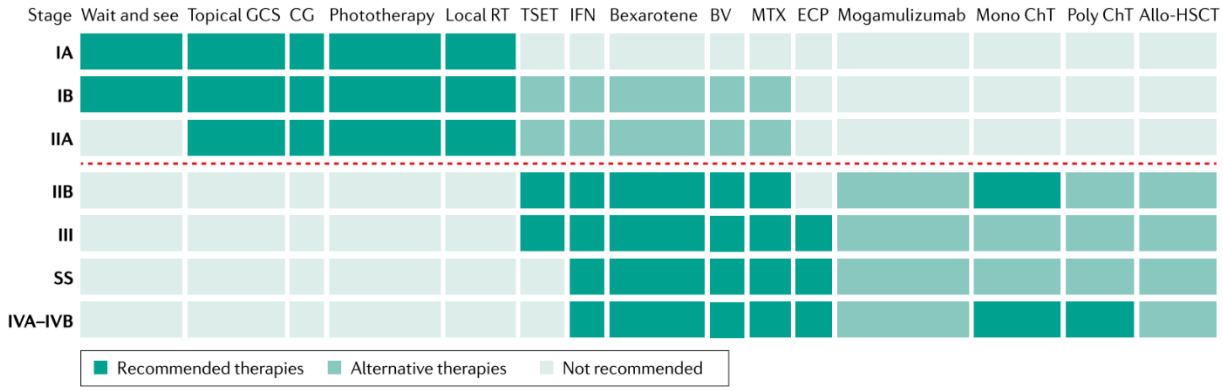

Figure 2: Overview of treatment options for mycosis fungoides.
Allo-HSCT, allogeneic haematopoietic stem cell transplantation; BV, Brentuximab-Vedotin; CG, chlormethine gel; ChT, chemotherapy; ECP, extracorporeal photopheresis; GCS, glucocorticosteroids; IFN, interferon; MTX, methotrexate; RT, radiotherapy; TSET, total skin electron therapy.
Reproduced from: Dummer, R. *et al.* Cutaneous T cell lymphoma. *Nat. Rev. Dis. Prim.* 7, 61 (2021).

1.1.3 *Signalling Pathways Governing Benign T-Cell Activity*

Before exploring the malignant properties of neoplastic T cells in MF, this section provides a brief overview of the three primary signalling pathways that govern benign T-cell function, activity, and proliferation. This section partially adopts content from the introduction of Publication 3 [23].

The first step in T-cell activation is the antigenic stimulation of the T cell receptor (TCR) in conjunction with CD3, activating TCR signalling. Second, co-stimulation is required to augment TCR signalling. Co-stimulation is mediated by various molecules, including CD28 and members of the tumour necrosis factor receptor superfamily (TNFRSF). Downstream, both TCR signalling and co-stimulation converge on key pathways such as PI3K/AKT, NFAT, and NF-κB [24]. Third, cytokine signalling sustains T-cell activity over longer time periods by activating the JAK-STAT pathway. For CD8+ T cells, this process requires cytokines like interleukin (IL)-12 and interferon (IFN)-α/β, whereas CD4+ T cells depend on IL-1 [25,26].

Because TCR signalling, co-stimulating pathways like NF-κB signalling, and cytokine signalling by JAK-STAT are recurrently mutated and aberrantly activated in T cell lymphomas, a ‘three-signal-model’ of T cell lymphoma pathogenesis has been proposed [27].

1.1.4 *Molecular and Transcriptional Landscape of Aetiology and Pathology*

Homologous to the phenotypic and clinical plasticity observed in MF, its molecular and transcriptional landscape demonstrates significant heterogeneity, contributing to an incomplete understanding of the molecular underpinnings of aetiology and pathogenesis [28].

Genomic profiling studies have revealed a diverse mutational spectrum: More than 50 driver mutations were identified to date [28], however, most are only infrequently prevalent [3]. CTCL-specific mutations can be broadly classified into two categories: i) canonical cancer genes commonly mutated across various cancer types, and ii) mutations in genes associated with pathways implicated in the 'three-signal model' of T-cell lymphoma. In addition, skin homing receptor *CCR4* was also found to be recurrently mutated. Example mutations of canonical cancer genes (category i) include genes involved in DNA damage repair like *TP53*, cell cycle regulation (e.g., *CDKN2A, RB1*), apoptosis (e.g., *FAS*), epigenetic regulation (e.g., *ARID1A*, *DNMT3A*), and the MAPK pathway (e.g., *KRAS*, *BRAF*, *MAPK1*). T cell lymphoma specific mutations (category ii) were found in TCR signalling (e.g., *PRKCQ*, *PDCD1*, *CD28*, *PLCG1*), NF-κB signalling (e.g., *TNFRSF1B*, *NFKB2*), and JAK-STAT signalling (e.g., *JAK1*, *JAK3*, *STAT3*, *STAT5B*) [29].

Downstream, the transcriptome exhibits an intricate network of signalling pathways, including TCR, NF-κB, JAK-STAT, PI3K/AKT, and MAPK, as well as those controlling cell cycle and apoptosis (Figure 3). These dysregulated signalling pathways collectively govern neoplastic T cell fate in a wide range of functions, such as polarization, proliferation, survival, cell cycle, and production of various cytokines that stimulate neoplastic T cells in an autocrine fashion [3,28,30]. Furthermore, these pathways do not operate in isolation but rather form an intricate, interconnected network, with signalling in one pathway often activating others [30].

Importantly, transcriptomic profiling revealed substantial heterogeneity both between patients and among lesions within the same patient. Bulk and single-cell RNA sequencing (RNAseq) demonstrated distinct transcriptional profiles in MF lesions of the same stage and over time [28,31,32].

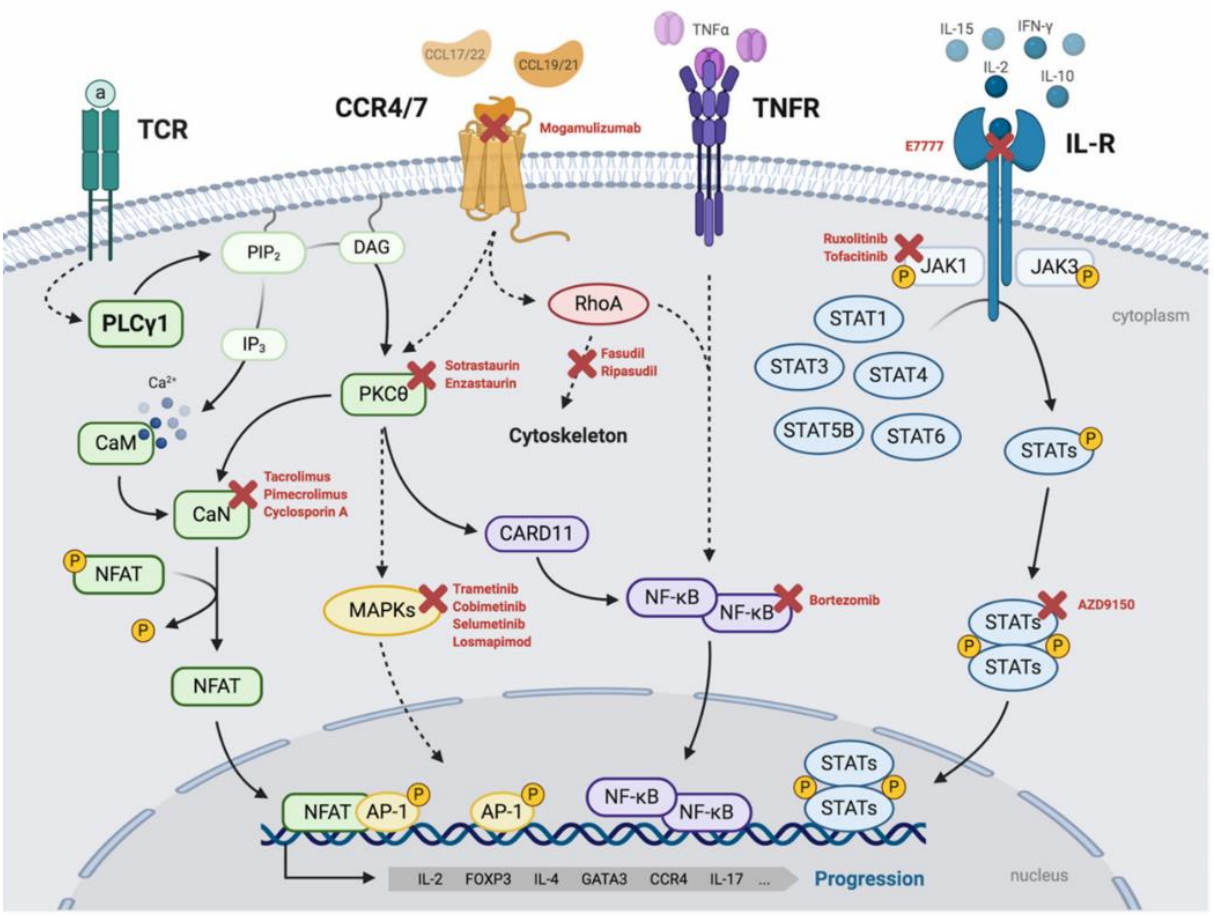

Figure 3: Overview of aberrant pathways in CTCL.
Key pathways include TCR signalling via PLCγ1–NFAT/AP-1 and NF-κB, chemokine receptor signalling (CCR4/CCR7) via MAPK and RhoA, TNFR-mediated NF-κB activation, and cytokine receptor signalling via the JAK–STAT pathway. These cascades converge to drive expression of genes central to T-cell proliferation, survival, and inflammation, including IL-2, IL-4, IL-17, FOXP3, GATA3, and CCR4. The **X** denoted in red shows approved (e.g., Mogamulizumab) and possible treatments to block/supress disease signalling.
Reproduced from: García-Díaz, N., Piris, M.Á., Ortiz-Romero, P.L. & Vaqué, J.P. *Cancers (Basel).* 13, 1931 (2021).

Furthermore, the pool of neoplastic T cells of individual SS patients was found to heterogeneously express surface markers characteristic of effector memory (T_{EM}), central memory (T_{CM}), stem cell memory (T_{SCM}), naïve (T_N), and transitional memory (T_{TM}) T cell phenotypes [28,33]. It was suggested that external or surrounding factors like the tumour microenvironment (TME) may shape the differentiation of neoplastic T cells, depending on the signal they receive [28]. Although the finding of phenotypic plasticity was observed in SS, a similar phenomenon is conceivable in MF, since the finding of phenotypic plasticity of neoplastic SS T cells contrasts with the previous understanding of the T cell subset phenotype of SS: Campbell et al. [8] proposed that neoplastic T cells in SS arise from mature T_{CM}, whereas neoplastic T cells in MF originate from mature T_{EM}

cells. This concept has been widely accepted, as it provides a rational for the distinct clinical behaviours of MF and SS [28].

Nevertheless, a series of studies mapped the cell of origin to early thymocytes, where the initial oncologic transformation occurs between the Double Negative (DN) states DN1 and DN3. These 'pre-malignant' clones are thought to infiltrate the skin, may divide into different clonotype branches, and potentially seed into other lesions or skin sites through the circulation [34–38]. Thus, it is still up to debate whether the cell of origin s derived from mature T cells or from early thymocytes.

Likewise, the aetiologic agent that causes neoplastic transformation in MF remains uncertain [3]. A wide array of potential carcinogens has been proposed, including exposure to chemicals like glyphosate, a medical history of eczema, and putative viral agents [39]. The latter has drawn considerable attention over the past decades, as oncoviruses are implicated in the development of various lymphomas, including two entities of CTCL [40]. Specifically, retroviral insertion into genes of the *RUNX* family has been shown to interfere with thymocyte differentiation into mature T cells [41]. Interestingly, MF patients exhibit an elevated risk to develop secondary virus-initiated lymphomas, either concurrently with MF or later in time [42–48]. However, the role of viruses in the aetiology of MF remains enigmatic [49]. Findings from various studies have yielded conflicting results, and are summarized in section 1.3.1 *Viruses in CTCL.*

1.1.5 *Implications for Microbial Factors in the Development of CTCL*

Besides genetic predisposition [3], it has long been hypothesized that a strong external stimulus is required to transform 'pre-malignant' into T cells neoplastic ones. Chronic antigenic stimulation is thought to drive persistent T-cell expansion and cutaneous inflammation [50], both of which are hallmarks of MF pathogenesis [3]. In support, the mutational spectrum in the TCR signalling cascade is not being considered sufficient to activate signalling alone, suggesting the need for external stimuli [29]. Given that neoplastic T cells predominantly reside in the epidermis [3,4] and that human skin is in constant interaction with a plethora of microbes [51], infectious agents might provide the additional stimulus necessary to provoke MF aetiopathogenesis [49].

Indeed, several observations support the role of infectious agents in the pathogenesis of CTCL: From an epidemiological perspective, CTCL occurs at an elevated frequency in immunosuppressed individuals compared to the general population [52]. CTCL has been observed in post-organ transplantation patients, where it often exhibits an aggressive clinical course [53]. Similarly, a high prevalence of CTCL has been correlated with a high incidence of HIV-infected individuals within the same geographic region [52]. Supporting this, CTCL patients are highly susceptible to bacterial skin infection with the risk of infection increasing as the disease progresses. Notably, morbidity in CTCL patients is often attributed not to the lymphoma itself, but rather to secondary infections [52,54,55].

From a biological perspective, CTCL is characterized by an oligoclonal expansion of neoplastic T cells, which is in contrast to the clonal pattern in other lymphomas. This oligoclonality has been attributed to the stimulation of respective neoplastic T cells by viral or bacterial superantigens [49,52,56,57].

Clinically relevant superantigens are produced by *Staphylococcus aureus* (*S. aureus*) [58]. Several early studies attempted to correlate *S. aureus* outgrowth with CTCL disease severity [59], but no definitive role for *S. aureus* in CTCL pathogenesis has been established [60]. Nevertheless, antibiotic treatment leads to significant clinical improvement in a subset of MF patients [59]. Notably, diseases progression in CTCL mouse model was attenuated under germ-free conditions and reinforced upon the presence of microbiota [61], suggesting that the microbiome, and potentially *S. aureus*, plays a role in modulating CTCL activity. Therefore, studies investigating the microbiome of CTCL patients are warranted.

1.2 The Human Skin Microbiome

The study of the human skin microbiome began with Antoni van Leeuwenhoek's microscopic observations in 1683 and advanced significantly with Kligman’s research in the 1950s using improved culture techniques [62]. The term “human microbiome,” referring to the collective genome of microorganisms inhabiting the body, was introduced by Joshua Lederberg in 2000 [63].

Unlike the well-studied gut microbiome, research on the skin microbiome is relatively recent. It involves identifying and characterizing microbial communities, assessing their abundance, and understanding their role in skin health and disease. While only about 200 microorganisms are classified as truly pathogenic, the majority are commensal or facultative pathogens [62].

The skin microbiome contributes to immune modulation and skin homeostasis, but dysbiosis can create conditions conducive to infections, supporting the concept of the hologenome, which considers the host and microbiome as a single ecological unit. From a genetic perspective, the metagenome refers to the total genetic content of skin microbes, while the meta-transcriptome encompasses their gene expression profiles. Understanding the complexity of the skin microbiome and its dynamic interactions with the host has profound implications for skin health and the development of targeted therapeutic strategies [62].

1.2.1 *The Skin Microbiome in Health and Disease*

The human skin, functioning as both a physical barrier and a habitat for microbial communities, is home to a manifold of microbiota, including bacteria, fungi, viruses, and archaea. These microbes play crucial roles in immune system education, pathogen defence, and skin homeostasis [51]. Bacteria have the highest frequency within the skin microbiome, followed by viruses and fungi, while archaea represent a minor kingdom [51,64,65]. The composition of the microbial communities primarily varies with the physiology of specific skin sites, categorized as sebaceous (e.g., face, chest), moist (e.g., elbow creases, inguinal crease), dry (e.g., forearms, palms), and the feet (e.g., toenail, plantar heel) [51]. Sebaceous areas are dominated by Propionibacteria and Staphylococci, moist and feet areas by Corynebacteria and Staphylococci, and dry areas

by Streptococci. In contrast, fungal communities, particularly Malassezia spp., are relatively stable across body sites, though their diversity increases in areas like the feet [51]. Interestingly, under healthy conditions, the microbiome profiles exhibit temporal stability even on strain level [66].

With a colonization of 1 million bacteria per cm^2 of adult skin, the microbiota exerts an extraordinary pressure on the immune system. This results in high numbers of immune cells governing the skin, including ~20 billion effector memory T cells, setting it among the largest reservoirs of memory T cells in the human body [67]. This mutual alliance has evolved closely and educated the cutaneous immune system in both innate and adaptive arms to allow maintenance of commensals while eliminating pathogens. For instance, keratinocytes bind to microbial pathogen-associated molecular patterns (PAMPs) through pattern recognition receptors (PRRs), resulting in the secretion of antimicrobial peptides (AMPs). These molecules have bactericidal activity and can be targeted to specific species or genera or exhibit broad-spectrum activity. As a first line of defence, some AMPs are constitutively expressed, while others are transiently controlled by specific members of the skin microbiome, such as *Propionibacterium* spp. [62,67,68]. The skin microbiome also discretely controls Interleukin (IL) 1 expression, which is a central mediator of innate immunity and inflammation and is expressed by various cutaneous cell populations [67,69]. Notably, under steady-state conditions, this process induces Interferon (IFN) gamma and IL-17 response by effector memory T cells (T_{EM}) in the absence of classical inflammation, a process termed “homeostatic immunity”. In the case of infection, these “pre-activated” lymphocytes provide improved protection. Thus, the skin microbiota can serve as an endogenous adjuvant of cutaneous immunity [68].

While under homeostatic conditions a delicate network of microbe-microbe and microbe-host interactions balances cutaneous immunity, many cutaneous diseases are associated with shifts in the skin microbiome, termed dysbiosis [51,68]. Much attention was attracted by the contribution of the skin microbiome to atopic dermatitis (AD), a chronic and relapsing inflammatory disorder. Gene mutations that compromise the skin barrier are common, and disease flares are often exacerbated or triggered by the overgrowth of specific *S. aureus* strains, which differ from asymptomatic AD patients [51,70,71]. Notably, *S. aureus*, a natural commensal of the healthy skin microbiota,

exemplifies how commensal bacteria can transition into pathogenic states under dysbiotic conditions [68]. Targeted eradication of *S. aureus* correlates with improvements in AD severity, underscoring its role in disease progression [71,72]. In psoriasis (Pso), another chronic inflammatory skin disorder, microbiome perturbations are more complex and multifaceted. Pso is driven by a combination of genetic predisposition and environmental factors, leading to dermal immune cell infiltration and keratinocyte hyperproliferation, which results in the formation of characteristic scaly plaques. Impaired immunological tolerance to the cutaneous microbiota has been implicated in Pso pathogenesis, suggesting that microbial dysbiosis may act as a contributing factor in disease onset and progression [71]. The Pso skin dysbiosis is characterized by a decrease in beneficial microbes, such as *Cutibacterium acnes* (*C. acnes*) and *Staphylococcus epidermidis* (*S. epidermidis*), and an overgrowth of *S. aureus*, which contributes to inflammation and keratinocyte proliferation through toxin secretion and immune activation. Additionally, *Streptococcus pyogenes* (*S. pyogenes*) has been implicated in triggering and exacerbating the disease via superantigen-mediated immune responses. The potential role of fungal species, such as Malassezia spp. and *Candida albicans* (*C. albicans*), in Pso remains unclear but is suspected to contribute to lesion persistence and immune modulation [71]. Further skin disorders which are associated with cutaneous dysbiosis are seborrheic dermatitis, acne, rosacea [73].

1.2.2 *The Microbiome and Cancer*

The human microbiome has garnered significant interest in cancer research in recent years. Studies found a perturbed microbiome in many microbial niches in human cancer patients' bodies, including the gastrointestinal tract, respiratory tract, genitourinary tract, and the skin. Notably, also an intratumoural microbiome was described, modulating the tumour microenvironment (TME) and therapeutic response [74,75].

Three landmark papers from 2018 showed that systemic antibiotics corroborated immune checkpoint blockade (ICB) in patients with epithelial tumours [76], while greater microbial diversity and the presence of specific beneficial bacteria correlated with improved ICB responses in melanoma patients [77,78]. Similar microbiome-driven influences have been reported for other immunotherapies, such as CAR T cell therapy [79,80] and allogeneic hematopoietic stem cell transplantation [81].

Despite these promising findings, cancer-associated microbiome profiles exhibit considerable variability between individuals, complicating the generalization of results. However, this inter-individual heterogeneity likely reflects the true biological diversity of the microbiome and could account for the variability in clinical outcomes among cancer patients. As a result, targeting the microbiome holds potential as a personalized therapeutic strategy [74,75].

One mechanism by which the microbiome exerts its immune-modulating effects is through the production of secondary bile acids, metabolic byproducts of microbial activity. These secondary bile acids have been shown to suppress the differentiation of T helper 17 (Th17) cells [82,83], while promoting the expansion of regulatory T cells (Treg) [82–84], thereby shifting the host's immune balance toward an immunosuppressive state [85].

While the majority of research on the microbiome's role in cancer pathogenesis has focused on the intestinal microbiome, the contribution of the skin microbiome has been less studied [75]. Nonetheless, growing interest has emerged in exploring its potential involvement in skin cancer development. Although studies on melanoma have been limited and show only minor concordance, research on non-melanoma skin cancers has yielded more consistent and conclusive findings [86].

In this group of keratinocyte cancers, including basal cell carcinoma (BCC), squamous cell carcinoma (SCC), and the SCC precursor actinic keratosis (AKs), microbial dysbiosis is characterized by a shift from a commensal-dominated environment to one enriched with potentially pathogenic species, contributing to chronic inflammation and immune dysregulation [87].

In SCC and its precursor AKs, studies have identified an overrepresentation of *S. aureus* at the expense of *C. acnes* and *S. epidermidis*, with distinct strains of *C. acnes* observed between healthy skin and SCC lesions [88]. Mechanistically, *S. aureus* may promote local inflammation, DNA damage, and tumour cell proliferation by inducing keratinocytes to express IL-6, IL-8, AMPs, and tumor necrosis factor alpha (TNF-α) [86]. Furthermore, an increased prevalence of beta human papillomaviruses (β-HPV) has been detected in SCC and AK, with some β-HPV genotypes potentially contributing to tumorigenesis by inducing chronic and self-maintaining inflammation [86,87]. In contrast, BCC exhibits a

distinct microbial profile, with a lower prevalence of *S. aureus* compared to SCC. Instead, an increased abundance of Streptococci has been reported in BCC lesions, suggesting a different microbial influence in its pathogenesis [86].

1.3 The Microbiome of Cutaneous T cell Lymphoma

Before the advent of next-generation sequencing (NGS) technologies, which enable comprehensive microbiome analysis, investigations relied on culture-based methods or molecular biology techniques such as polymerase chain reaction. While these approaches are highly precise, they are designed to target specific organisms of interest and are limited to identifying known microbiota, thereby overlooking a vast array of uncharacterized microorganisms referred to as the 'microbial dark matter' [89].

To date, numerous studies investigated the microbial flora of MF and SS patients, of which the majority utilized non-sequencing based methods [60,90]. Most research has focused on the role of bacteria in CTCL, followed by viruses, while fungi and archaea remain largely unexplored [91]. The next two sections present current knowledge of the microbiome patterns in CTCL, with a focus on sequencing-based investigations of the CTCL skin microbiome.

1.3.1 *Viruses in CTCL*

A wide array of possible environmental factors capable of initiating T cell proliferation and disease progression have been investigated [49,92,93]. As outlined above, viruses are suspected to act as carcinogen due to their involvement in various lymphomas, including two entities of CTCL [40]. However, viral profiling has yet to establish a conclusive role in CTCL pathogenesis [49,94].

The retrovirus Human T-Lymphotropic Virus (HTLV), a known causative agent of adult T-cell leukaemia/lymphoma (ATLL), has been linked to MF due to clinical and histopathological similarities between the diseases [95,96], as well as the detection of HTLV-specific sequences and virus-like particles in MF patient samples [49]. However, other studies found mixed HTLV detection rates in skin and blood of MF patients and even in healthy controls [94]. Despite these inconsistencies, it has been proposed that HTLV may act indirectly, promoting chronic antigenic stimulation and persistent T-cell activation in skin-homing T cells rather than exerting a direct oncogenic effect [49].

Epstein-Barr Virus (EBV) has long been investigated for its potential role in CTCL due to its oncogenic involvement in multiple lymphomas and its ability to establish long-term latent infections that promote chronic antigenic stimulation and T-cell hyperproliferation Some studies have shown higher EBV seropositivity and elevated antibody titres in CTCL patients compared to healthy controls, along with the detection of EBV genetic material in CTCL lesions [49]. However, many findings are inconsistent, with several studies failing to detect EBV in most CTCL samples or reporting only a minority of positive cases [49,94].

Similarly, profiling of other Herpesviridae has not pinpointed any definitive oncogenic involvement yet. Cytomegalovirus (CMV) has been linked to CTCL due to the high seropositivity rates in patients. However, inconsistent findings — such as only spurious detection of CMV DNA in skin lesions — suggest that its presence is largely due to the immunosuppressed state of CTCL patients rather than any direct involvement in tumour development [49]. T-lymphotropic HHV-6 and HHV-7 infections have been inconsistently detected, often with low rates around 5% and a maximum of 25%, failing to provide significant evidence for involvement in CTCL. Likewise, no clear association has been established between HHV-8, the causative agent of Kaposi's sarcoma, and CTCL. Although viral DNA has occasionally been detected, follow-up studies failed to replicate these findings [49].

1.3.2 *Bacteria in CTCL*

Given the evidence supporting a role for *S. aureus* in CTCL (outlined in section *1.1.5 Implications for Microbial Factors in the Development of CTCL*), several studies investigated this microbe using non-sequencing-based methods. Most of these studies found that a large proportion of CTCL patients is culture positive for *S. aureus* and associated it's presence with disease progression [54,59,97–103]. The pathogenic effect of *S. aureus* is attributed to two classes of virulence factors, staphylococcal superantigens and staphylococcal enterotoxins, which lead to clonal expansion of (malignant) T cells [59], or the activation of JAK-STAT signalling in neoplastic T cells [55], respectively.

Despite several compelling arguments of *S. aureus* involvement in CTCL pathogenesis [55,59], the situation is likely more complex than the mere presence of this microbe. *S. aureus* is a common commensal of the skin flora in healthy individuals [104], and studies

have failed to demonstrate a significantly higher prevalence of *S. aureus* in CTCL lesions compared to healthy skin or other inflammatory skin conditions [99]. Furthermore, although *S. aureus* eradication has been shown to induce remission in some cases, not all culture-positive CTCL patients benefit from antibiotic therapy [98,100,101]. These findings suggest that CTCL patients may suffer from a broader, more profound disturbance of the skin microbiome, which extends beyond the simple presence of *S. aureus*.

To address these shortcomings, several studies have characterized the microbiome of the skin [105–109], the gut [110,111], and the nose [112] using amplicon sequencing of the 16S ribosomal RNA (16S) and whole metagenome shotgun sequencing (WMS). However, many of these studies failed to achieve statistical significance, likely due to small sample sizes, inadequate sample stratification based on lesional or clinical stages, or the inherent limitations of 16S sequencing, which often lacks the resolution to identify microbes down to the species level.

Skin focused Microbiome Studies

In 2020, Salava et al. [105] conducted the first sequencing-based microbiome characterization of CTCL skin. Using both 16S sequencing and WMS, they examined 20 patients with early- and advanced-stage MF and found no significant differences in the microbial community between lesional and nonlesional skin. Nevertheless, their data suggested a trend toward microbiome destabilization on lesions compared to nonlesional skin [113], although the study lacked sample stratification by clinical stages or lesional stages.

One year later, Harkins et al. [106] investigated the microbial diversity in a small cohort of four MF patients with early- and late-stage disease using WMS and compared it to healthy individuals. They observed no statistically significant differences in overall microbial diversity. Nonetheless, the two corynebacterial species *C. tuberculostearicum* and *C. simulans* trended higher and two cutibacterial species *C. acnes* and *C. namnetense* trended lower on MF lesions — both trends correlating with disease severity. The lack of statistical significance was attributed to the small sample size [106].

Again one year later, Dehner et al. [107] combined 16S sequencing and culture-based techniques to analyse lesional and nonlesional skin from 7 early-stage MF patients and

healthy skin from controls. While no differences were seen in microbial α- and β-diversity metrics, *Bacillus safensis* was low but significantly more abundant in MF lesions compared to nonlesional and healthy skin. Alongside this, *S. aureus* was slightly, though nonsignificantly, more abundant on MF lesions. Notably, lesional T cells derived from two MF patients proliferated when exposed to *B. safensis* lesional isolate, but not when exposed to other patient isolates or unrelated bacteria. Similarly, CLA^+, $CCR4^+$, $CD4^+$ skin-homing T cells isolated from the peripheral blood of one patient also proliferated upon exposure to *B. safensis*. These findings suggest that *B. safensis*-reactive T cells could infiltrate the skin and contribute to local T-cell expansion. Supporting this hypothesis, the authors found that both cutaneous and circulating *B. safensis*-reactive T cells expressed high levels of inflammatory cytokines, including IL-21, IL-10, GM-CSF, IFN-γ, and TNF-α, potentially contributing to the chronic inflammation characteristic of early-stage MF. The authors further proposed that the early effects of *B. safensis* could be exacerbated by other inflammatory microbiota at later disease stages [107].

Similarly, Zhang et al. [108] found no significant alterations in microbial diversity between lesional and nonlesional skin in 39 MF patients using 16S sequencing. However, *Staphylococci* and *Corynebacteria* showed a positive correlation with symptom severity of erythema and skin thickness, while *Propionibacteria* correlated negatively with pain. Interestingly, patients who were on treatment (topical steroids, bexarotene, and imiquimod; radiation therapy; phototherapy; bleach bath) exhibited a diminished abundance of *Sphingomonas* spp. and an increased abundance of *Sarcina* spp, neither of which have been previously associated with skin infections. Notably, topical steroids did not alter the overall microbial composition [108].

Hooper et al. (2022/Skin-Study) [109] investigated microbial changes in the skin in response to UVB phototherapy, a standard-of-care treatment for early-stage MF, as assessed by mSWAT. Using 16S sequencing, the study included 40 CTCL patients (primarily MF) with early-stage (n = 20) and advanced-stage (n = 20) disease, of whom 25 received UVB therapy. While UVB therapy did not significantly alter overall microbial diversity, UVB responders presented with a more diverse skin microbiome compared to non-responders, particularly within the staphylococcal genus. Pre-UVB treatment, lesional and nonlesional skin of responders showed a significantly higher colonization by *S. capitis* and *S. warneri*. Over the course of UVB therapy, the abundance of *S. aureus* and

S. lugdunensis decreased in responders, whereas *S. warneri* abundance increased in non-responders. These findings support a link between MF disease severity and skin microbiome composition [109].

Gut focused Microbiome Studies

Hooper et al. (2022, Gut-Study) [110] investigated the gut microbiome in 38 CTCL patients (27 MF, 5 SS, 6 others) with early (n = 20) and advanced (n = 18) disease as well as healthy controls using 16S sequencing. They found that microbial α -diversity trended lower in CTCL patients, with significantly reduced α-diversity in advanced stages. Specific bacterial taxa, including *Actinobacteria* and *Anaerotruncus*, were significantly less abundant in CTCL patients, correlating with disease progression. Additionally, families such as *Eggerthellaceae* and *Lactobacillaceae* were reduced in patients with high skin disease burden. The observed microbial shifts shared similarities with dysbiosis patterns in AD but contrasted with those in psoriasis, reflecting immune-related parallels. For instance, *Lactobacillaceae* have cytokine-based anti-inflammatory activity [110], a hallmark of MF [3,114] and AD flares [115]. The findings suggest that gut dysbiosis might contribute to immune dysfunction and a pro-inflammatory environment in CTCL [110].

In a follow-up study, Nguyen et al. [111] extended their analyses of the gut microbiome to assess shifts introduced by UVB therapy. Using 16S sequencing, the study included 21 CTCL patients (primarily MF; unreported disease stage), of whom 13 received UVB therapy, as well as healthy controls. While the authors recapitulated non-affected diversity metrices in CTCL patients, UVB treatment did induce significant reduction of α- and β-diversity compared to healthy controls. Interestingly, microbial diversity did not differ between UVB responders and non-responders as assessed by mSWAT, neither pre- nor post-treatment. Nonetheless, certain taxa stratified responders and non-responders, albeit not significant after multiple comparison adjustments: *Sutterellaceae* trended higher in non-responders, while *Eggerthellaceae* and *Erysipelotrichaceae* trended higher in responders. Post-treatment, *Lachnospiraceae* trended higher in responders. As a biological explanation, the authors suggest that *Eggerthellaceae* exerts anti-inflammatory properties, potentially enhancing the efficacy of UVB therapy. Additionally, *Lachnospiraceae* produces short-chain fatty acid butyrate, which inhibits histone deacetylase, mimicking the mode of action of approved CTCL treatments like vorinostat

and romidepsin. Conversely, *Sutterellaceae* has pro-inflammatory properties and has been implicated in other inflammatory conditions, such as AD and ulcerative colitis. Last, functional analyses revealed increased inositol degradation pathways in CTCL-associated microbiota, suggesting modulation of T-cell activity via PI3K signalling [111].

Nasal focused Microbiome Studies

In addition to investigating the skin and gut microbiome of CTCL, Hooper et al. (2022/Nasal-Study) [112], conducted a study on the nasal microbiome in 45 CTCL patients (40 with MF and 5 with SS) with early (n = 26) and advanced stage (n = 19), as well as healthy controls. Using 16S sequencing, they found that α-diversity did not differ between CTCL patients and controls, β-diversity revealed distinct community structure sifts. While *S. aureus* and *S. epidermidis* where unchanged, several non-staphylococcal genera including *Roseomonas*, *Vibrio*, *Acinetobacter*, *Catenococcus*, and *Paracoccus* were significantly enriched in CTCL patients. Conversely, *Lachnospiraceae* NK4A136 group was reduced in CTCL patients. Notably, some enriched genera correlated positively with higher skin disease burden (i.e., mSWAT), whereas other enriched genera correlated negatively. Further, *Vibrio* abundance stratified patients into high and low mSWAT, as well as early- and late-stage disease. However, the mechanisms by which these genera exacerbate disease remain unclear, although some have been linked to AD, skin, and soft tissue infection [112]. Given the established role of S. aureus in mediating CTCL pathogenesis [59], and the lack of observed differences in *S. aureus* abundance in the studies by Hooper et al. [109,112] and others [112], the authors propose that *S. aureus* pathogenicity may result from a loss of regulatory control by commensal microbiota due to a global microbiome shift [112].

Introduction

Summary of findings

The collective findings from CTCL microbiome studies across skin, gut, and nasal microbiomes highlight microbial dysbiosis and its potential role in disease progression and immune dysregulation.

In the skin, no changes could be observed in α- and β-diversity [105–109], though a trend toward microbiome destabilization on CTCL lesions [105,106] can be surmised. Symptoms severity and CTCL lesions were associated with increased abundance of *C. simulans B. safensis*, and *Staphylococci*, and decreased abundance of *C. acnes*, S*. capitis* and *S. warneri* [106–109]. UVB therapy response was linked to alterations of several *Staphylococci*, including decrease of *S. aureus* [109]. Notably, *B. safensis* was mechanistically implicated in CTCL exacerbation by inducing T-cell proliferation and inflammation [107].

In the gut, CTCL patients exhibited lower microbial diversity in advanced stages, with reductions immune-regulating taxa (e.g., *Lactobacillaceae*, *Eggerthellaceae*), resembling AD-like dysbiosis [110]. UVB therapy further altered gut microbiota, with *Eggerthellaceae* and *Lachnospiraceae* enriched in UVB responders, potentially enhancing treatment efficacy through histone deacetylase inhibition [111].

The nasal microbiome showed distinct shifts, with *Roseomonas*, *Vibrio*, and *Acinetobacter* enriched in CTCL and *Vibrio* abundance stratifying patients by disease severity [112]. Despite the known role of *S. aureus* in CTCL pathogenesis, its abundance remained unchanged, suggesting pathogenicity may stem from a loss of microbiome balance rather than overgrowth [112].

Together, these studies suggest that CTCL-associated microbiome changes across multiple body sites may contribute to chronic immune stimulation, inflammation, and disease progression, with potential therapeutic implications for microbiome-targeted interventions.

1.4 Pathogenicity of *Staphylococcus aureus*

As a commensal of the skin, nasopharynx, and gastrointestinal tract, *S. aureus* is a common member of the human microbiome in homeostatic conditions [116]. However, under non-steady states, *S. aureus* is among the most frequent opportunistic pathogens, causing approximately $14 billion in health-care costs and 20,000 deaths annually in the United States [117]. It employs a broad array of virulence factors to establish infection, evade host immunity, and drive disease progression, particularly in the skin [117,118].

S. aureus disposes of several toxins that damage host cells through the formation of pores in the cytoplasmatic membrane [118,119].

Among them, α-toxin (also called α-hemolysin) is arguably the most infamous, targeting keratinocytes, erythrocytes, and leukocytes by binding to A Disintegrin and Metalloprotease 10 (ADAM10), a receptor widely expressed across human tissues. This interaction triggers inflammatory signalling and pyroptosis, leading to dermonecrosis and enhanced bacterial dissemination in skin infections [117,119].

The leukocidins are a class of bicompartment pore-forming toxins that include Panton-Valentine leucocidin (PVL), γ-toxin (also called γ-hemolysin) as well as the leukotoxins (Luk) LukAB and LukED [119]. These toxins bind distinct host receptors, with PVL and LukED targeting chemokine and complement receptors, while LukAB interacts with integrins [118,119]. This receptor specificity dictates cell-type and species specificity, with all *S. aureus* strains producing at least three leukocidins, while highly virulent strains can secrete five or more [119]. Interestingly, only 2-3% of *S. aureus* strains produce PVL, which is predominantly associated with clinical Methicillin-resistant *S. aureus* (MRSA) isolates and lung infection. However, its contribution to skin infections remains controversial [119]. While leukocidins are highly cytotoxic to immune cells like neutrophils, sublytic concentrations can drive pro-inflammatory responses, exacerbating chronic infection and immune dysregulation [117–119].

Phenol-soluble modulins (PSMs) are amphipathic, α-helical peptides secreted by S. aureus, playing a key role in immune evasion and inflammation. They are classified into α-type (highly cytolytic) and β-type (less cytolytic) [117]. Unlike pore-forming toxins, PSMs lyse host cells in a receptor-independent, detergent-like manner, with high cytolytic activity against neutrophils, particularly after phagocytosis, facilitating immune escape.

At sublytic concentrations, PSMs strongly stimulate keratinocytes, amplifying inflammation in skin infections [119]. Additionally, δ-toxin, a member of the PSM family, promotes Treg priming, which may contribute to immune tolerance and chronic infection [120].

Another mechanism to evade the hosts immune system is mediated by staphylococcal protein A (SpA), a multifunctional surface protein that disrupts both innate and adaptive immune responses. SpA binds to the Fcγ portion of Immunoglobulin G (IgG) in an anti-opsonic manner, preventing opsonization and phagocytosis by neutrophils [118]. Additionally, SpA acts as a B-cell superantigen, driving clonal expansion followed by apoptosis, thereby impairing adaptive immunity [116]. Beyond immune evasion, SpA SpA induces proinflammatory signaling by binding to TNF receptor 1 (TNFR1), triggering MAPK activation and upregulation of inflammatory cytokines, including IL-8, which enhances neutrophil recruitment [118]. In keratinocytes, SpA-mediated TNFR1 activation induces NF-κB signalling, promoting skin inflammation [121]. This mechanism has been validated in murine infection models, where TNFR1 knockout led to reduced bacterial virulence and systemic inflammation, underscoring SpA's role as a key driver of S. aureus pathogenicity [122].

To evade antimicrobial peptides (AMPs), a component of the innate immune system to control microbial growth [123], *S. aureus* employs multiple strategies. For instance, iron-regulated surface determinant protein A (isdA) enhances bacterial surface hydrophobicity, decreasing binding efficacy of AMPs β-Defensin 2 and cathelicidin (LL-37) [124]. The metalloprotease aureolysin, primarily involved in nutrient acquisition, also inhibits host immune responses by cleaving complement C3 [119] and degrading cathelicidin, β-Defensin 3, and Dermcidin [124,125]. Additionally, staphylokinase neutralizes α-defensins, abolishing their antimicrobial activity and further impairing host defense [125]. More AMP evading mechanisms are summarized in reviews [124] and [125].

1.5 Workflow of Microbiome Research

Microbiome sequencing has revolutionized microbial research by enabling the comprehensive analysis of microbial communities without the need for cultivation. Traditional culture-based methods, while historically fundamental to microbiology, are inherently limited by their inability to grow many microorganisms under standard laboratory conditions. A significant proportion of microbes, particularly those inhabiting complex environments such as the skin, remain unculturable, making it difficult to assess their diversity and functional potential. Sequencing-based approaches overcome this limitation by directly analysing microbial DNA, allowing for the identification of both culturable and unculturable organisms. In addition, sequencing provides a higher sensitivity for detecting low-abundance species that might otherwise be outcompeted in culture. Furthermore, microbiome sequencing techniques facilitate comprehensive taxonomic and functional characterization of microbial communities, and that simultaneously in bacteria, archaea, fungi, and viruses [126,127].

There are two primary sequencing strategies commonly used in microbiome research: amplicon – or marker gene - sequencing and whole metagenome shotgun sequencing (WMS). Amplicon sequencing targets highly variable regions within conserved motifs of ribosomal RNA for taxonomic classification of bacteria and archaea (16S rRNA) and fungi (internal transcribed spacer; ITS rRNA) [128]. This method is cost-effective and computationally less demanding, making it a practical choice for large-scale microbial community profiling. However, its resolution is limited, as it typically provides taxonomic classification at the genus level without distinguishing between species or strains. Additionally, biases arise from the selection of specific 16S or ITS variable regions, potentially skewing the representation of certain taxa [129,130].

By contrast, WMS provides a more comprehensive and less biased view of the microbiome by sequencing all genetic material in a sample. This approach enables the simultaneous classification of bacteria, archaea, fungi, and viruses down to the species- and strain-level. Additionally, WMS facilitates the identification of functional genes, allowing the reconstruction of metabolic pathways, virulence factors, and antibiotic resistance profiles [131]. However, WMS requires significantly deeper sequencing, more input DNA, and greater laboratory effort than amplicon-based techniques [127,129].

Introduction

Whole metagenomic profiling is a multi-step workflow depicted in Figure 4. Beginning with sample collection and microbial DNA extraction, which must be carefully standardized to minimize contamination and preserve microbial integrity. Sample collection should strive to increase microbial DNA while minimizing host DNA collection, as a higher microbial fraction increases sequencing depth for microbial genes [131]. Extraction of DNA involves multiple thermal, mechanical, chemical, and enzymatical steps to lyse the different cell walls from the diverse microbial species present in the sample [132]. Extracted DNA is then fragmented into smaller pieces (thus the naming "shotgun" sequencing) and ligated with sets of adapters and barcodes to form a sequencing library. Libraries of multiple samples are pooled and sequenced simultaneously on high throughput machines at read lengths of of 150 to 300 nucleotides paired-end [131]. After metagenomic data has been obtained, *in silico* processing starts with removal of host DNA, which has been naturally collected during the sampling process. Reconstruction of the microbial community composition and its functional properties can then be achieved with two different approach classes: Assembly-based and read-based profiling [129].

The former describes the *de novo* assembly of metagenomic reads into single microbial genomes of each species present in the sample, so called metagenomic assembled genomes (MAGs). MAGs are annotated to databases of known bacterial genomes and their functional properties. In conversion, unknown MAGs represent candidate phyla and species that have no cultured representative, which is an indispensable method to uncover microbial diversity. However, metagenome assembly comes with unique challenges: The coverage of each species' genome is dependent on its abundance in the sample and thus varies significantly. Further, multiple strains from the same bacterial species may be present, differing in small or big proportions of their genome. These facts often result in incomplete reconstructions, obscuring taxa from downstream analysis. Metagenomic-specific assemblers have been developed, but community consensus on best practice is lacking [129,131].

Read-based profiling assigns taxonomy and functional properties by comparing the unassembled DNA sequences against carefully curated databases [131]. For instance, MetaPhlAn provides a database with thousands of clade-specific marker genes to enable profiling down to the species level. Marker genes have been selected from virtually all

publicity available species pangenomes based on their discriminatory power [133,134]. Limitations of this method include the prior identification and sequencing of species. However, the number of available reference genomes is rapidly increasing, and certain habitats such as the human gut is considered to be very well characterized [131].

Resulting outputs are data matrices of samples versus microbial features like taxa, resistance or virulence genes, or pathways. Downstream analyses include determination of microbial diversity and comparison between different groups of samples, as well as traditional multivariate statistics and data science methods such ordination (e.g., Principal Component Analysis), clustering, differential abundance analysis, and learning classification (e.g., random forest or support vector machines) [129,131].

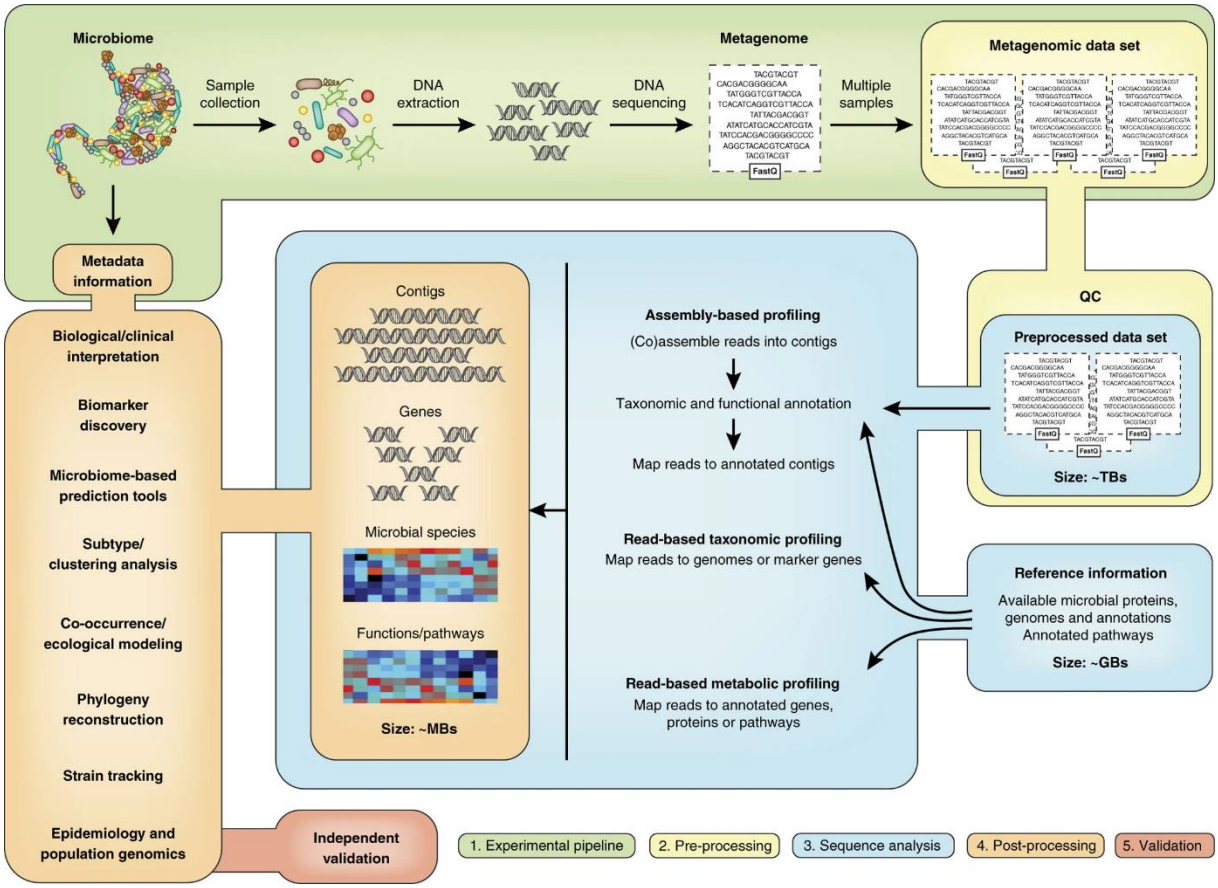

Figure 4: Overview of an archetypal Workflow in Whole Metagenomics Sequencing Analysis.
(1.) careful study design is crucial but often underestimated; (2.) computational pre-processing ensures data quality through adapter trimming, duplicate removal, and host DNA filtering; (3.) sequence analysis combines read-based and assembly-based approaches depending on the research goals; (4.) statistical post-processing enables interpretation of complex data; and (5.) validation is essential to confirm findings and reduce study-specific bias.
Adopted from: Quince, C., Walker, A.W., Simpson, J.T., Loman, N.J. & Segata, N. *Nat. Biotechnol.* 35, 833–844 (2017).

1.5.1 *Challenges of Human Skin Microbiome Research*

Despite its success, metagenomic sequencing presents several methodological and analytical challenges that complicate data interpretation and reproducibility.

First, microbiome datasets are high-dimensional, sparse, and compositional, meaning that changes in the observed abundance of one taxon inherently affect others. This compositionality complicates statistical analyses, as an increase in one microorganism's proportion forces a decrease in others, even if their absolute quantities remain unchanged. For example, a drug that selectively promotes the growth of a specific microbial genus may lead to an apparent decline in other taxa, despite no direct suppression [129].

Another major challenge is the inability of sequencing to differentiate between DNA from viable microbes and DNA from dead microbial cells [131]. This "live-dead-dilemma" is especially pertinent for skin microbiome, where DNA from lysed cells or extracellular sources could distort taxonomic and functional interpretations [135].

Additionally, unlike the gut microbiome, skin WMS samples are characterized by low microbial biomass and a disproportionately high fraction of host DNA, exceeding 90–95%. As a result, even high total read counts may yield limited microbial sequencing depth, potentially leading to underestimation of microbial diversity [51,131,136,137]. This constraint was illustrated in a benchmarking study using mock communities spiked with increasing levels of host DNA: when host DNA exceeded 90%, detection of low-abundance species significantly declined. This effect was further exacerbated when the total raw read number was reduced from 50 to 25 million reads per sample, resulting in the loss of up to 60% of very low-abundance species [137]. Nonetheless, several papers showed that WMS — even at shallow sequencing depths — offers clear advantages over 16S sequencing:

i. Unlike 16S, shallow WMS provides species-level taxonomic resolution, and correlates strongly with ultra-deep WMS species profiling (Spearman >0.99) [138,139].
ii. Shallow WMS also enables direct profiling of microbial functions, capturing genes and pathways that 16S-based inference methods (e.g., PICRUSt) miss [140].

Shallow WMS functional profiles yield spearman correlation of >0.97 compared to ultra-deep WMS [138,139].

iii. In addition, shallow WMS is less susceptible to technical variation, likely to biases introduced by library preparation artifacts, primer mismatches, and PCR amplification bias that affect 16S workflows [139,141].

To mitigate the inability to differentiate between live and dead cells as well as the challenge of low microbial biomass, complementary methods have been proposed. DNA-intercalating dyes can prevent amplification of DNA from membrane-compromised (i.e., dead) cells [142], while enzymatic pre-digestion can selectively remove DNA from dead microbial and/or living host cells before metagenomic sequencing [143,144]. However, these strategies remain imperfect, and no standardized approach has been universally adopted for skin microbiome research [145–147].

The integrity of microbiome analyses is also influenced by sample collection, DNA extraction, and storage conditions. Contamination can arise at all steps, emphasizing the need for standardized protocols. Given the low microbial load of skin samples, stringent controls are necessary, including positive controls (mock communities) to assess sequencing accuracy and negative controls to detect environmental contamination. Inconsistent handling across studies can lead to batch effects, reducing reproducibility [131,132].

A fundamental limitation of microbiome research is the difficulty in disentangling cause from effect. Observational metagenomic studies often reveal correlations between microbial taxa and disease, but they do not imply causality [148]. To confirm whether microbial changes drive disease progression or are merely a consequence of the disease state, longitudinal and experimental validation studies are needed [131].

Lastly, validation of microbiome biomarkers remains a significant hurdle. Disease-associated microbial signatures are often inconsistent across studies, likely due to differences in sequencing platforms, analytical pipelines, and cohort characteristics. Cross-study validation and standardized methodologies are essential to improve biomarker reproducibility and ensure clinical applicability [131].

1.6 Aim of this thesis

Mycosis fungoides is characterized by marked clinical and molecular heterogeneity. While emerging evidence suggests a role for the skin microbiome in disease progression, microbial dysbiosis remains to be firmly established, and its influence on host signalling and clinical outcomes is still poorly understood. This thesis aims to comprehensively explore the microbiome's role in MF through bioinformatic analyses, complemented by molecular and functional microbiology approaches. Specifically, the objectives are:

1. Review relevant transcriptomic and microbiome studies in MF to explore potential links between microbial composition and transcriptional heterogeneity.
2. Taxonomically characterize the MF skin microbiome using whole metagenome shotgun (WMS) sequencing across patch, plaque, and nonlesional skin, with comparison of diversity metrics and differential abundance.
3. Identify prognostic microbiome biomarkers capable of stratifying MF patients into clinically distinct subgroups based on microbiome composition alone.
4. Explore drivers of microbial shifts by measuring expression of host cutaneous antimicrobial peptides (AMPs) and determine resistance profiles of clinical MF skin isolates.
5. Characterize the pathogenic potential of the MF skin microbiome by screening WMS data for virulence genes. Clinical MF skin isolates, particularly *S. aureus*, will be further profiled for the WMS-identified virulence factor SpA.
6. Evaluate microbiome-mediated modulation of host TCR repertoires by analysing TCR diversity and epitope-binding predictions across skin and blood compartments.
7. Bioinformatically integrate metagenomic and transcriptomic data to investigate:
    a) Whether differential microbial colonization contributes to transcriptional heterogeneity in MF.e
    b) Whether *S. aureus* and SpA modulate host signalling pathways, including the TNFR–NF-κB axis.
8. Explore potential viral contributions to MF aetiopathogenesis by mining metagenomic and transcriptomic data for early virome signatures.

1.7 References of Introduction

1. Willemze, R.; Cerroni, L.; Kempf, W.; Berti, E.; Facchetti, F.; Swerdlow, S.H.; Jaffe, E.S. The 2018 Update of the WHO-EORTC Classification for Primary Cutaneous Lymphomas. *Blood* **2019**, *133*, 1703–1714, doi:10.1182/blood-2018-11-881268.
2. Ho, A.W.; Kupper, T.S. T Cells and the Skin: From Protective Immunity to Inflammatory Skin Disorders. *Nat. Rev. Immunol.* **2019**, *19*, 490–502, doi:10.1038/s41577-019-0162-3.
3. Dummer, R.; Vermeer, M.H.; Scarisbrick, J.J.; Kim, Y.H.; Stonesifer, C.; Tensen, C.P.; Geskin, L.J.; Quaglino, P.; Ramelyte, E. Cutaneous T Cell Lymphoma. *Nat. Rev. Dis. Prim.* **2021**, *7*, 61, doi:10.1038/s41572-021-00296-9.
4. Hwang, S.T.; Janik, J.E.; Jaffe, E.S.; Wilson, W.H. Mycosis Fungoides and Sézary Syndrome. *Lancet* **2008**, *371*, 945–957, doi:10.1016/S0140-6736(08)60420-1.
5. Bradford, P.T.; Devesa, S.S.; Anderson, W.F.; Toro, J.R. Cutaneous Lymphoma Incidence Patterns in the United States: A Population-Based Study of 3884 Cases. *Blood* **2009**, *113*, 5064–5073, doi:10.1182/blood-2008-10-184168.
6. Dobos, G.; de Masson, A.; Ram-Wolff, C.; Beylot-Barry, M.; Pham-Ledard, A.; Ortonne, N.; Ingen-Housz-Oro, S.; Battistella, M.; D'Incan, M.; Rouanet, J.; et al. Epidemiological Changes in Cutaneous Lymphomas: An Analysis of 8593 Patients from the French Cutaneous Lymphoma Registry*. *Br. J. Dermatol.* **2021**, *184*, 1059–1067, doi:10.1111/bjd.19644.
7. Scarisbrick, J.J.; Quaglino, P.; Prince, H.M.; Papadavid, E.; Hodak, E.; Bagot, M.; Servitje, O.; Berti, E.; Ortiz-Romero, P.; Stadler, R.; et al. The PROCLIPI International Registry of Early-stage Mycosis Fungoides Identifies Substantial Diagnostic Delay in Most Patients. *Br. J. Dermatol.* **2019**, *181*, 350–357, doi:10.1111/bjd.17258.
8. Campbell, J.J.; Clark, R.A.; Watanabe, R.; Kupper, T.S. Sézary Syndrome and Mycosis Fungoides Arise from Distinct T-Cell Subsets: A Biologic Rationale for Their Distinct Clinical Behaviors. *Blood* **2010**, *116*, 767–771, doi:10.1182/blood-2009-11-251926.
9. Hristov, A.C.; Tejasvi, T.; Wilcox, R.A. Cutaneous T-cell Lymphomas: 2023 Update on Diagnosis, Risk-stratification, and Management. *Am. J. Hematol.* **2023**, *98*, 193–209,

doi:10.1002/ajh.26760.

10. Willemze, R.; J. L. M. Meijer, C. Classification of Cutaneous T-cell Lymphoma: From Alibert to WHO-EORTC. *J. Cutan. Pathol.* **2006**, *33*, 18–26, doi:10.1111/j.0303-6987.2006.00494.x.

11. Nabil Nagshabandi, K.; Shadid, A.; Shadid, A.; Almuhanna, N.K. CD4/CD8 Double-Negative Mycosis Fungoides: A Review. *Dermatology Reports* **2024**, 247–250, doi:10.4081/dr.2024.9908.

12. Scarisbrick, J. Staging of Mycosis Fungoides and Sézary Syndrome : Time for an Update ? *Emj Eur. Med. J.* **2018**, 92–100.

13. Kempf, W.; Zimmermann, A.; Mitteldorf, C. Cutaneous Lymphomas—An Update 2019. *Hematol. Oncol.* **2019**, *37*, 43–47, doi:10.1002/hon.2584.

14. Ahn, C.S.; ALSayyah, A.; Sangüeza, O.P. Mycosis Fungoides: An Updated Review of Clinicopathologic Variants. *Am. J. Dermatopathol.* **2014**, *36*, 933–951, doi:10.1097/DAD.0000000000000207.

15. Olsen, E.A.; Whittaker, S.; Kim, Y.H.; Duvic, M.; Prince, H.M.; Lessin, S.R.; Wood, G.S.; Willemze, R.; Demierre, M.-F.; Pimpinelli, N.; et al. Clinical End Points and Response Criteria in Mycosis Fungoides and Sézary Syndrome: A Consensus Statement of the International Society for Cutaneous Lymphomas, the United States Cutaneous Lymphoma Consortium, and the Cutaneous Lymphoma Task Force of the E. *J. Clin. Oncol.* **2011**, *29*, 2598–2607, doi:10.1200/JCO.2010.32.0630.

16. Olsen, E.; Vonderheid, E.; Pimpinelli, N.; Willemze, R.; Kim, Y.; Knobler, R.; Zackheim, H.; Duvic, M.; Estrach, T.; Lamberg, S.; et al. Revisions to the Staging and Classification of Mycosis Fungoides and Sezary Syndrome: A Proposal of the International Society for Cutaneous Lymphomas (ISCL) and the Cutaneous Lymphoma Task Force of the European Organization of Research and Treatment of Ca. *Blood* **2007**, *110*, 1713–1722, doi:10.1182/blood-2007-03-055749.

17. Agar, N.S.; Wedgeworth, E.; Crichton, S.; Mitchell, T.J.; Cox, M.; Ferreira, S.; Robson, A.; Calonje, E.; Stefanato, C.M.; Wain, E.M.; et al. Survival Outcomes and Prognostic Factors in Mycosis Fungoides/Sézary Syndrome: Validation of the Revised International Society for Cutaneous Lymphomas/European Organisation for

Research and Treatment of Cancer Staging Proposal. *J. Clin. Oncol.* **2010**, *28*, 4730–4739, doi:10.1200/JCO.2009.27.7665.

18. Scarisbrick, J.J.; Kim, Y.H.; Whittaker, S.J.; Wood, G.S.; Vermeer, M.H.; Prince, H.M.; Quaglino, P. Prognostic Factors, Prognostic Indices and Staging in Mycosis Fungoides and Sézary Syndrome: Where Are We Now? *Br. J. Dermatol.* **2014**, *170*, 1226–1236, doi:10.1111/bjd.12909.

19. Whittaker, S.; Hoppe, R.; Prince, H.M. How I Treat Mycosis Fungoides and Sezary Syndrome. *Blood* **2016**, *127*, 3142–3153, doi:10.1182/blood-2015-12-611830.

20. Dippel, E.; Assaf, C.; Becker, J.C.; von Bergwelt-Baildon, M.; Bernreiter, S.; Cozzio, A.; Eich, H.T.; Elsayad, K.; Follmann, M.; Grabbe, S.; et al. S2k-Guidelines – Cutaneous Lymphomas (ICD10 C82 - C86): Update 2021. *JDDG J. der Dtsch. Dermatologischen Gesellschaft* **2022**, *20*, 537–554, doi:10.1111/ddg.14706.

21. Stadler, R.; Scarisbrick, J.J. Maintenance Therapy in Patients with Mycosis Fungoides or Sézary Syndrome: A Neglected Topic. *Eur. J. Cancer* **2021**, *142*, 38–47, doi:10.1016/j.ejca.2020.10.007.

22. de Masson, A.; Beylot-Barry, M.; Ram-Wolff, C.; Mear, J.-B.; Dalle, S.; D'Incan, M.; Ingen-Housz-Oro, S.; Orvain, C.; Abraham, J.; Dereure, O.; et al. Allogeneic Transplantation in Advanced Cutaneous T-Cell Lymphomas (CUTALLO): A Propensity Score Matched Controlled Prospective Study. *Lancet* **2023**, *401*, 1941–1950, doi:10.1016/S0140-6736(23)00329-X.

23. Licht, P.; Mailänder, V. Multi-Omic Data Integration Suggests Putative Microbial Drivers of Aetiopathogenesis in Mycosis Fungoides. *Cancers (Basel).* **2024**, *16*, 3947, doi:10.3390/cancers16233947.

24. Smith-Garvin, J.E.; Koretzky, G.A.; Jordan, M.S. T Cell Activation. *Annu. Rev. Immunol.* **2009**, *27*, 591–619, doi:10.1146/annurev.immunol.021908.132706.

25. Curtsinger, J.M.; Mescher, M.F. Inflammatory Cytokines as a Third Signal for T Cell Activation. *Curr. Opin. Immunol.* **2010**, *22*, 333–340, doi:10.1016/j.coi.2010.02.013.

26. Santarlasci, V.; Cosmi, L.; Maggi, L.; Liotta, F.; Annunziato, F. IL-1 and T Helper Immune Responses. *Front. Immunol.* **2013**, *4*, doi:10.3389/fimmu.2013.00182.

27. Wilcox, R.A. A Three-Signal Model of T-Cell Lymphoma Pathogenesis. *Am. J. Hematol.* **2016**, *91*, 113–122, doi:10.1002/ajh.24203.

28. Patil, K.; Kuttikrishnan, S.; Khan, A.Q.; Ahmad, F.; Alam, M.; Buddenkotte, J.; Ahmad, A.; Steinhoff, M.; Uddin, S. Molecular Pathogenesis of Cutaneous T Cell Lymphoma: Role of Chemokines, Cytokines, and Dysregulated Signaling Pathways. *Semin. Cancer Biol.* **2022**, *86*, 382–399, doi:10.1016/j.semcancer.2021.12.003.

29. Damsky, W.E.; Choi, J. Genetics of Cutaneous T Cell Lymphoma: From Bench to Bedside. *Curr. Treat. Options Oncol.* **2016**, *17*, 33, doi:10.1007/s11864-016-0410-8.

30. García-Díaz, N.; Piris, M.Á.; Ortiz-Romero, P.L.; Vaqué, J.P. Mycosis Fungoides and Sézary Syndrome: An Integrative Review of the Pathophysiology, Molecular Drivers, and Targeted Therapy. *Cancers (Basel).* **2021**, *13*, 1931, doi:10.3390/cancers13081931.

31. Litvinov, I. V.; Tetzlaff, M.T.; Thibault, P.; Gangar, P.; Moreau, L.; Watters, A.K.; Netchiporouk, E.; Pehr, K.; Prieto, V.G.; Rahme, E.; et al. Gene Expression Analysis in Cutaneous T-Cell Lymphomas (CTCL) Highlights Disease Heterogeneity and Potential Diagnostic and Prognostic Indicators. *Oncoimmunology* **2017**, *6*, e1306618, doi:10.1080/2162402X.2017.1306618.

32. Rassek, K.; Iżykowska, K. Single-Cell Heterogeneity of Cutaneous T-Cell Lymphomas Revealed Using RNA-Seq Technologies. *Cancers (Basel).* **2020**, *12*, 2129, doi:10.3390/cancers12082129.

33. Buus, T.B.; Willerslev-Olsen, A.; Fredholm, S.; Blümel, E.; Nastasi, C.; Gluud, M.; Hu, T.; Lindahl, L.M.; Iversen, L.; Fogh, H.; et al. Single-Cell Heterogeneity in Sézary Syndrome. *Blood Adv.* **2018**, *2*, 2115–2126, doi:10.1182/bloodadvances.2018022608.

34. Iyer, A.; Hennessey, D.; O'Keefe, S.; Patterson, J.; Wang, W.; Wong, G.K.-S.; Gniadecki, R. Skin Colonization by Circulating Neoplastic Clones in Cutaneous T-Cell Lymphoma. *Blood* **2019**, *134*, 1517–1527, doi:10.1182/blood.2019002516.

35. Hamrouni, A.; Fogh, H.; Zak, Z.; Ødum, N.; Gniadecki, R. Clonotypic Diversity of the T-Cell Receptor Corroborates the Immature Precursor Origin of Cutaneous T-Cell Lymphoma. *Clin. Cancer Res.* **2019**, *25*, 3104–3114, doi:10.1158/1078-0432.CCR-18-4099.

36. Iyer, A.; Hennessey, D.; O'Keefe, S.; Patterson, J.; Wang, W.; Salopek, T.; Wong, G.K.-S.; Gniadecki, R. Clonotypic Heterogeneity in Cutaneous T-Cell Lymphoma (Mycosis Fungoides) Revealed by Comprehensive Whole-Exome Sequencing. *Blood Adv.* **2019**, *3*, 1175–1184, doi:10.1182/bloodadvances.2018027482.

37. Iyer, A.; Hennessey, D.; O'Keefe, S.; Patterson, J.; Wang, W.; Wong, G.K.-S.; Gniadecki, R. Branched Evolution and Genomic Intratumor Heterogeneity in the Pathogenesis of Cutaneous T-Cell Lymphoma. *Blood Adv.* **2020**, *4*, 2489–2500, doi:10.1182/bloodadvances.2020001441.

38. Ren, J.; Qu, R.; Rahman, N.-T.; Lewis, J.M.; King, A.L.O.; Liao, X.; Mirza, F.N.; Carlson, K.R.; Huang, Y.; Gigante, S.; et al. Integrated Transcriptome and Trajectory Analysis of Cutaneous T-Cell Lymphoma Identifies Putative Precancer Populations. *Blood Adv.* **2022**, doi:10.1182/bloodadvances.2022008168.

39. Ghazawi, F.M.; Alghazawi, N.; Le, M.; Netchiporouk, E.; Glassman, S.J.; Sasseville, D.; Litvinov, I. V. Environmental and Other Extrinsic Risk Factors Contributing to the Pathogenesis of Cutaneous T Cell Lymphoma (CTCL). *Front. Oncol.* **2019**, *9*, 1–8, doi:10.3389/fonc.2019.00300.

40. Mesri, E.A.; Feitelson, M.A.; Munger, K. Human Viral Oncogenesis: A Cancer Hallmarks Analysis. *Cell Host Microbe* **2014**, *15*, 266–282, doi:10.1016/j.chom.2014.02.011.

41. Blyth, K.; Cameron, E.R.; Neil, J.C. The Runx Genes: Gain or Loss of Function in Canacer. *Nat. Rev. Cancer* **2005**, *5*, 376–387, doi:10.1038/nrc1607.

42. Väkevä, L.; Ranki, A.; Pukkala, E. Increased Risk of Secondary Cancers in Patients with Primary Cutaneous T Cell Lymphoma. *J. Invest. Dermatol.* **2000**, *115*, 62–65, doi:10.1046/j.1523-1747.2000.00011.x.

43. Kantor, A.F.; Curtis, R.E.; Vonderheid, E.C.; van Scott, E.J.; Fraumeni, J.F. Risk of Second Malignancy after Cutaneous T-Cell Lymphoma. *Cancer* **1989**, *63*, 1612–1615, doi:10.1002/1097-0142(19890415)63:8<1612::AID-CNCR2820630828>3.0.CO;2-C.

44. Amber, K.T.; Bloom, R.; Nouri, K. Second Primary Malignancies in CTCL Patients from 1992 to 2011: A SEER-Based, Population-Based Study Evaluating Time from

CTCL Diagnosis, Age, Sex, Stage, and CD30+ Subtype. *Am. J. Clin. Dermatol.* **2016**, *17*, 71–77, doi:10.1007/s40257-015-0155-3.

45. Brownell, I.; Etzel, C.J.; Yang, D.J.; Taylor, S.H.; Duvic, M. Increased Malignancy Risk in the Cutaneous T-Cell Lymphoma Patient Population. *Clin. Lymphoma Myeloma* **2008**, *8*, 100–105, doi:10.3816/CLM.2008.n.011.

46. Davis, T.H.; Morton, C.C.; Miller-Cassman, R.; Balk, S.P.; Kadin, M.E. Hodgkin's Disease, Lymphomatoid Papulosis, and Cutaneous T-Cell Lymphoma Derived from a Common T-Cell Clone. *N. Engl. J. Med.* **1992**, *326*, 1115–1122, doi:10.1056/NEJM199204233261704.

47. Wood, G.S.; Crooks, C.F.; Uluer, A.Z. Lymphomatoid Papulosis and Associated Cutaneous Lymphoproliferative Disorders Exhibit a Common Clonal Origin. *J. Invest. Dermatol.* **1995**, *105*, 51–55, doi:10.1111/1523-1747.ep12312548.

48. Steinhoff, M. Cutaneous T Cell Lymphoma and Classic Hodgkin Lymphoma of the B Cell Type within a Single Lymph Node: Composite Lymphoma. *J. Clin. Pathol.* **2004**, *57*, 329–331, doi:10.1136/jcp.2003.011882.

49. Mirvish, J.J.; Pomerantz, R.G.; Falo, L.D.; Geskin, L.J. Role of Infectious Agents in Cutaneous T-Cell Lymphoma: Facts and Controversies. *Clin. Dermatol.* **2013**, *31*, 423–431, doi:10.1016/j.clindermatol.2013.01.009.

50. TAN, R.S.-H.; BUTTERWORTH, C.M.; McLAUGHLIN, H.; MALKA, S.; SAMMAN, P.D. Mycosis Fungoides—a Disease of Antigen Persistence. *Br. J. Dermatol.* **1974**, *91*, 607–616, doi:10.1111/j.1365-2133.1974.tb12449.x.

51. Byrd, A.L.; Belkaid, Y.; Segre, J.A. The Human Skin Microbiome. *Nat. Rev. Microbiol.* **2018**, *16*, 143–155, doi:10.1038/nrmicro.2017.157.

52. Mirvish, E.D.; Pomerantz, R.G.; Geskin, L.J. Infectious Agents in Cutaneous T-Cell Lymphoma. *J. Am. Acad. Dermatol.* **2011**, *64*, 423–431, doi:10.1016/j.jaad.2009.11.692.

53. Ravat, F.E.; Spittle, M.F.; Russell-Jones, R. Primary Cutaneous T-Cell Lymphoma Occurring after Organ Transplantation. *J. Am. Acad. Dermatol.* **2006**, *54*, 668–675, doi:10.1016/j.jaad.2005.10.015.

54. Axelrod, P.I.; Lorber, B.; Vonderheid, E.C. Infections Complicating Mycosis Fungoides and Sézary Syndrome. *JAMA J. Am. Med. Assoc.* **1992**, *267*, 1354, doi:10.1001/jama.1992.03480100060031.

55. Willerslev-Olsen, A.; Krejsgaard, T.; Lindahl, L.; Bonefeld, C.; Wasik, M.; Koralov, S.; Geisler, C.; Kilian, M.; Iversen, L.; Woetmann, A.; et al. Bacterial Toxins Fuel Disease Progression in Cutaneous T-Cell Lymphoma. *Toxins (Basel).* **2013**, *5*, 1402–1421, doi:10.3390/toxins5081402.

56. Linnemann, T.; Gellrich, S.; Lukowsky, A.; Mielke, A.; Audring, H.; Sterry, W.; Walden, P. Polyclonal Expansion of T Cells with the TCR Vbeta Type of the Tumour Cell in Lesions of Cutaneous T-Cell Lymphoma: Evidence for Possible Superantigen Involvement. *Br. J. Dermatol.* **2004**, *150*, 1013–1017, doi:10.1111/j.1365-2133.2004.05970.x.

57. Vonderheid, E.C.; Boselli, C.M.; Conroy, M.; Casaus, L.; Espinoza, L.C.; Venkataramani, P.; Bigler, R.D.; Steve Hou, J. Evidence for Restricted Vβ Usage in the Leukemic Phase of Cutaneous T Cell Lymphoma. *J. Invest. Dermatol.* **2005**, *124*, 651–661, doi:10.1111/j.0022-202X.2004.23586.x.

58. Macias, E.S.; Pereira, F.A.; Rietkerk, W.; Safai, B. Superantigens in Dermatology. *J. Am. Acad. Dermatol.* **2011**, *64*, 455–472, doi:10.1016/j.jaad.2010.03.044.

59. Fujii, K. Pathogenesis of Cutaneous T Cell Lymphoma: Involvement of Staphylococcus Aureus. *J. Dermatol.* **2022**, *49*, 202–209, doi:10.1111/1346-8138.16288.

60. Łyko, M.; Jankowska-Konsur, A. The Skin Microbiome in Cutaneous T-Cell Lymphomas (CTCL)—A Narrative Review. *Pathogens* **2022**, *11*, 935, doi:10.3390/pathogens11080935.

61. Fanok, M.H.; Sun, A.; Fogli, L.K.; Narendran, V.; Eckstein, M.; Kannan, K.; Dolgalev, I.; Lazaris, C.; Heguy, A.; Laird, M.E.; et al. Role of Dysregulated Cytokine Signaling and Bacterial Triggers in the Pathogenesis of Cutaneous T-Cell Lymphoma. *J. Invest. Dermatol.* **2018**, *138*, 1116–1125, doi:10.1016/j.jid.2017.10.028.

62. Dréno, B.; Araviiskaia, E.; Berardesca, E.; Gontijo, G.; Sanchez Viera, M.; Xiang, L.F.;

Martin, R.; Bieber, T. Microbiome in Healthy Skin, Update for Dermatologists. *J. Eur. Acad. Dermatology Venereol.* **2016**, *30*, 2038–2047, doi:10.1111/jdv.13965.

63. Lederberg, J.; McCray, A.T. Ome Sweet 'Omics– A Genealogical Treasury of Words. *Sci.* **2001**.

64. Probst, A.J.; Auerbach, A.K.; Moissl-Eichinger, C. Archaea on Human Skin. *PLoS One* **2013**, *8*, e65388, doi:10.1371/journal.pone.0065388.

65. Moissl-Eichinger, C.; Probst, A.J.; Birarda, G.; Auerbach, A.; Koskinen, K.; Wolf, P.; Holman, H.-Y.N. Human Age and Skin Physiology Shape Diversity and Abundance of Archaea on Skin. *Sci. Rep.* **2017**, *7*, 4039, doi:10.1038/s41598-017-04197-4.

66. Oh, J.; Byrd, A.L.; Park, M.; Kong, H.H.; Segre, J.A. Temporal Stability of the Human Skin Microbiome. *Cell* **2016**, *165*, 854–866, doi:10.1016/j.cell.2016.04.008.

67. Belkaid, Y.; Segre, J.A. Dialogue between Skin Microbiota and Immunity. *Science (80-.).* **2014**, *346*, 954–959, doi:10.1126/science.1260144.

68. Belkaid, Y.; Tamoutounour, S. The Influence of Skin Microorganisms on Cutaneous Immunity. *Nat. Rev. Immunol.* **2016**, *16*, 353–366, doi:10.1038/nri.2016.48.

69. Garlanda, C.; Dinarello, C.A.; Mantovani, A. The Interleukin-1 Family: Back to the Future. *Immunity* **2013**, *39*, 1003–1018, doi:10.1016/j.immuni.2013.11.010.

70. Byrd, A.L.; Deming, C.; Cassidy, S.K.B.; Harrison, O.J.; Ng, W.-I.; Conlan, S.; Belkaid, Y.; Segre, J.A.; Kong, H.H. Staphylococcus Aureus and Staphylococcus Epidermidis Strain Diversity Underlying Pediatric Atopic Dermatitis. *Sci. Transl. Med.* **2017**, *9*, eaal4651, doi:10.1126/scitranslmed.aal4651.

71. Carmona-Cruz, S.; Orozco-Covarrubias, L.; Sáez-de-Ocariz, M. The Human Skin Microbiome in Selected Cutaneous Diseases. *Front. Cell. Infect. Microbiol.* **2022**, *12*, 1–9, doi:10.3389/fcimb.2022.834135.

72. Nakatsuji, T.; Hata, T.R.; Tong, Y.; Cheng, J.Y.; Shafiq, F.; Butcher, A.M.; Salem, S.S.; Brinton, S.L.; Rudman Spergel, A.K.; Johnson, K.; et al. Development of a Human Skin Commensal Microbe for Bacteriotherapy of Atopic Dermatitis and Use in a Phase 1 Randomized Clinical Trial. *Nat. Med.* **2021**, doi:10.1038/s41591-021-01256-2.

73. Ferček, I.; Lugović-Mihić, L.; Tambić-Andrašević, A.; Ćesić, D.; Grginić, A.G.; Bešlić, I.; Mravak-Stipetić, M.; Mihatov-Štefanović, I.; Buntić, A.-M.; Čivljak, R. Features of the Skin Microbiota in Common Inflammatory Skin Diseases. *Life* **2021**, *11*, 962, doi:10.3390/life11090962.

74. Cullin, N.; Azevedo Antunes, C.; Straussman, R.; Stein-Thoeringer, C.K.; Elinav, E. Microbiome and Cancer. *Cancer Cell* **2021**, *39*, 1317–1341, doi:10.1016/j.ccell.2021.08.006.

75. Sepich-Poore, G.D.; Zitvogel, L.; Straussman, R.; Hasty, J.; Wargo, J.A.; Knight, R. The Microbiome and Human Cancer. *Science (80-.).* **2021**, *371*, eabc4552, doi:10.1126/science.abc4552.

76. Routy, B.; Le Chatelier, E.; Derosa, L.; Duong, C.P.M.; Alou, M.T.; Daillère, R.; Fluckiger, A.; Messaoudene, M.; Rauber, C.; Roberti, M.P.; et al. Gut Microbiome Influences Efficacy of PD-1–Based Immunotherapy against Epithelial Tumors. *Science (80-.).* **2018**, *359*, 91–97, doi:10.1126/science.aan3706.

77. Matson, V.; Fessler, J.; Bao, R.; Chongsuwat, T.; Zha, Y.; Alegre, M.-L.; Luke, J.J.; Gajewski, T.F. The Commensal Microbiome Is Associated with Anti–PD-1 Efficacy in Metastatic Melanoma Patients. *Science (80-.).* **2018**, *359*, 104–108, doi:10.1126/science.aao3290.

78. Gopalakrishnan, V.; Spencer, C.N.; Nezi, L.; Reuben, A.; Andrews, M.C.; Karpinets, T. V.; Prieto, P.A.; Vicente, D.; Hoffman, K.; Wei, S.C.; et al. Gut Microbiome Modulates Response to Anti-PD-1 Immunotherapy in Melanoma Patients. *Science (80-.).* **2018**, *359*, 97–103, doi:10.1126/science.aan4236.

79. Smith, M.; Dai, A.; Ghilardi, G.; Amelsberg, K. V.; Devlin, S.M.; Pajarillo, R.; Slingerland, J.B.; Beghi, S.; Herrera, P.S.; Giardina, P.; et al. Gut Microbiome Correlates of Response and Toxicity Following Anti-CD19 CAR T Cell Therapy. *Nat. Med.* **2022**, *28*, 713–723, doi:10.1038/s41591-022-01702-9.

80. Stein-Thoeringer, C.K.; Saini, N.Y.; Zamir, E.; Blumenberg, V.; Schubert, M.-L.; Mor, U.; Fante, M.A.; Schmidt, S.; Hayase, E.; Hayase, T.; et al. A Non-Antibiotic-Disrupted Gut Microbiome Is Associated with Clinical Responses to CD19-CAR-T Cell Cancer Immunotherapy. *Nat. Med.* **2023**, *29*, 906–916, doi:10.1038/s41591-023-02234-6.

81. Peled, J.U.; Gomes, A.L.C.; Devlin, S.M.; Littmann, E.R.; Taur, Y.; Sung, A.D.; Weber, D.; Hashimoto, D.; Slingerland, A.E.; Slingerland, J.B.; et al. Microbiota as Predictor of Mortality in Allogeneic Hematopoietic-Cell Transplantation. *N. Engl. J. Med.* **2020**, *382*, 822–834, doi:10.1056/NEJMoa1900623.

82. Hang, S.; Paik, D.; Yao, L.; Kim, E.; Trinath, J.; Lu, J.; Ha, S.; Nelson, B.N.; Kelly, S.P.; Wu, L.; et al. Bile Acid Metabolites Control TH17 and Treg Cell Differentiation. *Nature* **2019**, *576*, 143–148, doi:10.1038/s41586-019-1785-z.

83. Paik, D.; Yao, L.; Zhang, Y.; Bae, S.; D'Agostino, G.D.; Zhang, M.; Kim, E.; Franzosa, E.A.; Avila-Pacheco, J.; Bisanz, J.E.; et al. Human Gut Bacteria Produce TH17-Modulating Bile Acid Metabolites. *Nature* **2022**, *603*, 907–912, doi:10.1038/s41586-022-04480-z.

84. Campbell, C.; McKenney, P.T.; Konstantinovsky, D.; Isaeva, O.I.; Schizas, M.; Verter, J.; Mai, C.; Jin, W.-B.; Guo, C.-J.; Violante, S.; et al. Bacterial Metabolism of Bile Acids Promotes Generation of Peripheral Regulatory T Cells. *Nature* **2020**, *581*, 475–479, doi:10.1038/s41586-020-2193-0.

85. Knochelmann, H.M.; Dwyer, C.J.; Bailey, S.R.; Amaya, S.M.; Elston, D.M.; Mazza-McCrann, J.M.; Paulos, C.M. When Worlds Collide: Th17 and Treg Cells in Cancer and Autoimmunity. *Cell. Mol. Immunol.* **2018**, *15*, 458–469, doi:10.1038/s41423-018-0004-4.

86. Ding, R.; Lian, S.B.; Tam, Y.C.; Oh, C.C. The Cutaneous Microbiome in Skin Cancer – A Systematic Review. *JDDG J. der Dtsch. Dermatologischen Gesellschaft* **2024**, *22*, 177–184, doi:10.1111/ddg.15294.

87. Squarzanti, D.F.; Zavattaro, E.; Pizzimenti, S.; Amoruso, A.; Savoia, P.; Azzimonti, B. Non-Melanoma Skin Cancer: News from Microbiota Research. *Crit. Rev. Microbiol.* **2020**, *46*, 433–449, doi:10.1080/1040841X.2020.1794792.

88. Voigt, A.Y.; Emiola, A.; Johnson, J.S.; Fleming, E.S.; Nguyen, H.; Zhou, W.; Tsai, K.Y.; Fink, C.; Oh, J. Skin Microbiome Variation with Cancer Progression in Human Cutaneous Squamous Cell Carcinoma. *J. Invest. Dermatol.* **2022**, *142*, 2773-2782.e16, doi:10.1016/j.jid.2022.03.017.

89. Rinke, C.; Schwientek, P.; Sczyrba, A.; Ivanova, N.N.; Anderson, I.J.; Cheng, J.-F.;

Darling, A.; Malfatti, S.; Swan, B.K.; Gies, E.A.; et al. Insights into the Phylogeny and Coding Potential of Microbial Dark Matter. *Nature* **2013**, *499*, 431–437, doi:10.1038/nature12352.

90. Jost, M.; Wehkamp, U. The Skin Microbiome and Influencing Elements in Cutaneous T-Cell Lymphomas. *Cancers (Basel).* **2022**, *14*, 1324, doi:10.3390/cancers14051324.

91. Rodríguez Baeza, D.; Bejarano Antonio, L.; González de Arriba, M.; Picó-Monllor, J.A.; Cañueto, J.; Navarro-Lopez, V. Cutaneous T-Cell Lymphoma and Microbiota: Etiopathogenesis and Potential New Therapeutic Targets. *Dermatol. Res. Pract.* **2024**, *2024*, 1–9, doi:10.1155/2024/9919225.

92. Mirvish, E.D.; Pomerantz, R.G.; Geskin, L.J. Infectious Agents in Cutaneous T-Cell Lymphoma. *J. Am. Acad. Dermatol.* **2011**, *64*, 423–431, doi:10.1016/j.jaad.2009.11.692.

93. Litvinov, I. V.; Shtreis, A.; Kobayashi, K.; Glassman, S.; Tsang, M.; Woetmann, A.; Sasseville, D.; Ødum, N.; Duvic, M. Investigating Potential Exogenous Tumor Initiating and Promoting Factors for Cutaneous T-Cell Lymphomas (CTCL), a Rare Skin Malignancy. *Oncoimmunology* **2016**, *5*, e1175799, doi:10.1080/2162402X.2016.1175799.

94. Angelova, A.; Rommelaere, J.; Ungerechts, G. The Complex Role of Infectious Agents in Human Cutaneous T-Cell Lymphoma Pathogenesis: From Candidate Etiological Factors to Potential Therapeutics. *Pathogens* **2024**, *13*, 184, doi:10.3390/pathogens13030184.

95. Arai, E.; Chow, K.C.; Li, C.Y.; Tokunaga, M.; Katayama, I. Differentiation between Cutaneous Form of Adult T Cell Leukemia/Lymphoma and Cutaneous T Cell Lymphoma by in Situ Hybridization Using a Human T Cell Leukemia Virus-1 DNA Probe. *Am. J. Pathol.* **1994**, *144*, 15–20.

96. Nagatani, T.; Matsuzaki, T.; Iemoto, G.; Kim, S.-T.; Baba, N.; Miyamoto, H.; Nakajima, H. Comparative Study of Cutaneous T-Cell Lymphoma and Adult T-Cell Leukemia/Lymphoma: Clinical, Histopathologic, and Immunohistochemical Analyses. *Cancer* **1990**, *66*, 2380–2386, doi:10.1002/1097-0142(19901201)66:11<2380::AID-CNCR2820661122>3.0.CO;2-H.

97. Jackow, C.M.; Cather, J.C.; Hearne, V.; Asano, A.T.; Musser, J.M.; Duvic, M. Association of Erythrodermic Cutaneous T-Cell Lymphoma, Superantigen-Positive Staphylococcus Aureus, and Oligoclonal T-Cell Receptor Vβ Gene Expansion. *Blood* **1997**, *89*, 32–40, doi:10.1182/blood.V89.1.32.

98. Talpur, R.; Bassett, R.; Duvic, M. Prevalence and Treatment of Staphylococcus Aureus Colonization in Patients with Mycosis Fungoides and Sézary Syndrome. *Br. J. Dermatol.* **2008**, *159*, 105–112, doi:10.1111/j.1365-2133.2008.08612.x.

99. Nguyen, V.; Huggins, R.H.; Lertsburapa, T.; Bauer, K.; Rademaker, A.; Gerami, P.; Guitart, J. Cutaneous T-Cell Lymphoma and Staphylococcus Aureus Colonization. *J. Am. Acad. Dermatol.* **2008**, *59*, 949–952, doi:10.1016/j.jaad.2008.08.030.

100. Emge, D.A.; Bassett, R.L.; Duvic, M.; Huen, A.O. Methicillin-Resistant Staphylococcus Aureus (MRSA) Is an Important Pathogen in Erythrodermic Cutaneous T-Cell Lymphoma (CTCL) Patients. *Arch. Dermatol. Res.* **2020**, *312*, 283–288, doi:10.1007/s00403-019-02015-7.

101. Vidulich, K.A.; Talpur, R.; Bassett, R.L.; Duvic, M. Overall Survival in Erythrodermic Cutaneous T-cell Lymphoma: An Analysis of Prognostic Factors in a Cohort of Patients with Erythrodermic Cutaneous T-cell Lymphoma. *Int. J. Dermatol.* **2009**, *48*, 243–252, doi:10.1111/j.1365-4632.2009.03771.x.

102. Lindahl, L.M.; Iversen, L.; Ødum, N.; Kilian, M. Staphylococcus Aureus and Antibiotics in Cutaneous T-Cell Lymphoma. *Dermatology* **2021**, 1–3, doi:10.1159/000517829.

103. Blaizot, R.; Ouattara, E.; Fauconneau, A.; Beylot-Barry, M.; Pham-Ledard, A. Infectious Events and Associated Risk Factors in Mycosis Fungoides/Sézary Syndrome: A Retrospective Cohort Study. *Br. J. Dermatol.* **2018**, *179*, 1322–1328, doi:10.1111/bjd.17073.

104. Oh, J.; Byrd, A.L.; Deming, C.; Conlan, S.; Kong, H.H.; Segre, J.A. Biogeography and Individuality Shape Function in the Human Skin Metagenome. *Nature* **2014**, *514*, 59–64, doi:10.1038/nature13786.

105. Salava, A.; Deptula, P.; Lyyski, A.; Laine, P.; Paulin, L.; Väkevä, L.; Ranki, A.; Auvinen, P.; Lauerma, A. Skin Microbiome in Cutaneous T-Cell Lymphoma by 16S and Whole-

Genome Shotgun Sequencing. *J. Invest. Dermatol.* **2020**, *140*, 2304-2308.e7, doi:10.1016/j.jid.2020.03.951.

106. Harkins, C.P.; MacGibeny, M.A.; Thompson, K.; Bubic, B.; Huang, X.; Brown, I.; Park, J.; Jo, J.-H.; Segre, J.A.; Kong, H.H.; et al. Cutaneous T-Cell Lymphoma Skin Microbiome Is Characterized by Shifts in Certain Commensal Bacteria but Not Viruses When Compared with Healthy Controls. *J. Invest. Dermatol.* **2021**, *141*, 1604–1608, doi:10.1016/j.jid.2020.10.021.

107. Dehner, C.A.; Ruff, W.E.; Greiling, T.; Pereira, M.S.; Redanz, S.; McNiff, J.; Girardi, M.; Kriegel, M.A. Malignant T Cell Activation by a Bacillus Species Isolated from Cutaneous T-Cell Lymphoma Lesions. *JID Innov.* **2022**, *2*, 100084, doi:10.1016/j.xjidi.2021.100084.

108. Zhang, Y.; Seminario-Vidal, L.; Cohen, L.; Hussaini, M.; Yao, J.; Rutenberg, D.; Kim, Y.; Giualiano, A.; Robinson, L.A.; Sokol, L. "Alterations in the Skin Microbiota Are Associated With Symptom Severity in Mycosis Fungoides." *Front. Cell. Infect. Microbiol.* **2022**, *12*, 1–10, doi:10.3389/fcimb.2022.850509.

109. Hooper, M.J.; Enriquez, G.L.; Veon, F.L.; LeWitt, T.M.; Sweeney, D.; Green, S.J.; Seed, P.C.; Choi, J.; Guitart, J.; Burns, M.B.; et al. Narrowband Ultraviolet B Response in Cutaneous T-Cell Lymphoma Is Characterized by Increased Bacterial Diversity and Reduced Staphylococcus Aureus and Staphylococcus Lugdunensis. *Front. Immunol.* **2022**, *13*, 1–14, doi:10.3389/fimmu.2022.1022093.

110. Hooper, M.J.; LeWitt, T.M.; Pang, Y.; Veon, F.L.; Chlipala, G.E.; Feferman, L.; Green, S.J.; Sweeney, D.; Bagnowski, K.T.; Burns, M.B.; et al. Gut Dysbiosis in Cutaneous T-cell Lymphoma Is Characterized by Shifts in Relative Abundances of Specific Bacterial Taxa and Decreased Diversity in More Advanced Disease. *J. Eur. Acad. Dermatology Venereol.* **2022**, *36*, 1552–1563, doi:10.1111/jdv.18125.

111. Nguyen, W.Q.; Chrisman, L.P.; Enriquez, G.L.; Hooper, M.J.; Griffin, T.L.; Ahmad, M.; Rahman, S.; Green, S.J.; Seed, P.C.; Guitart, J.; et al. Gut Microbiota Analyses of Cutaneous T-Cell Lymphoma Patients Undergoing Narrowband Ultraviolet B Therapy Reveal Alterations Associated with Disease Treatment. *Front. Immunol.* **2024**, *14*, 1–11, doi:10.3389/fimmu.2023.1280205.

112. Hooper, M.J.; LeWitt, T.M.; Veon, F.L.; Pang, Y.; Chlipala, G.E.; Feferman, L.; Green, S.J.; Sweeney, D.; Bagnowski, K.T.; Burns, M.B.; et al. Nasal Dysbiosis in Cutaneous T-Cell Lymphoma Is Characterized by Shifts in Relative Abundances of Non-Staphylococcus Bacteria. *JID Innov.* **2022**, *2*, 100132, doi:10.1016/j.xjidi.2022.100132.

113. Licht, P.; Mailänder, V. Transcriptional Heterogeneity and the Microbiome of Cutaneous T-Cell Lymphoma. *Cells* **2022**, *11*, 328, doi:10.3390/cells11030328.

114. Krejsgaard, T.; Lindahl, L.M.; Mongan, N.P.; Wasik, M.A.; Litvinov, I. V.; Iversen, L.; Langhoff, E.; Woetmann, A.; Odum, N. Malignant Inflammation in Cutaneous T-cell Lymphoma—a Hostile Takeover. *Semin. Immunopathol.* **2017**, *39*, 269–282, doi:10.1007/s00281-016-0594-9.

115. Peng, W.; Novak, N. Pathogenesis of Atopic Dermatitis. *Clin. Exp. Allergy* **2015**, *45*, 566–574, doi:10.1111/cea.12495.

116. Bear, A.; Locke, T.; Rowland-Jones, S.; Pecetta, S.; Bagnoli, F.; Darton, T.C. The Immune Evasion Roles of Staphylococcus Aureus Protein A and Impact on Vaccine Development. *Front. Cell. Infect. Microbiol.* **2023**, *13*, 1–10, doi:10.3389/fcimb.2023.1242702.

117. Otto, M. Basis of Virulence in Community-Associated Methicillin-Resistant Staphylococcus Aureus. *Annu. Rev. Microbiol.* **2010**, *64*, 143–162, doi:10.1146/annurev.micro.112408.134309.

118. Lacey, K.; Geoghegan, J.; McLoughlin, R. The Role of Staphylococcus Aureus Virulence Factors in Skin Infection and Their Potential as Vaccine Antigens. *Pathogens* **2016**, *5*, 22, doi:10.3390/pathogens5010022.

119. Cheung, G.Y.C.; Bae, J.S.; Otto, M. Pathogenicity and Virulence of Staphylococcus Aureus. *Virulence* **2021**, *12*, 547–569, doi:10.1080/21505594.2021.1878688.

120. Schreiner, J.; Kretschmer, D.; Klenk, J.; Otto, M.; Bühring, H.-J.; Stevanovic, S.; Wang, J.M.; Beer-Hammer, S.; Peschel, A.; Autenrieth, S.E. Staphylococcus Aureus Phenol-Soluble Modulin Peptides Modulate Dendritic Cell Functions and Increase In Vitro Priming of Regulatory T Cells. *J. Immunol.* **2013**, *190*, 3417–3426, doi:10.4049/jimmunol.1202563.

121. Claßen, A.; Kalali, B.N.; Schnopp, C.; Andres, C.; Aguilar-Pimentel, J.A.; Ring, J.; Ollert, M.; Mempel, M. TNF Receptor I on Human Keratinocytes Is a Binding Partner for Staphylococcal Protein A Resulting in the Activation of NF Kappa B, AP-1, and Downstream Gene Transcription. *Exp. Dermatol.* **2011**, *20*, 48–52, doi:10.1111/j.1600-0625.2010.01174.x.

122. Gómez, M.I.; Lee, A.; Reddy, B.; Muir, A.; Soong, G.; Pitt, A.; Cheung, A.; Prince, A. Staphylococcus Aureus Protein A Induces Airway Epithelial Inflammatory Responses by Activating TNFR1. *Nat. Med.* **2004**, *10*, 842–848, doi:10.1038/nm1079.

123. Gallo, R.L.; Hooper, L. V. Epithelial Antimicrobial Defence of the Skin and Intestine. *Nat. Rev. Immunol.* **2012**, *12*, 503–516, doi:10.1038/nri3228.

124. Ryu, S.; Song, P.; Seo, C.; Cheong, H.; Park, Y. Colonization and Infection of the Skin by S. Aureus: Immune System Evasion and the Response to Cationic Antimicrobial Peptides. *Int. J. Mol. Sci.* **2014**, *15*, 8753–8772, doi:10.3390/ijms15058753.

125. Otto, M. Staphylococcus Colonization of the Skin and Antimicrobial Peptides. *Expert Rev. Dermatol.* **2010**, *5*, 183–195, doi:10.1586/edm.10.6.

126. Chen, Y.E.; Tsao, H. The Skin Microbiome: Current Perspectives and Future Challenges. *J. Am. Acad. Dermatol.* **2013**, *69*, 143-155.e3, doi:10.1016/j.jaad.2013.01.016.

127. Sandhu, S.S.; Pourang, A.; Sivamani, R.K. A Review of next Generation Sequencing Technologies Used in the Evaluation of the Skin Microbiome: What a Time to Be Alive. *Dermatol. Online J.* **2019**, *25*, doi:10.5070/D3257044797.

128. Lundberg, D.S.; Yourstone, S.; Mieczkowski, P.; Jones, C.D.; Dangl, J.L. Practical Innovations for High-Throughput Amplicon Sequencing. *Nat. Methods* **2013**, *10*, 999–1002, doi:10.1038/nmeth.2634.

129. Knight, R.; Vrbanac, A.; Taylor, B.C.; Aksenov, A.; Callewaert, C.; Debelius, J.; Gonzalez, A.; Kosciolek, T.; McCall, L.I.; McDonald, D.; et al. Best Practices for Analysing Microbiomes. *Nat. Rev. Microbiol.* **2018**, *16*, 410–422, doi:10.1038/s41579-018-0029-9.

130. Claesson, M.J.; Clooney, A.G.; O'Toole, P.W. A Clinician's Guide to Microbiome

Analysis. *Nat. Rev. Gastroenterol. Hepatol.* **2017**, *14*, 585–595, doi:10.1038/nrgastro.2017.97.

131. Quince, C.; Walker, A.W.; Simpson, J.T.; Loman, N.J.; Segata, N. Shotgun Metagenomics, from Sampling to Analysis. *Nat. Biotechnol.* **2017**, *35*, 833–844, doi:10.1038/nbt.3935.

132. Kong, H.H.; Andersson, B.; Clavel, T.; Common, J.E.; Jackson, S.A.; Olson, N.D.; Segre, J.A.; Traidl-Hoffmann, C. Performing Skin Microbiome Research: A Method to the Madness. *J. Invest. Dermatol.* **2017**, *137*, 561–568, doi:10.1016/j.jid.2016.10.033.

133. Beghini, F.; McIver, L.J.; Blanco-Míguez, A.; Dubois, L.; Asnicar, F.; Maharjan, S.; Mailyan, A.; Manghi, P.; Scholz, M.; Thomas, A.M.; et al. Integrating Taxonomic, Functional, and Strain-Level Profiling of Diverse Microbial Communities with BioBakery 3. *Elife* **2021**, *10*, 1–42, doi:10.7554/eLife.65088.

134. Truong, D.T.; Franzosa, E.A.; Tickle, T.L.; Scholz, M.; Weingart, G.; Pasolli, E.; Tett, A.; Huttenhower, C.; Segata, N. MetaPhlAn2 for Enhanced Metagenomic Taxonomic Profiling. *Nat. Methods* **2015**, *12*, 902–903, doi:10.1038/nmeth.3589.

135. Acosta, E.M.; Little, K.A.; Bratton, B.P.; Lopez, J.G.; Mao, X.; Payne, A.S.; Donia, M.; Devenport, D.; Gitai, Z. Bacterial DNA on the Skin Surface Overrepresents the Viable Skin Microbiome. *Elife* **2023**, *12*, 1–21, doi:10.7554/eLife.87192.2.

136. Tett, A.; Pasolli, E.; Farina, S.; Truong, D.T.; Asnicar, F.; Zolfo, M.; Beghini, F.; Armanini, F.; Jousson, O.; De Sanctis, V.; et al. Unexplored Diversity and Strain-Level Structure of the Skin Microbiome Associated with Psoriasis. *npj Biofilms Microbiomes* **2017**, *3*, 14, doi:10.1038/s41522-017-0022-5.

137. Pereira-Marques, J.; Hout, A.; Ferreira, R.M.; Weber, M.; Pinto-Ribeiro, I.; van Doorn, L.-J.; Knetsch, C.W.; Figueiredo, C. Impact of Host DNA and Sequencing Depth on the Taxonomic Resolution of Whole Metagenome Sequencing for Microbiome Analysis. *Front. Microbiol.* **2019**, *10*, 1–9, doi:10.3389/fmicb.2019.01277.

138. Hillmann, B.; Al-Ghalith, G.A.; Shields-Cutler, R.R.; Zhu, Q.; Gohl, D.M.; Beckman, K.B.; Knight, R.; Knights, D. Evaluating the Information Content of Shallow Shotgun Metagenomics. *mSystems* **2018**, *3*, doi:10.1128/msystems.00069-18.

139. La Reau, A.J.; Strom, N.B.; Filvaroff, E.; Mavrommatis, K.; Ward, T.L.; Knights, D. Shallow Shotgun Sequencing Reduces Technical Variation in Microbiome Analysis. *Sci. Rep.* **2023**, *13*, 7668, doi:10.1038/s41598-023-33489-1.

140. Stothart, M.R.; McLoughlin, P.D.; Poissant, J. Shallow Shotgun Sequencing of the Microbiome Recapitulates 16S Amplicon Results and Provides Functional Insights. *Mol. Ecol. Resour.* **2023**, *23*, 549–564, doi:10.1111/1755-0998.13713.

141. Gohl, D.M.; Vangay, P.; Garbe, J.; MacLean, A.; Hauge, A.; Becker, A.; Gould, T.J.; Clayton, J.B.; Johnson, T.J.; Hunter, R.; et al. Systematic Improvement of Amplicon Marker Gene Methods for Increased Accuracy in Microbiome Studies. *Nat. Biotechnol.* **2016**, *34*, 942–949, doi:10.1038/nbt.3601.

142. Weinmaier, T.; Probst, A.J.; La Duc, M.T.; Ciobanu, D.; Cheng, J.-F.; Ivanova, N.; Rattei, T.; Vaishampayan, P. A Viability-Linked Metagenomic Analysis of Cleanroom Environments: Eukarya, Prokaryotes, and Viruses. *Microbiome* **2015**, *3*, 62, doi:10.1186/s40168-015-0129-y.

143. Amar, Y.; Lagkouvardos, I.; Silva, R.L.; Ishola, O.A.; Foesel, B.U.; Kublik, S.; Schöler, A.; Niedermeier, S.; Bleuel, R.; Zink, A.; et al. Pre-Digest of Unprotected DNA by Benzonase Improves the Representation of Living Skin Bacteria and Efficiently Depletes Host DNA. *Microbiome* **2021**, *9*, 123, doi:10.1186/s40168-021-01067-0.

144. Marotz, C.A.; Sanders, J.G.; Zuniga, C.; Zaramela, L.S.; Knight, R.; Zengler, K. Improving Saliva Shotgun Metagenomics by Chemical Host DNA Depletion. *Microbiome* **2018**, *6*, 42, doi:10.1186/s40168-018-0426-3.

145. Nocker, A.; Cheung, C.-Y.; Camper, A.K. Comparison of Propidium Monoazide with Ethidium Monoazide for Differentiation of Live vs. Dead Bacteria by Selective Removal of DNA from Dead Cells. *J. Microbiol. Methods* **2006**, *67*, 310–320, doi:10.1016/j.mimet.2006.04.015.

146. Ganda, E.; Beck, K.L.; Haiminen, N.; Silverman, J.D.; Kawas, B.; Cronk, B.D.; Anderson, R.R.; Goodman, L.B.; Wiedmann, M. DNA Extraction and Host Depletion Methods Significantly Impact and Potentially Bias Bacterial Detection in a Biological Fluid. *mSystems* **2021**, *6*, doi:10.1128/mSystems.00619-21.

147. Shi, Y.; Wang, G.; Lau, H.C.-H.; Yu, J. Metagenomic Sequencing for Microbial DNA in Human Samples: Emerging Technological Advances. *Int. J. Mol. Sci.* **2022**, *23*, 2181, doi:10.3390/ijms23042181.

148. Rohrer, J.M. Thinking Clearly About Correlations and Causation: Graphical Causal Models for Observational Data. *Adv. Methods Pract. Psychol. Sci.* **2018**, *1*, 27–42, doi:10.1177/2515245917745629.

2 Publication 1: Transcriptional Heterogeneity and the Microbiome of Cutaneous T-Cell Lymphoma

Licht, P. & Mailänder, V. Transcriptional Heterogeneity and the Microbiome of Cutaneous T-Cell Lymphoma. *Cells* **11,** 328 (2022). doi: 10.3390/cells11030328

Full-text link: https://www.mdpi.com/2073-4409/11/3/328

My contribution to this publication is detailed in the section *Contributions to Publications 1, 2, and 3*.

cells

MDPI

Review

Transcriptional Heterogeneity and the Microbiome of Cutaneous T-Cell Lymphoma

Philipp Licht [1] and Volker Mailänder [1,2,*]

[1] Dermatology Clinic, University Medical Center of the Johannes Gutenberg-University Mainz, Langenbeckstraße 1, 55131 Mainz, Germany; plicht@uni-mainz.de
[2] Max Planck Institute for Polymer Research, Ackermannweg 10, 55128 Mainz, Germany
* Correspondence: Volker.Mailaender@unimedizin-mainz.de

Abstract: Cutaneous T-Cell Lymphomas (CTCL) presents with substantial clinical variability and transcriptional heterogeneity. In the recent years, several studies paved the way to elucidate aetiology and pathogenesis of CTCL using sequencing methods. Several T-cell subtypes were suggested as the source of disease thereby explaining clinical and transcriptional heterogeneity of CTCL entities. Several differentially expressed pathways could explain disease progression. However, exogenous triggers in the skin microenvironment also seem to affect CTCL status. Especially *Staphylococcus aureus* was shown to contribute to disease progression. Only little is known about the complex microbiome patterns involved in CTCL and how microbial shifts might impact this malignancy. Nevertheless, first hints indicate that the microbiome might at least in part explain transcriptional heterogeneity and that microbial approaches could serve in diagnosis and prognosis. Shaping the microbiome could be a treatment option to maintain stable disease. Here, we review current knowledge of transcriptional heterogeneity of and microbial influences on CTCL. We discuss potential benefits of microbial applications and microbial directed therapies to aid patients with CTCL burden.

Keywords: cutaneous T-cell lymphoma (CTCL); mycosis fungoides (MF); Sézary syndrome (SS); transcriptome; microbiome; heterogeneity

Citation: Licht, P.; Mailänder, V. Transcriptional Heterogeneity and the Microbiome of Cutaneous T-Cell Lymphoma. *Cells* **2022**, *11*, 328. https://doi.org/10.3390/cells11030328

Academic Editors: Ivan V. Litvinov, Robert Gniadecki, Niels Ødum and Madeleine Duvic

Received: 29 September 2021
Accepted: 13 January 2022
Published: 19 January 2022

1. Introduction

Cutaneous T-cell lymphomas (CTCL) are a group of skin homing neoplastic malignancies comprising approximately 10% of total non-Hodgkin lymphomas (NHL) with Mycosis fungoides (MF) as the most common entity [1]. Primarily presenting as an indolent disease course initially, there might be a sudden progression to advanced stages including extracutaneous site involvement and a 5-year overall survival drop from >80% to 44% in higher stages [2–4]. One third of patients progress to advanced stage MF within 10 years [5]. Because of the indolent character of early stage CTCL, typically only late-stage patients are directed to systemic therapies that can cause severe side effects [6]. Preselection of patients with a poor prognosis would allow these subjects to receive more intensive treatments possibly improving disease control and survival. Several clinical variables and biological markers are discussed as prognostic factors. However, these parameters are partially subjective and imprecisely specified or show conflicting results across studies [5]. Furthermore, diagnosis is challenging and requires a complex combination of factors. Early stages mimicking other inflammatory skin diseases, as well as a variety of clinical manifestations that can highly differ from the typical appearance, are aggravating diagnostic hurdles [5,7]. Hence, interobserver variation for MF diagnosis is considerable, resulting in a median delay of 3 years before the definitive diagnosis is made since the first patient presentation [5]. These challenges underline the need for better diagnostic and prognostic tools [8]. The variable nature of CTCL comes in hand with strong transcriptome heterogeneity (inter-patient and intra-tumoural) on both the bulk [9] and the single-cell level [10].

Genes with potentially prognostic value were identified [9,11], but results emphasize the need for personalized precision medicine [10,12]. Moreover, skin barrier dysfunction and upregulated virus entry pathways [12] may reflect increased susceptibility for skin infections already clinically observed in CTCL patients [13]. Many different pathogens were observed in infected CTCL patients and incidence rates vary strongly [14], following the diverse character of CTCL in that manner. Infectious agents are discussed to play a role in CTCL aetiology and pathogenesis [15]. Indeed, exogenous factors like bacterial toxins can enhance disease progression via unspecific activation and expansion of T-cells [16]. Especially the mechanisms of how *Staphylococcus aureus* can aggravate the progression of CTCL have been investigated [17]. In general, several microbiota or a dysfunctional microbial community can influence cancers and other skin diseases [18,19]. Regarding CTCL, the complex microbiome patterns possibly influencing the course of this disease have only recently begun to be investigated [20,21]. Genomic methods to study microbiota can provide deep insights into shifted microbial communities relating disease [19].

In this review, we discuss current knowledge of transcriptional heterogeneity and the microbiome of CTCL. We will first show that CTCL seems to arise from malignant cells in the blood, leading to intra-patient heterogeneity. We also indicate first evidence of microbial implications on disease progression in CTCL and how differential colonization could lead to inter-patient heterogeneity. Then, we outline transcriptional heterogeneity on the inter- and intra-patient level and underline aspects that could point to microbial influence. Next, we summarize current knowledge of the microbiome in CTCL. Finally, we discuss the interplay between the microbiome and transcriptome of CTCL and suggest possible microbial applications in CTCL.

2. T-Cell Receptor Clonality

In the majority of cases the malignant T-cell exhibits a $CD4^+$ tissue resident effector memory phenotype [22]. The malignant T-cell might then disseminate via chronic antigenic stimulation leading to clonal proliferation [3]. It is believed that the first oncologic hit happens at the state of the mature tissue resident T-cell, but this understanding is recently challenged. It has been observed that malignant cells in lesions of the same patient can share the same T-cell receptor (TCR), and that a neoplastic clonotype can be found in the blood even months before its first skin occurrence [23]. With ongoing disease severity, there is a loss in TCR repertoire complexity and a shift towards a dominant clone [24]. Moreover, some of these clonotypes share the same TCR-gamma sequences but not TCR-beta and TCR-alpha, indicating an initial malignant transformation at the T-cell progenitor stage after TCR-gamma but before TCR-beta and –alpha reassembly [25,26]. Hence, a model of circulating and self-seeding T-cell clones is suggested (Figure 1): Early neoplastic clones may initially colonize the skin and other clones follow. Some early clones may mature and re-enter the circulation to self-seed into other lesions [23,25–27] leading to intra-patient heterogeneity.

High-throughput sequencing of the TCR-beta gene showed that MF patients with a tumour clone frequency (relative abundance of T-cell clones) in lesions less than 25% have a good prognosis for overall and progression-free survival, while this is inverse for tumour clone frequencies over 25%. However, such associations were not seen in patients with Sézary syndrome (SS), the leukemic variant of CTCL [8]. Interestingly, the most dominant TCR variable beta chain (TCR Vβ) family is found in frequencies comparable to SS patients [8,28]. Moreover, this specific TCR Vβ family is associated with *Staphylococcus aureus* (*S. aureus*) infections in a subset of CTCL patients [8,29]. This bacterium contributes to CTCL progression [30]. Because not all patients are colonized with *S. aureus* [14] and colonization with other commensals could protect against this pathogen [31,32], this could lead to a varying composition and prevalence of dominant malignant clones and therefore to inter-patient heterogeneity. Later, we will discuss the role of *S. aureus* in CTCL pathogenesis and its association with TCR Vβ in more detail.

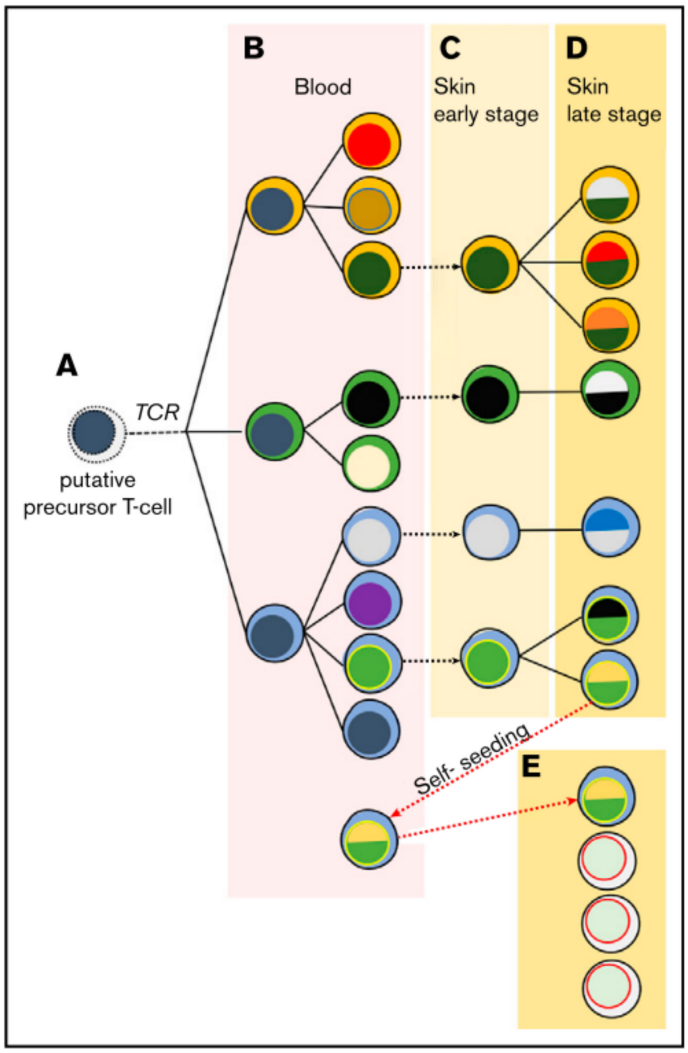

Figure 1. Suggested model of migrating malignant cells in CTCL. As a result of circulating and self-seeding malignant cells to other lesions, intra-patient heterogeneity may occur. (**A**) A putative precursor of a malignant T-cell undergoes malignant transformation before TCR-beta rearrangement, showing clonotypic heterogeneity (different cytoplasm colour). (**B**) In the blood the precursor expands and accumulates mutations, leading to different subclones (different colour of nucleus). (**C**,**D**) Lesions are seeded by malignant T-cells, where they progress malignancy and develop new subclones while disease further develops. (**E**) Some malignant cells may re-enter the circulation to self-seed into other lesions, increasing heterogeneity and disease progression. Reprinted with permission from ref. [27]. Copyright © 2020 American Society of Hematology.

3. Transcriptional Heterogeneity

A series of studies profiled the mutational landscape of CTCL [28,33–36]. However, an overall quite heterogeneous genomic picture is drawn, showing no well-defined alterations in fusion proteins, copy number, and somatic mutations. Gene modifications have been frequently found that are involved in specific cellular processes and signalling pathways [37]. Likewise, transcriptome analyses revealed a diverse picture: Litvinov et al. [9] used a targeted bulk RNA sequencing (RNA-seq) approach on mostly formaldehyde-fixed paraffin-embedded (FFPE) skin and a freshly snapped frozen specimen. The authors found differential heterogeneity between and even within the same patients that were sampled over the course of the disease with progressing MF stages. Unsupervised clustering showed intermixed groupings of CTCL stages and benign dermatoses. Similarly, cluster analyses

failed to produce clear results to distinguish between early versus advanced disease stages as well as indolent versus aggressive CTCL samples.

On the single gene level, however, 75 transcripts were found to be upregulated across different CTCL stages, including inflammation-mediating genes like STAT and CD70. The authors underlined differential expression of *TOX*, *FYB*, *LEF1*, *CCR4*, *ITK*, *EED*, *POU2AF*, *IL-26*, *STAT5*, *BLK*, *GTSF1* and *PSORS1C2*, as these genes were already characterized in previous investigations using quantitative RT-PCR [38].

Focusing on advanced disease stages, T-cell related genes like *TOX* and *FYB* were upregulated. In early disease stages that are about to progress, *TOX*, *FYB* and other genes were overexpressed as compared to samples with an indolent course [8,9,11,39]. These genes are also associated with decreased disease-specific survival and might thereby serve as prognostic markers [11]. As CTCL is characterized by unregulated expanding T-cells, genes involved in TCR signalling are associated with a high tumour cell frequency [8]. *TOX* is not an exclusive CTCL marker, since it has been shown to be upregulated in primary cutaneous B-cell lymphomas and benign dermatoses as well [40,41]. However, Litvinov et al. pointed out that *TOX* expression in CTCL was several magnitudes higher than in benign dermatoses, climaxing in most advanced stages [9]. Targeted RNA-seq provides an effective method to investigate (low-abundant) transcripts that have been selected based on previous considerations [42,43], but naturally also provides only a restricted picture. Routinely generated FFPE specimen in clinics provide an extensive source of samples, especially in the case of diseases with rarer incidences. However, because RNA is usually degraded in FFPE samples, results might not reflect the true biological information [44]. A follow-up study addressing differences between FFPE and fresh samples and possible batch effects found no significant influences [45], although trends can be observed.

3.1. Single Cell RNA Sequencing Reveals Transcriptional Heterogeneity

With the advent of single cell RNA sequencing (scRNA-seq), more detailed insights into the behaviour of single cells and their states within a specific context have emerged. This can lead to improved onco-biological knowledge leading to better treatment and precision medicine. Therefore, scRNA-seq might be superior to bulk RNA-seq, although the latter still provides less noisy and more precise data [42,46–48]. In the case of MF, the tumour microenvironment is composed of a significant proportion of infiltrative reactive immune cells including $CD8^+$ T-cells, regulatory T-cells (Tregs), dendritic cells (DCs), macrophages and mast cells. The infiltrative proportion decreases with disease progression and varies between patients [49,50]. Hence, bulk sequencing will determine average values of fluctuating percentages of malignant and benign cells and cannot assess unique transcriptome expression of tumour cells and its microenvironment [42,46]. Five studies utilized scRNA-seq for CTCL: Three investigated SS [51,52] with one study including a single MF subject [53] and two examined exclusively MF [12,54]. Gaydosik et al. [12] sequenced single cells of five advanced stage (IIB-IVA) MF patients. The lesions showed inter-patient heterogeneity as there was no overlap between cells from tumour samples or with cells from heathy controls revealed by clustering analysis. Focusing on lymphocytes, several gene expression clusters were found, mostly unique for specific MF samples. Enriched pathways in these clusters are associated with cell growth, proliferation and survival, translational reprogramming, metastasis, negative regulation of NK-mediated cytotoxicity against tumours, NK-cell signalling, and tumorigenic pathways known from other forms of cancers [12]. Noteworthy is the implication of a virus entry pathway which indicates exogenous triggers on CTCL.

Focusing only on actively proliferating lymphocytes of the five patients investigated revealed a shared panel of 17 genes that are overexpressed compared to healthy control individuals (Figure 2). Among other functions, these genes regulate cell cycle and survival, apoptosis, metabolism, and transportation of mRNA. Interestingly, the 17 genes were also expressed by *TOX*-positive cells and furthermore showed similar characteristics as the lymphocyte-tumour-clusters described above [12]. Hence, *TOX* might potentially serve

as a diagnostic and prognostic marker [9,12]. Although the TCR was not sequenced, expansion of constant TCR-beta chain was observed in the MF gene expression clusters [12], indicating TCR clonality [8]. Concerning tumour-infiltrating lymphocytes (TILs) in the tumour microenvironment, all but two MF samples showed overlapping patterns, also with healthy controls. However, in MF samples, several checkpoint inhibitory receptors were heterogeneously expressed in $CD4^+$ and $CD8^+$ TILs [12]. Patient-dependent expression of multiple inhibitory receptors have been reported to hinder an efficient antitumor response and hampers the development of a treatment regimen, thus requiring personalized therapies [12].

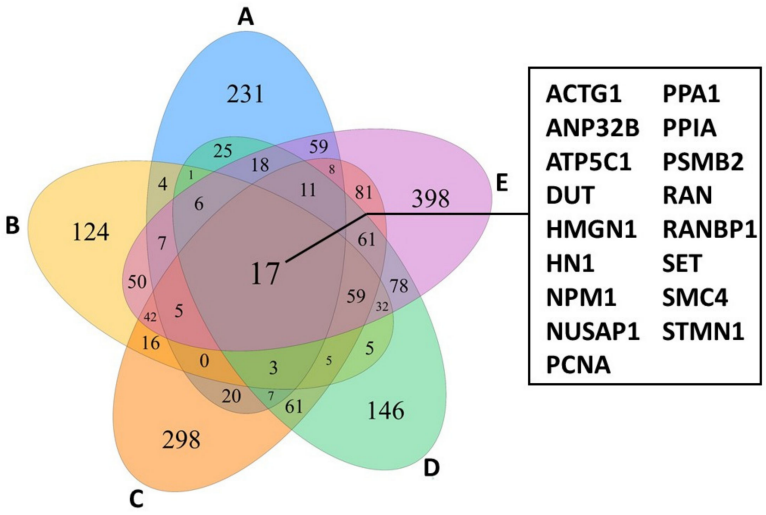

Figure 2. Venn diagram of proliferating lymphocytes from CTCL-lesions of 5 different patients (**A**–**E**) showing an overlap of 17 genes highly while only minor expression is observed in controls. The figure was created with specifications from [12].

Rindler et al. [54] showed intra-patient heterogeneity by investigating three body compartments of one advanced stage MF patient (skin, peripheral blood, and lymph node). Three clusters of malignant T-cells were identified by expression patterns and clonal TCR sequences. Two of the three malignant T-cell clusters exhibited comparable distributions of dominant TCR clonotypes between all investigated tissues, albeit one cluster was mainly present only in skin and blood. The third cluster showed clonality restricted to the skin, while the blood compartment was polyclonal. Differential gene expression revealed the malignant T-cell clusters as substantially heterogeneous. Pro-inflammatory markers not attributable to a specific T helper type were overexpressed in all tissues. However, in malignant skin cells mainly T helper 2 (Th2) cytokines were observed [54]. These cytokines have been linked to increased susceptibility for skin infections in CTCL [55] and might indicate microbial influence on skin cells.

To further investigate lineage relationships between malignant cells of the three body compartments, the authors used trajectory analysis. This computational method orders cells along branches based on similarities in their expression profile. As a result, lineage trees with branch points inferring cell fate are compiled. Mostly the resulting tree is 2-branched with a starting pre-branch (or root) [56,57]. Using this technique, the malignant skin and blood cells ordered at opposing branches. Skin cells accounted also for the starting pre-branch. Lymph node cells scattered alongside the whole trajectory. This indicates that lymph node cells share patterns with cells from both skin and blood. In the blood cell branch, loss of tissue retention can be observed while also retaining lymph node and skin homing ability [54]. Gene expression shows signatures for a central memory T-cell (Tcm)-like phenotype, which is typically attributed to SS [22]. Cells of the skin branch expressed markers associated with tissue retention and of tissue resident effector memory cells (Tem), which has been reported as the MF-typical tumour cell [22]. Pre-branched

skin cells discriminated from post-branched skin cells by expression of Th2 cytokines as opposed to Th22, Th17 and Th1 cytokines as well as cell motility genes [54]. It was recently shown that tissue resident T-cells (Trm) could re-join the circulation upon reactivation and resemble closer Tcm than recently activated Trm. Mature Trm can differentiate into Tcm, Tem and again into Trm with preferred homing to tissue of origin [58]. In conclusion, the adaptive ability of MF tumour cells for long lasting skin residency and dissemination through the circulation might contribute to the heterogeneous nature of MF [54].

Likewise, investigation by Borcherding and co-workers on Sézary syndrome revealed substantial heterogeneity within malignant T-cells of a single patient [52]. Overexpressed pathways differed significantly between clusters of malignant cells. Besides the typical Tcm type usually seen in SS [22], one cluster expressed markers specific to regulatory T-cells (Tregs). Trajectory analysis suggested transition of *FOXP3* (Tregs) positive cells to either *GATA3* (T helper 2 cells) or *IKZF2* (Tregs) positive cells, which may depend on the tumour micromilieu [52]. T helper 2 phenotype is often accompanied with bacterial infections in CTCL [59]. Since peripheral blood was investigated and some malignant cells transitioned into T helper 2 like phenotypes, this could indicate that these cells came into bacterial contact at the skin and moved back into circulation.

Both studies by Rindler et al. [54] and Borcherding et al. [52] found interesting aspects of cell fates potentially driving the malignant CTCL cell to develop into different cell (sub-)types and thereby constituting to intra-patient disease heterogeneity. Since these two investigations are based on samples of only a single patient, the results need to be validated and extended in bigger patient cohorts.

Buus et al. [51] support the heterogeneous picture showing surface marker expression of naïve T-cells (Tn), stem-cell memory T-cells (Tscm), and expression patterns not fitting Tn, Tcm, and Tscm. Using targeted gene expression profiling of relevant T-cell genes, inter-patient patterns were observed. Cells of each patient grouped into clusters, suggesting disparate functional background of malignant cells. The authors reported a 5-genes panel expressed by most cells (*S100A4*, *S100A10*, *IL7R*, *CCR7*, and *CXCR4*). Three of which comprise known functions in growth and migration of malignant T-cells (*IL7R*, *CCR7*, and *CXCR4I*, while the other two are well known cancer related molecules that have yet not been associated with CTCL [51].

Herrera et al. [53] interrogated surface marker expression, TCR-repertoire and transcriptome of matched skin and blood from SS and one leukemic MF patient on the single cell level. Malignant T-cells were defined based on clonal TCR sequences and transcriptional and surface marker patterns distinct to non-malignant T-cells. Matched skin and blood samples shared dominant TCR sequences, suggesting involvement of both tissues in CTCL. Among differentially expressed genes were transcripts typically affected in CTCL like *CD158K/KIR3DL2* [60] and *TOX* [9,41]. Comparing matched malignant cells derived from the blood and the skin of the same patients revealed several distinct groups thereby displaying intra-patient heterogeneity. Blood-derived cells showed a higher level of clonal diversity than skin-derived cells. Trajectory analysis suggests that malignant cells from the blood transition into skin-derived cells. Together, these findings show a strong tissue dependency regarding transcriptional activity. In skin samples, several upregulated pathways were unmasked: T-cell activation, TCR ligation, mitogen-induced transcripts, and cell cycle. Vice versa, T-cell quiescence and markers for resting T-cells were upregulated in blood counterparts [53]. Strikingly, some of those genes were also outlined by Rindler et al. in blood of an advanced stage MF patient [54]. Moreover, skin-derived cells exhibited higher T-cell activation, reduced T-cell resting and more highly proliferating lymphocytes. As this was not seen in a healthy donor as well as in a psoriasis patient, stimulating activity from the CTCL skin microenvironment can be suspected [53]. Adding to this, several exogenous factors are discussed as CTCL initiating or promoting [16]. Since phylogenetic analysis based on inferred genetic abnormalities showed no clear linear relationship between skin and blood sub-clones, the skin microenvironment seems to serve as driving factor in stimulation of malignant cells and the clonal expansion of few and specific

sub-clones [53]. Because varying proportions of colonizing microbiota on CTCL patients were reported [14], this could lead to inter-patient heterogeneity additive to intra-patient heterogeneity demonstrated by Herrra et al. [53]. On the other hand, decreased diversity of clonal diversity in skin cells in contrast to matched blood counterparts might indicate a homogenization of transcriptional activity by skewing of malignant cells from the blood to the skin compartment. In conclusion, microbial colonization might lead to skewing of malignant cells in the skin which can differ between CTCL lesions and between CTCL patients depending on the specific microbiome present.

3.2. Single Cell Transcriptome Signatures Suggest Microbial Influence on CTCL Heterogeneity

Taken together, several single cell transcriptomic signatures suggest exogeneous/microbial influence on CTCL heterogeneity. Gaydosik et al. found an upregulated pathway of endocytic virus entry. Dysregulation of epithelial-mesenchymal transition as well as skin-barrier dysfunction may reflect increased susceptibility to infections [12]. Additionally, typical cytokines for the T helper 2 (Th2) phenotype were upregulated in malignant skin cells in contrast to matched malignant cells from the blood and lymph node of the same patient [54]. Th2 cytokines were found to be associated with impaired production of S100 proteins [55]. S100 proteins contribute to tumorigenic processes in diverse cancers and expression patterns can be stage- and cancer subtype-specific. S100 inhibitors already are in clinical trials for e.g., melanoma [61]. In addition, some S100 family members are so called antimicrobial peptides (AMPs) with bactericidal activity [62]. In the scRNA-seq studies review, several S100 family members were differentially expressed [12,51,52,54]. Among them, S100A4, S100A8, S100A9 and S100A12 have known bactericidal activity or are implicated with bacterial infections [63–66]. Indeed, CTCL exhibits an impaired skin barrier and deficient expression of several AMPs leads to increased susceptibility for skin infections and bacterial toxins may play a major role in driving disease progression [55,59,67,68]. Since microbial colonization is not consistent between CTCL patients, as shown in an early study by Axelrod et al. [14] and extended by two investigations utilizing microbiomics [20,21], differential microbial colonization may account for transcriptional heterogeneity.

4. Microbiota and CTCL

4.1. Skin Barrier Dysfunction

Different exogenous triggers like skin resident microbiota are being discussed as CTCL provoking and/or promoting factors [16]. In a CTCL mouse model developed by Fanok et al. [34], disease progression was depended on microbial triggers. Mice housed under germ-free conditions were significantly less CTCL symptomatic [34]. Hence, there seems to be crosstalk between CTCL cells and/or the tumour microenvironment and microbiota. Indeed, MF presents with a skin barrier dysfunction [59]. It has been shown that malignant T-cells secrete galectins in CTCL [69]. This is a class of proteins with functions in several biological activities like cell proliferation and implications in inflammatory skin diseases and cancers [70–72]. In CTCL, galectins might induce morphological and histopathological changes via epidermal hyperproliferation, disorganized keratinocyte stratification and decreased attachment between the epithelial and mesenchymal layer [69]. Moreover, during CTCL progression, a shift in the inflammatory tumour micromilieu can be seen. In early stages, CTCL lesions typically present with a high abundance of benign reactive T helper 1 (Th1) cells, thereby expressing according Th1-markers. As the disease progresses, a decline in Th1 cells and its markers are observed. Concomitant, malignant T-cells and T helper 2 (Th2) cells increase, leading to a Th2 dominated inflammatory milieu [73]. Th2 cytokines like interleukin (IL)-4 and IL-13 suppress the appropriate expression of skin produced antimicrobials peptide (AMP) [74]. This effect is even more pronounced than in atopic dermatitis (AD) and psoriasis, which are other inflammatory skin diseases that often are overgrown by bacterial pathogens [55,59,67]. As already stated above, AMPs are differentially expressed in CTCL on the single cell level as well [12,51,52,54].

Further indication for the influencing effect of AMPs on CTCL progression is added by the discovery of geographic patterns of CTCL cases. They indicate a link between sunlight exposure leading to vitamin D expression which in turn upregulates AMPs: Demographic data from CTCL patients in Texas, USA, shows that several communities had five to twenty times higher incidences than the expected rate for the population [75]. On the other hand, only few communities were completely spared by CTCL. Among them are areas near El Paso, which is one of the sunniest cities in the USA with an annual sunshine of 84%. Sun exposure might therefore be a protective or a therapeutic factor [75,76]. Noteworthy, sun exposure has been shown to reduce risk for other non-Hodgkin lymphomas as well [77]. As it is well known, sunlight exposure leads to vitamin D production [78]. Vitamin D is already in use to treat other inflammatory skin diseases like AD [79] and psoriasis [80]. Moreover, vitamin D emerged as a possible cancer preventive agent which raises the question of its role in CTCL [81]. CTCL patients have vitamin D deficiency with a comparable prevalence to other cancer patients [82]. Under non-inflammatory conditions, vitamin D induces the expression of the cathelicidin LL-37, an AMP with strong antibacterial, antibiofilm, antifungal and antiviral actions. In return, microbial proteases (e.g., released by *Staphylococcus aureus*) might cleave LL-37 into inactive fragments [83].

In summary, CTCL presents with a dysfunctional skin barrier and reduced AMP production (either due to cytokine shifts during disease progression and/or environmental factors). This results in an enhanced skin permeability leading to greater susceptibility for skin infections [16,69].

4.2. Microbiome on CTCL Lesions

Many common skin diseases are associated with changes in the microbiota, which is termed dysbiosis [19]. While the overrepresentation of *Staphylococcus aureus* on CTCL lesions has been reported [84] and will be discussed later, other microorganisms may also play a role in disease progression. For example, interactions between skin commensals can comprise of competitively excluding one another, or synergies for mutual benefits. Especially interactions with *S. aureus* have been studied [19]. An early study assessed the relative abundance of microbes on CTCL involved skin using traditional culture-based methods [14]. However, more than 99% of all microorganisms still cannot be isolated by bacterial cultures even today [85]. The vast majority of microbial isolates belong to only four phyla and hence uncultured microbes are referred to as "microbial dark matter". Culture-based approaches select for appropriate microorganisms thereby underestimating the total diversity of the community [86]. There are several culture-independent methods to study the microbiome, each with their own advantages and disadvantages [87,88]. The most used method is amplicon sequencing, where marker genes like the 16S ribosome DNA (rDNA) with conserved regions are amplified. The process of 16S amplicon sequencing requires only low biomass and is not influenced by host DNA contamination but comes with PCR bias and a limited resolution. Whole-metagenomic shotgun sequencing (WMS) on the other hand is affected by host DNA but provides deeper resolution down to the microbial strain level and holds potential for functional analysis, e.g., screening for enriched pathways or virulence factors and antibiotic resistance genes [88,89].

Salava et al. used 16S and WMS to investigate the microbiome on early stage CTCL lesions while using non-lesional skin of the same patients as an internal control [21]. WMS data delivered higher resolution in the genus of propionibacteria as compared to 16s sequencing and subsequent analysis is therefore based on WMS. The authors observed patient and body site specific variation, which is to be expected [90]. No differences were found in terms of community diversity [21]. However, the presented data suggests a trend towards stable communities in non-lesional skin and an unpreserved microbiome composition on CTCL lesions. Hence, a dysbiotic flora might exist on lesional skin. Ten bacterial species were identified to be more abundant on non-lesional skin. Only two had been associated with cutaneous diseases before. These are *Serratia spp.* and *Pseudomonas spp.*, that affect the skin in nosocomial infections and immunocompromised patients [21]. Others reported

overrepresentation of *Staphylococci* on CTCL lesions using 16S sequencing. Moreover, the phylogenetic diversity was decreased, indicating a distinct microbiome as compared to healthy volunteers and psoriasis patients [30]. Psoriasis as an inflammatory disease is, among others, frequently confounded with early-stage MF [5]. Compared to atopic dermatitis (AD), decreased community diversity correlated significantly with flare and recovered post flare. Staphylococci increase during AD flare, whereas relative abundances of other microbial genera vary across AD disease states, pointing to the complex relationship present in microbial communities [91,92]. On the other hand, Harkins et al. [20] found no differences in the microbial diversity investigating early and advanced stage MF and SS patients compared to age-, sex- and sampling site-matched healthy volunteers. Fungal and viral abundances were low and showed no differences to healthy volunteers, contradicting hints about viral implications in CTCL [93]. Interestingly, *S. aureus* also showed no differences whereas other commensal staphylococcal species trended higher in MF but not in SS. Nonetheless, principal coordinate analysis showed separation of samples from healthy volunteers and advanced stage CTCL. This may be driven by overrepresentation of two corynebacterial species and decreased abundances of two cutibacterial species. Bacterial shifts, furthermore, seem to correlate with disease stage (Figure 3).

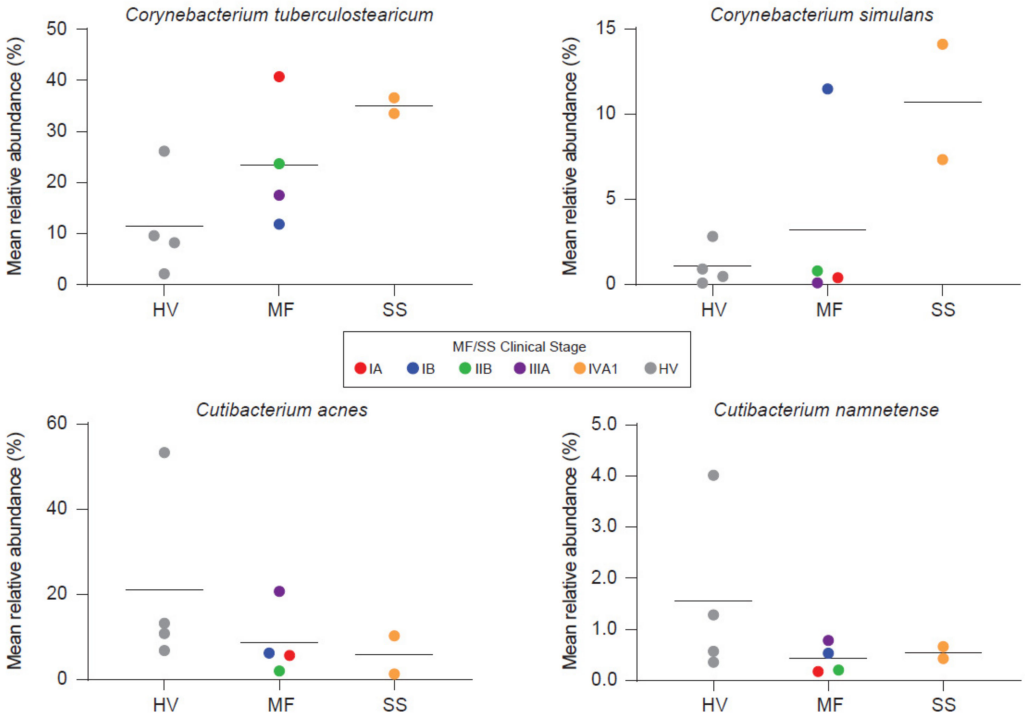

Figure 3. Besides *Staphylococcus aureus*, other organisms may also be linked with CTCL. Harkins et al. [20] found two corynebacteria to trend higher, whereas two cutibactactial species exhibited decreased abundances on CTCL lesions. Bacterial shifts seem to correlate with disease stage. HV = Healthy Volunteer. Reprinted with permission from ref. [20]. Copyright © 2021 Elsevier.

However, statistical significance was not reached, likely due to the small sample number [20]. *C. tuberculosearicum* can upregulate and/or induce inflammatory responses in keratinocyte derived cell lines in vitro and may contribute to cutaneous malignancies [94]. Besides this pathogenic role, corynebacteria also possess the ability to shift *S. aureus* towards commensalism via quorum sensing [95]. Furthermore, staphylococci like *S. epidermidis* and *S. hominis* are capable of controlling *S. aureus* virulence either indirectly through quorum sensing or directly via antimicrobial action in AD [31,32,96]. Under healthy conditions, *S. epidermidis* provides antagonistic action against *S. aureus* leading to negatively correlated colonization rates between these two bacteria [97]. Under disease/non-homeostatic skin flora conditions like AD, *S. aureus* abundance can increase substantially [92]. In parallel,

there might also be an increase in *S. epidermidis*, possibly reflecting an attempt to control the vast overrepresentation of *S. aureus* [92].

4.3. Staphylococcus aureus

Investigations show that CTCL lesions are often colonized by S. aureus [84]. This bacterium possesses a large repertoire of virulence factors [98]. Staphylococcal alpha-toxin (a-haemolysin) induces cell death in CTCL-derived benign cells leaving their malignant counterparts unharmed. Malignant cells dispose of several resistance mechanisms to a-haemolysin, favouring the survival of CTCL tumour cells upon toxin presentation [99]. Additionally, this toxin inhibits T-cell mediated cytotoxic anti-cancer responses, leading to tumour escape and continued persistence of respective cells [100]. Besides haemolysins, *S. aureus* produces staphylococcal enterotoxins (SEs) that can act as so-called superantigens [101]. Superantigens do not need to be processed by antigen presenting cells (APCs) but rather bind directly to the variable beta chain of the TCR and to the major histocompatibility complex class II (MHC II) outside of the antigen binding groove, thereby triggering clonal expansion and an upregulation of pro-inflammatory cytokines [102]. In a study investigating TCR clones in a big CTCL cohort via high-throughput sequencing, the most abundant TCR Vβ family was TRBV20 [8]. The staphylococcal toxin toxic shock syndrome toxin-1 (TSST-1) binds specifically to TRBV20 [103]. Moreover, TRBV20 expansion has been shown to correlate with TSST-1 level in clinical CTCL isolates. Besides TSST-1, other SEs were detected as well but not linked to TRBV20 ratios [29]. However, in another CTCL cohort, only staphylococcal enterotoxin A (SEA) but not TSST-1 or other SEs were found to be present on patient skin. SEA and staphylococcal enterotoxin E (SEE) were the only staphylococcal toxins to elicit disease-stimulating activity in SS patient-derived tumour cells in vitro [17]. Hence, this conflicting data might be caused by (i) other SEs than TSST-1 associating with TRBV20, (ii) specific host-pathogen interactions [104] that differed between the CTCL cohorts and/or (iii) microbe-microbe interactions leading to an altered expression of virulence factors [19]. Taken together, clonal expansion of malignant cells [50], loss of TCR repertoire complexity and TCR Vβ skewing [24] during CTCL disease course might (i) reflect the self-seeding mechanism described previously [27] and (ii) may be enhanced and/or triggered by superantigenic activity of colonizing microbes [68] that can also act specifically among themselves [19] and with the hosts skin immunity [104].

In Vitro, SEs can stimulate CTCL disease activity via cell-cell contact of malignant and benign T-cells [105], which may act in a T-T-cell interaction manner by T-cells bearing MHC II [106,107] (Figure 4). Cross-linked TCR-MHC II prompts the benign T-cells to produce IL-2 which in turn upregulates the Janus kinase 3/signal transducer and activator of transcription 3 (Jak3/Stat3) pathway. Activation of Jak3/Stat3 in malignant cells leads to secretion of soluble factors, supressing cell mediated cytotoxicity in benign immune cells and promoting aggregation of immunosuppressive regulatory T-cells. Furthermore, aberrant Jak3/Sat3 induces overexpression of IL-10, which dampens immunity by several means: Downregulation of Th1 responses (interferon-g, IL-12), favouring anergic and immunosuppressive T-cells, repression of DC maturation and promotion of immunoregulatory M2 macrophages [105]. In addition, SEs also activates the Stat5 protein and upregulates factors contributing to shifting the Th1 milieu to a Th2 dominated milieu [108]. The latter is usually seen in advanced stage CTCL [73]. Moreover, staphylococcal toxins disturb elimination of malignant cells by cytotoxic T-cells and induce upregulation of the regulatory T-cell marker FOXP3 [100,109]. Regulatory T-cells suppress autoimmunity leading to self-tolerance [110]. Together this might result in a reduced capacity of the immune system to clear malignant cells from tissues.

In conclusion, these results hold compelling evidence for the role of *S. aureus* on the progression of CTCL.

Because *S. aureus* is also a member of the physiological skin flora [19], specific strains might be responsible for CTCL progression. Indeed, SEs are a group of several toxins [101] and different *S. aureus* strains dispose of different SEs [98]. While some SEs showed

CTCL promoting activities (i.e., SEA and SEE), not all SEs act as CTCL stimulatory agents (e.g., TSST-1) [17]. Strain-level specificity was already shown to be related to AD and psoriasis at their disease severity [91,111]. Hence, not only the presence of *S. aureus*, but also the specific strain may be responsible for disease stimulating actions. Since TSST-1 was associated with the specific TCR Vβ family TRBV20 [8,29], but did not elicit stimulating activites in vitro [17], these conflicting results warrant further investigations.

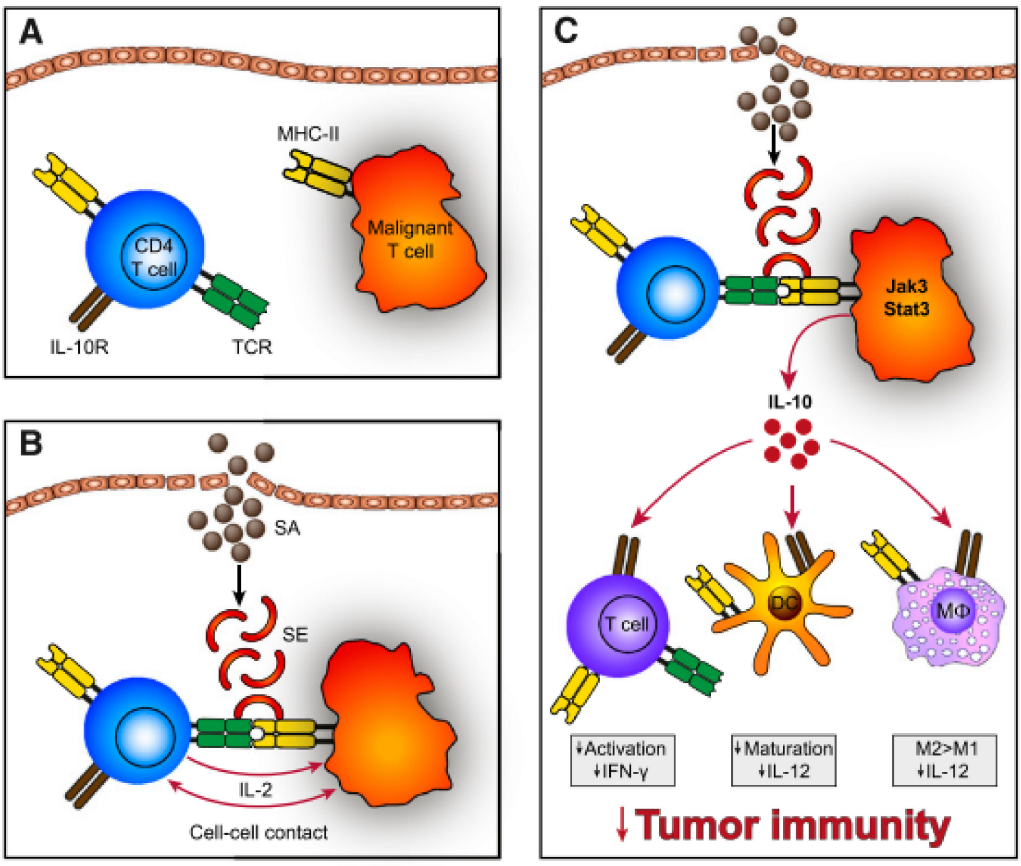

Figure 4. (**A**) Malignant T-cells often express a monoclonal TCR-V-beta chain with decreased function of the whole TCR complex. Hence, SEs do not stimulate the TCR directly but through activation of benign T-cells. (**B**) SEs bind to MHC II expressed on malignant T-cells, which crosslink to TCR of benign T-cells. Subsequently, establishing T-T-cell interaction and IL-2 is expressed. (**C**) These signals induce IL-10 expression, which dampens the immune response via impaired maturation of DCs, repressed expression of Th1 cytokines (interferon-g, IL-12), inhibition of T-cell activation and promoted development of M2 macrophages. Reprinted with permission from ref. [105]. Copyright © 2014 American Society of Hematology.

4.4. S. aureus Eradication

Because hospitalized CTCL patients suffer from recurrent staphylococcal sepsis, systemic antibiotic treatment is often applied. However, as a side benefit, rapid clinical improvement of CTCL burden in some patients has been observed [29,68]. In an early study, absence of *S. aureus* after antibiotic treatment over several months was linked to a decline in disease severity in 2 patients [112]. Another study reported skin improvement in the majority of 33 CTCL patients who are *S. aureus* positive after administering oral and topical (nares) antibiotic agents over a course of several months. Response to treatment was observed over all disease stages [84].

Lindahl et al. [113] showed that decreased CTCL severity and *S. aureus* colonization after antibiotic treatment is linked to a decrease in malignant T-cells and normalization of several markers and pathways typically upregulated in CTCL: Systemic antibiotics were

applied to six advanced stage MF patients and two SS patients over 24 days, who did not respond to standard treatment. Eradication of *S. aureus* resulted in significant disease improvement and a decrease in malignant T-cells depicted as the relative frequency of the most dominant TCR-beta clone. Microarray gene expression analysis revealed normalization of markers for cell proliferation, inflammatory response, neoplasia and the Stat3 and IL-2 pathways compared to healthy controls, even one month after cessation of antibiotic treatment. In isolated primary malignant cells, Staphylococcal enterotoxin A (SEA) led to an activation of Stat3 and IL2-Receptor, while antibiotics showed no effect. Together these findings strongly suggest that *S. aureus* directly or indirectly stimulate CTCL tumour cells, and that antibiotic mediated disease relief is depended [113]. Unfortunately, *S. aureus* re-emerges quickly in most patients after termination of systemic antibiotic application. This finding emphasizes the clinical need for appropriate management of CTCL infections. Lifelong antibiotic therapy is not feasible due to antibiotic side-effects and the risk of new antibiotic resistances [114]. One third of CTCL patients colonized by *S. aureus* are methicillin-resistant S. aureus (MRSA) [115], hence non-antibiotic treatment options are warranted. Duvic et al. [116] reported a new treatment regimen combining systemic antibiotics, antiseptic whirlpool bathing, corticosteroids with alternating topical antibiotics as well as antiseptic creams applied to ulcers, resulting in profound clinical response [116].

5. Conclusions

CTCL presents with substantial clinical and transcriptional heterogeneity that might originate from adaptive and functional plasticity of malignant T-cells [7,10,53,54]. However, *S. aureus* can highly influence disease course and eradication of this pathogen may result in profound clinical improvements [68,113]. CTCL patients have a dysfunctional skin barrier and are susceptible to infections [67]. On the single cell level, several pathways and differential expression of AMPs strongly suggest exogenous impact of pathogens [12,51,52,54]. In particular, a consistently higher activation score of skin T-cells in comparison with their blood counterparts and benign skin T-cells indicate the cutaneous microenvironment to promote expansion of malignant T-cells [53]. Some data suggest that microbial stimuli could lead to a homogenization of the transcriptional profile of malignant cells [53]. *S. aureus* seems to foster expansion of a specific TCR Vβ family [8], thereby skewing malignant cells to a few clones. Since *S. aureus* constitutes only a minor part of the complex microbiome on human skin with many other microbes orchestrating human health and disease [19], other microbes may also be implicated in CTCL. Only few microbiome studies dealing with CTCL have been carried out so far. They deliver not yet a consistent picture but rather seemingly display microbe colonization to be patient and CTCL stage dependent [20,21]. Since some microorganisms have protective properties for the host [31,32,96], the specific microbial community composition on CTCL lesions can be crucial for the virulence of pathogens. Taken together, while specific microorganism like *S. aureus* could lead to a homogenization of transcriptional response, observed transcriptional heterogeneity might at least in part also be attributed to differential microbial colonization between CTCL lesions and between CTCL patients. Of course, it could also be speculated that transcriptional heterogeneity of CTCL itself leads to the observed microbiome patterns. Thus, there could also be a reciprocal influence of the microbiome and transcriptome in CTCL. Studies investigating mechanistic relationships are needed to clarify this "chicken-and-egg" situation.

There is no curative therapy available until today and optimal treatment remains to be elucidated [117]. Early stages have comparably good 5-year overall survival and thus maintenance of stable disease is important [118]. Additionally, CTCL patients frequently suffer from pain, pruritus, as well as disfigurement consequently affecting health-related quality of life [119]. Shaping the microbiome as personalized skin precision medicine might be an option to relieve symptoms and prevent disease progression [120]. Recently, bacteriotherapy to control *S. aureus* in AD patients was successfully tested in a phase 1 clinical trial presumably leading to improvement in eczema severity [121]. However, understanding the complex microbiome patterns of CTCL is still in its infancy. Strain level diversity of

colonizing pathogenic and protective microorganisms on MF lesions remains to be illuminated to add knowledge about possible treatment regimen. In addition, investigating temporal microbial community shifts might be of interest as suggested by associations with AD opposed to healthy skin [92,122–124]. Owing to first hints about distinctive characteristics between cutaneous malignancies as well as between CTCL stages [20,30], microbial approaches could also be utilized as prognostic and diagnostic tools [120,125]. Further studies are needed to shed light on the relationship between CTCL and its microbiome. The high level of transcriptional heterogeneity on the single cell level emphasizes the need to expand the given results in bigger cohorts. Research is warranted to understand the (reciprocal) influence of differential microbial colonization on single tumour cells and its microenvironment.

Author Contributions: Conceptualization, P.L. and V.M.; writing—original draft preparation, P.L.; writing—review and editing, P.L. and V.M.; supervision, V.M. All authors have read and agreed to the published version of the manuscript.

Funding: This research received no external funding.

Acknowledgments: Permissions to reuse figures published elsewhere were obtained from the respective publishers. Figure 2 was created using the R! package 'VennDiagram' with specifications from Gaydosik et al. [12]. We would like to thank Katharina Maisenbacher (Max Planck Institute for Polymer Research) for preparing the graphical abstract.

Conflicts of Interest: The authors declare no conflict of interest.

References

1. Bradford, P.T.; Devesa, S.S.; Anderson, W.F.; Toro, J.R. Cutaneous lymphoma incidence patterns in the United States: A population-based study of 3884 cases. *Blood* **2009**, *113*, 5064–5073. [CrossRef] [PubMed]
2. Olsen, E.; Vonderheid, E.; Pimpinelli, N.; Willemze, R.; Kim, Y.; Knobler, R.; Zackheim, H.; Duvic, M.; Estrach, T.; Lamberg, S.; et al. Revisions to the staging and classification of mycosis fungoides and Sezary syndrome: A proposal of the International Society for Cutaneous Lymphomas (ISCL) and the cutaneous lymphoma task force of the European Organization of Research and Treatment of Ca. *Blood* **2007**, *110*, 1713–1722. [CrossRef] [PubMed]
3. Querfeld, C.; Zain, J.; Rosen, S.T. Primary cutaneous T-Cell lymphomas: Mycosis fungoides and Sezary syndrome. In *T-Cell and NK-Cell Lymphomas*; Springer: Cham, Switzerland, 2019; pp. 225–248.
4. Agar, N.S.; Wedgeworth, E.; Crichton, S.; Mitchell, T.J.; Cox, M.; Ferreira, S.; Robson, A.; Calonje, E.; Stefanato, C.M.; Wain, E.M.; et al. Survival Outcomes and Prognostic Factors in Mycosis Fungoides/Sézary Syndrome: Validation of the Revised International Society for Cutaneous Lymphomas/European Organisation for Research and Treatment of Cancer Staging Proposal. *J. Clin. Oncol.* **2010**, *28*, 4730–4739. [CrossRef]
5. Scarisbrick, J.J.; Quaglino, P.; Prince, H.M.; Papadavid, E.; Hodak, E.; Bagot, M.; Servitje, O.; Berti, E.; Ortiz-Romero, P.; Stadler, R.; et al. The PROCLIPI international registry of early-stage mycosis fungoides identifies substantial diagnostic delay in most patients. *Br. J. Dermatol.* **2019**, *181*, 350–357. [CrossRef]
6. Whittaker, S.; Hoppe, R.; Prince, H.M. How I treat mycosis fungoides and Sezary syndrome. *Blood* **2016**, *127*, 3142–3153. [CrossRef]
7. Kazakov, D.; Burg, G.; Kempf, W. Clinicopathological spectrum of mycosis fungoides. *J. Eur. Acad. Dermatol. Venereol.* **2004**, *18*, 397–415. [CrossRef] [PubMed]
8. De Masson, A.; O'Malley, J.T.; Elco, C.P.; Garcia, S.S.; Divito, S.J.; Lowry, E.L.; Tawa, M.; Fisher, D.C.; Devlin, P.M.; Teague, J.E.; et al. High-throughput sequencing of the T cell receptor β gene identifies aggressive early-stage mycosis fungoides. *Sci. Transl. Med.* **2018**, *10*, eaar5894. [CrossRef]
9. Litvinov, I.V.; Tetzlaff, M.T.; Thibault, P.; Gangar, P.; Moreau, L.; Watters, A.K.; Netchiporouk, E.; Pehr, K.; Prieto, V.G.; Rahme, E.; et al. Gene expression analysis in Cutaneous T-Cell Lymphomas (CTCL) highlights disease heterogeneity and potential diagnostic and prognostic indicators. *Oncoimmunology* **2017**, *6*, e1306618. [CrossRef]
10. Rassek, K.; Iżykowska, K. Single-Cell Heterogeneity of Cutaneous T-Cell Lymphomas Revealed Using RNA-Seq Technologies. *Cancers* **2020**, *12*, 2129. [CrossRef] [PubMed]
11. Lefrançois, P.; Xie, P.; Wang, L.; Tetzlaff, M.T.; Moreau, L.; Watters, A.K.; Netchiporouk, E.; Provost, N.; Gilbert, M.; Ni, X.; et al. Gene expression profiling and immune cell-type deconvolution highlight robust disease progression and survival markers in multiple cohorts of CTCL patients. *Oncoimmunology* **2018**, *7*, e1467856. [CrossRef]
12. Gaydosik, A.M.; Tabib, T.; Geskin, L.J.; Bayan, C.-A.; Conway, J.F.; Lafyatis, R.; Fuschiotti, P. Single-cell Lymphocyte Heterogeneity in Advanced Cutaneous T-cell Lymphoma Skin Tumors. *Clin. Cancer Res.* **2019**, *25*, 4443–4454. [CrossRef]
13. Lebas, E.; Arrese, J.E.; Nikkels, A.F. Risk Factors for Skin Infections in Mycosis Fungoides. *Dermatology* **2016**, *232*, 731–737. [CrossRef]

14. Axelrod, P.I. Infections Complicating Mycosis Fungoides and Sézary Syndrome. *JAMA J. Am. Med. Assoc.* **1992**, *267*, 1354. [CrossRef]
15. Mirvish, E.D.; Pomerantz, R.G.; Geskin, L.J. Infectious agents in cutaneous T-cell lymphoma. *J. Am. Acad. Dermatol.* **2011**, *64*, 423–431. [CrossRef] [PubMed]
16. Litvinov, I.V.; Shtreis, A.; Kobayashi, K.; Glassman, S.; Tsang, M.; Woetmann, A.; Sasseville, D.; Ødum, N.; Duvic, M. Investigating potential exogenous tumor initiating and promoting factors for Cutaneous T-Cell Lymphomas (CTCL), a rare skin malignancy. *Oncoimmunology* **2016**, *5*, e1175799. [CrossRef]
17. Willerslev-Olsen, A.; Krejsgaard, T.; Lindahl, L.M.; Litvinov, I.V.; Fredholm, S.; Petersen, D.L.; Nastasi, C.; Gniadecki, R.; Mongan, N.P.; Sasseville, D.; et al. Staphylococcal enterotoxin A (SEA) stimulates STAT3 activation and IL-17 expression in cutaneous T-cell lymphoma. *Blood* **2016**, *127*, 1287–1296. [CrossRef]
18. Schwabe, R.F.; Jobin, C. The microbiome and cancer. *Nat. Rev. Cancer* **2013**, *13*, 800–812. [CrossRef]
19. Byrd, A.L.; Belkaid, Y.; Segre, J.A. The human skin microbiome. *Nat. Rev. Microbiol.* **2018**, *16*, 143–155. [CrossRef] [PubMed]
20. Harkins, C.P.; MacGibeny, M.A.; Thompson, K.; Bubic, B.; Huang, X.; Brown, I.; Park, J.; Jo, J.-H.; Segre, J.A.; Kong, H.H.; et al. Cutaneous T-Cell Lymphoma Skin Microbiome Is Characterized by Shifts in Certain Commensal Bacteria but not Viruses when Compared with Healthy Controls. *J. Investig. Dermatol.* **2021**, *141*, 1604–1608. [CrossRef]
21. Salava, A.; Deptula, P.; Lyyski, A.; Laine, P.; Paulin, L.; Väkevä, L.; Ranki, A.; Auvinen, P.; Lauerma, A. Skin Microbiome in Cutaneous T-Cell Lymphoma by 16S and Whole-Genome Shotgun Sequencing. *J. Investig. Dermatol.* **2020**, *140*, 2304–2308. [CrossRef]
22. Campbell, J.J.; Clark, R.A.; Watanabe, R.; Kupper, T.S. Sézary syndrome and mycosis fungoides arise from distinct T-cell subsets: A biologic rationale for their distinct clinical behaviors. *Blood* **2010**, *116*, 767–771. [CrossRef]
23. Iyer, A.; Hennessey, D.; O'Keefe, S.; Patterson, J.; Wang, W.; Wong, G.K.-S.; Gniadecki, R. Skin colonization by circulating neoplastic clones in cutaneous T-cell lymphoma. *Blood* **2019**, *134*, 1517–1527. [CrossRef] [PubMed]
24. Yawalkar, N.; Ferenczi, K.; Jones, D.A.; Yamanaka, K.; Suh, K.-Y.; Sadat, S.; Kupper, T.S. Profound loss of T-cell receptor repertoire complexity in cutaneous T-cell lymphoma. *Blood* **2003**, *102*, 4059–4066. [CrossRef]
25. Hamrouni, A.; Fogh, H.; Zak, Z.; Ødum, N.; Gniadecki, R. Clonotypic Diversity of the T-cell Receptor Corroborates the Immature Precursor Origin of Cutaneous T-cell Lymphoma. *Clin. Cancer Res.* **2019**, *25*, 3104–3114. [CrossRef] [PubMed]
26. Iyer, A.; Hennessey, D.; O'Keefe, S.; Patterson, J.; Wang, W.; Salopek, T.; Wong, G.K.-S.; Gniadecki, R. Clonotypic heterogeneity in cutaneous T-cell lymphoma (mycosis fungoides) revealed by comprehensive whole-exome sequencing. *Blood Adv.* **2019**, *3*, 1175–1184. [CrossRef]
27. Iyer, A.; Hennessey, D.; O'Keefe, S.; Patterson, J.; Wang, W.; Wong, G.K.-S.; Gniadecki, R. Branched evolution and genomic intratumor heterogeneity in the pathogenesis of cutaneous T-cell lymphoma. *Blood Adv.* **2020**, *4*, 2489–2500. [CrossRef]
28. Wang, L.; Ni, X.; Covington, K.R.; Yang, B.Y.; Shiu, J.; Zhang, X.; Xi, L.; Meng, Q.; Langridge, T.; Drummond, J.; et al. Genomic profiling of Sézary syndrome identifies alterations of key T cell signaling and differentiation genes. *Nat. Genet.* **2015**, *47*, 1426–1434. [CrossRef] [PubMed]
29. Jackow, C.M.; Cather, J.C.; Hearne, V.; Asano, A.T.; Musser, J.M.; Duvic, M. Association of Erythrodermic Cutaneous T-Cell Lymphoma, Superantigen-Positive *Staphylococcus aureus*, and Oligoclonal T-Cell Receptor Vβ Gene Expansion. *Blood* **1997**, *89*, 32–40. [CrossRef]
30. Tegla, C.A.; Herrera, A.M.; Seffens, A.M.; Fanok, M.H.; Dean, G.; Kawaoka, J.; Laird, M.E.; Fulmer, Y.; Willerslev-Olsen, A.; Hymes, K.B.; et al. Skin Associated *Staphylococcus aureus* Contributes to Disease Progression in CTCL. *Blood* **2019**, *134*, 659. [CrossRef]
31. Williams, M.R.; Costa, S.K.; Zaramela, L.S.; Khalil, S.; Todd, D.A.; Winter, H.L.; Sanford, J.A.; O'Neill, A.M.; Liggins, M.C.; Nakatsuji, T.; et al. Quorum sensing between bacterial species on the skin protects against epidermal injury in atopic dermatitis. *Sci. Transl. Med.* **2019**, *11*, eaat8329. [CrossRef]
32. Nakatsuji, T.; Chen, T.H.; Narala, S.; Chun, K.A.; Two, A.M.; Yun, T.; Shafiq, F.; Kotol, P.F.; Bouslimani, A.; Melnik, A.V.; et al. Antimicrobials from human skin commensal bacteria protect against *Staphylococcus aureus* and are deficient in atopic dermatitis. *Sci. Transl. Med.* **2017**, *9*, eaah4680. [CrossRef]
33. Choi, J.; Goh, G.; Walradt, T.; Hong, B.S.; Bunick, C.G.; Chen, K.; Bjornson, R.D.; Maman, Y.; Wang, T.; Tordoff, J.; et al. Genomic landscape of cutaneous T cell lymphoma. *Nat. Genet.* **2015**, *47*, 1011–1019. [CrossRef]
34. Fanok, M.H.; Sun, A.; Fogli, L.K.; Narendran, V.; Eckstein, M.; Kannan, K.; Dolgalev, I.; Lazaris, C.; Heguy, A.; Laird, M.E.; et al. Role of Dysregulated Cytokine Signaling and Bacterial Triggers in the Pathogenesis of Cutaneous T-Cell Lymphoma. *J. Investig. Dermatol.* **2018**, *138*, 1116–1125. [CrossRef] [PubMed]
35. van Doorn, R.; van Kester, M.S.; Dijkman, R.; Vermeer, M.H.; Mulder, A.A.; Szuhai, K.; Knijnenburg, J.; Boer, J.M.; Willemze, R.; Tensen, C.P. Oncogenomic analysis of mycosis fungoides reveals major differences with Sézary syndrome. *Blood* **2009**, *113*, 127–136. [CrossRef] [PubMed]
36. Vermeer, M.H.; van Doorn, R.; Dijkman, R.; Mao, X.; Whittaker, S.; van Voorst Vader, P.C.; Gerritsen, M.-J.P.; Geerts, M.-L.; Gellrich, S.; Soderberg, O.; et al. Novel and Highly Recurrent Chromosomal Alterations in Sezary Syndrome. *Cancer Res.* **2008**, *68*, 2689–2698. [CrossRef] [PubMed]
37. Damsky, W.E.; Choi, J. Genetics of Cutaneous T Cell Lymphoma: From Bench to Bedside. *Curr. Treat. Options Oncol.* **2016**, *17*, 33. [CrossRef]

38. Litvinov, I.V.; Netchiporouk, E.; Cordeiro, B.; Zargham, H.; Pehr, K.; Gilbert, M.; Zhou, Y.; Moreau, L.; Woetmann, A.; Ødum, N.; et al. Ectopic expression of embryonic stem cell and other developmental genes in cutaneous T-cell lymphoma. *Oncoimmunology* **2014**, *3*, e970025. [CrossRef]
39. Scott, A.C.; Dündar, F.; Zumbo, P.; Chandran, S.S.; Klebanoff, C.A.; Shakiba, M.; Trivedi, P.; Menocal, L.; Appleby, H.; Camara, S.; et al. TOX is a critical regulator of tumour-specific T cell differentiation. *Nature* **2019**, *571*, 270–274. [CrossRef]
40. Schrader, A.M.R.; Jansen, P.M.; Willemze, R. TOX expression in cutaneous B-cell lymphomas. *Arch. Dermatol. Res.* **2016**, *308*, 423–427. [CrossRef]
41. Schrader, A.M.R.; Jansen, P.M.; Willemze, R. TOX expression in cutaneous T-cell lymphomas: An adjunctive diagnostic marker that is not tumour specific and not restricted to the $CD4^+$ $CD8^-$ phenotype. *Br. J. Dermatol.* **2016**, *175*, 382–386. [CrossRef] [PubMed]
42. Kuksin, M.; Morel, D.; Aglave, M.; Danlos, F.-X.; Marabelle, A.; Zinovyev, A.; Gautheret, D.; Verlingue, L. Applications of single-cell and bulk RNA sequencing in onco-immunology. *Eur. J. Cancer* **2021**, *149*, 193–210. [CrossRef] [PubMed]
43. Ozsolak, F.; Milos, P.M. RNA sequencing: Advances, challenges and opportunities. *Nat. Rev. Genet.* **2011**, *12*, 87–98. [CrossRef]
44. Esteve-Codina, A.; Arpi, O.; Martinez-García, M.; Pineda, E.; Mallo, M.; Gut, M.; Carrato, C.; Rovira, A.; Lopez, R.; Tortosa, A.; et al. A Comparison of RNA-Seq results from paired formalin-fixed paraffin-embedded and fresh-frozen glioblastoma tissue samples. *PLoS ONE* **2017**, *12*, e0170632. [CrossRef]
45. Lefrançois, P.; Tetzlaff, M.T.; Moreau, L.; Watters, A.K.; Netchiporouk, E.; Provost, N.; Gilbert, M.; Ni, X.; Sasseville, D.; Duvic, M.; et al. TruSeq-Based Gene Expression Analysis of Formalin-Fixed Paraffin-Embedded (FFPE) Cutaneous T-Cell Lymphoma Samples: Subgroup Analysis Results and Elucidation of Biases from FFPE Sample Processing on the TruSeq Platform. *Front. Med.* **2017**, *4*, 1–16. [CrossRef] [PubMed]
46. Fan, J.; Slowikowski, K.; Zhang, F. Single-cell transcriptomics in cancer: Computational challenges and opportunities. *Exp. Mol. Med.* **2020**, *52*, 1452–1465. [CrossRef] [PubMed]
47. Li, L.; Xiong, F.; Wang, Y.; Zhang, S.; Gong, Z.; Li, X.; He, Y.; Shi, L.; Wang, F.; Liao, Q.; et al. What are the applications of single-cell RNA sequencing in cancer research: A systematic review. *J. Exp. Clin. Cancer Res.* **2021**, *40*, 163. [CrossRef] [PubMed]
48. Streets, A.M.; Zhang, X.; Cao, C.; Pang, Y.; Wu, X.; Xiong, L.; Yang, L.; Fu, Y.; Zhao, L.; Tang, F.; et al. Microfluidic single-cell whole-transcriptome sequencing. *Proc. Natl. Acad. Sci. USA* **2014**, *111*, 7048–7053. [CrossRef]
49. Querfeld, C.; Zain, J. *T-Cell and NK-Cell Lymphomas*; Querfeld, C., Zain, J., Rosen, S.T., Eds.; Cancer Treatment and Research; Springer International Publishing: Cham, Switzerland, 2019; Volume 176.
50. Krejsgaard, T.; Lindahl, L.M.; Mongan, N.P.; Wasik, M.A.; Litvinov, I.V.; Iversen, L.; Langhoff, E.; Woetmann, A.; Odum, N. Malignant inflammation in cutaneous T-cell lymphoma—A hostile takeover. *Semin. Immunopathol.* **2017**, *39*, 269–282. [CrossRef]
51. Buus, T.B.; Willerslev-Olsen, A.; Fredholm, S.; Blümel, E.; Nastasi, C.; Gluud, M.; Hu, T.; Lindahl, L.M.; Iversen, L.; Fogh, H.; et al. Single-cell heterogeneity in Sézary syndrome. *Blood Adv.* **2018**, *2*, 2115–2126. [CrossRef]
52. Borcherding, N.; Voigt, A.P.; Liu, V.; Link, B.K.; Zhang, W.; Jabbari, A. Single-Cell Profiling of Cutaneous T-Cell Lymphoma Reveals Underlying Heterogeneity Associated with Disease Progression. *Clin. Cancer Res.* **2019**, *25*, 2996–3005. [CrossRef]
53. Herrera, A.; Cheng, A.; Mimitou, E.P.; Seffens, A.; George, D.D.; Bar-Natan, M.; Heguy, A.; Ruggles, K.V.; Scher, J.U.; Hymes, K.; et al. Multimodal single-cell analysis of cutaneous T cell lymphoma reveals distinct sub-clonal tissue-dependent signatures. *Blood* **2021**, *138*, 1456–1464. [CrossRef]
54. Rindler, K.; Bauer, W.M.; Jonak, C.; Wielscher, M.; Shaw, L.E.; Rojahn, T.B.; Thaler, F.M.; Porkert, S.; Simonitsch-Klupp, I.; Weninger, W.; et al. Single-cell RNA sequencing reveals tissue compartment-specific plasticity of mycosis fungoides tumor cells. *Front. Immunol.* **2021**, *12*, 666935. [CrossRef]
55. Wolk, K.; Mitsui, H.; Witte, K.; Gellrich, S.; Gulati, N.; Humme, D.; Witte, E.; Gonsior, M.; Beyer, M.; Kadin, M.E.; et al. Deficient cutaneous antibacterial competence in cutaneous T-Cell lymphomas: Role of Th2-mediated biased Th17 function. *Clin. Cancer Res.* **2014**, *20*, 5507–5516. [CrossRef]
56. Saelens, W.; Cannoodt, R.; Todorov, H.; Saeys, Y. A comparison of single-cell trajectory inference methods. *Nat. Biotechnol.* **2019**, *37*, 547–554. [CrossRef]
57. Papalexi, E.; Satija, R. Single-cell RNA sequencing to explore immune cell heterogeneity. *Nat. Rev. Immunol.* **2018**, *18*, 35–45. [CrossRef]
58. Fonseca, R.; Beura, L.K.; Quarnstrom, C.F.; Ghoneim, H.E.; Fan, Y.; Zebley, C.C.; Scott, M.C.; Fares-Frederickson, N.J.; Wijeyesinghe, S.; Thompson, E.A.; et al. Developmental plasticity allows outside-in immune responses by resident memory T cells. *Nat. Immunol.* **2020**, *21*, 412–421. [CrossRef]
59. Suga, H.; Sugaya, M.; Miyagaki, T.; Ohmatsu, H.; Kawaguchi, M.; Takahashi, N.; Fujita, H.; Asano, Y.; Tada, Y.; Kadono, T.; et al. Skin barrier dysfunction and low antimicrobial peptide expression in cutaneous T-cell lymphoma. *Clin. Cancer Res.* **2014**, *20*, 4339–4348. [CrossRef] [PubMed]
60. Moins-Teisserenc, H.; Daubord, M.; Clave, E.; Douay, C.; Félix, J.; Marie-Cardine, A.; Ram-Wolff, C.; Maki, G.; Beldjord, K.; Homyrda, L.; et al. CD158k is a reliable marker for diagnosis of Sézary syndrome and reveals an unprecedented heterogeneity of circulating malignant cells. *J. Investig. Dermatol.* **2015**, *135*, 247–257. [CrossRef] [PubMed]
61. Bresnick, A.R.; Weber, D.J.; Zimmer, D.B. S100 proteins in cancer. *Nat. Rev. Cancer* **2015**, *15*, 96–109. [CrossRef] [PubMed]
62. Park, A.J.; Okhovat, J.-P.; Kim, J. Antimicrobial peptides. In *Clinical and Basic Immunodermatology*; Springer International Publishing: Cham, Switzerland, 2017; pp. 81–95.

63. Bian, L.; Strzyz, P.; Jonsson, I.-M.; Erlandsson, M.; Hellvard, A.; Brisslert, M.; Ohlsson, C.; Ambartsumian, N.; Grigorian, M.; Bokarewa, M. S100A4 deficiency is associated with efficient bacterial clearance and protects against joint destruction during staphylococcal infection. *J. Infect. Dis.* **2011**, *204*, 722–730. [CrossRef] [PubMed]
64. Zhang, J.; Jiao, Y.; Hou, S.; Tian, T.; Yuan, Q.; Hao, H.; Wu, Z.; Bao, X. S100A4 contributes to colitis development by increasing the adherence of citrobacter rodentium in intestinal epithelial cells. *Sci. Rep.* **2017**, *7*, 12099. [CrossRef] [PubMed]
65. Corbin, B.D.; Seeley, E.H.; Raab, A.; Feldmann, J.; Miller, M.R.; Torres, V.J.; Anderson, K.L.; Dattilo, B.M.; Dunman, P.M.; Gerads, R.; et al. Metal chelation and inhibition of bacterial growth in tissue abscesses. *Science* **2008**, *319*, 962–965. [CrossRef]
66. Cole, A.M.; Kim, Y.-H.; Tahk, S.; Hong, T.; Weis, P.; Waring, A.J.; Ganz, T. Calcitermin, a novel antimicrobial peptide isolated from human airway secretions. *FEBS Lett.* **2001**, *504*, 5–10. [CrossRef]
67. Nakajima, R.; Miyagaki, T.; Kamijo, H.; Oka, T.; Shishido-Takahashi, N.; Suga, H.; Sugaya, M.; Sato, S. Decreased progranulin expression in Mycosis fungoides: A possible association with the high frequency of skin infections. *Eur. J. Dermatol.* **2018**, *28*, 790–794. [CrossRef] [PubMed]
68. Willerslev-Olsen, A.; Krejsgaard, T.; Lindahl, L.; Bonefeld, C.; Wasik, M.; Koralov, S.; Geisler, C.; Kilian, M.; Iversen, L.; Woetmann, A.; et al. Bacterial toxins fuel disease progression in cutaneous T-cell lymphoma. *Toxins* **2013**, *5*, 1402–1421. [CrossRef]
69. Thode, C.; Woetmann, A.; Wandall, H.H.; Carlsson, M.C.; Qvortrup, K.; Kauczok, C.S.; Wobser, M.; Printzlau, A.; Ødum, N.; Dabelsteen, S. Malignant T cells secrete galectins and induce epidermal hyperproliferation and disorganized stratification in a skin model of cutaneous T-cell lymphoma. *J. Investig. Dermatol.* **2015**, *135*, 238–246. [CrossRef] [PubMed]
70. Song, L.; Tang, J.; Owusu, L.; Sun, M.-Z.; Wu, J.; Zhang, J. Galectin-3 in cancer. *Clin. Chim. Acta* **2014**, *431*, 185–191. [CrossRef]
71. Rabinovich, G.A.; Toscano, M.A. Turning "sweet" on immunity: Galectin–glycan interactions in immune tolerance and inflammation. *Nat. Rev. Immunol.* **2009**, *9*, 338–352. [CrossRef]
72. Larsen, L.; Chen, H.-Y.; Saegusa, J.; Liu, F.-T. Galectin-3 and the skin. *J. Dermatol. Sci.* **2011**, *64*, 85–91. [CrossRef]
73. Stolearenco, V.; Namini, M.R.J.; Hasselager, S.S.; Gluud, M.; Buus, T.B.; Willerslev-Olsen, A.; Ødum, N.; Krejsgaard, T. cellular interactions and inflammation in the pathogenesis of cutaneous T-cell lymphoma. *Front. Cell Dev. Biol.* **2020**, *8*, 1–12. [CrossRef]
74. Howell, M.D.; Boguniewicz, M.; Pastore, S.; Novak, N.; Bieber, T.; Girolomoni, G.; Leung, D.Y.M. Mechanism of HBD-3 deficiency in atopic dermatitis. *Clin. Immunol.* **2006**, *121*, 332–338. [CrossRef] [PubMed]
75. Litvinov, I.V.; Tetzlaff, M.T.; Rahme, E.; Habel, Y.; Risser, D.R.; Gangar, P.; Jennings, M.A.; Pehr, K.; Prieto, V.G.; Sasseville, D.; et al. Identification of geographic clustering and regions spared by cutaneous T-cell lymphoma in Texas using 2 distinct cancer registries. *Cancer* **2015**, *121*, 1993–2003. [CrossRef] [PubMed]
76. Litvinov, I.V.; Tetzlaff, M.T.; Rahme, E.; Jennings, M.A.; Risser, D.R.; Gangar, P.; Netchiporouk, E.; Moreau, L.; Prieto, V.G.; Sasseville, D.; et al. Demographic patterns of cutaneous T-cell lymphoma incidence in Texas based on two different cancer registries. *Cancer Med.* **2015**, *4*, 1440–1447. [CrossRef]
77. Kricker, A.; Armstrong, B.K.; Hughes, A.M.; Goumas, C.; Smedby, K.E.; Zheng, T.; Spinelli, J.J.; De Sanjosé, S.; Hartge, P.; Melbye, M.; et al. Personal sun exposure and risk of non Hodgkin lymphoma: A pooled analysis from the interlymph consortium. *Int. J. Cancer* **2008**, *122*, 144–154. [CrossRef]
78. Wacker, M.; Holick, M.F. Sunlight and vitamin D. *Dermatoendocrinology* **2013**, *5*, 51–108. [CrossRef]
79. Hattangdi-Haridas, S.R.; Lanham-New, S.A.; Wong, W.H.S.; Ho, M.H.K.; Darling, A.L. Vitamin D deficiency and effects of vitamin D supplementation on disease severity in patients with atopic dermatitis: A systematic review and meta-analysis in adults and children. *Nutrients* **2019**, *11*, 1854. [CrossRef] [PubMed]
80. Barrea, L.; Savanelli, M.C.; Di Somma, C.; Napolitano, M.; Megna, M.; Colao, A.; Savastano, S. Vitamin D and its role in psoriasis: An overview of the dermatologist and nutritionist. *Rev. Endocr. Metab. Disord.* **2017**, *18*, 195–205. [CrossRef]
81. Garland, C.F.; Garland, F.C.; Gorham, E.D.; Lipkin, M.; Newmark, H.; Mohr, S.B.; Holick, M.F. The role of vitamin D in cancer prevention. *Am. J. Public Health* **2006**, *96*, 252–261. [CrossRef]
82. Talpur, R.; Cox, K.M.; Hu, M.; Geddes, E.R.; Parker, M.K.; Yang, B.Y.; Armstrong, P.A.; Liu, P.; Duvic, M. Vitamin D deficiency in mycosis fungoides and sézary syndrome patients is similar to other cancer patients. *Clin. Lymphoma Myeloma Leuk.* **2014**, *14*, 518–524. [CrossRef] [PubMed]
83. Bandurska, K.; Berdowska, A.; Barczyńska-Felusiak, R.; Krupa, P. Unique features of human cathelicidin LL-37. *BioFactors* **2015**, *41*, 289–300. [CrossRef] [PubMed]
84. Talpur, R.; Bassett, R.; Duvic, M. Prevalence and treatment of *Staphylococcus aureus* colonization in patients with mycosis fungoides and Sézary syndrome. *Br. J. Dermatol.* **2008**, *159*, 105–112. [CrossRef] [PubMed]
85. Locey, K.J.; Lennon, J.T. Scaling laws predict global microbial diversity. *Proc. Natl. Acad. Sci. USA* **2016**, *113*, 5970–5975. [CrossRef] [PubMed]
86. Rinke, C.; Schwientek, P.; Sczyrba, A.; Ivanova, N.N.; Anderson, I.J.; Cheng, J.-F.; Darling, A.; Malfatti, S.; Swan, B.K.; Gies, E.A.; et al. Insights into the phylogeny and coding potential of microbial dark matter. *Nature* **2013**, *499*, 431–437. [CrossRef]
87. Claesson, M.J.; Clooney, A.G.; O'Toole, P.W. A clinician' s guide to microbiome analysis. *Nat. Rev. Gastroenterol. Hepatol.* **2017**, *14*, 585–595. [CrossRef] [PubMed]
88. Liu, Y.-X.; Qin, Y.; Chen, T.; Lu, M.; Qian, X.; Guo, X.; Bai, Y. A practical guide to amplicon and metagenomic analysis of microbiome data. *Protein Cell* **2020**, *12*, 315. [CrossRef]
89. Franzosa, E.A.; Hsu, T.; Sirota-Madi, A.; Shafquat, A.; Abu-Ali, G.; Morgan, X.C.; Huttenhower, C. Sequencing and beyond: Integrating molecular "omics" for microbial community profiling. *Nat. Rev. Microbiol.* **2015**, *13*, 360–372. [CrossRef] [PubMed]

90. Oh, J.; Byrd, A.L.; Deming, C.; Conlan, S.; Kong, H.H.; Segre, J.A. Biogeography and individuality shape function in the human skin metagenome. *Nature* **2014**, *514*, 59–64. [CrossRef]
91. Byrd, A.L.; Deming, C.; Cassidy, S.K.B.; Harrison, O.J.; Ng, W.-I.; Conlan, S.; Belkaid, Y.; Segre, J.A.; Kong, H.H. *Staphylococcus aureus* and *Staphylococcus epidermidis* strain diversity underlying pediatric atopic dermatitis. *Sci. Transl. Med.* **2017**, *9*, eaal4651. [CrossRef]
92. Kong, H.H.; Oh, J.; Deming, C.; Conlan, S.; Grice, E.A.; Beatson, M.A.; Nomicos, E.; Polley, E.C.; Komarow, H.D.; Murray, P.R.; et al. Temporal shifts in the skin microbiome associated with disease flares and treatment in children with atopic dermatitis. *Genome Res.* **2012**, *22*, 850–859. [CrossRef]
93. Mirvish, J.J.; Pomerantz, R.G.; Falo, L.D.; Geskin, L.J. Role of infectious agents in cutaneous T-cell lymphoma: Facts and controversies. *Clin. Dermatol.* **2013**, *31*, 423–431. [CrossRef]
94. Altonsy, M.O.; Kurwa, H.A.; Lauzon, G.J.; Amrein, M.; Gerber, A.N.; Almishri, W.; Mydlarski, P.R. Corynebacterium tuberculostearicum, a human skin colonizer, induces the canonical nuclear factor-κB inflammatory signaling pathway in human skin cells. *Immun. Inflamm. Dis.* **2020**, *8*, 62–79. [CrossRef] [PubMed]
95. Ramsey, M.M.; Freire, M.O.; Gabrilska, R.A.; Rumbaugh, K.P.; Lemon, K.P. *Staphylococcus aureus* shifts toward commensalism in response to corynebacterium species. *Front. Microbiol.* **2016**, *7*, 1230. [CrossRef]
96. Cogen, A.L.; Yamasaki, K.; Sanchez, K.M.; Dorschner, R.A.; Lai, Y.; MacLeod, D.T.; Torpey, J.W.; Otto, M.; Nizet, V.; Kim, J.E.; et al. Selective antimicrobial action is provided by phenol-soluble modulins derived from *Staphylococcus epidermidis*, a normal resident of the skin. *J. Investig. Dermatol.* **2010**, *130*, 192–200. [CrossRef] [PubMed]
97. Lina, G.; Boutite, F.; Tristan, A.; Bes, M.; Etienne, J.; Vandenesch, F. Bacterial competition for human nasal cavity colonization: Role of *Staphylococcal agr* alleles. *Appl. Environ. Microbiol.* **2003**, *69*, 18–23. [CrossRef] [PubMed]
98. Otto, M. *Staphylococcus aureus* toxins. *Curr. Opin. Microbiol.* **2014**, *17*, 32–37. [CrossRef]
99. Blümel, E.; Willerslev-Olsen, A.; Gluud, M.; Lindahl, L.M.; Fredholm, S.; Nastasi, C.; Krejsgaard, T.; Surewaard, B.G.J.; Koralov, S.B.; Hu, T.; et al. Staphylococcal alpha-toxin tilts the balance between malignant and non-malignant $CD4^+$ T cells in cutaneous T-cell lymphoma. *Oncoimmunology* **2019**, *8*, e1641387. [CrossRef]
100. Blümel, E.; Munir Ahmad, S.; Nastasi, C.; Willerslev-Olsen, A.; Gluud, M.; Fredholm, S.; Hu, T.; Surewaard, B.G.J.; Lindahl, L.M.; Fogh, H.; et al. *Staphylococcus aureus* alpha-toxin inhibits $CD8^+$ T cell-mediated killing of cancer cells in cutaneous T-cell lymphoma. *Oncoimmunology* **2020**, *9*, 1751561. [CrossRef]
101. Spaulding, A.R.; Salgado-Pabon, W.; Kohler, P.L.; Horswill, A.R.; Leung, D.Y.M.; Schlievert, P.M. Staphylococcal and streptococcal superantigen exotoxins. *Clin. Microbiol. Rev.* **2013**, *26*, 422–447. [CrossRef] [PubMed]
102. Macias, E.S.; Pereira, F.A.; Rietkerk, W.; Safai, B. Superantigens in dermatology. *J. Am. Acad. Dermatol.* **2011**, *64*, 455–472. [CrossRef]
103. Fraser, J.D.; Proft, T. The bacterial superantigen and superantigen-like proteins. *Immunol. Rev.* **2008**, *225*, 226–243. [CrossRef] [PubMed]
104. Belkaid, Y.; Tamoutounour, S. The influence of skin microorganisms on cutaneous immunity. *Nat. Rev. Immunol.* **2016**, *16*, 353–366. [CrossRef]
105. Krejsgaard, T.; Willerslev-Olsen, A.; Lindahl, L.M.; Bonefeld, C.M.; Koralov, S.B.; Geisler, C.; Wasik, M.A.; Gniadecki, R.; Kilian, M.; Iversen, L.; et al. Staphylococcal enterotoxins stimulate lymphoma-associated immune dysregulation. *Blood* **2014**, *124*, 761–770. [CrossRef] [PubMed]
106. Nisini, R.; Matricardi, P.M.; Fattorossi, A.; Biselli, R.; D'amelio, R. Presentation of superantigen by human T cell clones: A model of T-T cell interaction. *Eur. J. Immunol.* **1992**, *22*, 2033–2039. [CrossRef]
107. Helft, J.; Jacquet, A.; Joncker, N.T.; Grandjean, I.; Dorothée, G.; Kissenpfennig, A.; Malissen, B.; Matzinger, P.; Lantz, O. Antigen-specific T-T interactions regulate CD4 T-cell expansion. *Blood* **2008**, *112*, 1249–1258. [CrossRef]
108. Willerslev-Olsen, A.; Gjerdrum, L.M.R.; Lindahl, L.M.; Buus, T.B.; Pallesen, E.M.H.; Gluud, M.; Bzorek, M.; Nielsen, B.S.; Kamstrup, M.R.; Rittig, A.H.; et al. *Staphylococcus aureus* Induces Signal Transducer and Activator of Transcription 5—Dependent miR-155 Expression in Cutaneous T-Cell Lymphoma. *J. Invest. Dermatol.* **2021**, *141*, 2449–2458. [CrossRef]
109. Willerslev-Olsen, A.; Buus, T.B.; Nastasi, C.; Blümel, E.; Gluud, M.; Bonefeld, C.M.; Geisler, C.; Lindahl, L.M.; Vermeer, M.; Wasik, M.A.; et al. *Staphylococcus aureus* enterotoxins induce FOXP3 in neoplastic T cells in Sézary syndrome. *Blood Cancer J.* **2020**, *10*, 57. [CrossRef]
110. Beissert, S.; Schwarz, A.; Schwarz, T. Regulatory T Cells. *J. Investig. Dermatol.* **2006**, *126*, 15–24. [CrossRef] [PubMed]
111. Tett, A.; Pasolli, E.; Farina, S.; Truong, D.T.; Asnicar, F.; Zolfo, M.; Beghini, F.; Armanini, F.; Jousson, O.; De Sanctis, V.; et al. Unexplored diversity and strain-level structure of the skin microbiome associated with psoriasis. *NPJ Biofilms Microbiomes* **2017**, *3*, 14. [CrossRef]
112. Tokura, Y.; Yagi, H.; Ohshima, A.; Kurokawa, S.; Wakita, H.; Yokote, R.; Shirahama, S.; Flirukawa, F.; Takigawa, M. Cutaneous colonization with staphylococci influences the disease activity of Sézary syndrome: A potential role for bacterial superantigens. *Br. J. Dermatol.* **1995**, *133*, 6–12. [CrossRef]
113. Lindahl, L.M.; Willerslev-Olsen, A.; Gjerdrum, L.M.R.; Nielsen, P.R.; Blümel, E.; Rittig, A.H.; Celis, P.; Herpers, B.; Becker, J.C.; Stausbøl-Grøn, B.; et al. Antibiotics inhibit tumor and disease activity in cutaneous T-cell lymphoma. *Blood* **2019**, *134*, 1072–1083. [CrossRef] [PubMed]

114. Lindahl, L.M.; Iversen, L.; Ødum, N.; Kilian, M. *Staphylococcus aureus* and Antibiotics in Cutaneous T-Cell Lymphoma. *Dermatology* **2021**, *7*, 1–3. [CrossRef]
115. Emge, D.A.; Bassett, R.L.; Duvic, M.; Huen, A.O. Methicillin-resistant *Staphylococcus aureus* (MRSA) is an important pathogen in erythrodermic cutaneous T-cell lymphoma (CTCL) patients. *Arch. Dermatol. Res.* **2020**, *312*, 283–288. [CrossRef] [PubMed]
116. Lewis, D.J.; Holder, B.B.; Duvic, M. The "Duvic regimen" for erythrodermic flares secondary to *Staphylococcus aureus* in mycosis fungoides and Sézary syndrome. *Int. J. Dermatol.* **2018**, *57*, 123–124. [CrossRef]
117. Ansell, S.M. Non-Hodgkin lymphoma: Diagnosis and treatment. *Mayo Clin. Proc.* **2015**, *90*, 1152–1163. [CrossRef] [PubMed]
118. Stadler, R.; Scarisbrick, J.J. Maintenance therapy in patients with mycosis fungoides or Sézary syndrome: A neglected topic. *Eur. J. Cancer* **2021**, *142*, 38–47. [CrossRef]
119. Molloy, K.; Jonak, C.; Woei-A-Jin, F.J.S.H.; Guenova, E.; Busschots, A.M.; Bervoets, A.; Hauben, E.; Knobler, R.; Porkert, S.; Fassnacht, C.; et al. Characteristics associated with significantly worse quality of life in mycosis fungoides/Sézary syndrome from the prospective cutaneous lymphoma international prognostic index (PROCLIPI) study. *Br. J. Dermatol.* **2020**, *182*, 770–779. [CrossRef] [PubMed]
120. Grice, E. The skin microbiome: Potential for novel diagnostic and therapeutic approaches to cutaneous disease. *Semin. Cutan. Med. Surg.* **2014**, *33*, 98–103. [CrossRef]
121. Nakatsuji, T.; Hata, T.R.; Tong, Y.; Cheng, J.Y.; Shafiq, F.; Butcher, A.M.; Salem, S.S.; Brinton, S.L.; Rudman Spergel, A.K.; Johnson, K.; et al. Development of a human skin commensal microbe for bacteriotherapy of atopic dermatitis and use in a phase 1 randomized clinical trial. *Nat. Med.* **2021**, *27*, 700–709. [CrossRef] [PubMed]
122. Oh, J.; Byrd, A.L.; Park, M.; Kong, H.H.; Segre, J.A. Temporal stability of the human skin microbiome. *Cell* **2016**, *165*, 854–866. [CrossRef]
123. Grice, E.A.; Kong, H.H.; Conlan, S.; Deming, C.B.; Davis, J.; Young, A.C.; Bouffard, G.G.; Blakesley, R.W.; Murray, P.R.; Green, E.D.; et al. Topographical and temporal diversity of the human skin microbiome. *Science* **2009**, *324*, 1190–1192. [CrossRef]
124. Costello, E.K.; Lauber, C.L.; Hamady, M.; Fierer, N.; Gordon, J.I.; Knight, R. Bacterial community variation in human body habitats across space and time. *Science* **2009**, *326*, 1694–1697. [CrossRef] [PubMed]
125. Poore, G.D.; Kopylova, E.; Zhu, Q.; Carpenter, C.; Fraraccio, S.; Wandro, S.; Kosciolek, T.; Janssen, S.; Metcalf, J.; Song, S.J.; et al. Microbiome analyses of blood and tissues suggest cancer diagnostic approach. *Nature* **2020**, *579*, 567–574. [CrossRef] [PubMed]

3 Publication 2: The skin microbiome stratifies patients with cutaneous T cell lymphoma and determines event-free survival

Licht, P.*, Dominelli, N.*, Kleemann, J., Pastore, S., Müller, E.-S., Haist, M., Hartmann, K. S., Stege, H., Bros, M., Meissner, M., Grabbe, S., Heermann, R. & Mailänder, V. The skin microbiome stratifies patients with cutaneous T cell lymphoma and determines event-free survival. *npj Biofilms Microbiomes* **10,** 74 (2024). doi: 10.1038/s41522-024-00542-4

* denotes shared first authorship

Full-text link: https://www.nature.com/articles/s41522-024-00542-4

Supplementals: https://static-content.springer.com/esm/art%3A10.1038%2Fs41522-024-00542-4/MediaObjects/41522_2024_542_MOESM2_ESM.pdf

My contribution to this publication is detailed in the section *Contributions to Publications 1, 2, and 3*.

npj | biofilms and microbiomes

Article

Published in partnership with Nanyang Technological University

https://doi.org/10.1038/s41522-024-00542-4

The skin microbiome stratifies patients with cutaneous T cell lymphoma and determines event-free survival

Philipp Licht[1,7] ✉, Nazzareno Dominelli[2,7], Johannes Kleemann[3], Stefan Pastore[4,5], Elena-Sophia Müller[2], Maximilian Haist[1], Kim Sophie Hartmann[1], Henner Stege[1], Matthias Bros[1], Markus Meissner[3], Stephan Grabbe[1], Ralf Heermann[2] & Volker Mailänder[1,6] ✉

Mycosis fungoides (MF) is the most common entity of Cutaneous T cell lymphomas (CTCL) and is characterized by the presence of clonal malignant T cells in the skin. The role of the skin microbiome for MF development and progression are currently poorly understood. Using shotgun metagenomic profiling, real-time qPCR, and T cell receptor sequencing, we compared lesional and nonlesional skin of 20 MF patients with early and advanced MF. Additionally, we isolated *Staphylococcus aureus* and other bacteria from MF skin for functional profiling and to study the *S. aureus* virulence factor *spa*. We identified a subgroup of MF patients with substantial dysbiosis on MF lesions and concomitant outgrowth of *S. aureus* on plaque-staged lesions, while the other MF patients had a balanced microbiome on lesional skin. Dysbiosis and *S. aureus* outgrowth were accompanied by ectopic levels of cutaneous antimicrobial peptides (AMPs), including adaptation of the plaque-derived *S. aureus* strain. Furthermore, the plaque-derived *S. aureus* strain showed a reduced susceptibility towards antibiotics and an upregulation of the virulence factor *spa*, which may activate the NF-κB pathway. Remarkably, patients with dysbiosis on MF lesions had a restricted T cell receptor repertoire and significantly lower event-free survival. Our study highlights the potential for microbiome-modulating treatments targeting *S. aureus* to prevent MF progression.

Mycosis fungoides (MF) is a lymphoproliferative disorder of skin homing T cells and the most common entity of the heterogenous group of cutaneous T cell lymphoma (CTCL)[1]. MF patients usually present with multiple lesional areas in the skin that are classified into patches, plaques, and tumours, based on the extent of neoplastic T cell infiltration, the degree of inflammation and disease activity[1,2]. Clinical stages range from IA to IVB and consider, besides the skin lesions, also involvement of extracutaneous sites like the blood compartment[3]. Most patients keep in early-stages for their whole life (IA-IIA), yet up to one third of patients progresses to advanced stages within 10 years after diagnosis. In such cases, the 5-year overall survival drops dramatically from ~80% in early stages to 18% in most advanced stages[4,5] and may be accompanied by dissemination of malignant T cells into other organs[1,2]. Despite a better understanding of CTCL in recent decades, genomic drivers of MF pathogenesis remain elusive[1,2,6–9]. In consequence, there are no effective or sustainable therapies for advanced stage CTCL with the exception of hematopoietic stem cell transplantation, which comes with severe side effects[10]. As cure is not achievable but long-term survival is possible, maintenance of stable disease is aspired[11,12].

Postulated mechanisms of MF pathogenesis include the persistence of viral or bacterial agents from the skin microbiome that maintain chronic T cell expansion and cutaneous inflammation[13,14]. The importance of the skin microbiome for MF pathogenesis has previously been shown in a CTCL mouse model. Here, CTCL progression was attenuated under germ-free conditions and aggravated in the presence of microbiota[15]. In addition, systemic antibiotic therapy of MF patients sometimes leads to remission[16–18], and a number of studies suggest that *Staphylococcus aureus* can facilitate MF progression[19,20]. However, *S. aureus* is also a commensal of the physiological skin flora in healthy individuals[21] and not all MF patients benefit from *S.*

[1]University Medical Centre Mainz, Department of Dermatology, Mainz, Germany. [2]Johannes Gutenberg-University, Institute of Molecular Physiology (imP), Biocenter II, Microbiology and Biotechnology, Mainz, Germany. [3]University Hospital Frankfurt, Department of Dermatology, Venerology and Allergology, Frankfurt am Main, Germany. [4]University Medical Centre Mainz, Institute of Human Genetics, Mainz, Germany. [5]Johannes Gutenberg-University, Institute of Pharmaceutical and Biomedical Sciences, Mainz, Germany. [6]Max Planck Institute for Polymer Research, Mainz, Germany. [7]These authors contributed equally: Philipp Licht, Nazzareno Dominelli. ✉e-mail: plicht@uni-mainz.de; mailaend@mpip-mainz.mpg.de

aureus eradication[18,22]. Therefore, we hypothesized that MF patients have a more significant disturbance of the skin microbiome beyond the mere presence of pathogenic microbes like *S. aureus*.

So far, several reports characterized the MF skin microbiome[23–27] and indicated that (a) a destabilized microbiome and[23,28] (b) the abundance of certain microbial genera like *Cutibacteria* or *Staphylococci*[24,25] might be associated with disease severity. However, statistical significance was largely not reached, likely because of small sample sizes[24], characterization approaches that lacked resolution at the microbial species level, or because samples were not categorized based on clinical or lesional stages[28].

In this study, we investigated the role of the skin microbiome for MF pathogenesis in 20 patients with early- and advanced-stage MF using metagenomic sequencing, RT-qPCR and T cell receptor sequencing (TCRseq). We show that a subgroup of patients exhibited a substantial dysbiosis on MF lesions with concomitant outgrowth of *S. aureus* on plaque (termed ΔSA-positive) as compared to nonlesional skin, while the other subgroup had a balanced microbiome on these lesions (termed ΔSA-neutral). The perturbations in the former group might be caused by ectopic antimicrobial peptides eradicating the normal skin flora. While in the ΔSA-neutral subgroup physiological microbes with anti-*S. aureus* activity accumulated, the ΔSA-positive subgroup was dominated by *S. aureus*. Clinical isolate of this species showed increased adaptation to AMPs, which likely contributed to its outgrowth. Furthermore, *S. aureus* strains from lesional skin showed resistance towards common antibiotics and were highly virulent, thereby evading the host immune response and assaulting the T cell receptor repertoire. In addition, we observed a potential gain-of-function mutation in the virulence factor *spa* possibly rendering it highly potent to activate the NF-κB axis, a frequently overactivated feature in MF patient subgroups with progressive disease[29–31]. In accordance, we observed considerably reduced event-free survival in the ΔSA-positive subgroup. Our study highlights the importance of the skin microbiome for MF pathogenesis, thus opening new options for the treatment of MF.

Results

Characteristics of patient cohort and clinical specimens

To investigate the microbiome on MF lesions, we analysed metagenomic samples from patches (n = 19), plaques (n = 15) and nonlesional skin (n = 31) of 20 MF patients (8 females, 12 males) recruited from two skin cancer centres in Germany (Mainz, n = 14 patients and Frankfurt, n = 6 patients). Nonlesional skin from the contralateral body site of the same patients served as controls. Clinical samples were collected from patients with MF stages IA – IIB, with 15 patients displaying early-stage MF (stages IA–IIA), and 5 patients suffering from advanced-stage MF (IIB). We did not include tumour-stage lesions because these often ulcerate and might thereby offer a unique microbial habitat due to their moist wound characteristic[1,32]. The mean age at sampling was 66.4 ± 11.7 years, and the mean age at first diagnosis of MF was 60 ± 11.2 years. Patients were treated with common therapy (Table 1). In addition to metagenomic samples, that were collected for the entire patient cohort, we obtained skin punch biopsies from lesional and adjacent skin, as well as peripheral blood in a subset of patients. RT-qPCR (N = 24) was performed from the skin punch biopsies to study expression levels of antimicrobial peptides (AMPs). T cell receptor sequencing (TCRseq) was carried out on a total of 16 skin samples and 5 blood samples, obtained from 10 patients. Living bacterial isolates were picked from plaque and nonlesional skin of one patient (Pat1) and from healthy subjects. The patients clinical course including events (defined as death, start of new therapy and disease progression) and the time from observation start to event (TTE) were assessed. A summary of the patient characteristics is given in Table 1.

Analysis of rarefied microbial reads shows a dysbiosis on lesional MF skin

In a first analysis we clustered taxonomic profiles that were generated from rarefied metagenomic samples (Fig. 1a). As expected, clustering showed a strong grouping of specimens derived from the same patient, which justified our approach of using intra-patient controls[21]. By contrast, we observed no significant differences in the microbiome composition between the two study centres, and therefore did not consider these in subsequent analysis (see also Supplementary Fig. 1d). Overall, lesional samples appeared to have a lower microbial diversity compared to nonlesional controls. Remarkably, some patch and plaque samples from different patients clustered together, showing that the microbiome on lesional skin was altered in a uniform manner. To test whether the composition of the microbial community on patches and plaques differed from that of nonlesional skin, we calculated Shannon indices and Bray-Curtis dissimilarities from rarefied microbial reads. The α-diversity was reduced on MF lesions, with patch stage showing the strongest effect, but significance was not reached (Fig. 1b). However, β-diversity revealed a significant instability of the microbiome on MF lesions that increased with exacerbation of MF lesions (Fig. 1c). Moreover, α- and β-diversity of plaque skin exhibited a bimodal distribution. Several samples showed a strongly decreased Shannon Index and an affected microbiome stability, whereas others resembled the diversity-metrics of nonlesional skin. Notably, except for age, no significant associations with other demographics of the study cohort were found (Supplementary Fig. 1). We found a slightly, rather heterogenous decrease in microbial diversity with increasing age. Decreased microbial diversity is a known feature in elderly people[33] and was therefore to be expected. Interestingly, elder people were described to have reduced colonization with *S. aureus*[34]. Together, these results showed that dysbiosis is a common feature of MF lesions, which increased with exacerbation.

S. aureus colonization stratifies the MF patient cohort into two subgroups with distinct microbiome patterns

To understand which species accounted for the observed microbiome patterns on lesional skin, we set up a generalized linear mixed model (GLMM) using MaAsLin2[35]. We tested for differences in the abundance of microbial species on patches and plaques compared to nonlesional skin while adjusting for sequencing depth and the individuality of the patient's microbiome. Using this approach, we found that *S. aureus* was highly enriched on plaque while all other significantly associated microbial species were extremely reduced on patch and plaque (Fig. 2a, Supplementary Table 3). Among them were *S. hominis*, *S. epidermidis* and *Cutibacterium acnes*. These commensals can control *S. aureus* growth in other inflammatory skin conditions[36–39] and confer decreased release of inflammatory cytokines as well as recruitment of leucocytes in skin wounding healing[40].

When plotting the relative abundance of *S. aureus* patient-wise and differentiating between lesional stages, we noted a patient stratification into two subgroups: In one subgroup, the relative abundance of *S. aureus* did not change from nonlesional skin to plaque stage. In the other subgroup however *S. aureus* abundance substantially increased from nonlesional skin to plaque stage. We therefore referred to the first group as Δ *S. aureus*-neutral (ΔSA-neutral) and to the other group as Δ *S. aureus*-positive (ΔSA-positive) (Fig. 2b). Strikingly, when stratifying the α-diversity (Shannon Index) to the defined patient subgroups, the observed bimodality resolved: ΔSA-positive patients exhibited a significantly reduced α-diversity on plaques, and ΔSA-neutral patients in turn had a plaque microbiome which was as diverse as that on nonlesional skin (Fig. 2c). Likewise, the three commensals with anti-*S. aureus* activity were more prominent on plaques of ΔSA-neutral patients, albeit this association was above statistical significance ($p = 0.05–0.14$). This might be attributed to the fact that every plaque lesion of ΔSA-neutral patients was dominated by only one of the three commensals with anti-*S. aureus* action while the other two were minor constituents of the skin flora (Fig. 2d–f). When compiling *S. hominis*, *S. epidermidis* and *C. acnes*, *S. aureus*-inhibiting microbes were significantly more abundant on plaque than on nonlesional skin of ΔSA-neutral patients (Fig. 2g).

Increased and sustained expression of cutaneous antimicrobial peptides could lead to skin dysbiosis

The skin expresses a diverse repertoire of antimicrobial peptides (AMPs) to control microbial colonization and ensure epithelial integrity[41,42]. Under

https://doi.org/10.1038/s41522-024-00542-4

Table 1 | Patient characteristics, therapy regimen and clinical outcomes of the study cohort

Patient ID	Study Site	Sex	Age at Sampling (years)	Clinical Stage at Sampling	Metagenomics:Stage of Lesions (Body Site)	RT-qPCR: Stage of Lesions (Body Site)	TCRseq:Tissues included	ΔSA-subgroup	Therapy	Event	TTE (months)	Follow-up Time (months)
Pat1	MZ	f	81	IA	Plaque (hip), Patch (forearm)	Plaque (hip)	Skin (Plaque), Blood	positive	PUVA, Mechlorethamine	Yes	2.60	17.56
Pat2	MZ	f	57	IB	Plaque (thigh), Plaque (abdomen)	NA	NA	neutral	PUVA, UVB, topical steroids, Pimecrolimus, MTX, Bexarotene, Mogamulizumab	Yes	18.41	18.41
Pat3	MZ	f	47	IB	Patch (thigh)	Patch (thigh)	NA	neutral	topical steroids	Censored	Censored	17.95
Pat4	MZ	m	70	IIB	Plaque (upper back),Plaque (flank)	Plaque (upper back)	Skin (Plaque and nonlesional), Blood	positive	topical steroids, Bexarotene, Mogamulizumab, RTx	Yes	0.92	9.99
Pat5	MZ	f	73	IB	Patch (thigh),Patch (forearm)	Patch (thigh)	Skin (Patch and nonlesional)	neutral	topical steroids	Yes	13.87	17.10
Pat6	MZ	f	81	IA	Patch (breast)	Patch (breast)	Skin (Patch and nonlesional)	neutral	topical steroids, Mechlorethamine	Censored	Censored	15.55
Pat7	MZ	m	54	IB	Patch (forearm), Plaque (flank)	Plaque (flank)	Skin (Plaque and nonlesional)	neutral	PUVA, PEG-IFNα	Censored	Censored	16.11
Pat8	MZ	m	82	IIB	Plaque (head, parietal), Patch (upper back)	Patch (upper back)	Skin (Patch), Blood	positive	topical steroids, MTX, RTx	Yes	2.53	2.53
Pat9	MZ	m	63	IB	Plaque (forearm)	Plaque (forearm)	Skin (Plaque)	neutral	Topical steroids, PUVA, RTx	Yes	6.41	14.27
Pat10	MZ	m	49	IB	Patch (gluteus right), Patch (gluteus left)	Patch (gluteus left)	Skin (Patch)	neutral	NA	LFU	LFU	LFU
Pat11	MZ	m	61	IIB	Patch (wrist)	NA	NA	neutral	NA	LFU	LFU	LFU
Pat12	MZ	m	88	IA	Patch (abdomen), Patch (thigh)	Patch (thigh)	Skin (Patch and nonlesional), Blood	neutral	no special therapy, only moisturizing cremes	Censored	Censored	11.51
Pat13	MZ	m	66	IB	Patch (lower leg, front), Patch (lower leg, back)	Patch (lower leg, back)	NA	neutral	topical steroids	Censored	Censored	11.51
Pat14	MZ	m	62	IB	Plaque (forearm), Plaque (lower leg, front)	Plaque (lower leg, front)	Skin (Plaque and nonlesional), Blood	neutral	topical steroids, Silver iodide	Censored	Censored	11.05
Pat15	FFM	f	73	IB	2x Plaque (lower leg, front and gluteus)	NA	NA	positive	MTX, RTx	Yes	2.83	11.57
Pat16	FFM	f	58	IA	Plaque (scapula)	NA	NA	positive	MTX, Bexarotene	Yes	4.87	11.51
Pat17	FFM	m	83	IIB	2x Patch (hip and rips)	NA	NA	neutral	Bexarotene	Yes	7.00	7.00
Pat18	FFM	f	61	IB	2x Patch (thigh dorsal & abdominal)	NA	NA	neutral	no special therapy	Censored	Censored	9.99
Pat19	FFM	m	54	IIB	Patch (shoulder), Plaque (thigh)	NA	NA	neutral	Bexarotene	Censored	Censored	9.67
Pat20	FFM	m	65	IB	Plaque (forearm)	NA	NA	neutral	Bexarotene	Censored	Censored	11.11

f female, m male, *MZ* Mainz, Germany; *FFM* Frankfurt am Main, Germany; *PUVA* psoralen and UVA, *MTX* methotrexate, *PEG-IFNα* pegylated interferon alpha, *RTx* radiation therapy, *NA* not available, *LFU* lost to follow-up, *TTE* Time To Event.

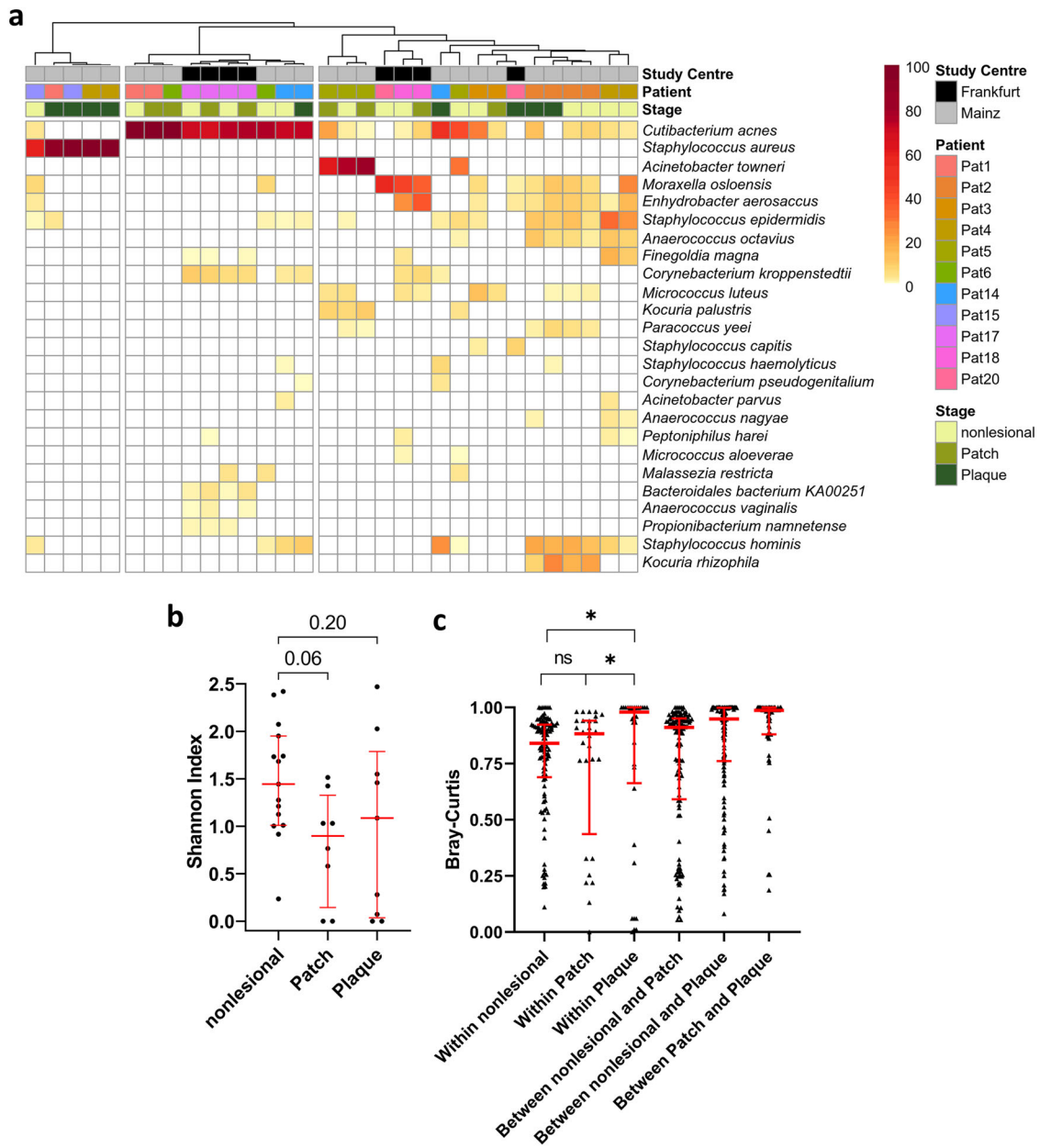

Fig. 1 | Analysis of rarefied metagenomic profiles. a Clustered taxonomic profiles of the 25 most abundant species present on nonlesional skin, patch, and plaque. Reads were rarefied to common depth prior to assignment of taxonomy. $n = 32$ metagenomic samples were left after rarefaction and included in the clustered heatmap. Displayed is the relative abundance in percent. **b** α-diversity (Shannon-Index) of $n = 32$ rarefied metagenomic samples (15 nonlesional, 8 patch, 9 plaque), one-way ANOVA corrected for multiple comparisons (Dunnett's test), dot plots with median and interquartile range. **c** β-diversity (Bray-Curtis) dissimilarities, pairwise PERMANOVA, dot plots with median and interquartile range. 2 degrees of freedom in **b** and **c**.

steady-state conditions, AMPs are constitutively produced at low rates but increase upon injury or inflammation[41,42]. MF is characterized by an inflammatory microenvironment and lesions might persist over long time periods[43]. In order to evaluate whether cutaneous AMPs may have contributed to the skin dysbiosis we obtained skin punch biopsies from the same MF lesions sampled for metagenomic profiling and analysed AMP expressions levels using RT-qPCR. Adjacent nonlesional skin served as control. RNA expression levels of the AMPs *hBD2*, *hBD3*, *S100A7*, and the calprotectin forming *S100A8* and *S100A9* were significantly increased in MF lesions but did not significantly differ between patch and plaque stage (Fig. 3a). This observation is consistent with the fact that these AMPs are known to be regulated by microbial recognition mechanisms[42,44]. In contrast, *hBD1* and *LL-37* are known to be constitutively expressed rather than inducible[42,44], which is in agreement with our results (Fig. 3a).

Next, we examined whether ectopic AMP levels affect growth of cutaneous bacterial species found on MF lesions. Clinical isolates of *S. aureus* and *S. hominis* were picked from plaque skin of Pat1 (termed *S. aureus* MFMZ1 and *S. hominis* MFMZ1, respectively). *S. aureus* (EM01) and *S. epidermidis* (MV01) picked from 2 healthy subjects served as negative controls. Another clinical *S. aureus* isolate historically picked from pleural fluid back in 1884 (*S. aureus* Rosenbach 1884, strain DSM11823) served as positive control[45]. All bacterial samples were exposed to increasing concentrations of hBD1, hBD3, LL-37 and calprotectin (a heterodimer consisting of S100A8 and S100A9).

Clinical isolates *S. aureus* MFMZ1, *S. hominis* MFMZ1 and *S. aureus* DSM 11823 survived at low concentrations of hBD3 (1 µg), while healthy subject-derived *S. epidermidis* MV01 was eradicated. All strains survived at low concentrations of LL-37 (1 µg, Fig. 3b). This was to be expected, because

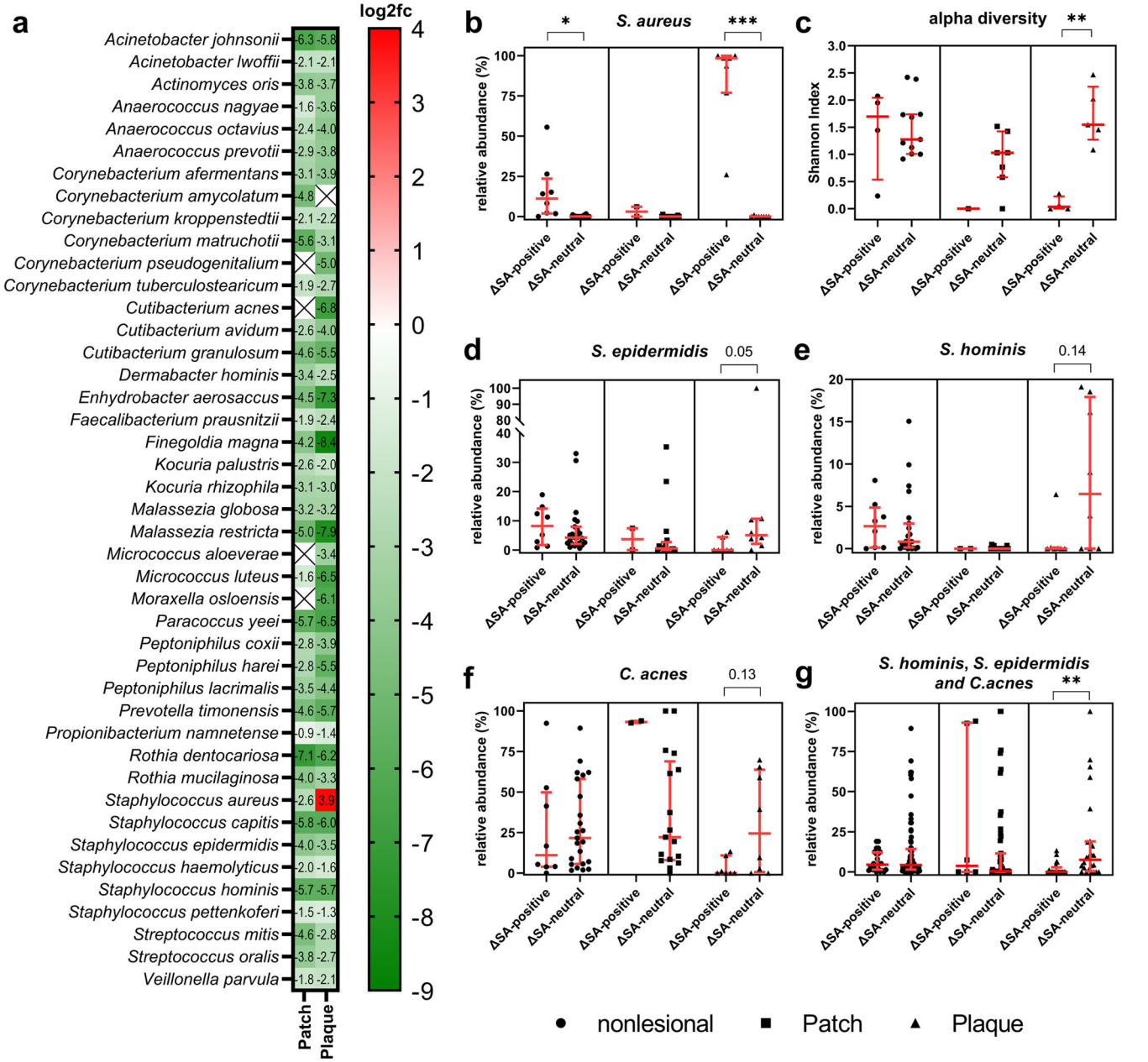

Fig. 2 | Differential abundance analysis of microbial species for N = 65 metagenomic samples. a log2 fold-change (log2fc) of microbial species present on patch (n = 19) and plaque (n = 15) compared to nonlesonial skin (n = 31). **b** *S. aureus* relative abundance increases from nonlesional skin to plaque in the ΔSA-positive subgroup, while this is not the case for the other subgroup (ΔSA-neutral). **c–g**, Shannon-Index and relative abundances of bacteria stratified to ΔSA-subgroups. Shannon Index is based on n = 32 metagenomic samples rarefied to common depth as in Fig. 1b. Depicted are dot plots with median and interquartile range, Kruskal-Wallis test (**b**, **d–g**) or one-way ANOVA with correction for multiple comparisons.

LL-37 was constitutively expressed in nonlesional skin and was also not induced by the disease (Fig. 3a). Hence, bacterial skin colonization requires resistance to LL-37 at least at low concentrations. Interestingly, *S. aureus* MFMZ1 showed the least reduction in survival at high concentrations of hBD3 and LL-37 compared to all other strains tested. (Fig. 3c). Furthermore, exposure to calprotectin resulted in decreased survival of only *S. hominis* MFMZ1, a bacterium with potential anti-*S. aureus* properties[36–40]. Surprisingly, hBD1 had a paradoxical effect on *S. aureus* MFMZ1, even augmenting its survival, while the survival of all other tested strains remained unchanged or decreased (Fig. 3c).

These data demonstrate that clinical isolates of *S. aureus*, and particularly that obtained from plaque of an MF patient, have considerable survival advantages under ectopic AMP application. As neoplastic T cells and reactive leucocyte infiltrate accumulate in MF lesions over time, plaques can be expected to persist longer than patches and, accordingly, the microbiome on plaques is exposed longer to high AMP levels than the microbiome on patches (and nonlesional skin). Given the fact that skin dysbiosis is most accentuated in patch stage (Fig. 2a), our results collectively indicate that most of the physiological skin flora is eradicated upon onset of increased AMP production. With ongoing persistence of MF lesions and high AMP levels, MF skin commensals eventually adopt to the new environmental conditions and (re-) colonize MF lesions.

MF skin lesions are colonized by distinct *S. aureus* strains that outgrow other MF skin commensals

We next asked why *S. aureus* outgrows only in the ΔSA-positive subgroup. Given the substantial survival advantages of *S. aureus* under high AMP expression levels and the observation of skin dysbiosis exclusively in the

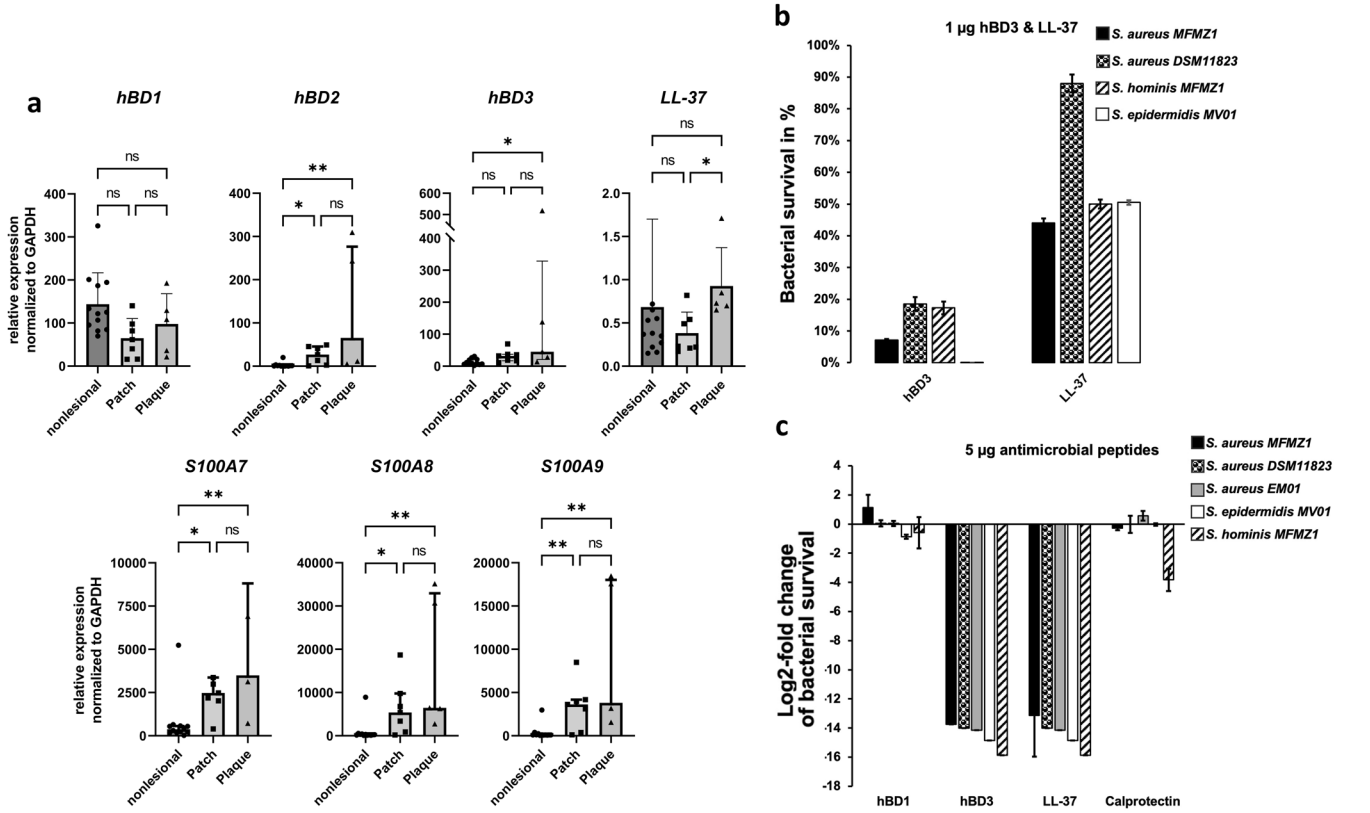

Fig. 3 | Cutaneous AMPs disturb the skin microbiome. a RNA expression level of antimicrobial peptides. Punch biopsies were taken from MF lesions (n = 7 patch, n = 5 plaque) and adjacent nonlesional skin (n = 12). Expression levels were determined with RT-qPCR and normalized to GAPDH. S100A8 and S100A9 together form the heterodimer calprotectin. Depicted are bar plots with median and interquartile range, Kruskal-Wallis test with multiple comparison correction. **b**, **c** Activities of AMPs against Staphylococci isolates. Survival of clinical isolates *S. aureus* MFMZ1 and *S. hominis* MFMZ1, clinical control strain *S. aureus* DSM11823 as well as isolates from healthy subjects *S. aureus* EM01 and *S. epidermidis* MV01 in presence of **b**, 1 µg and **c**, 5 µg AMPs. Bacterial survival was assessed by comparing number of colony forming units (CFU) with and without AMP treatment for each isolate and AMP. Displayed are bacterial survival for three biological replicates in percent (**b**) and log2-fold change (**c**), respectively.

ΔSA-positive subgroup (Fig. 2c), we first reasoned that cutaneous AMP levels of the ΔSA-neutral subgroup would be lower compared to the ΔSA-positive subgroup. Surprisingly, the AMP expression levels did not significantly differ between lesions of ΔSA-neutral and ΔSA-positive patients (Supplementary Fig. 2). There must hence be another factor or event allowing *S. aureus* to accumulate and outgrow competitive commensals. A potential explanation might be that *S. aureus* strains colonizing MF lesions differ from their nonlesional counterparts, since *S. aureus* is a common commensal of human skin flora but also a frequent pathogen in many diseases[21,32]. To test this hypothesis, we used the tool PanPhlAn[46] to profile bacterial strains in the MF microbiome by the presence and absence of genes in the respective species' pangenomes. Dimensionality reduction via principal component analysis (PCA) revealed that strains of *S. hominis, S. epidermidis* and *C. acnes* did not differ between MF lesions and nonlesional skin. In contrast, *S. aureus* strains present on plaques had a unique gene repertoire, clearly demonstrating that lesional *S. aureus* were of a different strain than their nonlesional counterparts (Fig. 4).

In order to validate these observations, we examined whether strain differences seen in the computational analysis could be transferred to the same living isolates tested before. In a disk diffusion assay, *S. aureus* MFMZ1 was considerably more resistant towards antibiotics typically used in the clinic than all other tested strains (Fig. 5). While Pat1-derived *S. epidermidis* MFMZ1 and healthy subject-derived *S. epidermidis* MV01 showed comparable susceptibilities, *S. aureus* MFMZ1 was notably more resistant than its counterpart from healthy skin (*S. aureus* EM01). Remarkably, the other clinical *S. aureus* DSM11823 strain was sensitive towards both β-lactam antibiotics, ampicillin and carbenicillin, as well as gentamycin, whereas *S. aureus* MFMZ1 was not (Fig. 5, Supplementary Table 1). We could further determine that *S. aureus* MFMZ1 was a methicillin resistant *S. aureus* (MRSA) strain, while *S. aureus* EM01 was not (Fig. 5b, c). *S. aureus* MFMZ1 not only demonstrated reduced susceptibility to antibiotics but also exhibited the strongest adaptation to the AMP conditions found on MF skin (Fig. 3b, c). In particular, this strain was not only resistant to hBD1, but its growth was even promoted by the AMP. Given that the other skin bacteria we tested in this assay did not show this effect, and were less resistant to other AMPs, likely provided *S. aureus* with an advantage over other skin commensals on plaques.

Taken together, *S. aureus* present on MF lesions was of a distinct strain that differed from its nonlesional counterpart, probably outcompeting other skin commensals by adapting more effectively to the unique environmental conditions of MF skin.

S. aureus strains on plaque of ΔSA-positive patients are highly virulent

Because *S. aureus* often acts as a pathogen[32], we next evaluated the virulent properties of the microbiome present on MF lesions. Utilizing ShortBRED[47], we profiled the whole metagenome sequencing (WMS) reads against the Virulence Factor Database (VFDB)[48] to detect the presence of virulence factors. Differences in virulence factor abundance between nonlesional skin and MF lesions were evaluated using MaAsLin 2.

Here, we found numerous virulence factors that were significantly more prevalent on plaques (Fig. 6a). Notably, the VFDB and the literature[49–52] link these virulence factors to *S. aureus*, affirming the exclusive increased abundance of this pathogen in plaque stage. Considering that *S.*

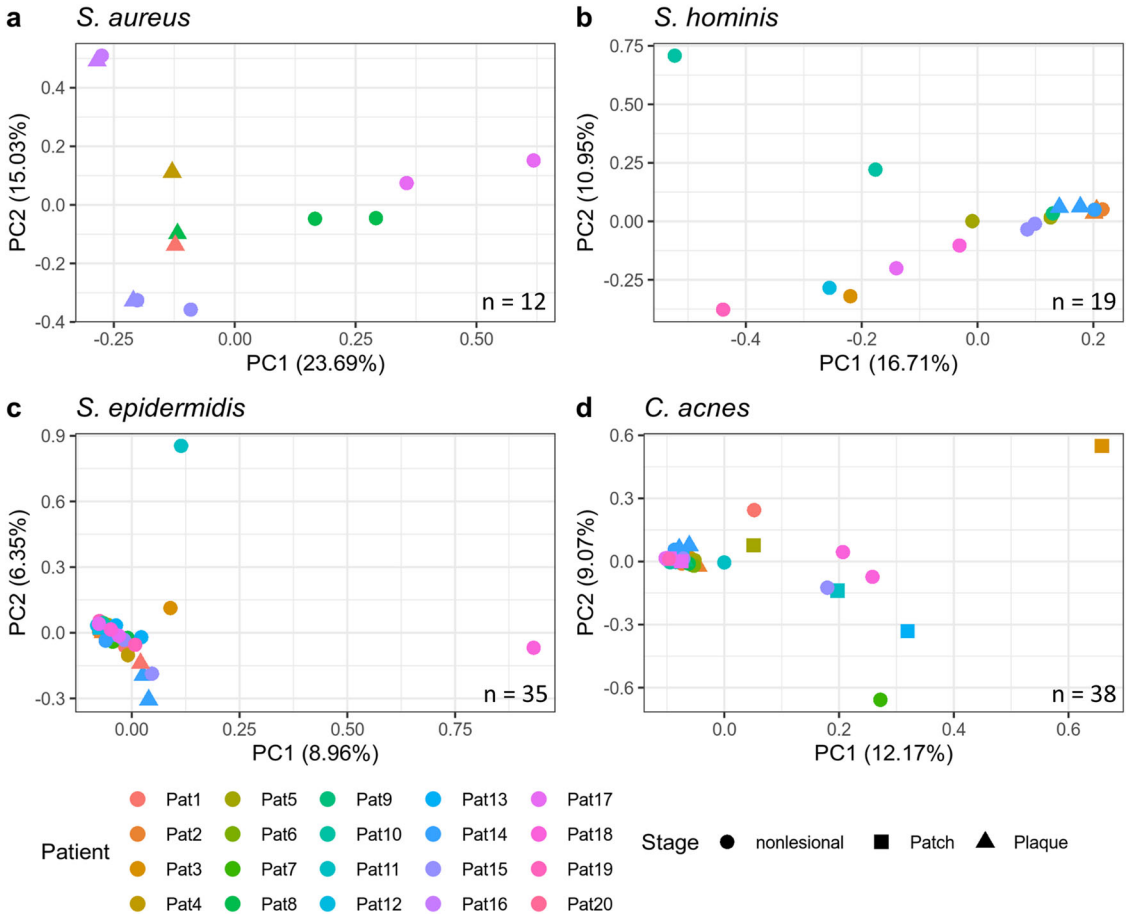

Fig. 4 | PCA of the gene repertoire in strains of four different microbial species present in the skin microbiome of MF patients. Only metagenomic samples with sufficient coverage of the species of interest are shown. S. aureus is the only species that exhibited strain differences between MF lesions and nonlesional skin, with principal component (PC) 1 being the discriminating factor. Pat15 and Pat16 each had the same strain present on plaque and nonlesional skin, indicating that *S. aureus* present on plaque spread into nonlesional areas of the skin (**a**). For *S. hominis* (**b**), *S. epidermidis* (**c**) and *C. acnes* (**d**) no such differences were found.

aureus was only upregulated in the ΔSA-positive subgroup (Fig. 2a, b), it is highly likely that the enriched virulence factors originated from *S. aureus* of ΔSA-positive patients.

Surprisingly, we did not find any superantigens, which are typically associated with disease progression in *S. aureus* infected CTCL patients[17,53–55]. However, we found an enrichment of α-hemolysin (*hly/hla*), another virulence factor of *S. aureus*, which is linked to MF pathogenesis[56,57]. *hly/hla* can form pores in human T cells, causing cellular damage[49]. In the context of MF, it was demonstrated that *hly/hla* preferentially induces cell death in benign T cells over malignant T cells[56] and inhibits cytotoxic T cell mediated killing of malignant T cells[57]. Furthermore, we identified an enrichment of several virulence factors that have not been associated with MF pathogenesis before (Fig. 6a). Most of the *S.* aureus-associated genes are components of larger complexes that orchestrate nutrition, immune evasion, spread of infection and secretion of virulence factors (Supplementary Material 1 provides a comprehensive overview of these virulence factors and their functional properties). In particular, we found a differential enrichment of Immunoglubin G binding protein A (*spa*), along with iron-regulated surface determinant protein A (*isdA*) and type VII secretion system protein D (*esaD*).

Since *isdA* was reported to confer resistance to the AMP hBD2[52], this virulence factor might have enabled *S. aureus* outgrowth on plaque despite the increased RNA-levels of *hBD2* in these lesions (Fig. 3a). An additional factor for *S. aureus* outgrowth may be *esaD*, which encodes a strong bactericidal for other bacteria than *S. aureus*, suppressing growth of competing commensals[58].

Of particular significance was the upregulation of *spa* on plaques: As previously reported, this virulence factor can activate the NF-κB (Nuclear factor kappa-light-chain-enhancer of activated B cells) pathway via tumour-necrosis factor-α (TNF-α) receptor 1 (TNFR1) through conserved IgG binding domains[59–65]. Several studies demonstrated that the TNF-α/NF-κB pathway is dysregulated in a subset of MF patients with poor clinical outcome[29–31], and *spa* could hence be the activating factor. We therefore next investigated *spa* in Pat1-derived isolate *S. aureus* MFMZ1 (*spa*_MFMZ1) and not only confirmed its presence within the genome (Fig. 6b), but also identified mutations via sequencing: Compared to *spa* of the *S. aureus* Newman strain serving as a reference (*spa*_NM, UniProt ID: A0A0H3K686), *spa*_MFMZ1 had an additional octapeptide repeat (Ins373PGKEDNNK) in the conserved IgG binding domain, resulting in a total of 12 repeats (Fig. 6c). It is known that the *spa* IgG binding domain is composed of a variable number of octapeptide repeats and activates inflammatory responses via interaction with the Fc fragment of IgG[66,67]. Strains of *S. aureus* with >7 repeats are generally considered more virulent as they can bind more precisely to the Fc fragment[68,69]. Notably, the IgG binding domain of *spa* also activates TNFR1 signalling through the same octapeptide repeats[59–64] where we detected the mutational insertion. Hence, the mutation-dependently increased number of octapeptide repeats of *spa* in the strain derived from MFMZ1 may enhance spa binding efficacy to TNFR1 and in turn pronouncedly activate the TNF-α/NF-κB axis.

In summary, these results show that *S. aureus* strains on plaque of ΔSA-positive patients were highly virulent and shaped environmental conditions to evade the host immune response, spread infection and may fuel disease

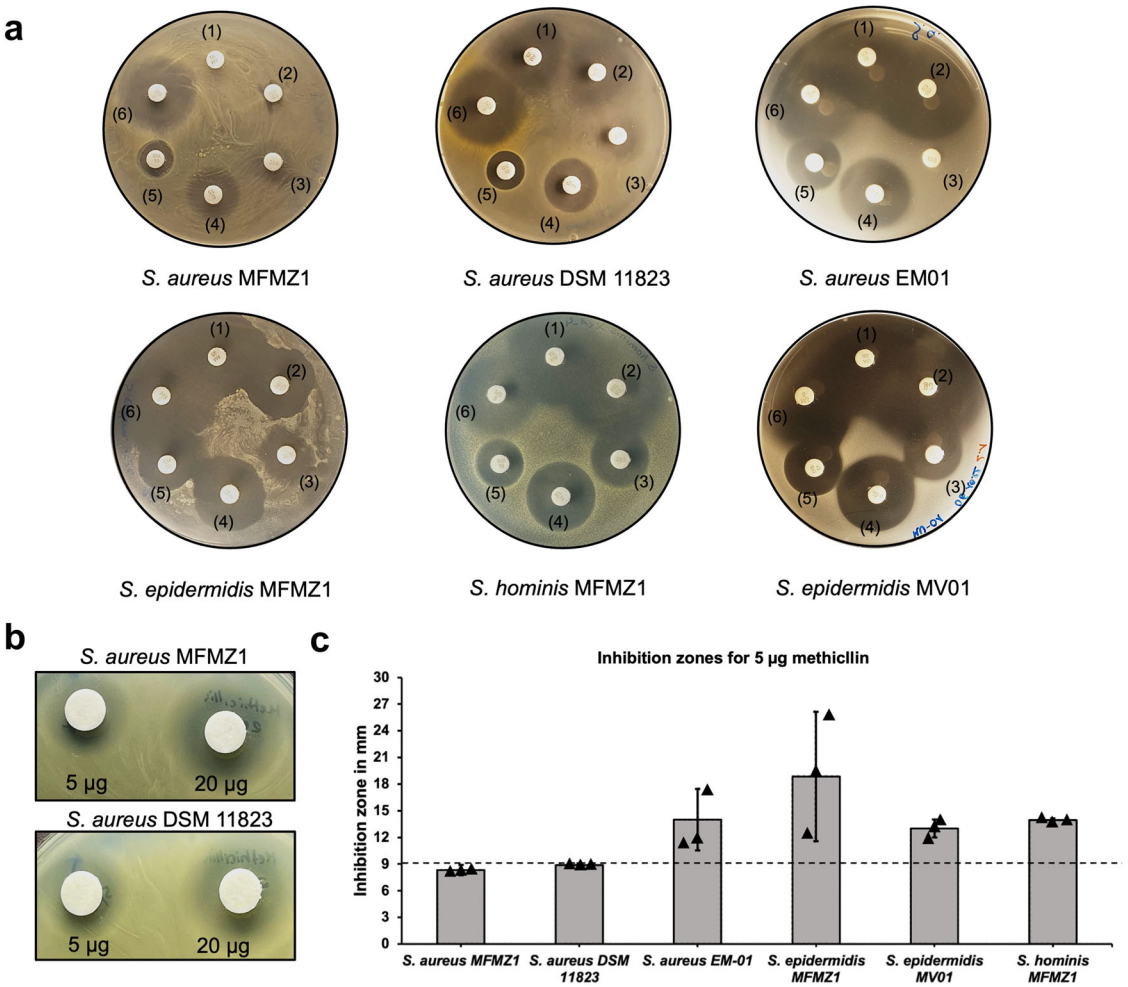

Fig. 5 | *Antibiotic diffusion assay.* The patient derived isolates *S. aureus* MFMZ1, *S. epidermidis* MFMZ1, and *S. hominis* MFMZ1 as well as positive control *S. aureus* DSM11823 and negative control strains derived from healthy patients *S. aureus* EM01 and *S. epidermidis* MV01 were tested on resistance towards a set of commonly used antibiotics in the clinic. **a** The antibiotics were applied using a Sensi-Disk dispenser with (1) 25 µg ampicillin, (2) 100 µg carbenicillin, (3) (23.75 µg) sulfamethoxazol + (1.25 µg) trimethoprim, (4) 15 µg erythromycin, (5) 10 µg gentamycin, and (6) 5 µg novobiocin. **b**, **c** The strains were additionally tested on methicillin resistance using 5 µg and 20 µg methicillin applied on sterile filter disks. The inhibition zone diameter for *S. aureus* MFMZ1 and DSM11823 strains was ≤ 9 mm, which indicates resistance towards methicillin according to the clinical and laboratory standards institute (CLSI[125]).

progression, as deduced from the potential gain-of-function mutation of spa in the MFMZ1 strain.

S. aureus assaults the T cell receptor repertoire and might promote malignancy and dissemination via spa

To assess a potential impact of *S. aureus* and its identified virulence factors on the malignant and benign T cell infiltrate, we further performed T cell receptor (TCR) sequencing in the skin and blood of MF patients. Surprisingly, although one might expect a skewed TCR repertoire in MF lesions due to the expansion of malignant T cells, instead, abundance and diversity increased with lesional stage (Fig. 7a, b). This augmentation might have been caused by tumour infiltrating lymphocytes (TILs)[70] and the expansion of more than just a single malignant clone resulting in oligoclonality[71–73]. Indeed, oligoclonality was detected in most MF lesions (Fig. 7d–k). Intriguingly, the TCR repertoire in plaques of the ΔSA-positive group was reduced (Fig. 7a, b). In addition, gene usage analysis of the T cell receptor β variable (TRBV) revealed that TRBV5-1, which another research paper linked to TILs in MF[74], was strongly expanded in plaque of the ΔSA-negative group but not in plaque of the ΔSA-positive group (Supplementary Fig. 3). We assumed that the reduction of both total TCR repertoire as well as TRBV5-1 in plaque of ΔSA-positive patients could be due to the virulence factor hla. Hla is known to kill benign T cells in MF[56,57], and we found this virulence factor enriched in the ΔSA-positive subgroup (Fig. 6a). Collectively, our data indicate that *S. aureus* affected the balance between malignant T cells and benign tumour infiltrating T cells.

We next examined whether T cells of MF patients were directed against the *S. aureus* virulence factors identified as enriched on plaque (Fig. 6a). Corresponding epitopes were obtained from the Immune Epitope Database (IEDB)[75], or, when not available in the IEDB, computationally predicted for both Major Histocompatibility Complex class I (MHC-I) and II (MHC-II). Binding Scores were calculated for the most abundant TCRs of a given sample and each of the epitopes (obtained and predicted) of *S. aureus* virulence factors. As expected, TCRs in patch, plaque and blood showed a significantly higher affinity for *S. aureus* virulence factors compared to TCRs in nonlesional skin (Fig. 7c). The increased binding affinity in blood and patch might be due to recirculation of benign skin resident T cells being called to sites of inflammation[76,77] as well as the recently described effect of clonal seeding by malignant T cells[71,73,78]. Analogues to the TCR repertoire, the binding affinity of TCRs in ΔSA-positive plaques was lower compared to ΔSA-neutral plaques, probably caused by the virulence factor hla which preferentially kills benign reactive infiltrate over malignant T cells[56,57]. Notably, dominant T cell clones of MF lesions were also detected in nonlesional skin and the blood (Fig. 7d–k). In all tissues tested, the MHC-II epitope of spa was among the epitopes that was recognized most often by

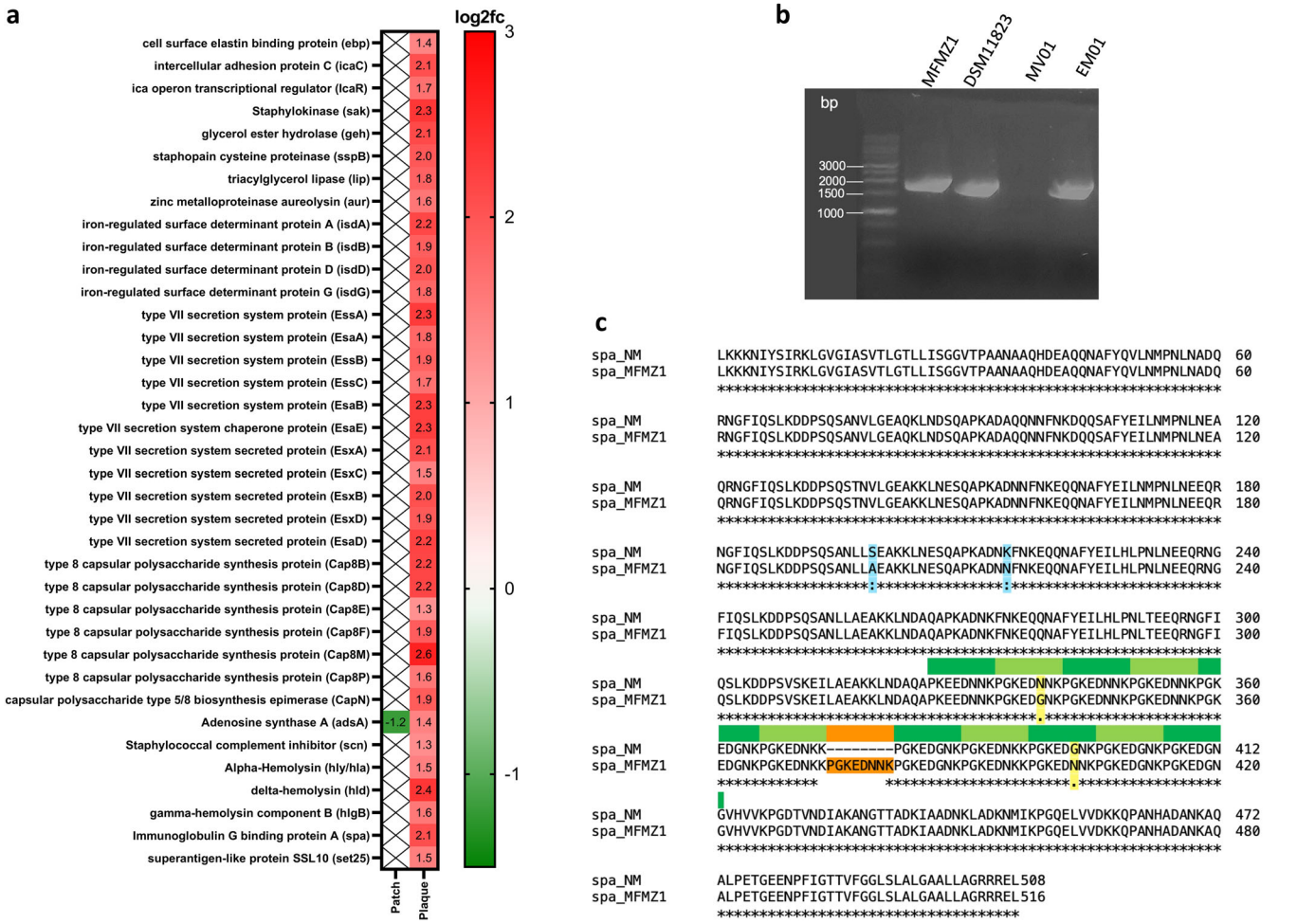

Fig. 6 | Virulence factors of the MF microbiome. a Differential abundance analysis of the virulence gene repertoire. Displayed are log2 fold-change (log2fc) of virolence genes on patch (n = 19) and plaque (n = 15) compaired to nonlesional (n = 31). **b** Agarose gel electrophoresis of spa genes from Staphylococci isolates after PCR amplification. From left to right: spa from S. aureus MFMZ1, *S. aureus* DSM11823 (positive control), *S. epidermidis* MV01 (negative control), and *S. aureus* EM01. All detected spa genes are located between the 1500 and 2000 bp line. **c** ClustalΩ alignment of spa from *S. aureus* MFMZ1 (spa_MFMZ1) with spa from the *S. aureus* Newman strain (spa_NM, UniProt ID: A0A0H3K686). spa_MFMZ1 was found to be 24 bp/8 aa longer than spa_NM (1551 bp/516 aa vs. 1527 bp/508 aa) due to the insertion of an additional octapeptide repeat (marked in orange) in the conserved IgG binding domain (marked in green). Furthermore, amino acid variations could be detected in the B-domain (S199A, K215N, marked light blue) and in one of the octapeptide domains of spa_MFMZ1 (N349K, G403N, marked in yellow).

TCRs (Supplementary Fig. 4). MHC-II interacts with the TCR of CD4 + T cells, which is the T cell subset that undergoes malignant transformation in MF[79]. As already outlined above, spa is known to activate NF-κB and to trigger inflammation[59,60,63–65], typical characteristics of progressive MF[2]. Collectively, our results indicate that the plaque-enriched *S. aureus* virulence factors, and of these especially spa, were recognized by T cells in MF lesions and that those clones might disseminate into other tissue compartments, thus driving pathogenesis.

ΔSA-positive patients have an inferior event-free survival

We demonstrated that *S. aureus* strains on MF lesions differed from non-lesional counterparts being highly virulent, and dominated the plaque microbiome of ΔSA-positive patients, which had a comprised TCR repertoire that specifically recognized *S. aureus* virulence factors. Hence, the ΔSA-positive subgroup might undergo a more severe course of disease. Therefore, the clinical response of the MF study cohort was monitored while patients were treated with approved MF therapy adequate to the patients' individual situation. Event-free survival (EFS) was evaluated using Kaplan-Meier analysis. Events were defined as death, start of new therapy and disease progression. Two out of 20 patients were lost to follow-up (LFU) for clinical assessment and therefore excluded from analysis. 9 out of 18 patients experienced an event during the observation period (2.5–18.4 months, median 11.5). Metrics are summarized in Table 1.

Patients in the ΔSA-positive group exhibited a strikingly inferior EFS with a hazard ratio of 11.91 (95% confidence interval 1.44 to 98.36) (Fig. 8). Median EFS was 2.6 months in the ΔSA-positive group and not reached in the ΔSA-neutral group. No EFS associations were found for age and gender, however, EFS was significantly lower for patients treated systemically and when undergoing radiotherapy, respectively (Supplementary Fig. 5a, b). This is to be expected as these lines of therapy are chosen in advanced-stage or refractory early-stage MF[80], and are thus associated with poor clinical course[4]. The cohort analysed consists of 14 patients in early-stage (IA-IIA) MF and 4 patients in advanced-stage (IIB) MF. Since advanced-stage MF tends to progress faster than early-stages[4], joining clinical stages should be considered with caution. Notably, the four 4 stage IIB MF patients were distributed equally between the ΔSA-subgroups (two each) and independent Kaplan-Meier analysis of early- and advanced stage MF patients yielded similar results (Supplementary Fig. 5d, e) as the joint analysis depicted in Fig. 8.

This demonstrates that the skin-microbiome stratifies MF patients into two subgroups with distinct clinical outcomes, opening-up the potential of new treatment regimens.

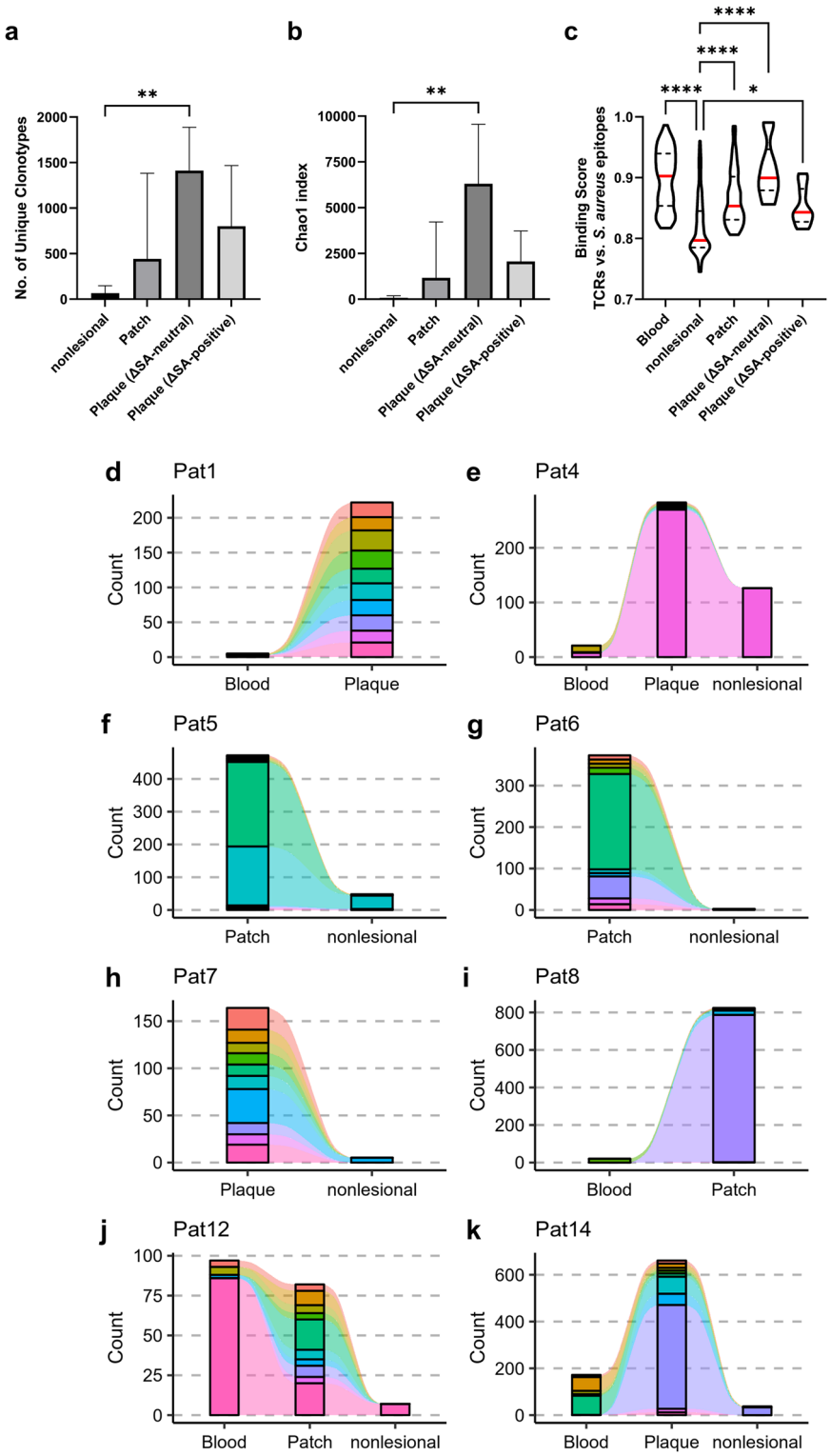

Fig. 7 | The TCR repertoire is affected by S. aureus. **a**, **b**, α-diversity of the TCR repertoire in MF lesions and nonlesional skin. Plaque samples are stratified according to ΔSA-subgroup. **c** For each given pair of TCR and *S. aureus* epitope, a Binding Score (1 = perfect binding, 0 = no binding) was calculated. Epitopes were downloaded from the IEDB or, if not available, predicted for identified virulence factors of plaque-associated S. aureus strains. n = 275, displayed are the median (red), 1st and 3rd quantile, Kruskal-Wallis test corrected for multiple comparisons. **d–k**, Presentation of the top abundant TCRs in MF lesions and their contribution to the TCR repertoire in nonlesional skin and blood in the same patients. Counts represent the summed abundance of TCR clones and were normalized across all patients (by subsampling to common sequencing depth). Dominant clones in MF lesions were detectable in other tissues as well.

Discussion

An increasing body of evidence demonstrated the profound impact of human body colonizing microbes on the cancer disease course, especially enabled by the advent of new sequencing technologies[81]. While the gut microbiome has been in the focus of investigations, the skin microbiome is increasingly recognized for its role in modulating the cutaneous immune system and its resulting implications for several inflammatory and neoplastic skin conditions[82]. A convincing body of evidence proposes the influence of single bacterial agents, especially *S. aureus*, on MF pathogenesis[14–20]. However, *S. aureus* is also a physiological commensal on healthy skin[21] and not every MF patient was found to be skin colonized by this species[17,18]. Additionally, while systemic or topical antibiotic treatment successfully eliminated *S. aureus* in the majority of culture-positive MF patients, only 53% – 58% responded to therapy[18,22].

In this study, we investigated the role of the skin microbiome in 20 MF patients using metagenomic sequencing. We obtained several findings that give novel insights into the pathophysiological role of the skin microbiome

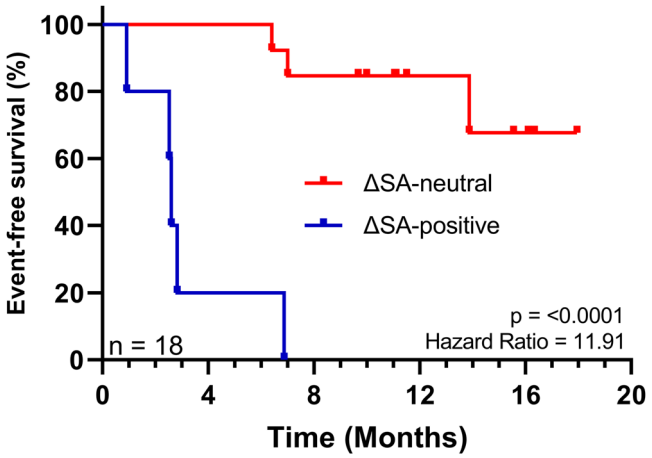

Fig. 8 | Event-free survival Kaplan-Meier curves. Patient Enrolment started in September 2020 and was completed in April 2021. The follow-up period lasted until May 2022. The Log-rank test was used to determine differences between survival curves (1 degree of freedom).

for MF progression along with potential mechanisms that underly these distinct changes:

First, we were able to identify microbiome patterns that stratified our patient cohort into the two subgroups ΔSA-positive and ΔSA-neutral. In the ΔSA-positive subgroup, the relative abundance of *S. aureus* increased from nonlesional skin to plaque, a significant dysbiosis existed on plaque, the TCR repertoire was assaulted and EFS was strongly decreased.

Second, we observed an overexpression of AMPs in MF lesions as compared to nonlesional skin, which is in accordance with previous reports[83–85]. In addition, our results revealed that clinical isolates of MF skin commensals were more resistant to several of these AMPs as compared to microbial isolates from healthy skin. Notably, the AMP hBD1 even augmented growth of plaque-derived *S. aureus* (Fig. 3c), probably acting like a co-factor. Therefore, we reasoned that the sustained and sublytic expression of AMPs might initially eradicate the physiological skin flora while, eventually, some commensals adopt to the new conditions and develop resistances, allowing them to live under ectopic AMP levels of MF skin. Besides this indirect disease promoting effect, AMPs may also directly drive MF progression. In particular, AMPs were reported to recruit $CD4^+$ (memory) T cells[86,87], which represent the neoplastic T cell subtype in MF[79]. This interaction might result in a positive feedback loop in which the production of AMPs recruits neoplastic T cells, that enhance the inflammatory microenvironment and augment AMP levels. Although AMP expression levels were increased in MF lesions, they did not differ between ΔSA-positive and ΔSA-neutral patients. Thus, enhanced AMP levels might not explain the molecular and clinical differences of the two patient subgroups.

Rather, this study identified that *S. aureus* strains on plaques of the ΔSA-positive subgroup were distinct from their nonlesional counterparts, displaying a unique gene repertoire and being considerably more resistant towards commonly used antibiotics than all other tested bacteria. Further, we identified several virulence genes that were enriched in the plaque microbiome of ΔSA-positive patients. Interestingly, our analysis did not reveal the presence of staphylococcal superantigens within the pool of virulence genes, which have been regarded as a significant factor in *S. aureus*-dependent MF progression so far[17,53–55]. Instead, our attention was drawn to the virulence factor *spa*. It has been shown that spa activates the NF-κB pathway and induces inflammation by serving as ligand for the TNFR1[59–65]. Also, it was reported that *S. aureus* triggers the release of TNF-α in keratinocytes[88], which in turn may activate NF-κB in malignant T cells in a paracrine fashion. In line, several studies showed that the NF-κB pathway is recurrently deregulated in a subset of MF patients with an inferior disease course[29–31,89]. Notably, our results revealed that *spa* of the plaque-derived *S. aureus* isolate MFMZ1 contained a potential gain-of-function mutation that may render it even more potent in activating the TNFR1/NF-κB axis[59,60,68,69,90]. Therefore, stimulation of the NF-κB pathway by spa could account for the inferior EFS of the ΔSA-positive subgroup. Consistent with these findings, our results from TCRseq demonstrated that plaque-enriched *S. aureus* virulence factors, and spa in particular, were recognized by T cells in MF lesions. Given that those clones also presented in blood and nonlesional skin, indicates that these specific T cell clones might disseminate into other tissue compartments, thus driving pathogenesis.

Collectively, our results provide a strong rationale for treating MF patients with microbiome-modulating drugs. Since we showed that the presence of *S. aureus* alone is not necessarily associated with an aggravated disease course, we suggest stratifying MF patients into ΔSA-subgroups rather than subjecting all *S.* aureus-positive MF patients to antibiotic therapy[18,22]. In addition, more precise microbiome-modulating drugs are warranted because antibiotics also eradicate the physiological skin flora and provoke microbial resistances[28,91]. An appropriate therapeutic approach could be bacteriotherapy by transferring the microbiome or a single bacterial species of nonlesional skin onto MF lesions. In previous reports, *S. epidermis* was found to inhibit growth of malignant cells in skin neoplasms in vitro and in vivo while sparing normal keratinocytes[92]. Moreover, a clinical phase 1 trial showed that patients with atopic dermatitis (AD) benefit from re-introduction of an *S. hominis* strain onto AD lesions that was isolated from nonlesional AD skin[93]. AD and MF share some molecular characteristics of the inflammatory microenvironment[94,95] and, moreover, some MF microbiome patterns identified by us in the present study were also observed in AD. In particular, AD severity is associated with an increase of *S. aureus*, concomitant α-diversity decrease[96], and distinct *S. aureus* strains between AD lesions and nonlesional skin[97]. Thus, re-introduction of *S. hominis* on MF plaque may be a therapeutic option. In addition, our results suggest that *S. epidermidis*, *S. hominis* and *C. acnes* could help to maintain stable disease in MF patients as those commensals were significantly counterbalanced to *S. aureus* in the ΔSA-neutral group exhibiting fewer progressive events. In line, all three commensals were found beneficial for protection against *S. aureus* in clinical settings[36–39].

Limitations of our study are the small patient cohort, the location of the two study centres that lie within the same geographic area which might add a selection bias to the *S. aureus* strains[98], the small amount of patients from which clinical microbial species were isolated, and the relatively short follow-up period for the usually indolent course of MF. Furthermore, the lack of a healthy control group would have allowed for more definitive conclusions on the composition and the functional properties of microbes found in nonlesional skin of MF patients. In particular, our analysis could not identify a specific factor or event that facilitated *S. aureus* outgrowth on plaques of ΔSA-positive patients, after most of the normal skin flora is eradicated upon the onset of aberrant AMP expression. Since we demonstrated that lesional *S. aureus* strains differed from their nonlesional counterparts, it may be possible that ΔSA-positive patients were overgrown with this virulent *S. aureus* strain during a period of decreased microbial defence barrier, opening a "window of opportunity". In turn, ΔSA-neutral patients did not experience such an event and their skin microbiome was able to recover, (re-)building an intact microbial defence barrier. Additional research involving larger patient cohorts, an expanded range of clinical bacterial isolates, and functional assays is required to elucidate the underlying cause of *S. aureus* overgrowth in the ΔSA- positive subgroup.

Also, we cannot definitively determine whether the disturbance in the microbiome was a consequence of our proposed mechanism, where initial infiltration of malignant T cells led to ectopic AMP expression, or if the skin was rather initially infected with a virulent and AMP-resistant *S. aureus* strain, triggering ectopic AMP levels resulting in secondarily acquired dysbiosis. Of note, *S. aureus* was more abundant on nonlesional skin of ΔSA-positive patients (Fig. 2b), which would support the alternative hypothesis at first sight. In contrast, our results indicate that the lesional *S. aureus* strain may have spread into nonlesional areas of the skin, as suggested by two ΔSA-positive patients with the same virulent *S. aureus* strain present on both plaque and nonlesional skin (Fig. 4a). In line, it was shown

that MF patients have a comprised physical skin barrier even in nonlesional skin, rendering them more susceptible to infections[83,84].

Open issues also remain about the role of *C. acnes* in MF pathogenesis. While this species displays anti-*S. aureus*-activity[36], C. *acnes* also is an opportunistic pathogen in various infectious diseases and induces secondary aggregation as well as biofilm formation of *S. aureus*[99,100]. In addition, *C. acnes* can cause inflammation, which is a chronic condition in MF and boosts progression[1,2,99]. Linking *C. acnes* to the pathogenesis of (early-stage) MF seems therefore plausible. Indeed, *C. acnes* was highly abundant on patches of ΔSA-positive patients (Fig. 2f). Yet, our results involved only two data points and *C. acnes* was upregulated in some patches of ΔSA-neutral patients as well (Fig. 2f). Further research is therefore warranted to understand if *C. acnes* plays a role in MF pathogenesis.

In summary, our study offers comprehensive insights into the skin microbiome of MF patients and identified dysregulation of the skin microbiome and concomitant outgrowth of virulent *S. aureus* strains as critical components that can stratify MF patients into distinct subgroups of MF severity. The microbiome perturbations might be caused by an aberrant AMP production, enabling the outgrowth of AMP-resistant *S. aureus*. Strains of this pathogen harboured several virulent properties, most notably the virulence factor *spa*, which likely drove the pathogenesis in the ΔSA-positive subgroup with inferior prognosis. Although our study is exploratory in its nature, our data provide a strong rational to treat the skin of MF patients with drugs that either reconstitute a physiological skin flora or build up epithelial integrity. One possibility could be bacteriotherapy with commensals that we identified being counterbalanced to *S. aureus*. Further studies are needed to explore the underlying mechanism why one subgroup experiences *S. aureus* outgrowth while the other subgroup is spared, if *S. aureus* activates NF-κB via spa to fuel MF progression, and to delineate the role of other commensals such as *C. acnes* in MF progression.

Methods

Patient recruitment and clinical specimens

Patients were recruited from two skin cancer centres in Germany, the Department of Dermatology, University Medical Centre Mainz, and the Department of Dermatology, Venerology and Allergology, University Hospital Frankfurt am Main. Eligibility criteria included diagnosis of MF, aged between 18 and 90 years, no antibiotic treatment at a minimum of 1 month prior to sampling, no showering or application of cremes and antiseptic agents at a minimum of 24 h prior to sampling. Patients with allergies against local anaesthetics were excluded from skin biopsies. The following clinical specimens were taken, all at the same visit: Microbiome swabs from lesional and nonlesional skin, skin punch biopsies from the same lesions and nonlesional skin, peripheral blood.

Microbiome sampling and DNA extraction

We sampled up to two separate lesions from each patient. To account for the high individuality of microbiome profiles[21,101], we included intra-patient controls instead of other subjects with e.g., healthy skin or patients with skin conditions other than MF. To this end, we collected nonlesional skin samples from the contralateral site of lesional samples of the same MF patient.

procedure and DNA extraction was performed as described previously with a few modifications[21,24,102]. A swab-scrape-swab procedure was used to sample microbes from the skin. Yeast cell lysis buffer from the MasterPure Yeast DNA Purification Kit (MPY80200, Lucigen, USA) was aliquoted into individual collection tubes holding baskets with a semi-permeable valve (NAO™ Basket 4103CS01, COPAN, USA). A sterile swab (FLOQSwab 4N6, NAO™ Basket 4103CS01, COPAN, USA) pre-moistened in the aliquoted buffer was brushed vigorously over the skin and placed back into the collection tube holding the basket and buffer. Then, a surgical scalpel was carefully scraped over the same skin area and placed into the tube holding the buffer-containing basket. This was followed by brushing the skin with the same swab used in the first step. The swab was placed into the collection tube and the swab head was clipped off. The collection tube was directly placed on dry ice and stored at −80 °C until DNA extraction. The whole sampling procedure was performed wearing sterile gloves and surgical masks.

To extract the DNA, frozen samples were first thawed at 37 °C for 10 min on a heated shaking block. Samples were then treated with 1 µl ReadyLyse Lysozyme solution (MGP04100, Lucigen, USA) at 37 °C for 60 min on a heated shaking block. After incubation, the sample solution was separated from the swab head with the help of the semi-permeable valve in the baskets by centrifuging at 12,000 g for 2 min at room temperature. The basket containing the swab head was discarded. Then, beads (Pathogen Lysis Tubes, 19092, Qiagen, Germany) were added into the collection tube to mechanically disrupt cells using a TissueLyser II (85300, Qiagen, Germany) for 10 min at 30 Hz. Samples were then incubated at 67 °C for 30 min and placed on ice for 5 min. After adding 150 µl MPC precipitation reagent from the MasterPure Yeast DNA Purification Kit, cell debris was spun down and the supernatant was transferred to a fresh DNA LoBind Tube (0030108051, Eppendorf, Germany). Samples were combined with an equal volume of 100% ethanol (15420665, Fisher BioReagents, USA) and purified using the PureLink Genomic DNA Mini Kit (K182002, Invitrogen, USA) according to the manufacturer's instruction. Finally, DNA was eluted in 25 µl 0.1 TE.

Preparation of metagenomic libraries and Whole Metagenome Sequencing

Illumina sequencing libraries were created using the NEBNext Ultra II FS DNA Library Prep Kit (E7805L, New England Biolabs, USA) in combination with NEBNext Multiplex Oligos, Dual Index Set 1 (E7600S, New England Biolabs, USA) according to the manufacturer's instructions. Library qualities were assessed with the 2100 Bioanalyzer (G2939BA, Agilent, USA) and Qubit 2.0 (Q32866, Invitrogen, USA). Whole Metagenome sequencing was performed on Illumina NovaSeq 6000 at 150 bp paired-end to an average of 47,519 million raw reads (7.13 Gbp) per sample.

To control for consistency in DNA extraction and metagenomic library preparation, we included a standardized mock community of inactivated microbial cells (ZymoBIOMICS Microbial Community Standard, Zymo Research, USA) and thereof derived microbial DNA (ZymoBIOMICS Microbial Community DNA Standard, Zymo Research, USA) that we processed and sequenced alongside the MF-metagenomic samples. Clustering analysis of the microbial community profiles obtained from both standards revealed high similarity between each processing batch and concordance with the manufacturer's specifications (Supplementary Fig. 6).

Metagenomic profiling

Preparation steps and analysis of metagenomic samples were conducted using the bioBakery toolsuit[103]. Raw reads were first quality checked, trimmed and human reads were filtered out with KneadData version 0.7.10, which integrates the tools FastQC 0.11.9[104], Trimmomatic 0.33[105], and Bowtie2 2.4.1[106]. An average of 1,312 million non-human, quality-filtered reads (0.34 Gbp) were obtained per sample and used for all subsequent steps. More non-human reads were retained from nonlesional skin compared to MF lesions, probably due to the nature of MF lesions being scaly[2]. In consequence a greater proportion of human skin cells were sampled from MF lesions compared to nonlesional skin. A similar effect was observed in a study investigating the skin microbiome of Psoriasis using a similar analysis pipeline[107].

Taxonomic profiles were generated with MetaPhlAn 3.0.2[103,108] successfully for a total of $N = 65$ metagenomic samples. Relative abundances of each clade were obtained with the flag –analysis_type rel_ab. Taxonomic tables of each sample were merged with the merge_metaphlan_tables.py script and only the species level retained. To profile virulence genes, protein sequences were obtained from the Virulence Factor Database (VFDB)[48]. These were used as input to the Identify-mode of ShortBRED[47]. Briefly, ShortBRED clusters proteins of interest into families and finds markers for every built family that are unique against an exhaustive database of proteins (UniRef90). Then, ShortBRED-Quantify uses translated search to quantify

the identified protein markers in metagenomic reads and normalizes results to produce a functional profile. Differential abundance analyses were conducted with MaAsLin 2[35] building a generalized linear mixed model, with stage being the dependent variable and patient and number of non-human reads as co-variates. Relative abundances were log-scaled and nonlesional skin was set to reference level for the dependent variable (i.e., stage). Other settings were left to default.

Strain profiling was performed with PanPhlAn 3.1[46]. The tool characterizes the gene composition of individual strains by mapping metagenomic samples against the pangenome of a species of interest. For profiling, the least stringent option was carried out by adding respective flags as described in the manual (--min_coverage 1 --left_max 1.70 --right_min 0.30). The resulting binary table showing presence/absence of genes was loaded into R! and a PCA was performed with the internal prcomp function. Plots were generated with GraphPad PRISM 9 and ggplot2[109].

Diversity analysis and clustering of taxonomic profiles from rarefied metagenomic samples

Diversity metrics and clustering analysis was carried out from metagenomic reads rarefied to common depth. To generate rarefaction curves, non-human reads were subsampled to increasing depths using seqkit 0.15.0[110] with subsequent taxonomic profiling. Rarefaction curves resembled those of another study investigating the skin microbiome of psoriasis patients using a similar analysis pipeline[107]. Generally, more unique species were observed on nonlesional skin than on MF lesions (Supplementary Fig. 7). This could be associated with the higher sequencing depth of nonlesional skin. Yet, also at a given subsampled depth nonlesional skin presented with more unique microbial species, showing that the differences are rather of a biological than a technical nature[107]. For diversity analysis and clustering of taxonomic profiles, metagenomic reads were subsampled to 141,703 reads. Lesional skin samples tended to have less non-human reads and thus more lesional samples were filtered out by rarefaction compared to nonlesional samples. Thus, to maintain the intrapatient sample-control regimen, nonlesional samples without a counterpart from lesional skin were filtered out, resulting in a total of 32 samples for subsequent analyses. Shannon-Index and Bray-Curtis dissimilarities were calculated with the R! package vegan[111]. The same package was also used to calculate PERMANOVA with the adonis function as well as PERMDISP with the betadisper function. A statistically significant signal from adonis was only considered trustworthy with concomitant non-significant signal from betadisper to rule out inhomogeneity of dispersion among groups. Pairwise comparisons were performed with the R! package pairwiseAdonis[112]. Clustering and plotting of taxonomic profiles were done with the R! package pheatmap.

Skin biopsies, peripheral blood, and RNA extraction

4 mm punch biopsies were obtained from the same lesions sampled for metagenomics and at the same visit. The punch biopsies were immediately shock frozen and kept in liquid nitrogen until processed. RNA was extracted using the RNeasy Fibrous Tissue Mini Kit (74704, Qiagen, Germany) along with the TissueLyser II (85300, Qiagen, Germany) according to the manufacturer's instructions. Peripheral blood mononuclear cells (PBMCs) were isolated from freshly drawn blood using density gradient centrifugation (Histopaque-1077, SIGMA-ALDRICH, Germany) and kept in liquid nitrogen until processed. PBMCs were thawed at 37 °C, washed in pre-warmed RPMI 1640 medium (31870-025, Gibco, USA) including 10% FCS and counted using the Countess 3 machine (ThermoFisher Scientific, USA). To enrich the T cell population, the Pan T Cell Isolation Kit human (Miltenyi Biotec, Germany) was used according to the manufacturer's instructions. Directly thereafter total RNA was extracted with the RNeasy Plus Mini Kit (Qiagen, Germany) according to the manufacturer's instructions.

RT-qPCR of AMPs

First, synthesize of first strand cDNA was carried out with M-MuLV Reverse Transcriptase (M0253L) using both Random Hexamer Primer (S1330S) and Oligo(dT) Primer (S1316S) (all from New England Biolabs, USA) at a total reaction volume of 20 µl and incubated as noted in the manual. Final cDNA was quantified on a NanoDrop 2000c (ND-2000, ThermoFisher Scientific, USA). For RT-qPCR the primaQUANT SYBRGreen Master Mix (SL-9902HRB, Steinbrenner Laborsysteme, Germany) was used with 400 ng template as input at a total reaction volume of 25 µl. The 7300 Real-Time PCR System (Applied Biosystems, USA) was used with an initial denaturation at 95 °C for 10 min followed by 40 cycles of 95 °C for 15 s and 60 °C for 1 min. The runs were evaluated via melting curves. Primers for AMPs and housekeeping gene were used from literature or self-designed and are listed in Supplementary Table 2.

T cell receptor sequencing and analysis

Illumina sequencing libraries were constructed with the NEBNext Immune Sequencing Kit, human (E6320, New England Biolabs, USA) according to the manufacturer's instructions with 200 ng total RNA as starting material. The optimal number of PCR cycles for target amplification was determined for each sample by RT-qPCR as outlined in the manual. Final libraries were quality checked via Qubit 2.0 (Q32866, Invitrogen, USA) and the 2100 Bioanalyzer (G2939BA, Agilent, USA). Because of the low T cell proportion especially in nonlesional skin, samples with inappropriate TCR libraries were excluded from further analysis. A total of 21 libraries (16 from MF skin, 5 from PBMCs enriched for T cells) were pooled and then sequenced on a MiSeq (Illumina, USA) with 10% PhiX. Sequencing was performed running 300 bp PE using a 600-cycle V3 reagent kit to an average of 0.98 million reads per sample.

The sequencing data were uploaded to the Galaxy web platform and processed with the pRESTO toolkit[113] implemented in a publicity available workflow at https://usegalaxy.org/u/bradlanghorst/w/presto-nebnext-immune-seq-workflow-v320 using default parameters. Subsequently, the R toolkit immunarch 0.7.0 was used to analyse the TCR repertoire and to visualize T cell clonotype tracking as well as TCR gene usage[114]. To investigate if TCRs recognize *S. aureus* virulence factors that we identified as enriched on plaque, we downloaded corresponding epitopes from the IEDB (https://www.iedb.org/)[75]. If an epitope of was not available, it was predicted with an online tool for both MHC-II and MHC-I (http://tools.iedb.org/main/tcell/). A table was constructed containing pairs of the most abundant TCR clones with each epitope (i.e., epitopes received from the IEDB and epitopes predicted with the online tool). The python tool ERGO-II was used to calculate a binding score of each TCR-epitope pair. The higher the binding score, the higher the probability that the TCR recognizes and binds the epitope[115].

Although plaque samples of Pat1 and Pat7 did not show monoclonal expansion according to our RNA-based TCR sequencing approach, we confirmed the diagnosis of MF during the further clinical course: Pat1 developed a tumour (T2b, >7 cm diameter), and several patch and plaque lesions. Regarding Pat7, we detected T cell clonality against a polyclonal background using the clinical standard-of-care BIOMED-2 protocol. BIOMED-2 is a DNA-based TCR sequencing approach[116], whereas we performed RNA-based TCR sequencing. Both methods differ in several aspects, e.g., RNA-based TCR sequencing has a higher sensitivity and detects more TCR clones[117,118].

Isolation of clinical microbial species and functional analyses

Clinical isolates of microbial species were obtained from the same MF patients enroled in the metagenomic survey. The skin was swabbed several times, spread on a *Staphylococcus* Vogel-Johnson agar [1% (w/v) casein peptone, 1% (w/v) mannitol, 1% (w/v) glycine, 0.5% (w/v) yeast extract, 0.5% (w/v) lithium chloride, 0.5% (w/v) dipotassium phosphate, 0.0025% (w/v) phenol red, 0.02% (v/v) potassium tellurite, 2% (w/v) agar, pH 7.2][119,120], and samples were incubated at 37 °C overnight. *S. aureus* colonies should appear small, black surrounded by a green-yellow zone, while *S. epidermidis* strains appear grey-black without zones. Putative *S. aureus* and *S. epidermidis* colonies were picked and checked via colony PCR using *Staphylococcus tuf* specific primers (TStaG422: GGCCGTGTTGAAC GTGGTCAAATCA & TStag765: TIACCATTTCAGTACCTTCTGG

TAA) according to[121]. The achieved fragments were sequenced to identify the *Staphylococcus* strain.

Antibiotic diffusion assay was performed to determine antibiotic resistances of clinical *Staphylococci* isolates. Therefore, 100 µl of an overnight culture were pipetted into 20 ml melted 0.8% semi solid HD agar (w/v) and poured into petri dishes. After solidification, 5 antibiotics (25 µg ampicillin, 100 µg carbenicillin, 23.75 µg sulfomethoxazol + 1.25 µg trimetophrim, 15 µg erythromycin, and 5 µg novobiocin) were applied using Sensi-Disc™ BD dispenser. Furthermore, resistance/sensitivity towards an additional antibiotic, methicillin, was separately tested applying 5 µg and 20 µg on sterile filter disks. The plates were kept for 2 h at 4 °C to allow antibiotics to diffuse. Afterwards the plates were incubated at 37 °C for 24 h. Antibiotic sensitivity became visible as degradation zone around the filter disks. Halo size was measured using ImageJ.

Antibacterial assay was performed to test whether the clinical isolates exhibit resistance towards selected AMPs, as described in[122]. Overnight cultures of bacterial strains were harvested, washed in 1x PBS [137 mM NaCl, 2.7 mM KCl, 10 mM Na_2HPO_4, 1.8 mM KH_2PO_4, pH 7.2], and resuspended in 10 mM sodium phosphate buffer (NaPi; pH 6.8). Afterwards, 10 µl of a 10^6 cells/ml bacterial suspension were inoculated into 190 µl of 10 mM sodium phosphate buffer (10^4 cells in 200 µl final volume) w/o various AMP concentrations (1 and 5 µg) and incubated for 2 h at 37 °C. 100 µl of the reaction mixture were plated on TSB agar plates [peptone/tryptone 1.7% (w/v), soy peptone 0.3% (w/v), D(+)-glucose 0.25% (w/v), NaCl 0.5% (w/v), K2HPO4 0.25% (w/v), meat extract 0.3% (w/v), pH 7.3] and then incubated at 37 °C overnight. The number of CFU was determined and the antibacterial effect was assessed by determining survival rate of AMP-treated *S. aureus* compared to the total number of cells in the control experiment. Three biological replicates were tested.

Identification and sequencing of spa was performed to determine whether the *spa* gene was present in clinical isolates. Therefore, *spa*-specific primers (Supplementary Table 2) were designed for gene amplification and PCR was performed using Q5® high-fidelity DNA polymerase from NEB according to the manufacturers protocol. As a control, PCR was performed using *S. aureus* EM01 and *S. epidermidis* MV01 obtained from the two healthy patients enroled in this study. After detecting positive amplicons via 1.5% (w/v) agarose gel electrophoresis and purification with „*HiYield*® PCR Clean-Up & Gel-Extraction Kit" (SLG) the genes were sequenced through the Sanger method[123] by StarSeq® GmbH (Mainz). For sequencing the respective primers for *spa* were used. For more accurate result the sample was further sequenced using an additional primer *spa*_mid: cttaaaagatgacccaagcc binding in the middle of the gene. Sequencing data were analyzed, and alignments of gene and amino acid sequences were performed using Benchling (https://www.benchling.com/) and the online implementation of ClustalΩ (ref.124, https://www.ebi.ac.uk/Tools/msa/clustalo/) using default parameters.

Reporting summary

Further information on research design is available in the Nature Research Reporting Summary linked to this article.

Data availability

All relevant data are available from the authors: WMS Sequencing data and associated analysis files can be accessed at the Gene Expression Omnibus (GEO) under GSE221149 (https://www.ncbi.nlm.nih.gov/geo/query/acc.cgi?acc=GSE221149). TCR Sequencing data and associated analysis files can be accessed under GSE218874 (https://www.ncbi.nlm.nih.gov/geo/query/acc.cgi?acc=GSE218874). Both are part of the SuperSeries GSE221150 (https://www.ncbi.nlm.nih.gov/geo/query/acc.cgi?acc=GSE221150).

Code availability

The code used for the analyses can be found at https://github.com/phlicht/Code_for_analyses_and_graphs/tree/main.

Received: 27 November 2023; Accepted: 31 July 2024;
Published online: 29 August 2024

References

1. Hwang, S. T., Janik, J. E., Jaffe, E. S. & Wilson, W. H. Mycosis fungoides and Sézary syndrome. *Lancet* **371**, 945–957 (2008).
2. Dummer, R. et al. Cutaneous T cell lymphoma. *Nat. Rev. Dis. Prim.* **7**, 61 (2021).
3. Olsen, E. et al. Revisions to the staging and classification of mycosis fungoides and Sezary syndrome: a proposal of the International Society for Cutaneous Lymphomas (ISCL) and the cutaneous lymphoma task force of the European Organization of Research and Treatment of Ca. *Blood* **110**, 1713–1722 (2007).
4. Agar, N. S. et al. Survival Outcomes and Prognostic Factors in Mycosis Fungoides/Sézary Syndrome: Validation of the Revised International Society for Cutaneous Lymphomas/European Organisation for Research and Treatment of Cancer Staging Proposal. *J. Clin. Oncol.* **28**, 4730–4739 (2010).
5. Scarisbrick, J. J. et al. The PROCLIPI international registry of early-stage mycosis fungoides identifies substantial diagnostic delay in most patients. *Br. J. Dermatol.* **181**, 350–357 (2019).
6. Da Silva Almeida, A. C. et al. The mutational landscape of cutaneous T cell lymphoma and Sézary syndrome. *Nat. Genet* **47**, 1465–1470 (2015).
7. Choi, J. et al. Genomic landscape of cutaneous T cell lymphoma. *Nat. Genet.* **47**, 1011–1019 (2015).
8. Damsky, W. E. & Choi, J. Genetics of Cutaneous T Cell Lymphoma: From Bench to Bedside. *Curr. Treat. Options Oncol.* **17**, 33 (2016).
9. Rassek, K. & Iżykowska, K. Single-Cell Heterogeneity of Cutaneous T-Cell Lymphomas Revealed Using RNA-Seq Technologies. *Cancers (Basel)* **12**, 2129 (2020).
10. de Masson, A. et al. Allogeneic transplantation in advanced cutaneous T-cell lymphomas (CUTALLO): a propensity score matched controlled prospective study. *Lancet* https://doi.org/10.1016/S0140-6736(23)00329-X (2023).
11. Ansell, S. M. Non-Hodgkin Lymphoma: Diagnosis and Treatment. *Mayo Clin. Proc.* **90**, 1152–1163 (2015).
12. Stadler, R. & Scarisbrick, J. J. Maintenance therapy in patients with mycosis fungoides or Sézary syndrome: A neglected topic. *Eur. J. Cancer* **142**, 38–47 (2021).
13. Tan, R. S.-H., Butterworth, C. M., Mclaughlin, H., Malka, S. & Samman, P. D. Mycosis fungoides—a disease of antigen persistence. *Br. J. Dermatol* **91**, 607–616 (1974).
14. Mirvish, J. J., Pomerantz, R. G., Falo, L. D. & Geskin, L. J. Role of infectious agents in cutaneous T-cell lymphoma: Facts and controversies. *Clin. Dermatol.* **31**, 423–431 (2013).
15. Fanok, M. H. et al. Role of Dysregulated Cytokine Signaling and Bacterial Triggers in the Pathogenesis of Cutaneous T-Cell. *Lymphoma J. Invest. Dermatol.* **138**, 1116–1125 (2018).
16. Lindahl, L. M. et al. Antibiotics inhibit tumor and disease activity in cutaneous T-cell lymphoma. *Blood* **134**, 1072–1083 (2019).
17. Jackow, C. M. et al. Association of Erythrodermic Cutaneous T-Cell Lymphoma, Superantigen-Positive Staphylococcus aureus, and Oligoclonal T-Cell Receptor Vβ Gene Expansion. *Blood* **89**, 32–40 (1997).
18. Talpur, R., Bassett, R. & Duvic, M. Prevalence and treatment of Staphylococcus aureus colonization in patients with mycosis fungoides and Sézary syndrome. *Br. J. Dermatol.* **159**, 105–112 (2008).
19. Willerslev-Olsen, A. et al. Bacterial Toxins Fuel Disease Progression in Cutaneous T-Cell Lymphoma. *Toxins (Basel)* **5**, 1402–1421 (2013).
20. Fujii, K. Pathogenesis of cutaneous T cell lymphoma: Involvement of Staphylococcus aureus. *J. Dermatol.* **49**, 202–209 (2022).
21. Oh, J. et al. Biogeography and individuality shape function in the human skin metagenome. *Nature* **514**, 59–64 (2014).

22. Emge, D. A., Bassett, R. L., Duvic, M. & Huen, A. O. Methicillin-resistant Staphylococcus aureus (MRSA) is an important pathogen in erythrodermic cutaneous T-cell lymphoma (CTCL) patients. *Arch. Dermatol. Res.* **312**, 283–288 (2020).
23. Salava, A. et al. Skin Microbiome in Cutaneous T-Cell Lymphoma by 16S and Whole-Genome Shotgun Sequencing. *J. Invest. Dermatol.* **140**, 2304–2308.e7 (2020).
24. Harkins, C. P. et al. Cutaneous T-Cell Lymphoma Skin Microbiome Is Characterized by Shifts in Certain Commensal Bacteria but not Viruses when Compared with Healthy. *Controls J. Invest. Dermatol.* **141**, 1604–1608 (2021).
25. Zhang, Y. et al. "Alterations in the Skin Microbiota Are Associated With Symptom Severity in Mycosis Fungoides". *Front. Cell. Infect. Microbiol.* **12**, 1–10 (2022).
26. Dehner, C. A. et al. Malignant T Cell Activation by a Bacillus Species Isolated from Cutaneous T-Cell Lymphoma Lesions. *JID Innov.* **2**, 100084 (2022).
27. Hooper, M. J. et al. Nasal Dysbiosis in Cutaneous T-Cell Lymphoma Is Characterized by Shifts in Relative Abundances of Non-Staphylococcus Bacteria. *JID Innov.* **2**, 100132 (2022).
28. Licht, P. & Mailänder, V. Transcriptional Heterogeneity and the Microbiome of Cutaneous T-Cell Lymphoma. *Cells* **11**, 328 (2022).
29. Tracey, L. et al. Mycosis fungoides shows concurrent deregulation of multiple genes involved in the TNF signaling pathway: an expression profile study. *Blood* **102**, 1042–1050 (2003).
30. Shin, J. et al. Lesional gene expression profiling in cutaneous T-cell lymphoma reveals natural clusters associated with disease outcome. *Blood* **110**, 3015–3027 (2007).
31. Ungewickell, A. et al. Genomic analysis of mycosis fungoides and Sézary syndrome identifies recurrent alterations in TNFR2. *Nat. Genet.* **47**, 1056–1060 (2015).
32. Byrd, A. L., Belkaid, Y. & Segre, J. A. The human skin microbiome. *Nat. Rev. Microbiol.* **16**, 143–155 (2018).
33. Luna, P. C. Skin Microbiome as Years Go By. *Am. J. Clin. Dermatol.* **21**, 12–17 (2020).
34. Leung, M. H. Y., Wilkins, D. & Lee, P. K. H. Insights into the pan-microbiome: skin microbial communities of Chinese individuals differ from other racial groups. *Sci. Rep.* **5**, 11845 (2015).
35. Mallick, H. et al. Multivariable association discovery in population-scale meta-omics studies. *PLoS Comput. Biol.* **17**, e1009442 (2021).
36. Shu, M. et al. Fermentation of Propionibacterium acnes, a Commensal Bacterium in the Human Skin Microbiome, as Skin Probiotics against Methicillin-Resistant Staphylococcus aureus. *PLoS One* **8**, e55380 (2013).
37. Cogen, A. L. et al. Selective Antimicrobial Action Is Provided by Phenol-Soluble Modulins Derived from Staphylococcus epidermidis, a Normal Resident of the Skin. *J. Invest. Dermatol.* **130**, 192–200 (2010).
38. Nakatsuji, T. et al. Antimicrobials from human skin commensal bacteria protect against Staphylococcus aureus and are deficient in atopic dermatitis. *Sci. Transl. Med*. **9**, eaah4680 (2017).
39. Williams, M. R. et al. Quorum sensing between bacterial species on the skin protects against epidermal injury in atopic dermatitis. *Sci. Transl. Med.* **11**, eaat8329 (2019).
40. Lai, Y. et al. Commensal bacteria regulate Toll-like receptor 3–dependent inflammation after skin injury. *Nat. Med.* **15**, 1377–1382 (2009).
41. Mangoni, M. L., Mcdermott, A. M. & Zasloff, M. Antimicrobial peptides and wound healing: Biological and therapeutic considerations. *Exp. Dermatol.* **25**, 167–173 (2016).
42. Gallo, R. L. & Hooper, L. V. Epithelial antimicrobial defence of the skin and intestine. *Nat. Rev. Immunol.* **12**, 503–516 (2012).
43. Stolearenco, V. et al. Cellular Interactions and Inflammation in the Pathogenesis of Cutaneous T-Cell Lymphoma. *Front. Cell Dev. Biol.* **8**, 1–12 (2020).
44. Park, A. J., Okhovat, J.-P. & Kim, J. Antimicrobial Peptides. in *Clinical and Basic Immunodermatology* 81–95 (Springer International Publishing, Cham, 2017). https://doi.org/10.1007/978-3-319-29785-9_6.
45. Rosenbach, F. J. *Mikro-Organismen Bei Den Wund-Infections-Krankheiten Des Menschen*. (Wiesbaden, 1884).
46. Scholz, M. et al. Strain-level microbial epidemiology and population genomics from shotgun metagenomics. *Nat. Methods* **13**, 435–438 (2016).
47. Kaminski, J. et al. High-Specificity Targeted Functional Profiling in Microbial Communities with ShortBRED. *PLOS Comput. Biol.* **11**, e1004557 (2015).
48. Liu, B., Zheng, D., Zhou, S., Chen, L. & Yang, J. VFDB 2022: a general classification scheme for bacterial virulence factors. *Nucleic Acids Res*. **50**, (2022).
49. Cheung, G. Y. C., Bae, J. S. & Otto, M. Pathogenicity and virulence of Staphylococcus aureus. *Virulence* **12**, 547–569 (2021).
50. Otto, M. Staphylococcus aureus toxins. *Curr. Opin. Microbiol.* **17**, 32–37 (2014).
51. Tan, S.-Y., Tay, S. S., Sumaria, N., Roediger, B. & Weninger, W. *Clinical and Basic Immunodermatology*. *Clinical and Basic Immunodermatology* (Springer International Publishing, Cham, 2017). https://doi.org/10.1007/978-3-319-29785-9.
52. Clarke, S. R. et al. The Staphylococcus aureus Surface Protein IsdA Mediates Resistance to Innate Defenses of Human Skin. *Cell Host Microbe* **1**, 199–212 (2007).
53. Woetmann, A. et al. Nonmalignant T cells stimulate growth of T-cell lymphoma cells in the presence of bacterial toxins. *Blood* **109**, 3325–3332 (2007).
54. Willerslev-Olsen, A. et al. Staphylococcal enterotoxin A (SEA) stimulates STAT3 activation and IL-17 expression in cutaneous T-cell lymphoma. *Blood* **127**, 1287–1296 (2016).
55. TOKURA, Y. et al. Cutaneous colonization with staphylococci influences the disease activity of Sézary syndrome: a potential role for bacterial superantigens. *Br. J. Dermatol.* **133**, 6–12 (1995).
56. Blümel, E. et al. Staphylococcal alpha-toxin tilts the balance between malignant and non-malignant CD4 + T cells in cutaneous T-cell lymphoma. *Oncoimmunology* **8**, e1641387 (2019).
57. Blümel, E. et al. Staphylococcus aureus alpha-toxin inhibits CD8 + T cell-mediated killing of cancer cells in cutaneous T-cell lymphoma. *Oncoimmunology* **9**, 1751561 (2020).
58. Cao, Z., Casabona, M. G., Kneuper, H., Chalmers, J. D. & Palmer, T. The type VII secretion system of Staphylococcus aureus secretes a nuclease toxin that targets competitor bacteria. *Nat. Microbiol.* **2**, 16183 (2017).
59. Gómez, M. I. et al. Staphylococcus aureus protein A induces airway epithelial inflammatory responses by activating TNFR1. *Nat. Med.* **10**, 842–848 (2004).
60. Gómez, M. I., O'Seaghdha, M., Magargee, M., Foster, T. J. & Prince, A. S. Staphylococcus aureus Protein A Activates TNFR1 Signaling through Conserved IgG Binding Domains. *J. Biol. Chem.* **281**, 20190–20196 (2006).
61. Mendoza Bertelli, A. et al. Staphylococcus aureus protein A enhances osteoclastogenesis via TNFR1 and EGFR signaling. *Biochim. Biophys. Acta - Mol. Basis Dis.* **1862**, 1975–1983 (2016).
62. Ledo, C. et al. Protein A Modulates Neutrophil and Keratinocyte Signaling and Survival in Response to Staphylococcus aureus. *Front. Immunol.* **11**, 1–15 (2021).
63. Claßen, A. et al. TNF receptor I on human keratinocytes is a binding partner for staphylococcal protein A resulting in the activation of NF kappa B, AP-1, and downstream gene transcription. *Exp. Dermatol.* **20**, 48–52 (2011).
64. Claro, T. et al. Staphylococcus aureus protein A binding to osteoblast tumour necrosis factor receptor 1 results in activation of

nuclear factor kappa B and release of interleukin-6 in bone infection. *Microbiology* **159**, 147–154 (2013).
65. Ren, L.-R. et al. Staphylococcus aureus Protein A induces osteoclastogenesis via the NF-κB signaling pathway. *Mol. Med. Rep.* **16**, 6020–6028 (2017).
66. Martin, F. J. *et al*. Staphylococcus aureus activates type I IFN signaling in mice and humans through the Xr repeated sequences of protein A. *J. Clin. Invest*. https://doi.org/10.1172/JCI35879 (2009).
67. O'Halloran, D. P., Wynne, K. & Geoghegan, J. A. Protein A Is Released into the Staphylococcus aureus Culture Supernatant with an Unprocessed Sorting Signal. *Infect. Immun.* **83**, 1598–1609 (2015).
68. Frénay, H. M. E. et al. Molecular typing of methicillin-resistantStaphylococcus aureus on the basis of protein A gene polymorphism. *Eur. J. Clin. Microbiol. Infect. Dis.* **15**, 60–64 (1996).
69. Montesinos, I., Salido, E., Delgado, T., Cuervo, M. & Sierra, A. Epidemiologic Genotyping of Methicillin-Resistant Staphylococcus aureus by Pulsed-Field Gel Electrophoresis at a University Hospital and Comparison with Antibiotyping and Protein A and Coagulase Gene Polymorphisms. *J. Clin. Microbiol.* **40**, 2119–2125 (2002).
70. Gaydosik, A. M. et al. Single-Cell Lymphocyte Heterogeneity in Advanced Cutaneous T-cell Lymphoma Skin Tumors. *Clin. Cancer Res.* **25**, 4443–4454 (2019).
71. Iyer, A. et al. Skin colonization by circulating neoplastic clones in cutaneous T-cell lymphoma. *Blood* **134**, 1517–1527 (2019).
72. Yawalkar, N. et al. Profound loss of T-cell receptor repertoire complexity in cutaneous T-cell lymphoma. *Blood* **102**, 4059–4066 (2003).
73. Iyer, A. et al. Branched evolution and genomic intratumor heterogeneity in the pathogenesis of cutaneous T-cell lymphoma. *Blood Adv*. **4**, 2489–2500 (2020).
74. Iyer, A. et al. Clonotypic heterogeneity in cutaneous T-cell lymphoma (mycosis fungoides) revealed by comprehensive whole-exome sequencing. *Blood Adv*. **3**, 1175–1184 (2019).
75. Vita, R. et al. The Immune Epitope Database (IEDB): 2018 update. *Nucleic Acids Res*. **47**, D339–D343 (2019).
76. Watanabe, R. et al. Human skin is protected by four functionally and phenotypically discrete populations of resident and recirculating memory T cells. *Sci. Transl. Med.* **7**, 279ra39–279ra39 (2015).
77. Fonseca, R. et al. Developmental plasticity allows outside-in immune responses by resident memory T cells. *Nat. Immunol.* **21**, 412–421 (2020).
78. Kirsch, I. R. et al. TCR sequencing facilitates diagnosis and identifies mature T cells as the cell of origin in CTCL. *Sci. Transl. Med.* **7**, 1–14 (2015).
79. Campbell, J. J., Clark, R. A., Watanabe, R. & Kupper, T. S. Sézary syndrome and mycosis fungoides arise from distinct T-cell subsets: a biologic rationale for their distinct clinical behaviors. *Blood* **116**, 767–771 (2010).
80. Trautinger, F. et al. EORTC consensus recommendations for the treatment of mycosis fungoides/Sézary syndrome. *Eur. J. Cancer* **42**, 1014–1030 (2006).
81. Cullin, N., Azevedo Antunes, C., Straussman, R., Stein-Thoeringer, C. K. & Elinav, E. Microbiome and cancer. *Cancer Cell* **39**, 1317–1341 (2021).
82. Yu, Y., Dunaway, S., Champer, J., Kim, J. & Alikhan, A. Changing our microbiome: probiotics in dermatology. *Br. J. Dermatol*. bjd.18088 https://doi.org/10.1111/bjd.18088 (2019).
83. Nakajima, R. et al. Decreased progranulin expression in Mycosis fungoides: a possible association with the high frequency of skin infections. *Eur. J. Dermatol.* **28**, 790–794 (2018).
84. Suga, H. et al. Skin Barrier Dysfunction and Low Antimicrobial Peptide Expression in Cutaneous T-cell Lymphoma. *Clin. Cancer Res.* **20**, 4339–4348 (2014).
85. Wolk, K. et al. Deficient Cutaneous Antibacterial Competence in Cutaneous T-Cell Lymphomas: Role of Th2-Mediated Biased Th17 Function. *Clin. Cancer Res.* **20**, 5507–5516 (2014).
86. Yang, D. et al. β-Defensins: Linking Innate and Adaptive Immunity Through Dendritic and T Cell CCR6. *Science (80-.)*. **286**, 525–528 (1999).
87. Jinquan, T. et al. Psoriasin: A Novel. *Chemotactic Protein J. Invest. Dermatol.* **107**, 5–10 (1996).
88. Aufiero, B. et al. Staphylococcus aureus induces the expression of tumor necrosis factor-? in primary human keratinocytes. *Int. J. Dermatol.* **46**, 687–694 (2007).
89. Park, J. et al. Genomic analysis of 220 CTCLs identifies a novel recurrent gain-of-function alteration in RLTPR (p.Q575E). *Blood* **130**, 1430–1440 (2017).
90. Garofalo, A. et al. The Length of the Staphylococcus aureus Protein A Polymorphic Region Regulates Inflammation: Impact on Acute and Chronic Infection. *J. Infect. Dis.* **206**, 81–90 (2012).
91. Frieri, M., Kumar, K. & Boutin, A. Antibiotic resistance. *J. Infect. Public Health* **10**, 369–378 (2017).
92. Nakatsuji, T. et al. A commensal strain of Staphylococcus epidermidis protects against skin neoplasia. *Sci. Adv*. **4**, (2018).
93. Nakatsuji, T. et al. Development of a human skin commensal microbe for bacteriotherapy of atopic dermatitis and use in a phase 1 randomized clinical trial. *Nat. Med*. https://doi.org/10.1038/s41591-021-01256-2 (2021).
94. Krejsgaard, T. et al. Malignant inflammation in cutaneous T-cell lymphoma—a hostile takeover. *Semin. Immunopathol.* **39**, 269–282 (2017).
95. Brandt, B. E. Th2 Cytokines and Atopic Dermatitis. *J. Clin. Cell. Immunol.* **2**, 110 (2011).
96. Kong, H. H. et al. Temporal shifts in the skin microbiome associated with disease flares and treatment in children with atopic dermatitis. *Genome Res*. **22**, 850–859 (2012).
97. Byrd, A. L. et al. Staphylococcus aureus and Staphylococcus epidermidis strain diversity underlying pediatric atopic dermatitis. *Sci. Transl. Med.* **9**, eaal4651 (2017).
98. Nübel, U. et al. Frequent emergence and limited geographic dispersal of methicillin-resistant Staphylococcus aureus. *Proc. Natl Acad. Sci.* **105**, 14130–14135 (2008).
99. Achermann, Y., Goldstein, E. J. C., Coenye, T. & Shirtliff, M. E. Propionibacterium acnes: from Commensal to Opportunistic Biofilm-Associated Implant Pathogen. *Clin. Microbiol. Rev.* **27**, 419–440 (2014).
100. Wollenberg, M. S. et al. Propionibacterium-produced coproporphyrin III induces staphylococcus aureus aggregation and Biofilm formation. *MBio* **5**, 1–10 (2014).
101. Grice, E. A. et al. Topographical and Temporal Diversity of the Human Skin Microbiome. *Science (80-)* **324**, 1190–1192 (2009).
102. Oh, J. Human, Bacterial and Fungal Amplicon Collection and Processing for Sequencing. *BIO-PROTOCOL* **5**, (2015).
103. Beghini, F. et al. Integrating taxonomic, functional, and strain-level profiling of diverse microbial communities with bioBakery 3. *Elife* **10**, 1–42 (2021).
104. Andrews, S. & Babraham I. FastQC: A Quality Control Tool for High Throughput Sequence Data. (2010).
105. Bolger, A. M., Lohse, M. & Usadel, B. Trimmomatic: a flexible trimmer for Illumina sequence data. *Bioinformatics* **30**, 2114–2120 (2014).
106. Langmead, B. & Salzberg, S. L. Fast gapped-read alignment with Bowtie 2. *Nat. Methods* **9**, 357–359 (2012).
107. Tett, A. et al. Unexplored diversity and strain-level structure of the skin microbiome associated with psoriasis. *npj Biofilms Microbiomes* **3**, 14 (2017).
108. Truong, D. T. et al. MetaPhlAn2 for enhanced metagenomic taxonomic profiling. *Nat. Methods* **12**, 902–903 (2015).
109. Wickham, H. *Ggplot2: Elegant Graphics for Data Analysis*. (Springer-Verlag New York, 2016).
110. Shen, W., Le, S., Li, Y. & Hu, F. SeqKit: A Cross-Platform and Ultrafast Toolkit for FASTA/Q File Manipulation. *PLoS One* **11**, e0163962 (2016).

111. Dixon, P. VEGAN, a package of R functions for community ecology. *J. Veg. Sci.* **14**, 927–930 (2003).
112. Martinez Arbizu, P. pairwiseAdonis: Pairwise multilevel comparison using adonis. at https://github.com/pmartinezarbizu/pairwiseAdonis (2020).
113. Vander Heiden, J. A. et al. pRESTO: a toolkit for processing high-throughput sequencing raw reads of lymphocyte receptor repertoires. *Bioinformatics* **30**, 1930–1932 (2014).
114. ImmunoMind Team. immunarch: An R Package for Painless Bioinformatics Analysis of T-Cell and B-Cell Immune Repertoires. at https://doi.org/10.5281/zenodo.3367200 (2019).
115. Springer, I., Tickotsky, N. & Louzoun, Y. Contribution of T Cell Receptor Alpha and Beta CDR3, MHC Typing, V and J Genes to Peptide Binding Prediction. *Front. Immunol*. **12**, (2021).
116. van Dongen, J. J. M. et al. Design and standardization of PCR primers and protocols for detection of clonal immunoglobulin and T-cell receptor gene recombinations in suspect lymphoproliferations: Report of the BIOMED-2 Concerted Action BMH4-CT98-3936. *Leukemia* **17**, 2257–2317 (2003).
117. Genolet, R. et al. TCR sequencing and cloning methods for repertoire analysis and isolation of tumor-reactive TCRs. *Cell Rep. Methods* **3**, 100459 (2023).
118. Mazzotti, L. et al. T-Cell Receptor Repertoire Sequencing and Its Applications: Focus on Infectious Diseases and Cancer. *Int. J. Mol. Sci.* **23**, 8590 (2022).
119. Vogel, R. A. & Johnson, M. Modification of the Tellurite-Glycine Medium for use in the Identification of Staphylococcus aureus. *Public Health Lab.* **18**, 131–133 (1960).
120. Zebovitz, E., Evans, J. B. & Niven, C. F. Tellurite-glycine agar: a selective plating medium for the quantitative detection of coagulase-positive staphylococci. *J. Bacteriol.* **70**, 686–690 (1955).
121. Martineau, F. et al. Development of a PCR Assay for Identification of Staphylococci at Genus and. *Species Lev. J. Clin. Microbiol.* **39**, 2541–2547 (2001).
122. Midorikawa, K. et al. Staphylococcus aureus Susceptibility to Innate Antimicrobial Peptides, β-Defensins and CAP18, Expressed by Human Keratinocytes. *Infect. Immun.* **71**, 3730–3739 (2003).
123. Sanger, F., Nicklen, S. & Coulson, A. R. DNA sequencing with chain-terminating inhibitors. *Proc. Natl Acad. Sci.* **74**, 5463–5467 (1977).
124. Madeira, F. et al. The EMBL-EBI search and sequence analysis tools APIs in 2019. *Nucleic Acids Res* **47**, W636–W641 (2019).
125. Oladipo, I. C., Ogunsona, S. B. & Abayomi, M. A. Methicillin-resistant Staphylococcus aureus (MRSA) as a cause of nosocomial infection in Ibadan, Nigeria. *Eur. J. Pharm. Med. Res*. 135–139 (2019).

Acknowledgements

This study received no funding.

Author contributions

Clinical data coordination: P.L., J.K., M.H., H.S., M.M., V.M.; Clinical fieldwork: P.L., J.K., M.H., H.S., M.M., V.M.; Conceptualization: P.L., N.D., M.B., S.G., V.M.; Data curation: P.L., N.D., S.P., J.K., E.S.M., K.S.H., ; Formal analysis P.L., N.D., S.P., E.S.M., K.S.H.; Funding acquisition: P.L., V.M.; Investigation: P.L., N.D., S.P., J.H., E.S.M., K.S.H., M.H., H.S., M.B., M.M., S.G., R.H., V.M.; Project Administration: P.L., N.D., J.K., S.G., V.M.; Supervision: P.L., N.D., S.G., R.H., V.M.; Visualization: P.L., N.D.; Writing-original draft: P.L., N.D., M.H.; Writing, review, and editing: all authors. All authors read and approved the final manuscript.

Funding

Open Access funding enabled and organized by Projekt DEAL.

Competing interests

The authors declare no competing interests.

Ethics declarations

Ethics approval and consent to participate All procedures in this study were conducted in accordance with the Declaration of Helsinki from 1964 and its later amendments. Both local ethics committees responsible for the two study centres assigned ethical approval: The Medical Association of Rhineland-Palatine (Ethik-Kommisssion der Landesaerztekammer Rheinland-Pfalz), Germany (approval number: 2020-14813), and the ethics committee of the Faculty of Medicine, University of Frankfurt, Germany (approval number: 2021-46). All patients provided written informed consent.

Additional information

Supplementary information The online version contains supplementary material available at https://doi.org/10.1038/s41522-024-00542-4.

Correspondence and requests for materials should be addressed to Philipp Licht or Volker Mailänder.

Publication 2: The skin microbiome stratifies patients with cutaneous T cell lymphoma and determines event-free survival

3.1 Supplementals of Publication 2

Supplementary Material 1

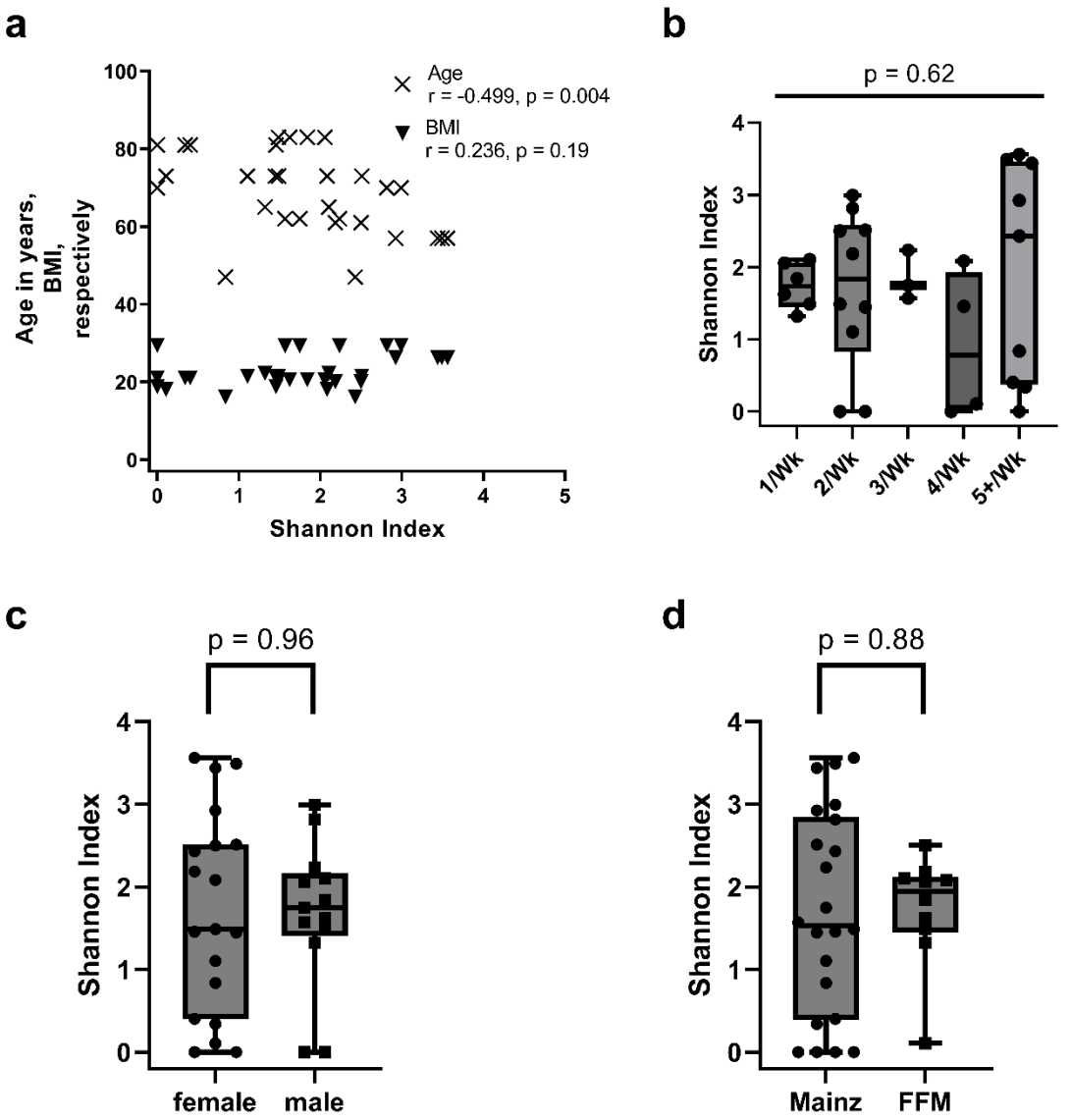

Supplementary Figure 1: Associations of α-diversity (Shannon Index) with demographic data. Reads were rarefied to common depth. a, Age in years and the BMI were correlated using spearman with the Shannon Index. **b,** Weekly Showering frequency. Wk = weekly. Kruskal-Wallis test, n = 32 **c,** Sex-related differences, Mann Whitney test, n = 32 **d,** Differences between study sites, FFM = Frankfurt am Main, Germany. Mann Whitney test, n = 32.

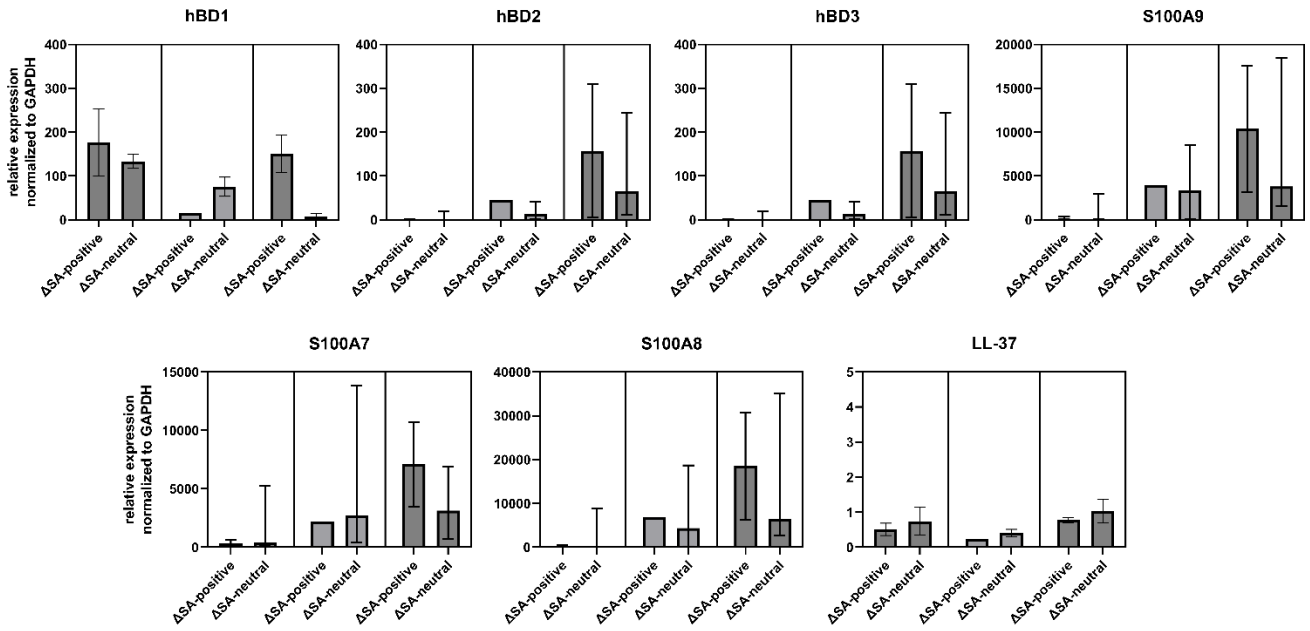

Supplementary Figure 2: Expression levels of AMPs stratified to ΔSA-positive and ΔSA-negative subgroups.

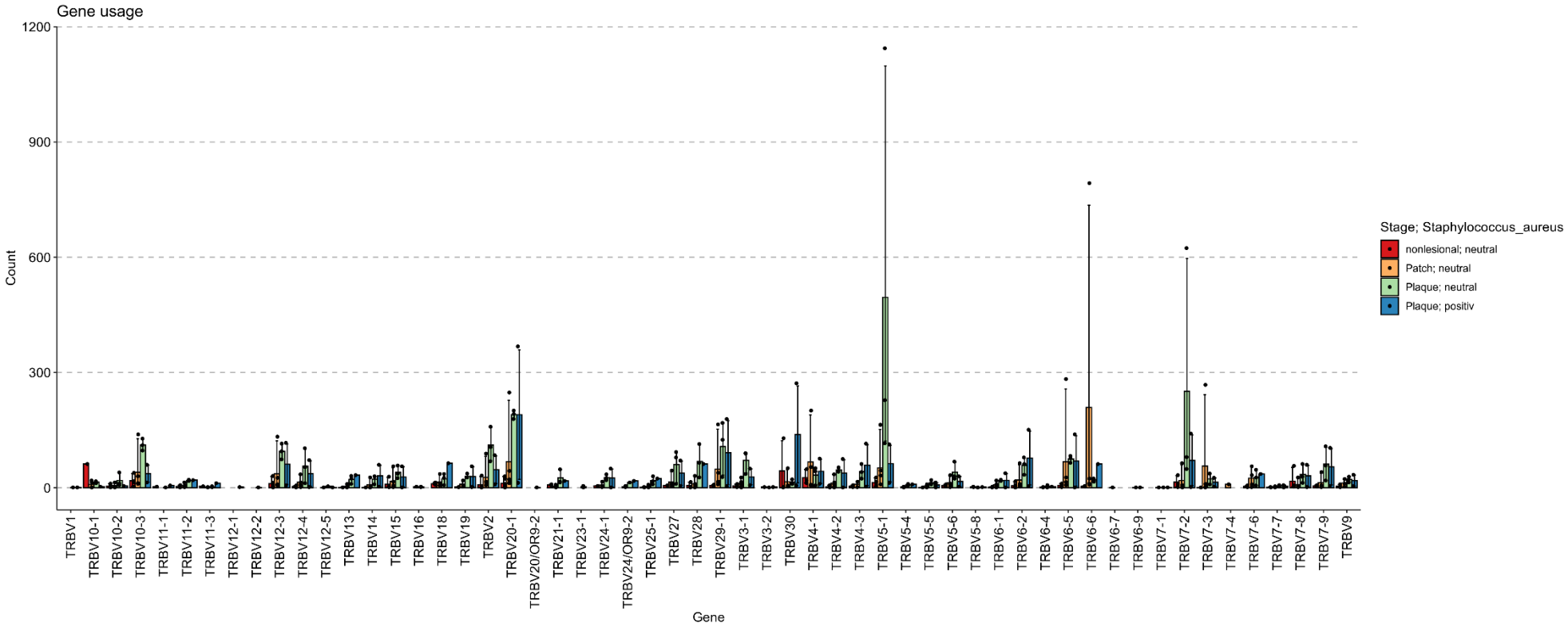

Supplementary Figure 3: TRBV Gene Usage of the TCR repertoire stratified to lesional stages and *S. aureus* status. TRBV5-1 is heavily reduced in Plaques with S. aureus. TRBV5-1 was linked to being tumour infiltrating lymphocytes by another investigation [1].

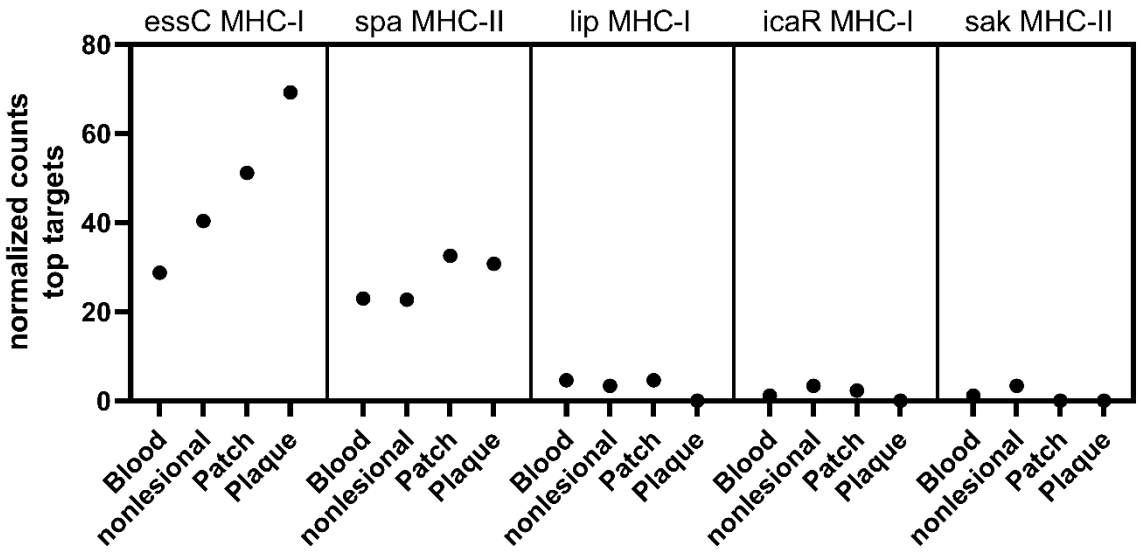

Supplementary Figure 4: Top epitope targets of T cell receptors. The epitopes that showed the highest binding score (strongest affinity) to TCRs in each sample were denoted and counted. The epitope for spa, a virulence factor enriched on Plaque of ΔSA-positive patients, is recognized by MHC-II with high affinity. spa was shown to trigger inflammation and survival via NF-κB [2,3] and CD4+ T cells are the subset of T cells that are malignant in MF [4].

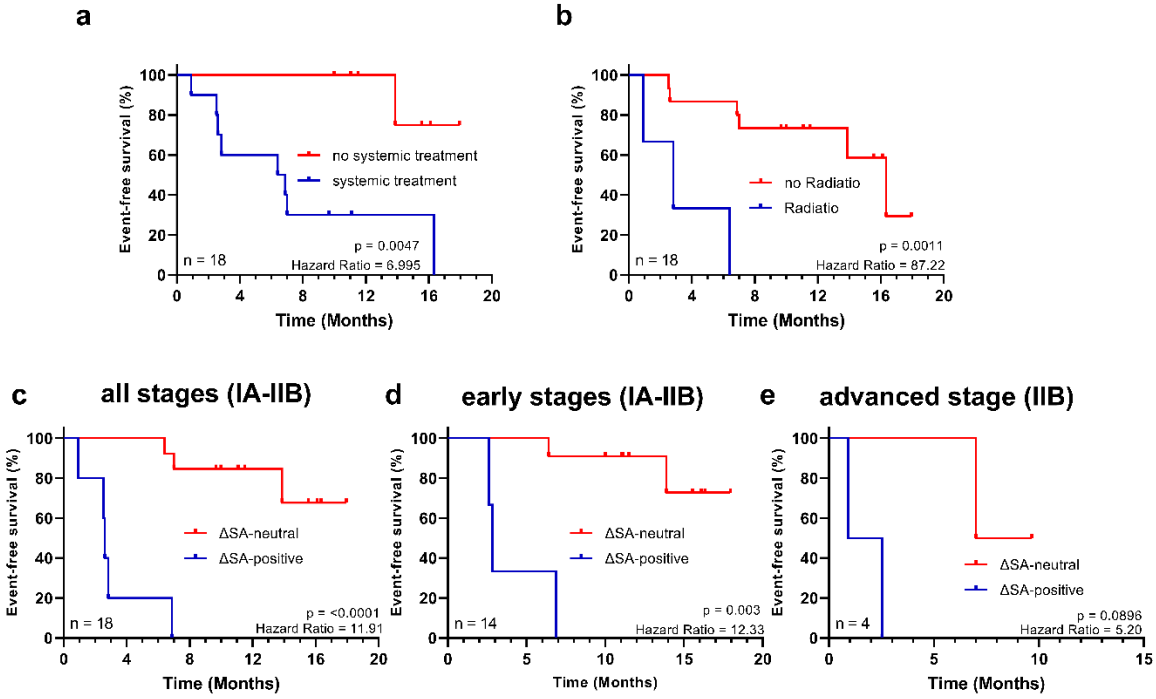

Supplementary Figure 5: Event-free survival Kaplan-Meier curves. The log-rank test was used to determine significance of differences between survival curves (1 degree of freedom). a, 95% Confidence Interval 2.801 to 39.14 **b,** 95% Confidence Interval 0.5117 to 91.12 **c,** 95% Confidence Interval 18.21 to 98.36 **d,** 95% Confidence Interval 0.74 to 206.5 **e,** 95% Confidence Interval 0.42 to 65.05.

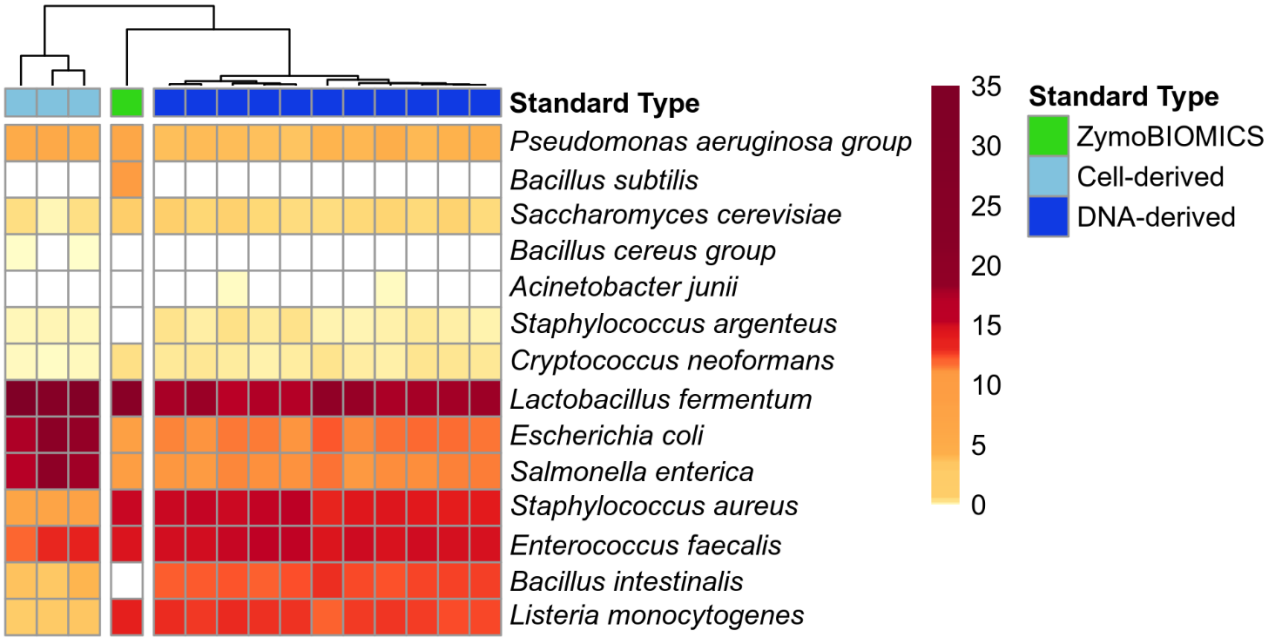

Supplementary Figure 6: High concordance of Cell- and DNA-derived positive controls with the suppliers' specifications. Control standards comprising of either a mock community of inactivated microbial cells (i.e., Cell-derived) or thereof derived microbial DNA (i.e., DNA-derived) processed with each batch of metagenomic sample DNA extraction and library preparation. The suppliers specified microbial composition of both standards is annotated as ZymoBIOMICS. Overall, both Cell-derived and DNA-derived standards showed high concordance between with the suppliers' specifications. *B. subtilis* was mistakenly classified as *B. intestinalis* and *B. cereus group* (very small read fractions in two Cell-derived control samples). A small fraction of reads belonging to *S. aureus* was mistakenly classified as *S. argenteus*. The latter organism is highly similar to *S. aureus* and was first described as a strain of this species, until *S. argenteus* was classified as individual organism [5,6]. Very small fractions of reads were mistakenly assigned to *A. junii* in two DNA-derived samples. Clustering was performed using Euclidean distance.

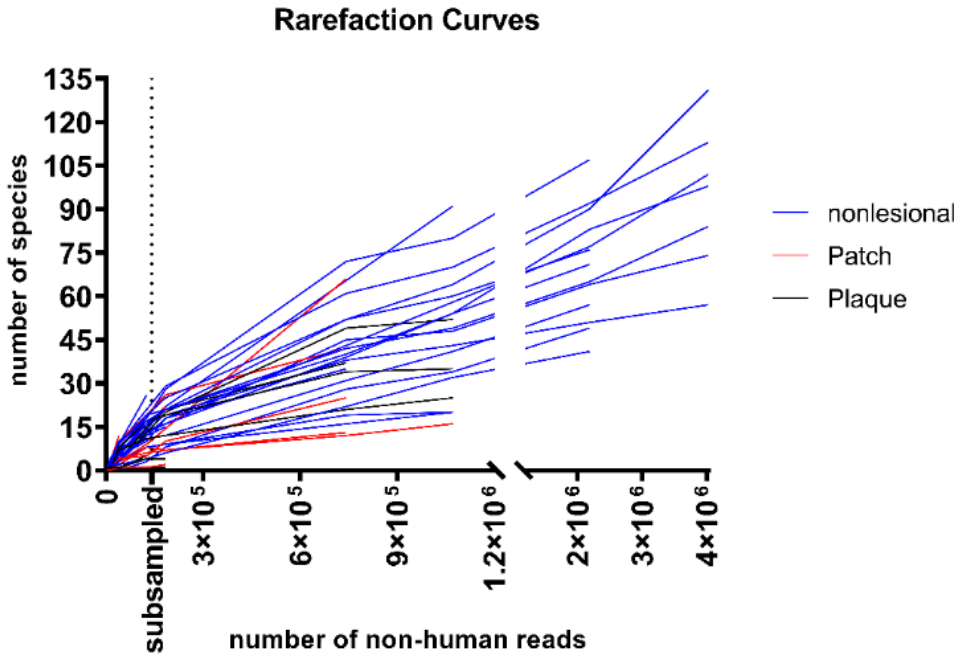

Supplementary Figure 7: Rarefaction curves. Non-human, quality-checked metagenomic reads were subsampled to increasing depths. For the analysis of diversity metrics and clustering taxonomic profiles samples were subsampled to 141,703 reads. At this point most metagenomic samples are still below the subsampling-threshold and the number of observed species are maximized.

Supplementary Table 1: Antibiotic diffusion assay. The patient derived isolates *S. aureus* MFMZ1, *S. epidermidis* MFMZ1, and *S. hominis* MFMZ1 as well as positive control *S. aureus* DSM11823 and negative control strains derived from healthy patients *S. aureus* EM01 and *S. epidermidis* MV01 were tested on resistance towards a set of commonly used antibiotics in the clinic. **a,** The antibiotics were applied using a Sensi-Disk dispenser with (1) 25 µg ampicillin, (2) 100 µg carbenicillin, (3) (23.75 µg) sulfamethoxazol + (1.25 µg) trimethoprim, (4) 15 µg erythromycin, (5) 10 µg gentamycin, and (6) 5 µg novobiocin. Measurement of halos indicating (s) sensitive, (i) intermediate, or (r) resistance effect of the antibiotics towards the tested Staphylococci strains. * indicates that the antibiotic showed an unclear categorization between i and r.

	S. aureus EM01	***S. aureus DSM 11823***	***S. aureus MFMZ1***	***S. hominis MFMZ1***	***S. epidermidis MFMZ1***	***S. epidermidis MV01***
(1) Ampicillin	24.0 mm (r)	27.1 mm (r)	0 mm (r)	34.4 mm (s)	33.4 mm (s)	36.1 mm (s)
(2) Carbenicillin	26.0 (s)	24.1 mm (i)	0 mm (r)	26.2 mm (s)	26.2 mm (s)	36.6 mm (s)
(3) Sulfamethoxazole + Trimethoprim	15.0 mm (i)	11.8 mm (i)	12.0 mm (i)	21.0 mm (s)	20.8 mm (s)	15.3 mm (s)
(4) Erythromycin	15.0 mm (i)	20.1 mm (i)	20.0 mm (i)	25.1 mm (s)	28.2 mm (s)	22.3 mm (s)
(5) Gentamycin	10.0 mm (r)	14.9 mm (s)	12.0 mm (i-r)*	14.4 mm (s)	25.9 mm (s)	15.9 mm (s)
(6) Novobiocin	24.0 mm (s)	28.5 mm (s)	29.4 mm (s)	27.0 mm (s)	38.2 mm (s)	33.1 mm (s)

Supplementary Table 2: Sequences of Primers for AMPs and quantification of Staphylococci quantification and virulence genes.

Gene	*Primers*	*Source*
GAPDH	F: 5'-TCAAGGCTGAGAACGGGAAG-3' R: 5'-CGCCCCACTTGATTTTGGAG-3'	[7]
hBD1	F: 5'-TGAGAACTTCCTACCTTCTGCTGTTT-3' R: 5'-GCCAAGGCCTGTGAGAAAGTTA-3'	[8]
hBD2	F: 5'-TGATGCCTCTTCCAGGTGTTT-3' R: 5'-GGATGACATATGGCTCCACTCTT-3'	[9]
hBD3	F: 5'-TGAGGATCCATTATCTTCTGTTTGCT-3' R: 5'-TTCTGTAATGTGTTTATGATTCCTCCA-3'	[8]
LL-37	F: 5'-TGACTTCAAGAAGGACGGGC-3' R: 5'-AGGGCACACACTAGGACTCT-3'	Self-Designed
S100A7	F: 5'-CTTCCTTAGTGCCTGTGACAAAAA-3' R: 5'-AAAGACAGAAACTCAGAAAAATCAATCT-3'	[10]
S100A8	F: 5'-ATGCCGTCTACAGGGATGAC-3' R: 5'-ACGCCCATCTTTATCACCAG-3'	[11]
S100A9	F: 5'-CAGCTGGAACGCAACATAGA-3' R: 5'-TCAGCTGCTTGTCTGCATTT-3'	[10]
spa	F: 5'-GATTTTGCGGTTTTAAGCC-3' R: 5'-GAGTAGAAAGTGTTGAGGC-3'	Self-Designed

References

1. Iyer A, Hennessey D, O'Keefe S, Patterson J, Wang W, Salopek T, et al. Clonotypic heterogeneity in cutaneous T-cell lymphoma (mycosis fungoides) revealed by comprehensive whole-exome sequencing. Blood Adv [Internet]. 2019;3:1175–84. Available from: https://ashpublications.org/bloodadvances/article/3/7/1175/247276/Clonotypic-heterogeneity-in-cutaneous-Tcell

2. Gómez MI, Lee A, Reddy B, Muir A, Soong G, Pitt A, et al. Staphylococcus aureus protein A induces airway epithelial inflammatory responses by activating TNFR1. Nat Med [Internet]. 2004;10:842–8. Available from: http://www.nature.com/articles/nm1079

3. Gómez MI, O'Seaghdha M, Magargee M, Foster TJ, Prince AS. Staphylococcus aureus Protein A Activates TNFR1 Signaling through Conserved IgG Binding Domains. J Biol Chem [Internet]. 2006;281:20190–6. Available from: https://linkinghub.elsevier.com/retrieve/pii/S0021925819763339

4. Campbell JJ, Clark RA, Watanabe R, Kupper TS. Sézary syndrome and mycosis fungoides arise from distinct T-cell subsets: a biologic rationale for their distinct clinical behaviors. Blood [Internet]. 2010;116:767–71. Available from: https://ashpublications.org/blood/article/116/5/767/107723/Sézary-syndrome-and-mycosis-fungoides-arise-from

5. Holt DC, Holden MTG, Tong SYC, Castillo-Ramirez S, Clarke L, Quail MA, et al. A Very Early-Branching Staphylococcus aureus Lineage Lacking the Carotenoid Pigment Staphyloxanthin. Genome Biol Evol [Internet]. 2011;3:881–95. Available from: https://academic.oup.com/gbe/article/doi/10.1093/gbe/evr078/591113

6. Tong SYC, Schaumburg F, Ellington MJ, Corander J, Pichon B, Leendertz F, et al. Novel staphylococcal species that form part of a Staphylococcus aureus-related complex: the non-pigmented Staphylococcus argenteus sp. nov. and the non-human primate-associated Staphylococcus schweitzeri sp. nov. Int J Syst Evol Microbiol [Internet]. 2015;65:15–22. Available from: https://www.microbiologyresearch.org/content/journal/ijsem/10.1099/ijs.0.062752-0

7. Dahn ML, Dean CA, Jo DB, Coyle KM, Marcato P. Human-specific GAPDH qRT-PCR is an accurate and sensitive method of xenograft metastasis quantification. Mol Ther - Methods Clin Dev [Internet]. The Author(s); 2021;20:398–408. Available from: https://doi.org/10.1016/j.omtm.2020.12.010

8. Wolk K, Mitsui H, Witte K, Gellrich S, Gulati N, Humme D, et al. Deficient Cutaneous Antibacterial Competence in Cutaneous T-Cell Lymphomas: Role of Th2-Mediated Biased Th17 Function. Clin Cancer Res [Internet]. 2014;20:5507–16. Available from: http://clincancerres.aacrjournals.org/lookup/doi/10.1158/1078-0432.CCR-14-0707

9. Gambichler T, Skrygan M, Appelhans C, Tomi NS, Reinacher-Schick A, Altmeyer P, et al. Expression of human β-defensins in patients with mycosis fungoides. Arch Dermatol Res [Internet]. 2007;299:221–4. Available from: http://link.springer.com/10.1007/s00403-007-0749-6

10. Suga H, Sugaya M, Miyagaki T, Ohmatsu H, Kawaguchi M, Takahashi N, et al. Skin Barrier Dysfunction and Low Antimicrobial Peptide Expression in Cutaneous T-cell Lymphoma. Clin Cancer Res [Internet]. 2014;20:4339–48. Available from: http://clincancerres.aacrjournals.org/lookup/doi/10.1158/1078-0432.CCR-14-0077

11. Nakajima R, Miyagaki T, Kamijo H, Oka T, Shishido-Takahashi N, Suga H, et al. Decreased progranulin expression in Mycosis fungoides: a possible association with the high frequency of skin infections. Eur J Dermatol [Internet]. 2018;28:790–4. Available from: http://www.ncbi.nlm.nih.gov/pubmed/30530405

B. Liu, D. Zheng, S. Zhou, L. Chen, J. Yang, Nucleic Acids Res. 50 (2022).
E. Blümel *et al.*, *Oncoimmunology*. **8**, e1641387 (2019).
E. Blümel *et al.*, *Oncoimmunology*. **9**, 1751561 (2020).
F. Alonzo, V. J. Torres, *Microbiol. Mol. Biol. Rev.* **78**, 199–230 (2014).
G. Y. C. Cheung, J. S. Bae, M. Otto, *Virulence*. **12**, 547–569 (2021).
D. A. Bloes, D. Kretschmer, A. Peschel, *Nat. Rev. Microbiol.* **13**, 95–104 (2015).

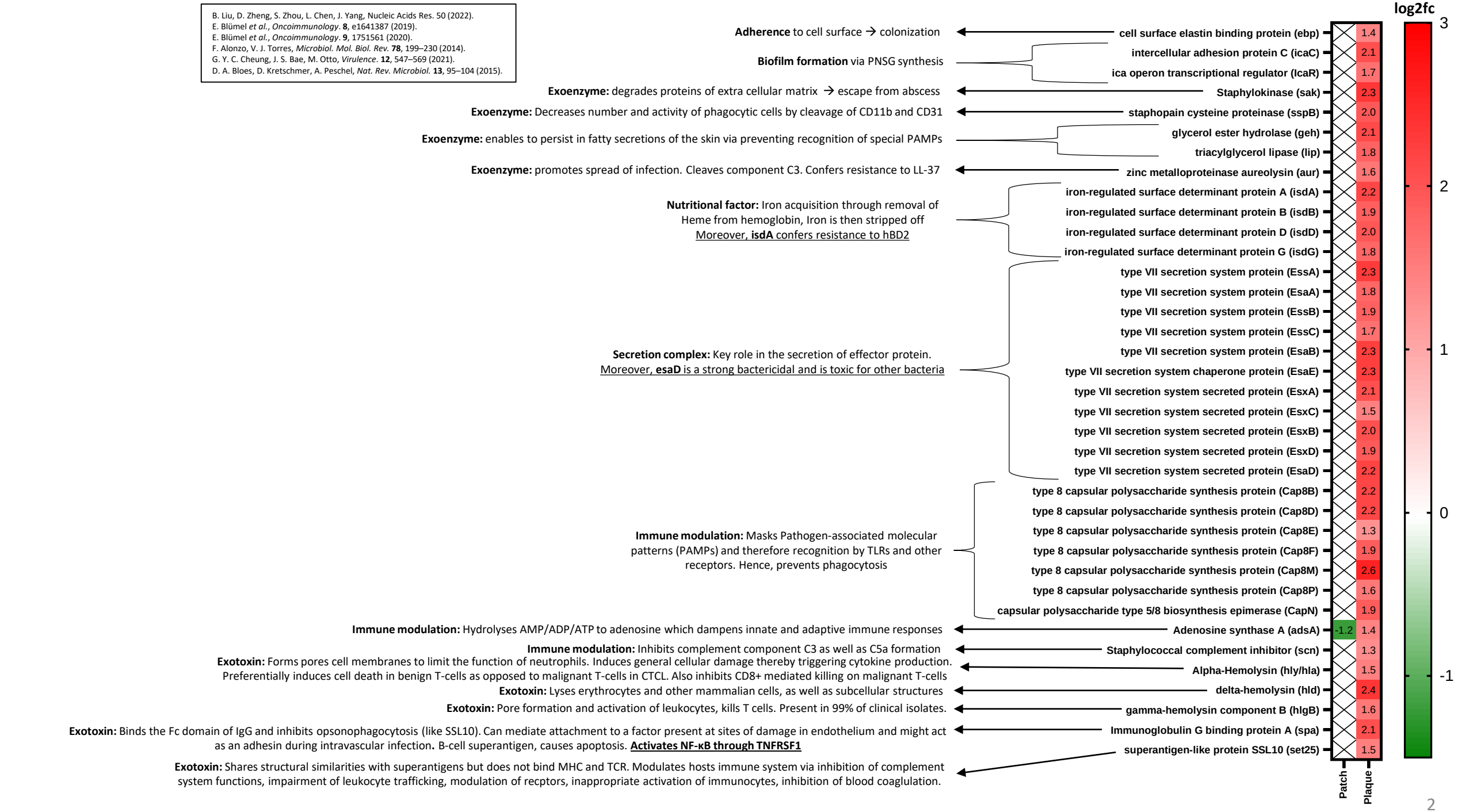

Supplementary Table 3: Differential Abundances Analysis of Microbial Species

feature	value	coef	fc	log2fc	stderr	N	N.not.zero	pval	qval
Malassezia_restricta	Plaque	-5,49759065	0,00409663	-7,93134677	0,96641785	65	43	9,57E-07	8,42E-05
Corynebacterium_matruchotii	Patch	-3,88813895	0,02048343	-5,60939878	0,75238701	65	19	5,70E-06	0,00025086
Cutibacterium_acnes	Plaque	-4,70187664	0,00907822	-6,78337412	0,96957971	65	58	1,64E-05	0,00048228
Finegoldia_magna	Plaque	-5,85585726	0,00286308	-8,44821622	1,26111871	65	44	2,56E-05	0,00056297
Micrococcus_luteus	Plaque	-4,53207265	0,01075835	-6,53839873	0,9868459	65	39	3,87E-05	0,00056718
Staphylococcus_hominis	Patch	-3,94654105	0,01932142	-5,6936552	0,85499377	65	38	3,43E-05	0,00056718
Rothia_dentocariosa	Patch	-4,94328864	0,00713111	-7,13165801	1,09690569	65	25	5,11E-05	0,00062085
Cutibacterium_granulosum	Plaque	-3,81563192	0,02202379	-5,50479324	0,86285818	65	37	6,44E-05	0,00062085
Peptoniphilus_harei	Plaque	-3,82016496	0,02192418	-5,51133305	0,87366953	65	29	7,06E-05	0,00062085
Acinetobacter_johnsonii	Patch	-4,35588335	0,0128311	-6,2842113	0,983059	65	23	5,89E-05	0,00062085

Staphylococcus_capitis	Patch	-4,04559864	0,01749923	-5,83656509	0,94172039	65	42	9,53E-05	0,00070631
Streptococcus_mitis	Patch	-3,17925775	0,04161653	-4,58669938	0,73932587	65	26	9,63E-05	0,00070631
Staphylococcus_epidermidis	Patch	-2,74912933	0,06398355	-3,96615525	0,64964189	65	52	0,00010746	0,00072745
Corynebacterium_amycolatum	Patch	-3,29483564	0,03707414	-4,75344303	0,77704325	65	23	0,00011939	0,00075047
Cutibacterium_granulosum	Patch	-3,17089086	0,0419662	-4,57462851	0,76885349	65	37	0,0001678	0,00086859
Staphylococcus_hominis	Plaque	-3,93660708	0,01951431	-5,67932351	0,95776374	65	38	0,00016682	0,00086859
Paracoccus_yeei	Plaque	-4,48238915	0,01130637	-6,4667206	1,08616949	65	24	0,00015464	0,00086859
Paracoccus_yeei	Patch	-3,92939304	0,0196556	-5,66891585	0,96834152	65	24	0,00019545	0,00095552
Malassezia_restricta	Patch	-3,46911874	0,03114446	-5,0048804	0,86147204	65	43	0,00022318	0,00103368
Staphylococcus_capitis	Plaque	-4,1502077	0,01576114	-5,98748406	1,05556515	65	42	0,00029093	0,00128007
Moraxella_osloensis	Plaque	-4,2330349	0,01450829	-6,10697846	1,11388662	65	44	0,00044957	0,00188392

Corynebacterium_pseudogenitalium	Plaque	-3,4577321	0,0315011 2	-4,9884529 5	0,9211501 6	65	38	0,0005058 2	0,0020232 8
Acinetobacter_johnsonii	Plaque	-4,0041773 5	0,0182392 9	-5,7768068 1	1,0997490 9	65	23	0,0006813 9	0,0026070 5
Rothia_dentocariosa	Plaque	-4,2648501 5	0,0140539 7	-6,1528781 7	1,2307992 9	65	25	0,0012114 6	0,0044420 2
Streptococcus_oralis	Patch	-2,6005408 6	0,0742334 2	-3,7517874	0,7604503 7	65	23	0,0013348 9	0,0046988 2
Staphylococcus_epidermidis	Plaque	-2,4432386 9	0,0868790 2	-3,5248483 4	0,7268300 1	65	52	0,0015340 3	0,0051921 2
Rothia_mucilaginosa	Patch	-2,7982445 7	0,0609169	-4,0370135 6	0,8376472 5	65	18	0,0017673 1	0,0057601 1
Kocuria_rhizophila	Patch	-2,1158990 7	0,1205248 8	-3,0525971	0,6543407	65	23	0,0023930 5	0,0074572 9
Anaerococcus_nagyae	Plaque	-2,4994748 1	0,0821281 2	-3,6059799 1	0,7803253 7	65	23	0,0025016 9	0,0074572 9
Anaerococcus_octavius	Plaque	-2,7795762 9	0,0620648	-4,0100809 3	0,8705023	65	25	0,0025422 6	0,0074572 9
Corynebacterium_afermentans	Plaque	-2,6909997 5	0,0678131 1	-3,8822919 9	0,8550683 2	65	27	0,0028107 4	0,0077327 7
Prevotella_timonensis	Plaque	-3,9761321 1	0,0187580 5	-5,7363460 8	1,2566805	65	24	0,0028119 2	0,0077327 7

Peptoniphilus_coxii	Plaque	-2,7292672	0,0652671	-3,9375003	0,8679519	65	19	0,0029407	0,0078419
Dermabacter_hominis	Patch	-2,3465563	0,0956981	-3,3853652	0,7692607	65	17	0,0038100	0,0098612
Peptoniphilus_lacrimalis	Plaque	-3,0257822	0,0485198	-4,3652809	1,0051708	65	20	0,0041929	0,0105421
Enhydrobacter_aerosaccus	Plaque	-5,0664233	0,0063049	-7,3093037	1,7529145	65	39	0,0059848	0,0146297
Prevotella_timonensis	Patch	-3,2126148	0,0402512	-4,6348234	1,1206124	65	24	0,0063673	0,015144
Corynebacterium_afermentans	Patch	-2,1474980	0,1167759	-3,0981847	0,7650405	65	27	0,0072216	0,0167237
Kocuria_rhizophila	Plaque	-2,0707986	0,1260850	-2,9875309	0,7360217	65	23	0,0074250	0,0167538
Cutibacterium_avidum	Plaque	-2,8032887	0,0606104	-4,0442908	1,0152980	65	19	0,0081531	0,0179368
Acinetobacter_lwoffii	Patch	-1,4803677	0,227554	-2,1357191	0,5482789	65	20	0,0099075	0,0212650
Staphylococcus_haemolyticus	Patch	-1,3856427	0,2501629	-1,9990598	0,5138684	65	21	0,0102242	0,0214222
Corynebacterium_tuberculostearicum	Plaque	-1,9010008	0,1494190	-2,7425644	0,7147350	65	21	0,0107841	0,0215682

Peptoniphilus_lacrimalis	Patch	-2,3925063	0,0914003 2	-3,4516569 7	0,8990547	65	20	0,0107072 4	0,0215682 8
Staphylococcus_aureus	Plaque	2,6868051 7	14,684685 8	3,8762405	1,0221438 9	65	30	0,0119399 7	0,0233492 7
Veillonella_parvula	Plaque	-1,4357269 9	0,2379423 2	-2,0713162 1	0,5573044 4	65	20	0,0130553 9	0,0249755 3
Veillonella_parvula	Patch	-1,2734923 9	0,2798525 6	-1,8372611 6	0,4997859	65	20	0,0141245	0,0258949 1
Finegoldia_magna	Patch	-2,8853679	0,0558342 4	-4,1627059 6	1,1300142 1	65	44	0,0138891 5	0,0258949 1
Corynebacterium_matruchotii	Plaque	-2,1395803 9	0,1177042 2	-3,0867620 2	0,8444220 1	65	19	0,0149143 2	0,0267849 1
Peptoniphilus_harei	Patch	-1,9658067 6	0,1400428 6	-2,8360596 6	0,7790213 3	65	29	0,0152354 3	0,0268143 5
Peptoniphilus_coxii	Patch	-1,9167682 6	0,1470815 2	-2,7653120 6	0,7736397 7	65	19	0,0170965 1	0,0294998 7
Malassezia_globosa	Patch	-2,2128226 7	0,1093914 4	-3,1924283	0,8995987 2	65	22	0,0180162 6	0,0304890 6
Anaerococcus_prevotii	Plaque	-2,6293023 2	0,0721287 7	-3,7932814 2	1,0912704 4	65	18	0,0199233 6	0,0330802 9
Rothia_mucilaginosa	Plaque	-2,2566339 2	0,1047023 3	-3,2556345 7	0,9392857 3	65	18	0,0207074 1	0,0334462 9

Acinetobacter_lwoffii	Plaque	-1,4768311	0,2283601	-2,1306169	0,6159279	65	20	0,0209039	0,0334462
			9	1	7			3	9
Micrococcus_aloeverae	Plaque	-2,3470974	0,0956463	-3,3861458	0,9991977	65	19	0,0231519	0,0358813
		2	8	1	9			3	5
Streptococcus_mitis	Plaque	-1,9493750	0,1423630	-2,8123537	0,8288787	65	26	0,0232413	0,0358813
		7	1	5	7			3	5
Propionibacterium_namnetense	Plaque	-0,9364258	0,3920265	-1,3509769	0,4008480	65	21	0,0244004	0,0370213
		5		3	3				
Staphylococcus_pettenkoferi	Patch	-1,0511062	0,3495508	-1,5164257	0,4610836	65	18	0,0272256	0,0406076
			6	1	9				7
Actinomyces_oris	Patch	-2,6178118	0,0729623	-3,7767041	1,1646701	65	21	0,0296959	0,0428401
		1	4	2	8			9	1
Kocuria_palustris	Patch	-1,8233718	0,1614803	-2,6305695	0,8111242	65	19	0,0296218	0,0428401
		8	4	7	6			6	1
Streptococcus_oralis	Plaque	-1,8682821	0,1543886	-2,6953613	0,8517200	65	23	0,0333257	0,0473010
		4	5	7	5			6	7
Malassezia_globosa	Plaque	-2,2034796	0,1104182	-3,1789491	1,0070454	65	22	0,0340259	0,0475282
		2	8	3	4			2	7
Anaerococcus_octavius	Patch	-1,6699568	0,1882551	-2,4092384	0,7766523	65	25	0,0369340	0,0507843
		3	9	4	1			5	2
Corynebacterium_tuberculostearicum	Patch	-1,347524	0,2598829	-1,9440661	0,6376825	65	21	0,0402516	0,0544945
			4	9	7			5	4

Anaerococcus_prevotii	Patch	-2,03496965	0,1306844 5	-2,93584062	0,9748344	65	18	0,0423675 4	0,0564900 6
Dermabacter_hominis	Plaque	-1,72231055	0,1786528 8	-2,48476888	0,8619874 6	65	17	0,0516172 7	0,0677958 1
Faecalibacterium_prausnitzii	Plaque	-1,678031	0,1867413 1	-2,420887	0,8471575	65	18	0,0530095 7	0,0679280 3
Enhydrobacter_aerosaccus	Patch	-3,10278167	0,0449240 6	-4,47636773	1,5610513 3	65	39	0,0532617 5	0,0679280 3
Staphylococcus_aureus	Patch	-1,79088513	0,1668124 5	-2,58370109	0,9088453 4	65	30	0,0554761 3	0,0697414 2
Cutibacterium_avidum	Patch	-1,7732156	0,1697861 5	-2,55820935	0,9074049 4	65	19	0,0566840 3	0,0702562 6
Actinomyces_oris	Plaque	-2,5379307	0,0790297 7	-3,66146004	1,3045183 6	65	21	0,0580250 1	0,0709194 5
Staphylococcus_haemolyticus	Plaque	-1,08330035	0,3384765 9	-1,56287205	0,5779216 3	65	21	0,0681603 8	0,0821659 4
Corynebacterium_kroppenstedtii	Patch	-1,48418683	0,2266866	-2,14122897	0,8011893 4	65	28	0,0710149 5	0,0844502 1
Staphylococcus_pettenkoferi	Plaque	-0,91446118	0,4007324 9	-1,31928861	0,5155782 3	65	18	0,0824695 1	0,0967642 3
Faecalibacterium_prausnitzii	Patch	-1,3174793	0,2678095 2	-1,90072085	0,7605913 2	65	18	0,0894476 1	0,1035709 1

Propionibacterium_namnetense	Patch	-0,60847385	0,54418074	-0,8778422	0,35630347	65	21	0,09521696	0,10881938
Corynebacterium_kroppenstedtii	Plaque	-1,4970951	0,22377927	-2,15985168	0,90073816	65	28	0,10389972	0,11722019
Kocuria_palustris	Plaque	-1,40860988	0,24448291	-2,03219449	0,90929245	65	19	0,12836	0,141196
Anaerococcus_nagyae	Patch	-1,08152017	0,33907968	-1,56030378	0,6958318	65	23	0,12726176	0,141196
Micrococcus_luteus	Patch	-1,10972418	0,32964987	-1,60099357	0,8778293	65	39	0,21311585	0,23153327

Supplementary Table 4: Differential Abundances Analysis of Virulence Genes

feature	value	coef	fc	log2fc	stderr	N	N.not.0	pval	qval
(cap8M) type 8 capsular polysaccharide synthesis protein Cap8M [Capsule (VF0003) - Immune modulation (VFC0258)] [Staphylococcus aureus subsp. aureus MW2]	Plaque	1,79447686	6,01632653	2,58888287	0,56140402	65	17	0,00238604	0,07158114
(hld) delta-hemolysin [-hemolysin (VF0007) - Exotoxin (VFC0235)] [Staphylococcus aureus subsp. aureus MW2]	Plaque	1,63885211	5,14925533	2,36436381	0,59339576	65	7	0,00776988	0,10391755
(sak) Staphylokinase precursor [Staphylokinase (VF0021) - Exoenzyme (VFC0251)] [Staphylococcus aureus subsp. aureus MW2]	Plaque	1,62416901	5,07420067	2,34318058	0,43220667	65	14	0,00044645	0,05357401

(essA) type VII secretion system protein EssA, monotopic membrane protein [Type VII secretion system (VF0403) - Effector delivery system (VFC0086)] [Staphylococcus aureus subsp. aureus MW2]	Plaque	1,59685407	4,93747502	2,30377345	0,64946357	65	10	0,01731959	0,10391755
(esaE) type VII secretion system chaperone protein [Type VII secretion system (VF0403) - Effector delivery system (VFC0086)] [Staphylococcus aureus subsp. aureus MW2]	Plaque	1,571273	4,81277094	2,26686776	0,44427223	65	15	0,00093933	0,05635985
(esaB) type VII secretion system protein EsaB [Type VII secretion system (VF0403) - Effector delivery system (VFC0086)] [Staphylococcus aureus subsp. aureus MW2]	Plaque	1,56951905	4,80433698	2,26433735	0,62031179	65	12	0,01444507	0,10391755
(esaD) type VII secretion system secreted protein, a nuclease toxin EsaD [Type VII secretion system (VF0403) - Effector delivery system (VFC0086)] [Staphylococcus aureus subsp. aureus MW2]	Plaque	1,53071132	4,62146299	2,20834963	0,57653013	65	13	0,01044238	0,10391755
(cap8B) type 8 capsular polysaccharide synthesis protein Cap8B [Capsule (VF0003) - Immune modulation (VFC0258)] [Staphylococcus aureus subsp. aureus MW2]	Plaque	1,50781735	4,51686132	2,17532062	0,60849744	65	12	0,01665397	0,10391755
(cap8D) type 8 capsular polysaccharide synthesis protein Cap8D [Capsule (VF0003) - Immune modulation (VFC0258)] [Staphylococcus aureus subsp. aureus MW2]	Plaque	1,50669137	4,51177829	2,17369617	0,59512364	65	11	0,01455379	0,10391755

(isdA) iron-regulated surface determinant protein A [Isd (VF0015) - Nutritional/Metabolic factor (VFC0272)] [Staphylococcus aureus subsp. aureus str. Newman]	Plaque	1,49726282	4,46943864	2,16009364	0,56152265	65	10	0,01010552	0,10391755
(geh) glycerol ester hydrolase [Lipase (VF0012) - Exoenzyme (VFC0251)] [Staphylococcus aureus subsp. aureus MW2]	Plaque	1,47054387	4,35160122	2,12154635	0,52854085	65	8	0,00734715	0,10391755
(spa) Immunoglobulin G binding protein A precursor [SpA (VF0017) - Exotoxin (VFC0235)] [Staphylococcus aureus subsp. aureus MW2]	Plaque	1,43449496	4,19752456	2,06953877	0,65002904	65	9	0,03153937	0,14556632
(esxA) type VII secretion system secreted protein EsxA [Type VII secretion system (VF0403) - Effector delivery system (VFC0086)] [Staphylococcus aureus subsp. aureus MW2]	Plaque	1,42815607	4,17100105	2,06039368	0,49629191	65	21	0,00595724	0,10391755
(icaC) intercellular adhesion protein C, involved in polysaccharide intercellular adhesin(PIA) synthesis [Intercellular adhesion proteins (VF0014) - Biofilm (VFC0271)] [Staphylococcus aureus subsp. aureus MW2]	Plaque	1,42733293	4,16756916	2,05920614	0,57095955	65	13	0,01585216	0,10391755
(esxB) type VII secretion system secreted protein EsxB [Type VII secretion system (VF0403) - Effector delivery system (VFC0086)] [Staphylococcus aureus subsp. aureus MW2]	Plaque	1,42065402	4,13982707	2,04957051	0,43971082	65	13	0,00228099	0,07158114
(isdD) iron-regulated surface determinant protein D [Isd (VF0015) - Nutritional/Metabolic factor (VFC0272)] [Staphylococcus aureus subsp. aureus str. Newman]	Plaque	1,37213874	3,94377641	1,97957776	0,50296924	65	11	0,00881067	0,10391755

(sspB) staphopain cysteine proteinase SspB [Staphopain (VF0006) - Exoenzyme (VFC0251)] [Staphylococcus aureus subsp. aureus MW2]	Plaque	1,35391851	3,87257054	1,95329152	0,54207889	65	12	0,01575994	0,10391755
(esxD) type VII secretion system secreted protein EsxD [Type VII secretion system (VF0403) - Effector delivery system (VFC0086)] [Staphylococcus aureus subsp. aureus MW2]	Plaque	1,34144719	3,82457438	1,9352992	0,55125895	65	14	0,01873092	0,10703384
capN) capsular polysaccharide type 5/8 biosynthesis epimerase CapN [Capsule (VF0003) - Immune modulation (VFC0258)] [Staphylococcus aureus subsp. aureus MW2]	Plaque	1,32550829	3,76409814	1,91230424	0,58363711	65	19	0,02740781	0,1426702
(cap8F) type 8 capsular polysaccharide synthesis protein Cap8F [Capsule (VF0003) - Immune modulation (VFC0258)] [Staphylococcus aureus subsp. aureus MW2]	Plaque	1,31557888	3,72690779	1,89797913	0,52541653	65	13	0,01566541	0,10391755
isdB) iron-regulated surface determinant protein B, haemoglobin receptor [Isd (VF0015) - Nutritional/Metabolic factor (VFC0272)] [Staphylococcus aureus subsp. aureus str. Newman]	Plaque	1,29881047	3,66493451	1,87378742	0,52623901	65	15	0,01718483	0,10391755
(essB) type VII secretion system protein EssB, monotopic membrane protein [Type VII secretion system (VF0403) - Effector delivery system (VFC0086)] [Staphylococcus aureus subsp. aureus MW2]	Plaque	1,29315565	3,64426846	1,86562924	0,5697769	65	13	0,02762377	0,1426702
(lip) triacylglycerol lipase precursor [Lipase (VF0012) - Exoenzyme (VFC0251)] [Staphylococcus aureus subsp. aureus MW2]	Plaque	1,27337489	3,57289036	1,83709164	0,49845452	65	9	0,01388927	0,10391755

(isdG) iron-regulated surface determinant protein G [Isd (VF0015) - Nutritional/Metabolic factor (VFC0272)] [Staphylococcus aureus subsp. aureus str. Newman]	Plaque	1,2435211	3,46780247	1,79402172	0,55097313	65	12	0,02853404	0,1426702
(esaA) type VII secretion system protein EsaA [Type VII secretion system (VF0403) - Effector delivery system (VFC0086)] [Staphylococcus aureus subsp. aureus MW2]	Plaque	1,24247471	3,46417571	1,79251211	0,56655199	65	17	0,03300159	0,14667374
(essC) type VII secretion system protein EssC, FtsK/SpoIIIE family ATPase [Type VII secretion system (VF0403) - Effector delivery system (VFC0086)] [Staphylococcus aureus subsp. aureus MW2]	Plaque	1,15810679	3,18389978	1,67079493	0,55363047	65	10	0,04168571	0,16606933
(icaR) ica operon transcriptional regulator IcaR [Intercellular adhesion proteins (VF0014) - Biofilm (VFC0271)] [Staphylococcus aureus subsp. aureus MW2]	Plaque	1,15236021	3,1656557	1,66250435	0,57975442	65	17	0,05198515	0,17704151
aur) zinc metalloproteinase aureolysin [Aureolysin (VF0024) - Exoenzyme (VFC0251)] [Staphylococcus aureus subsp. aureus MW2]	Plaque	1,11031699	3,03532041	1,60184881	0,5025413	65	7	0,03135327	0,14556632
(hlgB) gamma-hemolysin component B [-hemolysin (VF0011) - Exotoxin (VFC0235)] [Staphylococcus aureus subsp. aureus MW2]	Plaque	1,09618961	2,99274077	1,58146732	0,53335407	65	8	0,04465572	0,16606933
(cap8P) type 8 capsular polysaccharide synthesis protein Cap8P [Capsule (VF0003) - Immune modulation (VFC0258)] [Staphylococcus aureus subsp. aureus MW2]	Plaque	1,09553203	2,99077343	1,58051862	0,58247511	65	14	0,0659863	0,19822864

(set25) superantigen-like protein SSL10 [SSLs (VF0990) - Exotoxin (VFC0235)] [Staphylococcus aureus subsp. aureus MW2]	Plaque	1,03892936	2,82618956	1,49885823	0,54956235	65	13	0,06444136	0,19822864
(esxC) type VII secretion system secreted protein EsxC [Type VII secretion system (VF0403) - Effector delivery system (VFC0086)] [Staphylococcus aureus subsp. aureus MW2]	Plaque	1,03131103	2,80474054	1,48786731	0,49975523	65	16	0,04422772	0,16606933
(hly/hla) Alpha-Hemolysin precursor [-hemolysin (VF0001) - Exotoxin (VFC0235)] [Staphylococcus aureus subsp. aureus MW2]	Plaque	1,03114068	2,80426279	1,48762155	0,49657481	65	11	0,04270114	0,16606933
(adsA) Adenosine synthase A [AdsA (VF0422) - Immune modulation (VFC0258)] [Staphylococcus aureus subsp. aureus MW2]	Plaque	1,00479985	2,73136055	1,44961977	0,48931096	65	11	0,04566907	0,16606933
(ebp) cell surface elastin binding protein [EbpS (VF0008) - Adherence (VFC0001)] [Staphylococcus aureus subsp. aureus MW2]	Plaque	0,99864452	2,71459974	1,44073949	0,51599598	65	16	0,05838319	0,18935088
scn) complement inhibitor SCIN [SCIN (VF0425) - Immune modulation (VFC0258)] [Staphylococcus aureus subsp. aureus MW2]	Plaque	0,92725376	2,52755837	1,33774441	0,49284981	65	9	0,06607621	0,19822864
(cap8E) type 8 capsular polysaccharide synthesis protein Cap8E [Capsule (VF0003) - Immune modulation (VFC0258)] [Staphylococcus aureus subsp. aureus MW2]	Plaque	0,89285938	2,44210258	1,2881238	0,44915379	65	11	0,05208613	0,17704151
(lpxC) UDP-3-O-acyl-N-acetylglucosamine deacetylase [LPS (VF0466) - Immune modulation (VFC0258)] [Acinetobacter baumannii ACICU]	Plaque	-0,34595691	0,70754298	-0,49911032	0,16390827	65	8	0,04042482	0,16606933
(pilH) twitching motility protein PilH [Type IV pili (VF0082) - Adherence (VFC0001)] [Pseudomonas aeruginosa PAO1]	Patch	-0,63699687	0,52887833	-0,91899222	0,32202245	65	19	0,05311245	0,17704151

(pilG) twitching motility response regulator PilG [TFP (VF1334) - Adherence (VFC0001)] [Acinetobacter baumannii ACICU]	Plaque	-0,79383656	0,45210693	-1,14526407	0,31467571	65	8	0,01511838	0,10391755
(adsA) Adenosine synthase A [AdsA (VF0422) - Immune modulation (VFC0258)] [Staphylococcus aureus subsp. aureus MW2]	Patch	-0,81071167	0,44454159	-1,16960971	0,44149748	65	11	0,07289897	0,21336284

4 Publication 3: Multi-Omic Data Integration Suggests Putative Microbial Drivers of Aetiopathogenesis in Mycosis Fungoides

Licht, P. & Mailänder, V. Multi-Omic Data Integration Suggests Putative Microbial Drivers of Aetiopathogenesis in Mycosis Fungoides. *Cancers (Basel).* **16,** 3947 (2024). doi: 10.3390/cancers16233947

Full-text link: https://www.mdpi.com/2072-6694/16/23/3947

Supplementals: https://www.mdpi.com/article/10.3390/cancers16233947/s1

My contribution to this publication is detailed in the section *Contributions to Publications 1, 2, and 3*.

cancers

MDPI

Article

Multi-Omic Data Integration Suggests Putative Microbial Drivers of Aetiopathogenesis in Mycosis Fungoides

Philipp Licht [1] and Volker Mailänder [1,2,*]

[1] Department of Dermatology, University Medical Centre Mainz, 55131 Mainz, Germany; plicht@uni-mainz.de
[2] Max Planck Institute for Polymer Research, 55128 Mainz, Germany
* Correspondence: mailaend@mpip-mainz.mpg.de

Simple Summary: This research aims to better understand the causes of Mycosis fungoides (MF)—a disease where a type of immune cell, the T cell, malignantly transforms into cancer. It is not yet fully understood what triggers MF or how it progresses, partly because it varies so much between patients and because there is debate about whether the disease begins in immature T cells (thymocytes) or in more mature T cells (memory T cells). Recent findings suggest that bacteria living on the skin, particularly a harmful strain of Staphylococcus aureus, may aggravate MF by triggering specific pathways in T cells. To investigate this hypothesis, we explored the gene expression and microbial abundance of MF patients' skin with advanced statistical methods. We found that varied microbial skin colonization between patients may explain why the skin gene expression is so different from patient to patient. We also observed additional evidence that *S. aureus* might indeed trigger pathways in mature T cells that fuel cancer progression. Further, our statistical model suggested that certain viruses, like Epstein–Barr virus, could play a role in starting the disease by disrupting thymocytes (immature T cells). Based on these results, we speculate that both perspectives on the origin of MF could be correct, immature (thymocytes) and mature T cells: Thymocytes undergo malignant transformation, possibly caused by viruses, and bacteria like *S. aureus* fuel the malignant T cells to become prominent cancer cells. Our research could help uncover the complex interplay between bacteria, viruses, and T cells in MF. The findings may pave the way for new treatments targeting the skin microbiome or T cell pathways, offering hope for better management of this challenging disease.

Abstract: Background: Mycosis fungoides (MF) represents the most prevalent entity of cutaneous T cell lymphoma (CTCL). The MF aetiopathogenesis is incompletely understood, due to significant transcriptomic heterogeneity and conflicting views on whether oncologic transformation originates in early thymocytes or mature effector memory T cells. Recently, using clinical specimens, our group showed that the skin microbiome aggravates disease course, mainly driven by an outgrowing, pathogenic *S. aureus* strain carrying the virulence factor spa, which was shown by others to activate the T cell signalling pathway NF-κB. Methods: To explore the role of the skin microbiome in MF aetiopathogenesis, we here performed RNA sequencing, multi-omic data integration of the skin microbiome and skin transcriptome using Multi-Omic Factor Analysis (MOFA), virome profiling, and T cell receptor (TCR) sequencing in 10 MF patients from our previous study group. Results: We observed that inter-patient transcriptional heterogeneity may be largely attributed to differential activation of T cell signalling pathways. Notably, the MOFA model resolved the heterogenous activation pattern of T cell signalling after denoising the transcriptome from microbial influence. The MOFA model suggested that the outgrowing *S. aureus* strain evoked signalling by non-canonical NF-κB and IL-1B, which in turn may have fuelled the aggravated disease course. Further, the MOFA model indicated aberrant pathways of early thymopoiesis alongside enrichment of antiviral innate immunity. In line with this, viral prevalence, particularly of Epstein–Barr virus (EBV), trended higher in both lesional skin and the blood compared to nonlesional skin. Additionally, TCRs in both MF skin lesions and the blood were significantly more likely to recognize EBV peptides involved in latent infection. Conclusions: First, our findings suggest that *S. aureus* with its virulence factor spa fuels MF progression through non-canonical NF-κB and IL-1B signalling. Second, our data provide insights into the potential role of viruses in MF aetiology. Last, we propose a model of microbiome-driven

check for updates

Citation: Licht, P.; Mailänder, V. Multi-Omic Data Integration Suggests Putative Microbial Drivers of Aetiopathogenesis in Mycosis Fungoides. *Cancers* **2024**, *16*, 3947. https://doi.org/10.3390/cancers16233947

Academic Editors: Annunziata Gloghini and Giancarlo Pruneri

Received: 17 September 2024
Revised: 16 November 2024
Accepted: 21 November 2024
Published: 25 November 2024

MF aetiopathogenesis: Thymocytes undergo initial oncologic transformation, potentially caused by viruses. After maturation and skin infiltration, an outgrowing, pathogenic *S. aureus* strain evokes activation and maturation into effector memory T cells, resulting in aggressive disease. Further studies are warranted to verify and extend our data, which are based on computational analyses.

Keywords: cutaneous T cell lymphoma (CTCL); Mycosis fungoides (MF); microbiome; transcriptomics; multi-omics; data integration; bioinformatics; computational biology; disease signalling; NF-κB; IL-1B; *Staphylococcus aureus*; protein A; microbiome-driven pathogenesis

1. Introduction

Cutaneous T cell lymphoma (CTCL) is a heterogeneous group of non-Hodgkin T cell lymphomas with skin homing properties. The most common entity is Mycosis fungoides (MF), with an incidence rate of 4.1 cases per million in the USA [1,2]. MF patients present with several to many cutaneous lesions that are formed by the infiltration of neoplastic T cells and benign reactive lymphocytes. With disease progression, both neoplastic and benign infiltrates accumulate, resulting in inflammatory reddening of skin lesions [1,3,4]. Depending on the degree of lymphocyte infiltration and inflammation, lesions are classified into the stages patch, plaque, and tumour. As MF is a lymphoproliferative disorder which can involve extracutaneous compartments like the blood, a clinical staging system considers these events and classifies patients into stages IA–IVB [1,5]. In early stages (IA–IIA), MF is an indolent disease with a 5-year disease-specific survival of 89%, which, however, dramatically drops to ~20% in the most advanced stages [5]. Because the aetiology and pathogenesis of MF are incompletely understood, treatment options are limited, and a cure is almost not achievable [6,7].

MF is thought to arise from mature, skin-resident CD4+ T cells [8], which resemble the phenotype of tissue-resident effector memory T cells [9]. However, others suggest that the initial oncologic transformation takes place during early thymopoiesis, specifically during the double-negative (DN) stages DN-1 through DN-3. Those "premalignant clones" may then migrate to the skin, where they proliferate [10–15]. The causative agent responsible for the oncogenic transformation of T cells in MF remains uncertain [1]. Viruses are among the potential factors considered due to their involvement in various lymphoma types, including even two other entities of CTCL [16]. Viral involvement in MF is further supported by the elevated risk of MF patients to develop one or more virus-initiated lymphoma types, either simultaneously with MF or later in time [17–23]. However, the role of viruses in the aetiology of MF remains unclear, as findings from different studies have yielded conflicting results [24–26].

Likewise, the molecular drivers of MF pathogenesis remain incompletely understood [27,28]. In benign T cells, three signals orchestrate activity and proliferation: First, an initial T cell response is initiated by antigenic stimulation of the T cell receptor (TCR) together with CD3. Second, co-stimulation is required to augment TCR signalling, which is mediated by various molecules, including CD28 and the tumour necrosis factor receptor superfamily (TNFRSF). Downstream, both TCR signalling and co-stimulation converge on PI3K/AKT, NFAT, and NF-κB [29]. Third, sustained T cell activity is promoted by cytokines, which activate JAK-STAT. While CD8+ T cells require interleukin (IL) 12 and interferon (IFN) α/β to initiate signal three, CD4+ T cells require IL-1 [30,31]. Because these pathways are frequently dysregulated in T cell lymphomas, a "three-signal model" of T cell lymphoma pathogenesis has been proposed [32]. In MF, dysregulation of TCR, TNFRSF/NF-κB, and JAK-STAT pathways is recurrently observed, demonstrating the involvement of all three "T cell lymphoma promoting" signalling pathways [33–38]. However, the MF transcriptome exhibits substantial variability between patients and among lesions within the same patient [27,39], which impedes the identification of a shared pathogenic pathway to date.

It has been proposed that the skin microbiome contributes to or evokes transcriptional heterogeneity [40]. In agreement, we recently identified a subgroup of MF patients with a significantly aggravated disease course and outgrowth of a distinct, pathogenic *S. aureus* strain on plaque lesions. Conversely, another MF patient subgroup presented with a more balanced skin microbiome and a favourable prognosis. Reflecting the differing prevalences of *S. aureus* between the two subgroups, we referred to the subgroup with aggravated disease and *S. aureus* outgrowth as ΔSA-positive, while the other subgroup was termed ΔSA-neutral. Notably, the virulence factor staphylococcal protein A (spa) was highly abundant in the genome of *S. aureus* in the ΔSA-positive subgroup [41]. It has been demonstrated that spa activates the NF-κB pathway [42,43], which is involved in T cell co-stimulation [29], and is a component of the "three-signal model" of T cell lymphoma pathogenesis [32]. Moreover, some studies observed aberrant NF-κB activity in subsets of MF patients with aggressive disease [44–46]. We thus theorized that the skin microbiome shapes MF disease signalling, resulting in exacerbated malignancy.

To investigate our hypothesis, we here performed bulk RNA sequencing (RNAseq), multi-omic data integration of the microbiome and the transcriptome using Multi-Omic Factor Analysis (MOFA) (48), virome profiling, and T cell receptor sequencing (TCRseq). Our analyses yielded three main findings:

First, our data indicated that inter-patient transcriptional heterogeneity was largely driven by differential expression of pathways involved in T cell signalling. Strikingly, denoising the transcriptome from microbial influence using MOFA pronouncedly reduced the heterogeneous activation pattern of T cell signalling pathways. This advocated that the skin microbiome had a substantial impact on MF disease signalling.

Second, the MOFA model suggested that *S. aureus* with its virulence factor spa induced ectopic activity of both non-canonical NF-κB and IL-1B signalling. While non-canonical NF-κB signalling leads to survival and proliferation of naïve T cells and their differentiation into effector memory T cells (49), IL-1B facilitates sustained CD4+ T cell activation [30,31]. Given that CD4+ effector memory T cells are the malignant T cell subset in MF (*9*), spa-bearing *S. aureus* may induce or augment the phenotypic characteristics of MF, resulting in aggressive disease.

Third, the MOFA model implied augmented antiviral immune response along with enriched pathways involved in early thymopoiesis between DN1 and DN3. Viral prevalence, particularly of Epstein–Barr virus (EBV) and human papillomavirus 71 (HPV), trended higher in both lesional skin and the blood. In line with this, TCRs in both MF skin lesions and the blood were significantly more likely to recognize epitopes of EBV compared to TCRs in nonlesional skin. Notably, the most frequently recognized EBV-epitopes were derived from proteins orchestrating latent EBV infection. Collectively, our findings provide evidence to support potential viral involvement in the aetiology of MF, considering that (I) malignant MF T cells infiltrate the skin from the blood (50), (II) the initial oncologic transformation of malignant T cells in MF was mapped between DN1 and DN3 (10–15), and (III) latent EBV infection can induce non-Hodgkin lymphoma, including peripheral T cell lymphoma [47,48].

Taking findings from our preceding and this study together, we present a speculative model delineating microbiome-driven MF aetiopathogenesis: The initial oncologic transformation occurs during early thymopoiesis, possibly induced by viral infection. Following maturation and skin infiltration, outgrowth of a spa-bearing *S. aureus* strain exacerbates disease by activating both non-canonical NF-κB and IL-1B signalling, resulting in the differentiation of naïve T cells into effector memory T cells with sustained activity. Our study sheds light on the critical role of the microbiome in MF aetiopathogenesis.

2. Materials and Methods

2.1. Patients and Clinical Specimens

The patient group comprised a subset of patients included in our previous study [41] that were recruited from the Department of Dermatology, University Medical Centre Mainz,

Germany. Clinical specimens included metagenomic samples from the skin, skin punch biopsies, and peripheral blood (see Table 1). Metagenomic skin samples were obtained using a swab–scrape–swab procedure described earlier [41]. In brief, a pre-moistened swab was brushed over the skin, then the same skin area was gently scraped with a scalpel, and then it was brushed again with the same swab. To address the interindividual profile of skin microbiomes [49], nonlesional skin from the contralateral site of the sampled lesion was used as a control. The skin biopsies were obtained with 4 mm punches from the same MF lesions sampled for the metagenome and were immediately snap frozen and stored at −80 °C until RNA extraction. Peripheral blood was drawn for the isolation of peripheral blood mononuclear cells (PBMCs) and subsequently enriched for the T cell fraction. For full details, please refer to [41].

Table 1. Study group, clinical specimens, and patient metadata. This study group is a subset of the group enrolled in Licht et al. [41], in which we characterized the skin microbiome of MF patients. We demonstrated that *S. aureus* abundance is increased on MF lesions compared to nonlesional skin in a subgroup of patients (ΔSA-positive), while S. aureus abundance does not change in the other subgroup (ΔSA-neutral). ΔSA-positive patients exhibit a poor clinical course compared to ΔSA-neutral patients. Patient IDs in this study match the given patient IDs in Licht et al. [41]. NA = not available; f = female; m = male.

Patient ID	Sex	Age (Years)	Clinical Stage	ΔSA-Subgroup	Stage of Lesion (Body Site)	RNAseq: Tissues Included	TCRseq: Tissues Included
Pat1	f	81	IA	positive	plaque (hip)	lesion, blood	lesion, blood
Pat3	f	47	IB	neutral	patch (thigh)	lesion, nonlesional	NA
Pat4	m	70	IIB	positive	plaque (upper back)	lesion, nonlesional, blood	lesion, nonlesional, blood
Pat5	f	73	IB	neutral	patch (thigh)	lesion, nonlesional	lesion, nonlesional
Pat7	m	54	IB	neutral	plaque (flank)	lesion, nonlesional, blood	lesion, nonlesional
Pat8	m	82	IIB	positive	patch (upper back)	lesion, nonlesional, blood	lesion, blood
Pat9	m	63	IB	neutral	plaque (forearm)	lesion, nonlesional	lesion
Pat10	m	49	IB	neutral	patch (gluteus)	lesion, nonlesional	lesion
Pat13	m	66	IB	neutral	patch (lower leg, back)	lesion, nonlesional	NA
Pat14	m	62	IB	neutral	plaque (lower leg, front)	lesion, nonlesional	lesion, nonlesional, blood

2.2. RNA Sequencing and Bioinformatic Analysis of the Transcriptome

Total RNA was extracted from skin biopsies and T cell enriched PBMCs as described previously [41]. Total RNA was sent to Novogene Company Ltd. (Cambridge, UK) for library preparation and sequencing. Briefly, after a quality check with Caliper Life Sciences GX II (Hopkinton, MA, USA), 400 ng RNA was used as input for the NEBNext Ultra RNA Library Prep Kit (New England Biolabs, Ipswich, MA, USA). One sample (nonlesional skin of Pat1) was excluded due to low RNA quality. After the quality check, libraries were

sequenced on a NovaSeq 6000 (Illumina, San Diego, CA, USA) at 150 bp paired-end to an average of 78.74 (range 63.82–94.20) million raw reads, with 11.81 (range 9.57–14.13) giga base pairs (Gbp) per sample.

For the transcriptome analysis, raw reads were quality-checked with Fastqc version 0.11.9 [50], and subsequently aligned against the human reference genome Ensembl built GRCh38.p13 using STAR 2.7.9a with the flag –quantMode GeneCounts [51]. The data were loaded into DESeq2 version 1.36.0 [52], filtered for genes with a minimum of ten cumulative counts over all samples, and normalized using the internal DESeq2 method. Subsequently, a differential expression analysis using the Wald test was carried out, adjusted for influences from individual patients which may have been introduced by the paired-sample design. To account for multiple testing, *p*-values were adjusted using Benjamini–Hochberg and genes with <0.05 adjusted *p*-value were considered significant. Volcano plots were created using the R package EnhancedVolcano [53]. For principal component analyses, the data were first transformed with the variance-stabilization method (vst) and then analysed using the plotPCA function within DESeq2. The PCA was visualized using ggplot2 [54].

Gene set enrichment analysis was performed using the R package pathfindeR [55]. Log2 fold-changes of significantly deregulated genes determined by DESeq2 were used as input. The Reactome database [56] was used to find enriched pathways. Because we were particularly interested in signalling pathways that might orchestrate MF pathogenesis, we screened the literature for pathways that were described as deregulated in T cell lymphomas or CTCL. The Reactome database was subsequently filtered to retain only pathways that contain at least one of the following terms (case-insensitive): cascade, signal, signalling, signaling, pathway, transition, cycle, regulation, activation, keratinization, cornified, antimicrobial, interferon, IFN, stimulation, stimuli, activate, receptor, TLR. Enriched pathways were clustered using the pathfindeR function cluster_enriched_terms. Plots were created using pathfindeR.

Upregulated pathways in the plaque stage that, according to the literature, may have been elicited by *S. aureus* were further investigated using PCA. Therefore, the influence from the paired-sample design was regressed out from the normalized and rlog-transformed count matrix with the removeBatchEffect function from the limma package [57]. For three differentially regulated pathways of interest in the plaque stage, up- and downregulated genes according to pathfindeR were determined. The corrected count matrix was filtered for the genes of interest and plaque stage samples and parsed into the prcomp R stats function to perform PCA. ggplot2 was used for visualization.

2.3. Multi-Omic Data Integration

We utilized the R implementation of MOFA (Multi-Omic Factor Analysis) version 1.6.0 [58] to integratively analyse the microbiome and transcriptome datasets. MOFA integrates multiple omics datasets by discovering latent factors that capture both shared and omic-specific patterns of variation. These latent factors help to identify key biological signals, denoise the data, and identify relationships between different omics layers.

The microbiome dataset was created in our preceding study where we characterized the MF skin microbiome using shotgun metagenomics and MetaPhlAn 3.0.2 [41,59,60]. To obtain absolute counts of microbial taxa (rather than the relative abundance, which is the default in MetaPhlAn and was used in our previous study), the metagenome was re-profiled including the flag -t rel_ab_w_read_stats using MetaPhlAn 3.0.2 with the intermediate bowtie2 mapping files as input. The resulting profiles were filtered to retain only taxa on the species level and normalized using the wrench method, which accounts for sparse metagenomic count data and is implemented in the R package wrench [61]. The normalized data were log2-transformed with a pseudocount of 1. To select highly variable species for the MOFA model, 50 species with the highest variance were filtered (with the R base function var) and used for all subsequent steps.

The transcriptome dataset was created in this study as described above. After mapping and normalization with STAR 2.7.9a and DESeq2 version 1.36.0 (described above), the data

were transformed with the regularized logarithm using the rlog function implemented in DESeq2 [52]. As recommended by the MOFA authors, the large transcriptome dataset was restricted to not overrepresent the smaller microbiome dataset in the MOFA model. Therefore, the top 5000 highly variable genes were selected based on the median absolute deviation calculated with the R base function mad. The MOFA model was trained with a single group, the option scale_views set to TRUE, convergence_mode set to slow, and eight factors.

Gene set enrichment analysis was performed with the MOFA function run_enrichment, which is based on principal component gene set enrichment (PCGSE) [62] using only genes with positive weights as input. The Reactome database, filtered for pathways of interest (see the above section of transcriptome analysis), was used as a background. Pathway enrichment plots were generated with ggplot2.

For the heatmaps in Figure 2A,B, an identical set of genes were plotted using the R package pheatmap (refer to the caption of Figure 2 for more details on gene selection). The heatmap in Figure 2A shows the normalized gene counts, while the heatmap in Figure 2B shows the denoised version of the data, explained by the latent factors of the MOFA model. This means that the MOFA model reconstructs the input data (transcriptome and microbiome) based on the latent factors and shows patterns that are shared between the omics layers and that are omics-specific. The denoised heatmap in Figure 2B was generated with the MOFA function plot_data_heatmap with argument denoise set to TRUE. Internally, plot_data_heatmap uses pheatmap for heatmap plotting, with the MOFA trained data as input. The code used for Figure 2B (and other figures) can be found in the Data Availability Statement.

2.4. Virus Profiling

The virome present on superficial skin layers was profiled via re-analysis of the microbiome dataset generated in our previous investigation [41]. Briefly, human skin was brushed topically with swabs, and whole metagenomic sequencing was performed and subsequently profiled with MetaPhlAn 3.0.2. While viruses were excluded in our previous study, here we activated the flag for viral identification (--add_viruses). The resulting profiles were filtered to retain only viruses.

The virome present in deeper skin layers was profiled using RNAseq reads generated from skin punch biopsies. In contrast to the swabbing procedure, punch biopsies obtain the entire depth of skin layers. Virome profiles from RNAseq reads were generated with the VIRTUS pipeline [63]. Briefly, non-human reads were filtered out through alignment to the human reference genome Ensembl built GRCh38.p13. Next, unmapped (i.e., non-human) reads were aligned against 762 viral genomes. Heatmaps visualizing the virome profile were generated with the R package pheatmap [64].

2.5. Assessment of TCR–Epitope Binding

To investigate whether T cells of MF patients recognize EBV-epitopes, the T cell receptor was sequenced as described previously [41]. Briefly, RNA isolated from skin punch biopsies and T cell enriched PBMCs of MF patients were subjected to library preparation spanning the variable part of the TCR using the NEBNext Immune Sequencing Kit, human (E6320, New England Biolabs, USA), and sequenced on a MiSeq (Illumina, USA) running 300 bp PE. The sequencing data were processed with the pRESTO toolkit [65] (https://usegalaxy.org/u/bradlanghorst/w/presto-nebnext-immune-seq-workflow-v320, accessed on 20 May 2019) and the R package immunearch [66]. EBV-epitopes were obtained from the Immune Epitope Database (IEDB) (https://www.iedb.org/, accessed on 2 April 2019) [67]. The Tool ERGO-II [68] was used to determine binding scores of pairs of TCRs and EBV-epitopes. The closer the binding score is to 1, the higher the probability that a TCR recognizes the epitope [68].

3. Results

3.1. Study Group and Clinical Specimens

The study group consisted of 10 MF patients (mean age at sampling: 64.7 years; range: 47 to 82 years) and was a subset of patients that were enrolled in our preceding investigation where we characterized the MF skin microbiome [41]. To ensure traceability, IDs of included patients in this study were adopted from our previous investigation [41]. In that study, we found that a subgroup of patients presented with an increased abundance of *S. aureus* on MF lesions compared to nonlesional skin of the same patient. We termed this subgroup ΔSA-positive as opposed to the ΔSA-neutral subgroup, where *S. aureus* abundance was consistent between MF lesions and nonlesional skin of the same patient. The ΔSA-positive subgroup had a strong dysbiosis and a significantly aggravated disease course compared to the ΔSA-neutral subgroup [41]. Of the 10 MF patients included in the present study, 3 were in the ΔSA-positive subgroup and 7 were in the ΔSA-neutral subgroup.

Clinical specimens included skin swabs and punch biopsies of lesional skin (5 patch stage and 5 plaque stage) and matched nonlesional skin of the same MF patients as an intra-patient control (10 nonlesional skin samples). For more details about the rationale of using internal controls, please refer to Licht, Dominelli et al. [41]. Additionally, blood was drawn in four patients for the isolation of peripheral blood mononuclear cells (PBMCs). All clinical specimens were taken at the same visit. Skin punch biopsies were used for RNAseq. Where sufficient material was available, skin punch biopsies and PBMCs were used for TCRseq. Shotgun metagenomics from skin swabs were initially carried out in our previous investigation [41] and re-analysed in the present study in a multi-omic data integration approach together with the skin transcriptome. Table 1 summarizes patient metadata, clinical specimens, and data modalities used in the present study.

3.2. Transcriptional Heterogeneity May Be Largely Driven by Differential Activation of Pathways of the "Three-Signal Model" of T Cell Lymphoma Pathogenesis

A number of studies investigated the CTCL transcriptome [27,39] and uncovered various mechanisms of disease progression [33–38]. However, the transcriptome was also found to exhibit significant heterogeneity among patients, complicating the identification of a common pathological mechanism [27,39,46,69–73].

To explore the root of transcriptional heterogeneity, we employed differential gene expression analysis and gene set enrichment analysis (GSEA). Principal component analysis (PCA) of the MF skin transcriptome clearly separated nonlesional skin, patch, and plaque via principal component (PC) 1. However, lesional samples also spread along PC2, demonstrating strong inter-patient transcriptional heterogeneity (Figure 1A). Likewise, GSEA recovered several aberrant pathways known to promote MF exacerbation, such as chemokine signalling [74] (Supplementary Material S2), but also showed substantial activation differences between patients in both patch and plaque lesions (Supplementary Material S3). Notably, pathways of the "three-signal model" of T cell lymphoma pathogenesis exhibited different activation patterns between patch and plaque (Table 2): TCR signalling was enriched in both patch and plaque, whereas interleukin-13 (IL-13) signalling, CD28 co-stimulation, and co-stimulation through death receptors activating NF-κB [44,45] were enriched solely in the plaque stage.

Next, we aimed to assess whether pathways of the "three-signal model" for T cell lymphoma pathogenesis [32] replicate transcriptional heterogeneity. To this end, we compiled a list of genes that are (I) members of the "three-signal model" for T cell lymphomas and (II) were differentially expressed in either or both patch and plaque stages. A clustered heatmap of these genes closely resembled the pattern of the PCA of the entire transcriptome (Figure 2A): Nonlesional skin and plaque samples formed separate clusters, while patch samples exhibited intermediate expression levels. Importantly, plaque samples displayed pronounced heterogeneity in RNA expression levels (Figure 2A). We thus reasoned that inter-patient transcriptional heterogeneity can, at least to some extent, be attributed to differential expression of pathways that orchestrate T cell lymphoma pathogenesis.

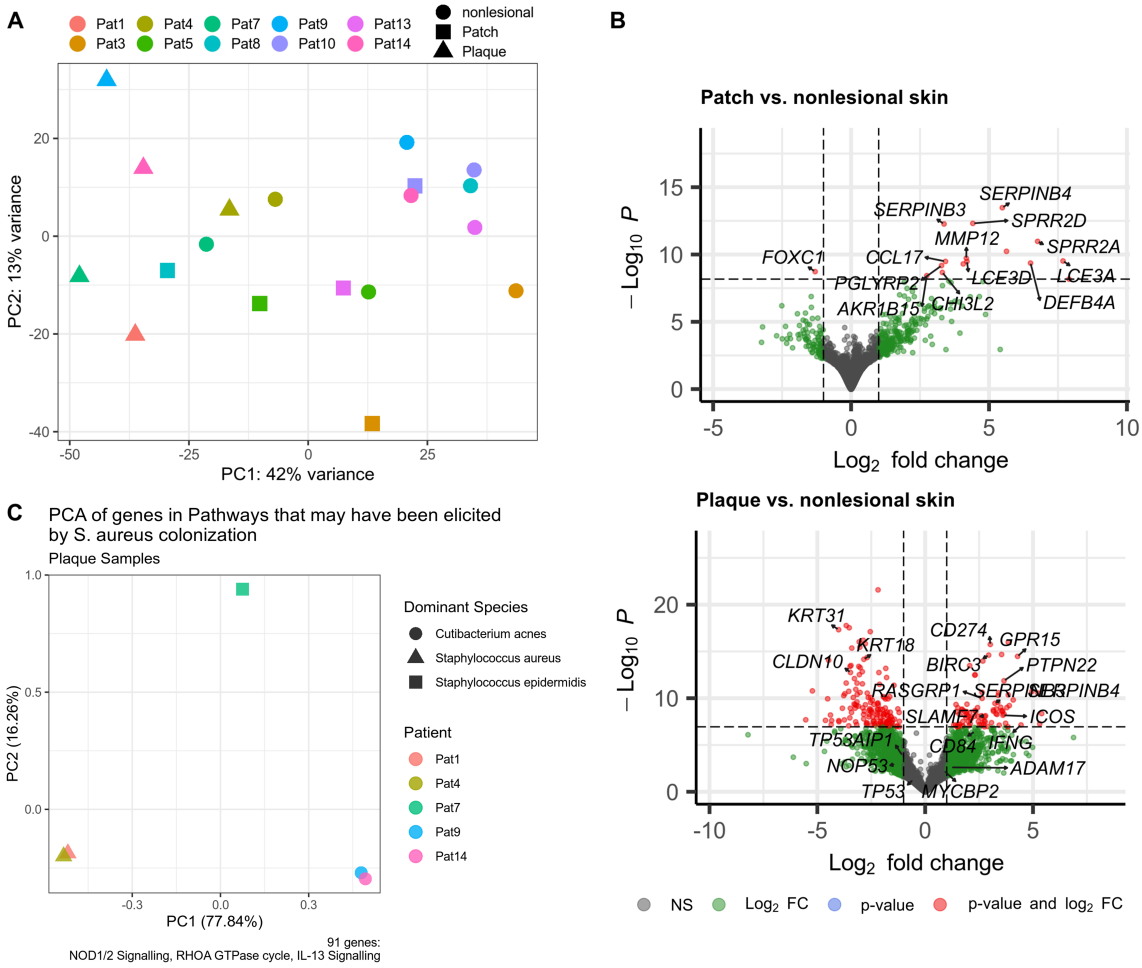

Figure 1. Analysis of the MF skin transcriptome. (**A**) Principal component analysis (PCA) showing inter-heterogeneity of plaque. (**B**) Volcano plots visualizing the distribution of gene fold-changes and statistical significance between patch or plaque and nonlesional skin. For the complete results table of DESeq2 differential gene expression analysis, refer to Supplementary Material S1. (**C**) PCA of genes belonging to upregulated pathways in the plaque stage that may have been elicited by *S. aureus* according to the literature [75–79]. PC = principal component, NS = not significant.

Table 2. Gene set enrichment analysis. Displayed are selected pathways of interest. Please refer to Supplementary Material S2 for the full GSEA list. log2fc = log2 fold-change, NA = not available, padj = *p*-value adjusted to multiple comparisons using Bonferroni.

Pathway	Patch log2fc	padj	Plaque log2fc	padj
Keratinization	6.35	3.6×10^{-5}	1.18	7.1×10^{-8}
Antimicrobial peptides	8.69	1.4×10^{-5}	NA	NA
TCR signalling	4.74	1.3×10^{-7}	1.63	1.4×10^{-14}
CD28 co-stimulation	NA	NA	1.74	1.1×10^{-5}
Non-canonical NF-kB pathway	NA	NA	1.34	4.3×10^{-11}
Interleukin-13 signalling	NA	NA	1.41	6.2×10^{-4}
IFN-γ signalling	8.32	6.7×10^{-5}	1.83	5.8×10^{-3}
Death receptor signalling	NA	NA	1.85	6.4×10^{-21}
Toll-Like Receptor 4 (TLR4) Cascade	2.55	1.5×10^{-2}	1.31	6.4×10^{-19}
NOD1/2 signalling pathway	NA	NA	1.84	4.3×10^{-17}
RHOA GTPase cycle	NA	NA	1.62	4×10^{-29}
Regulation of TP53 activity	NA	NA	1.28	1.8×10^{-10}

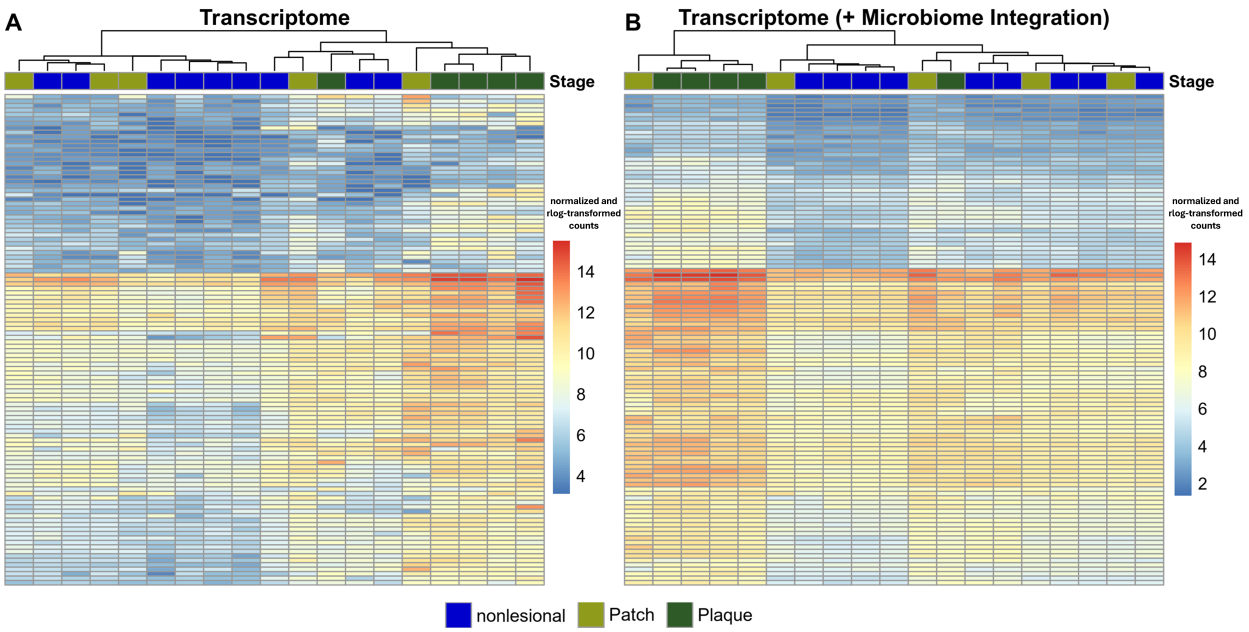

Figure 2. Clustered heatmap of genes involved in the "three-signal model" of T cell lymphoma pathogenesis. The clustered heatmap was created with genes involved in the "three-signal model" of T cell lymphoma pathogenesis that were differentially expressed in the patch and/or plaque stage and were included in the MOFA model (5000 highly variable genes; see Methods and Supplementary Material S6). Raw gene counts were normalized using the median of ratios and rlog-transformed with the DESeq2 package [52]. (**A**) Shown are normalized RNA expression levels before integration of the microbiome. Notably, although only genes of the "three-signal model" of T cell lymphoma pathogenesis were included, the clustering resembled the patterns of the PCA, which was based on the entire transcriptome. Despite clustering together, plaque samples exhibited a high degree of heterogeneity. (**B**) After data integration of the transcriptome with the microbiome, the heterogeneity of plaque samples was largely resolved, suggesting that the microbiome had a strong impact on MF disease signalling. Please refer to the Methods section for information on how the denoised heatmap was generated.

3.3. The MF Skin Transcriptome Shows Responses to Microbial Stimuli

Since differential microbial skin colonization may contribute to transcriptional heterogeneity [40], and we recently identified that the skin microbiome stratifies MF patients and determines the clinical course [41], our next objective was to identify microbial responses in the skin transcriptome.

As expected, we uncovered enriched pathways likely activated by the skin microbiome (Table 2 and Supplementary Material S2). Notably, Toll-Like Receptor 4 (TLR4) was upregulated in patch and showed attenuated activity in plaque. The pathway senses lipopolysaccharides, a cell wall constituent of Gram-negative bacteria, and activates inflammatory responses as well as pyroptosis, which is a form of programmed necrosis. Pyroptosis protects the host from microbial infection but, if overactivated, can also lead to pathological inflammation [80], a typical condition of progressive MF [4]. In accordance, we recently showed that the skin microbiome of patches is strongly dysbiotic, while dysbiosis on plaques was observed only on a subgroup of MF patients [41], providing a potential explanation for the differential TLR4 activation between patch and plaque.

Conversely, several microbe-associated pathways were uniquely upregulated in plaque lesions, potentially driven by the outgrowth of a distinct S. aureus strain harbouring virulence factors such as α-hemolysin and spa [41]. The innate immune sensor NOD2 (nucleotide-binding oligomerization domain 2) recognizes small peptides derived from the peptidoglycan cell wall component of Gram-positive bacteria like *S. aureus*. Importantly, NOD2 mediates protective responses specifically against *S. aureus* through its interaction

with the virulence factor α-hemolysin [75,76]. Additionally, we observed enhanced activity of the RHOA GTPase cycle, a pathway that *S. aureus* can exploit via its virulence factor spa to facilitate epithelial invasion [77]. Further, we also noted enrichment of IL-13 signalling, consistent with reports that IL-13 expression is induced in healthy skin upon *S. aureus* exposure [78,79]. Interestingly, malignant T cells in the skin of MF patients express IL-13, whereas malignant T cells found in lymph nodes and blood do not [46]. To further investigate whether the upregulation of NOD1/2 signalling, the RHOA GTPase cycle, and IL-13 signalling might have been elicited by the microbiome, as suggested by the literature, we conducted PCA of genes regulating these pathways (Figure 1C). Plaque samples with *S. aureus* as the dominant species in the microbiome clearly separate from those with other dominant species.

Collectively, we noted several enriched pathways that may be attributed to microbial stimuli, consistent with the microbiome patterns identified on MF lesions in our preceding study [41]. Consequently, our findings indicated that distinct microbial colonization led to differential transcriptomic responses between patients.

3.4. Multi-Omic Data Integration of the Microbiome and the Transcriptome Resolves Transcriptional Heterogeneity

To investigate whether differential skin colonization elicited the heterogeneous expression of genes related to the "three-signal model" for T cell lymphoma pathogenesis, we performed data integration of the microbiome and the transcriptome using Multi-Omic Factor Analysis (MOFA) [58]. Briefly, MOFA can be seen as a multi-omic implementation of PCA and finds latent factors (comparable to principal components in PCA) that capture the main sources of variation across different omic data modalities (which are called views in the MOFA framework). Within the latent factors, weights are allocated to the features of the different views. Consequently, latent factors are characterized by feature weights, which indicate their importance or significance in the variation captured by the latent factor. Downstream, additional analyses such as gene set enrichment analysis (GSEA) can be conducted within each latent factor. The MOFA framework further enables the identification of each view's contribution to the variation captured by a latent factor across the entire multi-omic dataset [58].

Regarding the multi-omic dataset in this study, the weights of the microbes (features of the microbiome) and the weights of the genes (features of the transcriptome) characterize the latent factors. The MOFA model showed a good fit to the multi-omic dataset, as the patterns of the latent factors were congruent to the results observed in both the independent transcriptome analysis (see above) and our previous study on the MF skin microbiome [41] (see Supplementary Material S4). Latent factors 1 to 5 captured shared sources of variation present in both data modalities, indicating a reciprocal influence between the transcriptome and microbiome (Figure 3A). By leveraging the latent factors, MOFA reconstructs the input data to separate shared and specific variations in each data modality, thereby denoising the data and revealing underlying biological signals [58]. Strikingly, the differential expression of genes involved in the "three-signal model" of T cell lymphoma pathogenesis was resolved after integration of the microbiome and transcriptome data modalities (called denoised in MOFA2 terms; Figure 2B). This indicated that the lesion-specific microbiome heavily influences MF disease signalling. Please refer to the Methods section for information how the denoised heatmap was generated.

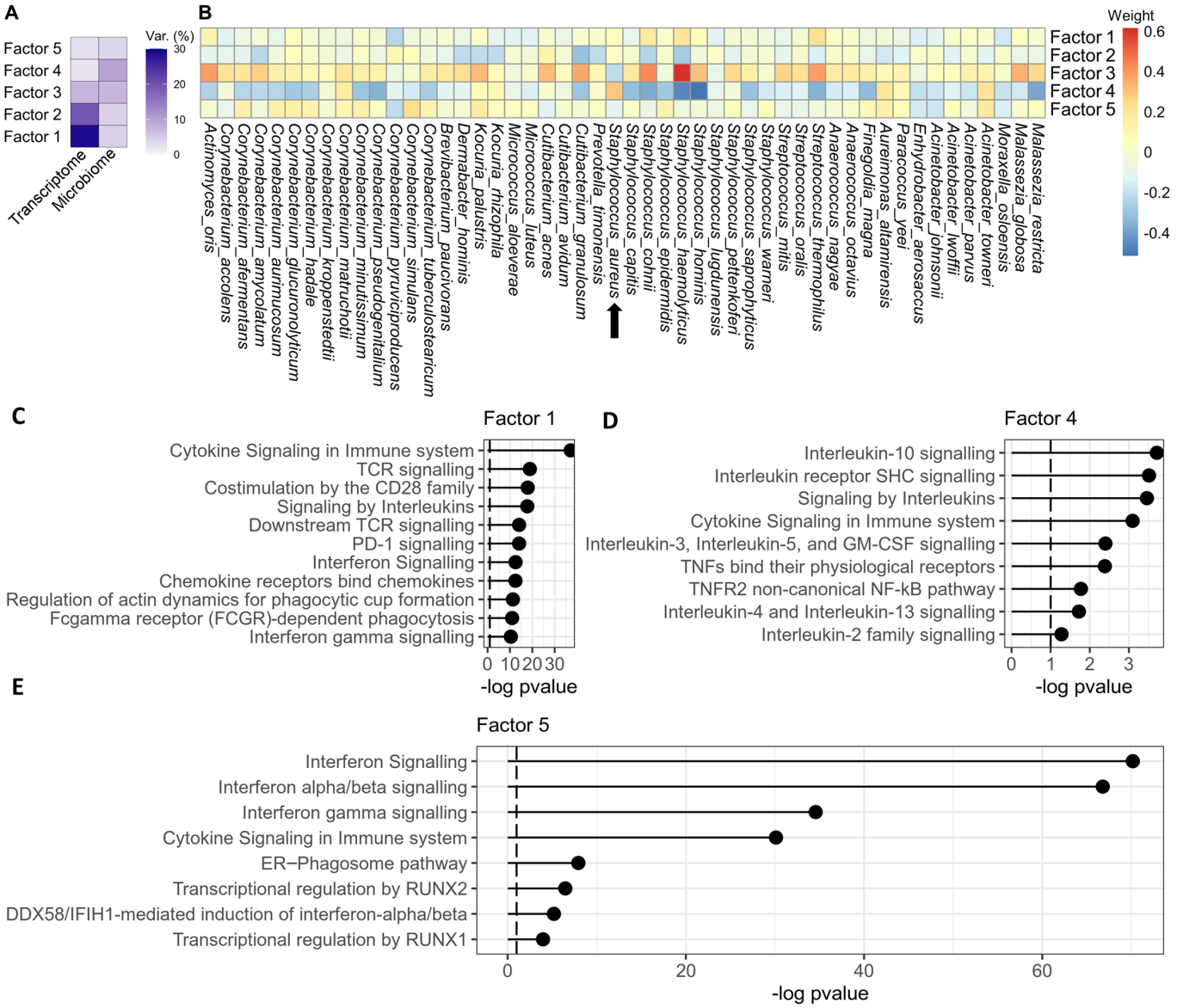

Figure 3. Overview of the latent factors of the MOFA model in the microbiome and transcriptome data modalities. (**A**) Overview of the latent factors capturing variances in the microbiome and transcriptome data modalities. Factor 4 captured the majority of variance in the microbiome, meaning that this factor captured important impacts of the microbiome on the transcriptome. (**B**) Overview of the feature weights of the microbiome per factor. (**C**–**E**) Gene set enrichment analysis. Factor 1 showed pathomechanisms of high and sustained T cell activity in MF (TCR signalling, CD28 co-stimulation, interleukin signals). Factor 4 showed pathways that were likely evoked by *S. aureus*. Factor 5 showed strong antivirus responses along with enrichment of RUNX1 and RUNX2 signalling, which have pivotal roles in thymopoiesis [81–84].

3.5. Spa-Bearing S. aureus Likely Activates Non-Canonical NF-κB and IL-1B Signalling

We next assessed the impact of the microbiome on MF disease signalling in more detail. **Factor 4** accounted for a substantial proportion of the total variance in the microbiome (Figure 3A), and *S. aureus* was the only microbiome feature with a positive weight. Notably, microbes with anti-*S. aureus* properties, such as *S. hominis* and *S. epidermidis* [85–87], displayed markedly negative weights. Thus, the microbiome feature weights exhibited a pattern similar to plaque lesions of the ΔSA-positive subgroup. These patients presented with *S. aureus* outgrowth and an aggravated clinical course [41].

In the transcriptome, the following pathways controlling T cell activity were enriched: Interleukin signalling, particularly IL-1B, and non-canonical NF-κB signalling (Figure 3D, Supplementary Material S5). While non-canonical NF-κB serves as a co-stimulator and generates and maintains effector memory T cells [88,89], IL-1B signalling facilitates sustained activation of CD4+ T cells [32]. In agreement, the malignant T cell subset in MF is thought to be CD4+ effector memory T cells [9]. Regarding IL-1B signalling, Chng et al. [90] reported that human keratinocytes express IL-1B when challenged with *S. aureus*. This suggests that outgrowth of virulent *S. aureus* may stimulate the tumour microenvironment to activate malignant T cells via IL-1B in a paracrine fashion.

Regarding non-canonical NF-κB signalling, we intriguingly observed that the stimulating ligand, TNF-α [91], displayed an almost neutral weight in factor 4 (Supplementary Material S5), indicating an alternative stimulation route. Instead, we previously identified high abundance of the virulence factor staphylococcal protein A (spa) in the genome of the *S. aureus* strain colonizing ΔSA-positive patients. It was reported that spa can activate the NF-κB pathway [42,43], and some studies associated aggressive CTCL with upregulated NF-κB signalling [44–46]. Notably, several genes emphasized in these studies exhibited positive weights in factor 4 (e.g., *LTA*, *LTB*, *BIRC3*, *TNFSF13*, *TNFSF14*, *TNFRSF1B*, and *TNFRSF7*; Supplementary Material S5). Owing to the almost neutral weight of the NF-κB stimulating agent TNF-α and the presence of spa as an alternative stimulator [41], we theorized that outgrowing, spa-bearing *S. aureus* strains upregulated non-canonical NF-κB signalling in MF patients with aggressive disease.

Collectively, the MOFA model indicated that the skin microbiome significantly influences MF disease signalling and is a major source of transcriptional heterogeneity. Further, the MOFA model suggested that *S. aureus* fuelled malignant T cells to promote the aggravated disease course of ΔSA-positive patients via two signalling axes: While spa may activate non-canonical NF-κB signalling, resulting in survival, proliferation, and naïve T cell differentiation into mature, effector memory T cells, the neoplastic T cell subset in MF [9], paracrine IL-1B signalling might facilitate sustained activation.

3.6. Aberrant Signalling of Early Thymopoiesis Alongside Enriched Antiviral Immunity Suggests Viral Involvement in MF Aetiology

Additionally to factor 4, our attention was drawn to the results of **factor 5**. While the microbiome weights showed only minimal signals (Figure 3B), GSEA identified significant upregulation of host defence signals against viruses (Figure 3E), indicating that factor 5 represented a source of variation independent of bacteria. In particular, GSEA showed upregulation of interferon alpha and beta (IFN-α/β) signalling, which is the first line of innate immune defence upon viral infection. Downstream, IFN-α/β signalling stimulates genes that inhibit the replication machinery of viruses at various mechanistic levels [92]. Several of these interferon-stimulated genes exhibited high weights in factor 5, for example *MX1*, *IFIT1*, *IFIT3*, *OAS1*, *OAS2*, *IFI27*, and *OASL* (Supplementary Material S5). *IFIT3*, which displayed the highest weight in factor 5, was shown to specifically boost antiviral signalling by IFN-α/β [93]. Further, GSEA found an enrichment of the ER–phagosome pathway (Figure 3E), which can be hijacked by viruses for their own translation, replication, and particle budding in order to spread into other host cells [94]. Notably, the phagosome-pathway genes *TAP1* and *TAP2*, which displayed high weights in factor 5 (Supplementary Material S5), are highly expressed by Epstein–Barr virus (EBV)-infected lymphocytes [95], and interact with Epstein–Barr-nuclear antigen 1 (EBNA1) [96].

Remarkably, EBV infection can lead to *RUNX1* expression [97,98], and signalling by *RUNX1* and *RUNX2* was significantly enriched in factor 5 (Figure 3E). The RUNX family is a frequent target of retroviral insertion [99–101], resulting in the development of several T cell lymphoma entities [102,103]. *RUNX1* regulates the expansion of mature CD4+ T cells [82], which constitutes the neoplastic T cell subset in MF [9]. Interestingly, both *RUNX1* and *RUNX2* are important regulators of early thymopoiesis during the double-negative

stages of T lymphocytes [81–84], a developmental step that has been mapped to the initial oncologic transformation of T cells in MF [10–15].

Since the transcriptome dataset included in the MOFA model was restricted to 5000 genes (see Methods section), we screened the entire transcriptomic dataset to investigate signals of aberrant thymopoiesis in more detail. It has been reported that ectopic expression of *RUNX2* strongly expands immature thymocytes during the double-negative stages, resulting in a preneoplastic state of thymocytes characterized by low proliferation rates [81]. However, concomitant overexpression of *MYC* rescues proliferation and facilitates differentiation. Additionally, *MYC* and *RUNX* collaboratively inhibit the tumour suppressor p53, resulting in decreased apoptosis of malignant T cells. Together, this ultimately leads to the accumulation of mature, neoplastic T cells [81,104]. In agreement with these reports, several genes were aberrantly expressed in the MF transcriptome (Supplementary Material S1): Besides *RUNX1* and *RUNX2*, we identified enriched *MYCBP2* (Figure 1B), which is a member of the c-myc family with the function to increase c-myc activity [105]. Further, although the pathway to regulate p53 activity was upregulated (Table 2), important components of the p53 machinery were downregulated (Figure 1B): These included the p53 gene *TP53* itself, the p53 stabilizing protein *NOP53* [106], and TP53AIP1, which is regulated by p53 and induces apoptosis [107]. A complete results table of DESeq2 differential gene expression analysis is available in Supplementary Material S1.

In summary, our data show dysregulation of pathways involved in early thymopoiesis, probably representing the initial oncologic transformation of T cells in MF. Moreover, factor 5 suggested a connection between viruses and MF aetiology given the concomitant upregulation of host responses to viruses and *RUNX1/2* signalling.

3.7. Increased Viral Prevalence and EBV-Epitope Recognition in MF Skin Lesions

In MF, malignant T cells circulate in the blood and infiltrate the upper dermis but have not been described to be present in the most superficial layers of the skin [108]. To determine whether viruses may be involved in in MF aetiology, we investigated viral prevalence in different layers of the skin and the blood of MF patients. To this end, we examined whole metagenomic sequencing (WMS) and RNAseq data. While the WMS data were generated from skin swabs and thus only contain material from superficial skin layers, the RNAseq data were generated from both the blood and skin punch biopsies representing the whole skin, including deeper skin layers like the epidermis and dermis.

In whole skin samples, total viral load trended higher in MF lesions compared to nonlesional skin (Figure 4B). In contrast, total viral load did not differ in superficial skin layers (Figure 4A). Among all viruses detected in MF lesions of whole skin samples, EBV and human papillomavirus 71 (HPV71) displayed the highest prevalence, albeit HPV71 was also frequently present in nonlesional skin. Remarkably, EBV and HPV71 were also present in the blood of some patients (Figure 4B). Both EBV and various human papillomaviruses are implicated in the development of cancer, including T cell lymphomas [109–111]. Since MF is characterized by the infiltration of circulating T cells from the blood into the skin [108], the concomitant presence of viruses in both compartments indicates a potential viral involvement in MF.

Next, we evaluated whether T cells of whole skin samples or T cells in the blood were directed against known EBV-epitopes obtained from the Immune Epitope Database (IEDB) [67]. We sequenced the TCRs of MF lesions, nonlesional skin, and blood and utilized ERGO-II [68] to calculate binding scores for the most abundant TCRs of a given sample with each of the EBV-epitopes. TCRs in MF lesions and the blood showed a significantly higher probability to recognize EBV-epitopes than T cells in nonlesional skin (Figure 4C), which agreed with the increased viral prevalence of MF lesions in whole skin samples. Interestingly, latent membrane protein (LMP) 1, LMP2, and Epstein–Barr-nuclear antigen (EBNA) 1 were the most frequently recognized EBV-epitopes by TCRs in the skin and blood (Figure 4D). An expression pattern of LMP1, LMP2, and EBNA1 represents a characteristic EBV gene profile of latency type I/II, commonly observed in EBV-induced

T cell lymphomas [112,113]. In NK/T cell lymphoma, LMP1 upregulates *CD274* (PD-L1) via the NF-κB axis [114], which agreed with our results of enriched *CD274* and NF-κB signalling in the plaque stage (Table 2, Figure 1B).

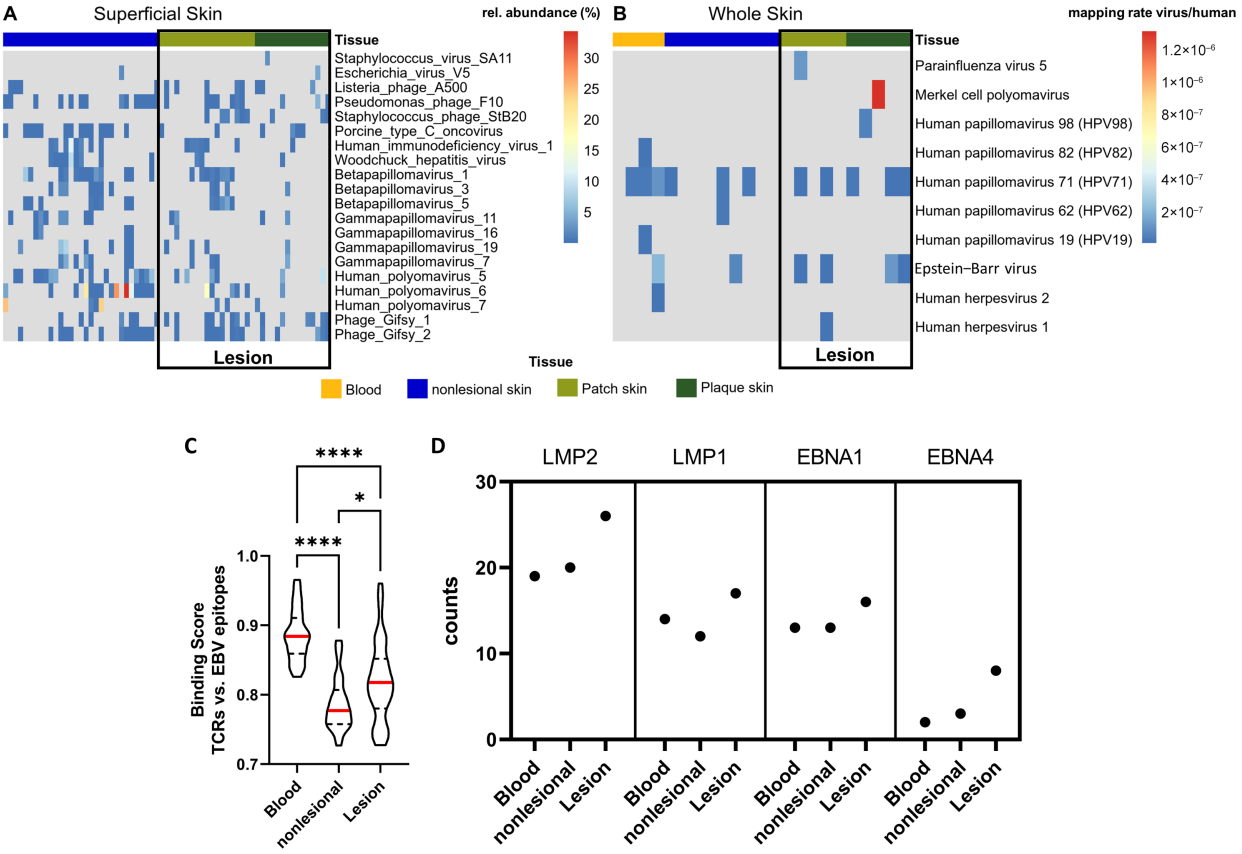

Figure 4. Viral association with MF. (**A**,**B**), Viral prevalence identified in WMS reads of superficial skin (**A**) and RNAseq reads of whole skin (**B**). Viral prevalence in MF lesions of whole skin trended higher compared to nonlesional skin, specifically EBV and HPV71 (**B**), whereas no difference was present on superficial skin (**A**). In (**A**), the top 20 viruses with the highest variation between MF lesions and nonlesional skin are shown. In (**B**), all viruses detected are shown. In (**C**,**D**), T cells in MF lesions and the blood specifically recognize EBV-epitopes. (**C**) The probability of TCRs in blood, nonlesional skin, and MF lesions to recognize EBV-epitopes was assessed using ERGO-II [68]. Binding scores (1 = perfect binding, 0 = no binding) were calculated for each TCR with each EBV-epitope. n = 175; displayed are violin plots with the median (red), 1st quartile, and 3rd quartile. Kruskal–Wallis test: * for $p \leq 0.05$, **** for $p \leq 0.0001$. (**D**) Displayed are the EBV-epitopes that were recognized most often by TCRs of MF patients.

Together, the trend of increased EBV and HPV71 prevalence in whole skin samples along with a significantly higher probability of EBV-epitope recognition by TCRs in MF lesions and the blood compared to nonlesional skin suggest viral involvement in MF aetiology.

4. Discussion

The clinical course of MF varies greatly, with some patients having only minor progress, whereas others suffer from fast progression and high disease burden [5,115]. Likewise, the transcriptome is tremendously heterogeneous, exhibiting patient and even lesion specificity [27,39,73]. Moreover, ambiguity exists about the initial oncologic transformation of malignant T cells, as studies from different groups mapped the event to either early thymocytes [10–15] or mature, effector memory T cells [9]. Consequently, a common

pathogenic mechanism of all patients or patient subgroups is still in doubt, resulting in a non-optimal treatment regimen [27]. We recently demonstrated that the skin microbiome of MF patients is altered, and identified a subgroup of patients that was overgrown with a distinct, pathogenic *S. aureus* strain. This subgroup exhibited a significantly aggravated disease course, possibly owing to the virulence factor spa, which was present in the *S. aureus* genome [41]. In line with this, others showed that spa can activate the NF-κB axis [42], which is recurrently deregulated in MF patients with aggressive disease [34,44–46,116]. We thus theorized that (I) the lesion-specific microbiome determines transcriptomic response, thereby contributing to or causing heterogeneity [40], and that (II) spa-bearing *S. aureus* elicits NF-κB signalling to fuel MF. Therefore, we investigated how the skin microbiome affects the skin transcriptome in a subset of 10 MF patients that were enrolled in our preceding study [41]. Using RNAseq, multi-omic data integration, virome profiling, and TCRseq, we obtained novel insights into the role of the microbiome in both the aetiology and pathogenesis of MF.

First, we recovered substantial transcriptomic heterogeneity on both gene and pathway levels and observed that this heterogeneity may be largely driven by differential expression of T cell signalling pathways. Strikingly, our results suggested that the differential T cell signalling pattern may have been caused by the skin microbiome, since denoising the transcriptome with the microbiome using MOFA considerably reduced heterogeneity (Figure 2A,B).

Second, latent factor 4 implied that *S. aureus* elicited upregulation of both non-canonical NF-κB and IL-1B signalling, which could explain the aggravated disease course of MF patients overgrown with a spa-bearing *S. aureus* strain. Non-canonical NF-κB signalling is known to promote survival and proliferation of thymocytes and mature T cells, induce differentiation of naïve T cells into effector memory T cells, and support clonal expansion [88,89], which are all common characteristics of malignant T cells in MF [1,8,9,117]. NF-κB signalling is typically initiated by the interaction of TNFα with either TNFRSF1A (also known as TNFR1) or TNFRSF1B (also known as TNFR2) [88,89]. However, the enrichment of non-canonical NF-κB signalling in factor 4 appeared to be independent of TNFα, since it displayed a very low weight. Instead, we propose that the *S. aureus* virulence factor spa induced non-canonical NF-κB signalling since Gómez et al. showed that spa activates TNFRSF1A [42,43]. In general, TNFRSF1A induces the canonical form of NF-κB signalling leading to apoptosis, while TNFRSF1B induces non-canonical NF-κB signalling resulting in survival and proliferation. However, there is some level of crosstalk between the two forms of NF-κB pathways. In highly activated T cells, such as the malignant T cells in MF, activation of TNFRSF1A results in survival rather than apoptosis [88,89,118]. Further, the extracellular domains of TNFRSF1A and TNFRSF1B exhibit a high degree of structural similarity [119], possibly allowing spa to activate both receptors. Additionally, while TNFRSF1A is expressed nearly ubiquitously across various cell types throughout the body, TNFRSF1B expression is considerably more restricted, including thymocytes and T cells [89]. Thus, spa may activate either TNFRSF1A, TNFRSF1B, or both to initiate non-canonical NF-κB signalling to fuel MF progression.

In agreement with our findings, a clinical study reported that systemic inhibition of NF-κB in CTCL patients induced a skin response in 30.4% of patients, whereas the blood response was mixed [120–122] Further, Shin et al. identified ectopic NF-κB signalling in 30.6% of MF patients and that these patients had an aggravated disease course compared to patients without ectopic NF-κB signalling [44]. We previously identified that 31.3% of MF patients were overgrown with the virulent, spa-bearing *S. aureus* strain and had an aggravated disease course [41]. Considering the comparable prevalences of the specified subgroups and the presumed NF-κB-activating effect of spa, this may suggest a potential association between skin colonization by a spa-carrying *S. aureus* strain and exacerbation of the disease in the aforementioned studies. Additional research on the spa-NF-κB interaction including mechanistic assays with bigger patient groups is warranted.

Regarding our finding of upregulated IL-1B signalling in factor 4, it was shown that *S. aureus* induces secretion of IL-1B by eosinophils [123], which infiltrate MF lesions [124]. Furthermore, human keratinocytes, skin-derived dendritic cells, and lymphocytes produce several cytokines, including IL-1A, IL-1B, and IL-4, when challenged with *S. aureus* or spa [90,125,126]. This suggests a paracrine stimulation of malignant T cells by the tumour microenvironment via cytokine signalling in response to *S. aureus*.

Last, we discovered evidence indicating viral involvement in the aetiology of MF. Latent factor 5 captured a concomitant upregulation of innate antivirus defence mechanisms and aberrant *RUNX1/2* signalling. The latter is known to coordinate thymopoiesis during double-negative (DN) stages DN1 through DN3 [81,82,127], which have been mapped to the initial oncologic transformation in MF [10–15]. We further observed that viral load, particularly of HPV71 and EBV, trended higher in both deeper skin layers of MF lesions and the blood compared to nonlesional skin, whereas superficial skin layers of MF lesions showed no difference. HPV71 was shown to degrade p53 [128], which can result in neoplasia [129]. Nevertheless, while certain papillomaviruses are categorized as high-risk factors for the onset of solid cancers [130] and have also been loosely linked to an elevated risk of lymphomas [131], HPV71 is generally regarded as having low oncogenic potential [132]. In contrast, EBV is a well-known oncovirus [133–135]. Remarkably, we found that T cells residing in MF lesions or in the blood were significantly more affinitive to EBV-epitopes than T cells of nonlesional skin (Figure 4C). Moreover, the most frequently recognized EBV-epitopes were epitopes of LMP1, LMP2, and EBNA1, which are genes commonly expressed by EBV in latent infection [113]. Although EBV has a strong B cell tropism, leading to B cell Hodgkin's lymphoma (HL) and non-Hodgkin's lymphoma (nHL) [133–135], the virus also infects T cells, thereby causing some entities of T cell nHL [47,48]. Notably, CTCL patients have an increased risk of developing secondary HL and nHL [17–20]. It has been proposed that a single precursor malignant T cell can trigger HL, CTCL, and lymphomatoid papulosis, a benign T cell neoplasm, in the same patient [21,22]. Others reported the simultaneous presence of HL and CTCL within the same lymph node and theorized that the two malignancies arise from distinct B and T cells [23], indicating that a common trigger induced oncogenesis.

To the best of our knowledge, we were the first to investigate viral prevalence in different skin compartments and found that EBV and HPV71 trended higher solely in deeper skin layers of MF lesions, where malignant T cells in MF reside [108]. Collectively, our data indicate that viruses, probably EBV and/or HPV71, might play a role in MF aetiology. However, the sample size was rather small and not all lesional and blood samples were positive for EBV and/or HPV71. Moreover, despite a significantly higher EBV-epitope recognition of these tissues defined by computational estimation, mechanistic assays are warranted for a definitive conclusion. Thus, hypotheses on viral involvement in MF need to be considered speculative at this point. Additional investigations with more participants and longitudinal viral monitoring across tissues and different skin compartments are necessary to determine whether viruses are the aetiologic agent in MF.

An open question remains whether the age distribution of our patient group may have influenced the skin condition/clinical appearance, since 7 out of 10 patients were aged 60 or older (4 ΔSA-neutral, 3 ΔSA-neutral). In skin-disease-free subjects, several skin integrity parameters such as hydration, sebum production, or cytokine production decrease with age [136,137]. Studies in MF have indicated that skin integrity and moisture levels are lower in comparison to age-matched healthy subjects, which could lead to an increased susceptibility to bacterial infection [138–140]. This implies that older MF patients could experience a more severe skin barrier defect than younger MF patients and hence could experience infections more frequently. Notably, a cut-point of 60 years of age has been identified as a clinically prognostic outcome factor. Given that 70% of the patients in our study group were aged 60 and older and were evenly distributed between the two ΔSA groups, this indicates appropriate age matching within our study group. However, bigger patient groups with a more diverse population are warranted.

Further limitations of our study are the small patient group size, the mono-centric nature of our study, and the lack of mechanistic assays to confirm our findings, which are based on computational analyses from primary clinical specimens.

Additionally, the skewed distribution of patients between the two ΔSA groups could have introduced bias. To mitigate this concern, we specifically opted to utilize MOFA2, which is an unsupervised method agnostic of grouping variables. Analogous to PCA, MOFA2 generates clusters based on integrated multi-omic profiles [58]. Therefore, the input to MOFA2 entails the entire group rather than a comparison of two (potentially imbalanced) groups. Importantly, despite the smaller size of the ΔSA-positive group compared to the ΔSA-neutral group, the MOFA2 model identified substantial upregulation of both non-canonical NF-κB and IL-1B signalling, which was largely disregarded by conventional GSEA (Supplementary Material S2, plaque vs. nonlesional skin). Nonetheless, our findings are based on a small patient group derived from our preceding study [41]. To assess the robustness of the MOFA2 model, we performed a thorough evaluation of (a.) the stability of our model throughout iterations and (b.) the robustness of our model against technical noise. Our assessment suggests that MOFA robustly detects the same latent factors and patterns with and without noise. Please refer to Supplementary Material S7 for the full stability assessment. The current study represents an in-depth investigation of a rather limited patient group, and further research is required for validation and generalization.

5. Conclusions

In this study, we provided novel insights into the role of the microbiome in MF aetiopathogenesis. First, our results indicated that the skin microbiome largely contributes to transcriptional heterogeneity. Second, our data suggest that a spa-bearing *S. aureus* strain, which overgrows a subgroup of MF patients with aggravated disease course, might evoke non-canonical NF-κB and IL-1B signalling in the skin. Third, our data collectively suggested that viruses, particularly EBV and HPV71, may be the aetiologic agent in MF.

Together with the results from our preceding study, these findings led us to propose a model of microbiome-driven MF aetiopathogenesis (Figure 5): The initial oncologic transformation could emerge during early thymopoiesis triggered by aberrant *RUNX* expression, potentially caused by viral infection such as with EBV and/or HPV71. Malignant T cells infiltrate the skin, leading the microenvironment to release AMPs. Eventually, this process eliminates microbes, resulting in skin dysbiosis and a diminished epithelial barrier. Additionally, certain AMPs attract CD4+ T cells, which could include malignant T cells, thereby augmenting the infiltration of (malignant) T cells into MF lesions. Over time, some microbes acquire resistance to AMPs and recolonize the lesions. In the ΔSA-neutral subgroup, microbes with anti-*S. aureus* properties accumulate, resulting in a balanced microbiome and favourable clinical course. However, in the ΔSA-positive subgroup, a virulent *S. aureus* strain carrying the virulence factor spa outgrows and activates non-canonical NF-κB and IL-1B signalling, resulting in the generation of mature effector memory T cells and poor outcome. Hence, both perspectives on the cells of origin in MF may apply: early T cell progenitors [10–14] and mature, effector memory T cells [8,9].

Additional research is warranted to validate and generalize our findings, which are based on a rather small patient group. Furthermore, research allowing mechanistic insights is needed to understand how the microbiome affects malignant T cells in MF.

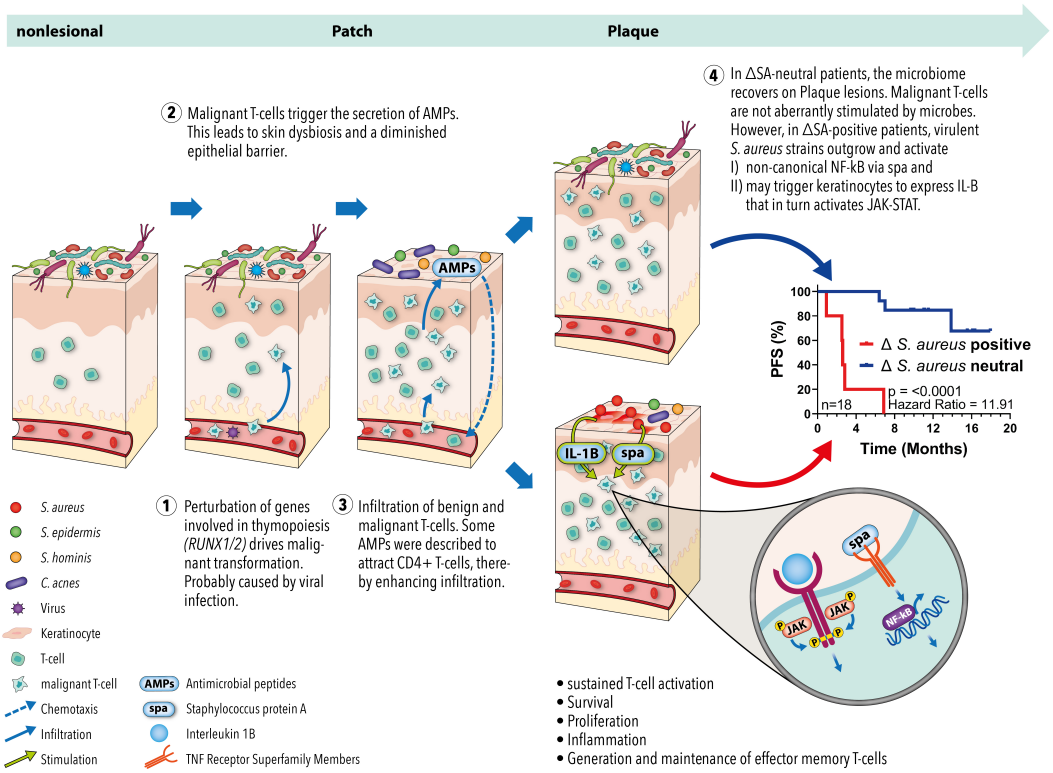

Figure 5. Proposed model of microbiome-driven MF aetiopathogenesis. T cell precursors undergo initial oncologic transformation due to aberrant expression of RUNX1 and RUNX2, probably caused by viruses like EBV and/or HPV71. After maturation and skin infiltration, the malignant T cells trigger the microenvironment to secrete AMPs. AMPs kill most of the physiological skin microbiota, resulting in dysbiosis and a diminished epithelial barrier. In addition, AMPs may recruit benign and malignant CD4+ T cells, establishing a loop of sustained dysbiosis and T cell infiltration. Since AMP levels remain constant over the disease course, some microbes eventually acquire resistance and recolonize the lesions. In the ΔSA-neutral subgroup, microbes with anti-S. aureus activity accumulate, resulting in a balanced microbiome that does not fuel the disease. However, in the ΔSA-positive subgroup, virulent S. aureus strains bearing the virulence factor spa overgrow and activate non-canonical NF-κB as well as IL-1B signalling. The two pathways cause inflammation, sustained activity, survival, and proliferation of T cells, as well as the generation and maintenance of effector memory T cells. These characteristics are hallmarks of malignant T cells in MF and may explain the significantly aggravated clinical course of the ΔSA-positive subgroup.

Supplementary Materials: The following supporting information can be downloaded at https://www.mdpi.com/article/10.3390/cancers16233947/s1: Supplementary Material S1: Differentially expressed genes in patch and plaque vs. nonlesional skin; Supplementary Material S2: Gene set enrichment analysis of patch and plaque vs. nonlesional skin; Supplementary Material S3: Heterogeneous activation pattern of pathways between nonlesional skin and patch or plaque, respectively; Supplementary Material S4: Characterization of the fitted MOFA2 model; Supplementary Figure S1: Total variance explained in the transcriptome and the microbiome data modalities by the MOFA model. Supplementary Material S5: Gene set enrichment analysis of each MOFA2 factor; Supplementary Material S6: Transcriptome input for the MOFA2 model. Supplementary Material S7: Stability Assessment of the MOFA model.

Author Contributions: Conceptualization, P.L. and V.M.; methodology, P.L.; validation, P.L. and V.M.; formal analysis, P.L.; investigation, P.L.; resources, V.M.; data curation, P.L.; writing—original draft preparation, P.L.; writing—review and editing, P.L. and V.M.; visualization, P.L.; supervision, V.M.; project administration, P.L. and V.M.; funding acquisition, P.L. and V.M. All authors have read and agreed to the published version of the manuscript.

Funding: This research received no external funding.

Institutional Review Board Statement: All procedures in this study were conducted in accordance with the Declaration of Helsinki from 1964 and its later amendments. The local ethics committee, the Medical Association of Rhineland-Palatine (Ethik-Kommisssion der Landesaerztekammer Rheinland-Pfalz), Germany, assigned ethical approval under number 2020-14813.

Informed Consent Statement: Informed consent was obtained from all subjects involved in this study.

Data Availability Statement: The code used to generate the plots in Figures 1, 2, 3 and 4A,B, Supplementary Figure S1, and Supplementary Material S5 was deposited on GitHub (https://github.com/phlicht/Multi-Omic_Data_Integration_in_MF). All datasets used in this study (i.e., RNAseq, WGS, and TCRseq) were deposited on the Gene Expression Omnibus (GEO) under the SuperSeries GSE221150 (https://www.ncbi.nlm.nih.gov/geo/query/acc.cgi?acc=GSE221150): RNA sequencing data and associated analysis files can be accessed under GSE221148 (https://www.ncbi.nlm.nih.gov/geo/query/acc.cgi?acc=GSE221148). This includes viral profiles from both whole skin biopsies and the blood. Microbiome sequencing data and associated analysis files can be accessed under GSE221149 (https://www.ncbi.nlm.nih.gov/geo/query/acc.cgi?acc=GSE221149). This includes re-analysed microbiome profiles with absolute counts and viral profiles from superficial skin layers. TCR Sequencing data and associated analysis files can be accessed under GSE218874 (https://www.ncbi.nlm.nih.gov/geo/query/acc.cgi?acc=GSE218874).

Acknowledgments: We thank Stefan Kindel, University Medical Centre Mainz, for the creation of the figure summarizing our proposed model of microbial-driven MF aetiopathogenesis.

Conflicts of Interest: The authors declare no conflicts of interest.

References

1. Dummer, R.; Vermeer, M.H.; Scarisbrick, J.J.; Kim, Y.H.; Stonesifer, C.; Tensen, C.P.; Geskin, L.J.; Quaglino, P.; Ramelyte, E. Cutaneous T Cell Lymphoma. *Nat. Rev. Dis. Prim.* **2021**, *7*, 61. [CrossRef]
2. Bradford, P.T.; Devesa, S.S.; Anderson, W.F.; Toro, J.R. Cutaneous Lymphoma Incidence Patterns in the United States: A Population-Based Study of 3884 Cases. *Blood* **2009**, *113*, 5064–5073. [CrossRef] [PubMed]
3. Nielsen, P.R.; Eriksen, J.O.; Sørensen, M.D.; Wehkamp, U.; Lindahl, L.M.; Bzorek, M.; Iversen, L.; Woetman, A.; Ødum, N.; Litman, T.; et al. Role of B-Cells in Mycosis Fungoides. *Acta Derm. Venereol.* **2021**, *101*, adv00413. [CrossRef] [PubMed]
4. Girardi, M.; Heald, P.W.; Wilson, L.D. The Pathogenesis of Mycosis Fungoides. *N. Engl. J. Med.* **2004**, *350*, 1978–1988. [CrossRef]
5. Olsen, E.; Vonderheid, E.; Pimpinelli, N.; Willemze, R.; Kim, Y.; Knobler, R.; Zackheim, H.; Duvic, M.; Estrach, T.; Lamberg, S.; et al. Revisions to the Staging and Classification of Mycosis Fungoides and Sezary Syndrome: A Proposal of the International Society for Cutaneous Lymphomas (ISCL) and the Cutaneous Lymphoma Task Force of the European Organization of Research and Treatment of Ca. *Blood* **2007**, *110*, 1713–1722. [CrossRef]
6. Whittaker, S.; Hoppe, R.; Prince, H.M. How I Treat Mycosis Fungoides and Sezary Syndrome. *Blood* **2016**, *127*, 3142–3153. [CrossRef] [PubMed]
7. Ansell, S.M. Non-Hodgkin Lymphoma: Diagnosis and Treatment. *Mayo Clin. Proc.* **2015**, *90*, 1152–1163. [CrossRef] [PubMed]
8. Kirsch, I.R.; Watanabe, R.; O'Malley, J.T.; Williamson, D.W.; Scott, L.-L.; Elco, C.P.; Teague, J.E.; Gehad, A.; Lowry, E.L.; LeBoeuf, N.R.; et al. TCR Sequencing Facilitates Diagnosis and Identifies Mature T Cells as the Cell of Origin in CTCL. *Sci. Transl. Med.* **2015**, *7*, 308ra158. [CrossRef]
9. Campbell, J.J.; Clark, R.A.; Watanabe, R.; Kupper, T.S. Sézary Syndrome and Mycosis Fungoides Arise from Distinct T-Cell Subsets: A Biologic Rationale for Their Distinct Clinical Behaviors. *Blood* **2010**, *116*, 767–771. [CrossRef]
10. Iyer, A.; Hennessey, D.; O'Keefe, S.; Patterson, J.; Wang, W.; Salopek, T.; Wong, G.K.-S.; Gniadecki, R. Clonotypic Heterogeneity in Cutaneous T-Cell Lymphoma (Mycosis Fungoides) Revealed by Comprehensive Whole-Exome Sequencing. *Blood Adv.* **2019**, *3*, 1175–1184. [CrossRef]
11. Hamrouni, A.; Fogh, H.; Zak, Z.; Ødum, N.; Gniadecki, R. Clonotypic Diversity of the T-Cell Receptor Corroborates the Immature Precursor Origin of Cutaneous T-Cell Lymphoma. *Clin. Cancer Res.* **2019**, *25*, 3104–3114. [CrossRef] [PubMed]
12. Iyer, A.; Hennessey, D.; O'Keefe, S.; Patterson, J.; Wang, W.; Wong, G.K.-S.; Gniadecki, R. Skin Colonization by Circulating Neoplastic Clones in Cutaneous T-Cell Lymphoma. *Blood* **2019**, *134*, 1517–1527. [CrossRef] [PubMed]
13. Iyer, A.; Hennessey, D.; O'Keefe, S.; Patterson, J.; Wang, W.; Wong, G.K.-S.; Gniadecki, R. Branched Evolution and Genomic Intratumor Heterogeneity in the Pathogenesis of Cutaneous T-Cell Lymphoma. *Blood Adv.* **2020**, *4*, 2489–2500. [CrossRef] [PubMed]
14. Iyer, A.; Hennessey, D.; Gniadecki, R. Clonotype Pattern in T-Cell Lymphomas Map the Cell of Origin to Immature Lymphoid Precursors. *Blood Adv.* **2022**, *6*, 2334–2345. [CrossRef]

15. Ren, J.; Qu, R.; Rahman, N.-T.; Lewis, J.M.; King, A.L.O.; Liao, X.; Mirza, F.N.; Carlson, K.R.; Huang, Y.; Gigante, S.; et al. Integrated Transcriptome and Trajectory Analysis of Cutaneous T-Cell Lymphoma Identifies Putative Precancer Populations. *Blood Adv.* **2022**, *7*, 445–457. [CrossRef]
16. Mesri, E.A.; Feitelson, M.A.; Munger, K. Human Viral Oncogenesis: A Cancer Hallmarks Analysis. *Cell Host Microbe* **2014**, *15*, 266–282. [CrossRef]
17. Väkevä, L.; Ranki, A.; Pukkala, E. Increased Risk of Secondary Cancers in Patients with Primary Cutaneous T Cell Lymphoma. *J. Investig. Dermatol.* **2000**, *115*, 62–65. [CrossRef]
18. Kantor, A.F.; Curtis, R.E.; Vonderheid, E.C.; van Scott, E.J.; Fraumeni, J.F. Risk of Second Malignancy after Cutaneous T-Cell Lymphoma. *Cancer* **1989**, *63*, 1612–1615. [CrossRef]
19. Amber, K.T.; Bloom, R.; Nouri, K. Second Primary Malignancies in CTCL Patients from 1992 to 2011: A SEER-Based, Population-Based Study Evaluating Time from CTCL Diagnosis, Age, Sex, Stage, and CD30+ Subtype. *Am. J. Clin. Dermatol.* **2016**, *17*, 71–77. [CrossRef]
20. Brownell, I.; Etzel, C.J.; Yang, D.J.; Taylor, S.H.; Duvic, M. Increased Malignancy Risk in the Cutaneous T-Cell Lymphoma Patient Population. *Clin. Lymphoma Myeloma* **2008**, *8*, 100–105. [CrossRef]
21. Davis, T.H.; Morton, C.C.; Miller-Cassman, R.; Balk, S.P.; Kadin, M.E. Hodgkin's Disease, Lymphomatoid Papulosis, and Cutaneous T-Cell Lymphoma Derived from a Common T-Cell Clone. *N. Engl. J. Med.* **1992**, *326*, 1115–1122. [CrossRef] [PubMed]
22. Wood, G.S.; Crooks, C.F.; Uluer, A.Z. Lymphomatoid Papulosis and Associated Cutaneous Lymphoproliferative Disorders Exhibit a Common Clonal Origin. *J. Investig. Dermatol.* **1995**, *105*, 51–55. [CrossRef]
23. Steinhoff, M. Cutaneous T Cell Lymphoma and Classic Hodgkin Lymphoma of the B Cell Type within a Single Lymph Node: Composite Lymphoma. *J. Clin. Pathol.* **2004**, *57*, 329–331. [CrossRef]
24. Mirvish, E.D.; Pomerantz, R.G.; Geskin, L.J. Infectious Agents in Cutaneous T-Cell Lymphoma. *J. Am. Acad. Dermatol.* **2011**, *64*, 423–431. [CrossRef]
25. Mirvish, J.J.; Pomerantz, R.G.; Falo, L.D.; Geskin, L.J. Role of Infectious Agents in Cutaneous T-Cell Lymphoma: Facts and Controversies. *Clin. Dermatol.* **2013**, *31*, 423–431. [CrossRef]
26. Dulmage, B.O.; Feng, H.; Mirvish, E.; Geskin, L. Black Cat in a Dark Room: The Absence of a Directly Oncogenic Virus Does Not Eliminate the Role of an Infectious Agent in Cutaneous T-Cell Lymphoma Pathogenesis. *Br. J. Dermatol.* **2015**, *172*, 1449–1451. [CrossRef] [PubMed]
27. García-Díaz, N.; Piris, M.Á.; Ortiz-Romero, P.L.; Vaqué, J.P. Mycosis Fungoides and Sézary Syndrome: An Integrative Review of the Pathophysiology, Molecular Drivers, and Targeted Therapy. *Cancers* **2021**, *13*, 1931. [CrossRef] [PubMed]
28. Yumeen, S.; Girardi, M. Insights into the Molecular and Cellular Underpinnings of Cutaneous T Cell Lymphoma. *Yale J. Biol. Med.* **2020**, *93*, 111–121.
29. Smith-Garvin, J.E.; Koretzky, G.A.; Jordan, M.S. T Cell Activation. *Annu. Rev. Immunol.* **2009**, *27*, 591–619. [CrossRef]
30. Curtsinger, J.M.; Mescher, M.F. Inflammatory Cytokines as a Third Signal for T Cell Activation. *Curr. Opin. Immunol.* **2010**, *22*, 333–340. [CrossRef]
31. Santarlasci, V.; Cosmi, L.; Maggi, L.; Liotta, F.; Annunziato, F. IL-1 and T Helper Immune Responses. *Front. Immunol.* **2013**, *4*, 182. [CrossRef] [PubMed]
32. Wilcox, R.A. A Three-Signal Model of T-Cell Lymphoma Pathogenesis. *Am. J. Hematol.* **2016**, *91*, 113–122. [CrossRef] [PubMed]
33. McGirt, L.Y.; Jia, P.; Baerenwald, D.A.; Duszynski, R.J.; Dahlman, K.B.; Zic, J.A.; Zwerner, J.P.; Hucks, D.; Dave, U.; Zhao, Z.; et al. Whole-Genome Sequencing Reveals Oncogenic Mutations in Mycosis Fungoides. *Blood* **2015**, *126*, 508–519. [CrossRef] [PubMed]
34. Ungewickell, A.; Bhaduri, A.; Rios, E.; Reuter, J.; Lee, C.S.; Mah, A.; Zehnder, A.; Ohgami, R.; Kulkarni, S.; Armstrong, R.; et al. Genomic Analysis of Mycosis Fungoides and Sézary Syndrome Identifies Recurrent Alterations in TNFR2. *Nat. Genet.* **2015**, *47*, 1056–1060. [CrossRef]
35. Da Silva Almeida, A.C.; Abate, F.; Khiabanian, H.; Martinez-Escala, E.; Guitart, J.; Tensen, C.P.; Vermeer, M.H.; Rabadan, R.; Ferrando, A.; Palomero, T. The Mutational Landscape of Cutaneous T Cell Lymphoma and Sézary Syndrome. *Nat. Genet.* **2015**, *47*, 1465–1470. [CrossRef]
36. Choi, J.; Goh, G.; Walradt, T.; Hong, B.S.; Bunick, C.G.; Chen, K.; Bjornson, R.D.; Maman, Y.; Wang, T.; Tordoff, J.; et al. Genomic Landscape of Cutaneous T Cell Lymphoma. *Nat. Genet.* **2015**, *47*, 1011–1019. [CrossRef]
37. Damsky, W.E.; Choi, J. Genetics of Cutaneous T Cell Lymphoma: From Bench to Bedside. *Curr. Treat. Options Oncol.* **2016**, *17*, 33. [CrossRef]
38. Pérez, C.; Mondéjar, R.; García-Díaz, N.; Cereceda, L.; León, A.; Montes, S.; Durán Vian, C.; Pérez Paredes, M.G.; González-Morán, A.; Miguel, V.; et al. Advanced-stage Mycosis Fungoides: Role of the Signal Transducer and Activator of Transcription 3, Nuclear Factor-κB and Nuclear Factor of Activated T Cells Pathways. *Br. J. Dermatol.* **2020**, *182*, bjd.18098. [CrossRef]
39. Dulmage, B.O.; Geskin, L.J. Lessons Learned from Gene Expression Profiling of Cutaneous T-Cell Lymphoma. *Br. J. Dermatol.* **2013**, *169*, 1188–1197. [CrossRef]
40. Licht, P.; Mailänder, V. Transcriptional Heterogeneity and the Microbiome of Cutaneous T-Cell Lymphoma. *Cells* **2022**, *11*, 328. [CrossRef]
41. Licht, P.; Dominelli, N.; Kleemann, J.; Pastore, S.; Müller, E.-S.; Haist, M.; Hartmann, K.S.; Stege, H.; Bros, M.; Meissner, M.; et al. The Skin Microbiome Stratifies Patients with Cutaneous T Cell Lymphoma and Determines Event-Free Survival. *NPJ Biofilms Microbiomes* **2024**, *10*, 74. [CrossRef] [PubMed]

42. Gómez, M.I.; Lee, A.; Reddy, B.; Muir, A.; Soong, G.; Pitt, A.; Cheung, A.; Prince, A. Staphylococcus Aureus Protein A Induces Airway Epithelial Inflammatory Responses by Activating TNFR1. *Nat. Med.* **2004**, *10*, 842–848. [CrossRef] [PubMed]
43. Gómez, M.I.; O'Seaghdha, M.; Magargee, M.; Foster, T.J.; Prince, A.S. Staphylococcus Aureus Protein A Activates TNFR1 Signaling through Conserved IgG Binding Domains. *J. Biol. Chem.* **2006**, *281*, 20190–20196. [CrossRef]
44. Shin, J.; Monti, S.; Aires, D.J.; Duvic, M.; Golub, T.; Jones, D.A.; Kupper, T.S. Lesional Gene Expression Profiling in Cutaneous T-Cell Lymphoma Reveals Natural Clusters Associated with Disease Outcome. *Blood* **2007**, *110*, 3015–3027. [CrossRef]
45. Tracey, L.; Villuendas, R.; Dotor, A.M.; Spiteri, I.; Ortiz, P.; García, J.F.; Peralto, J.L.R.; Lawler, M.; Piris, M.A. Mycosis Fungoides Shows Concurrent Deregulation of Multiple Genes Involved in the TNF Signaling Pathway: An Expression Profile Study. *Blood* **2003**, *102*, 1042–1050. [CrossRef]
46. Rindler, K.; Bauer, W.M.; Jonak, C.; Wielscher, M.; Shaw, L.E.; Rojahn, T.B.; Thaler, F.M.; Porkert, S.; Simonitsch-Klupp, I.; Weninger, W.; et al. Single-Cell RNA Sequencing Reveals Tissue Compartment-Specific Plasticity of Mycosis Fungoides Tumor Cells. *Front. Immunol.* **2021**, *12*, 666935. [CrossRef] [PubMed]
47. Gru, A.A.; Haverkos, B.H.; Freud, A.G.; Hastings, J.; Nowacki, N.B.; Barrionuevo, C.; Vigil, C.E.; Rochford, R.; Natkunam, Y.; Baiocchi, R.A.; et al. The Epstein-Barr Virus (EBV) in T Cell and NK Cell Lymphomas: Time for a Reassessment. *Curr. Hematol. Malig. Rep.* **2015**, *10*, 456–467. [CrossRef]
48. Heslop, H.E. Biology and Treatment of Epstein-Barr Virus–Associated Non-Hodgkin Lymphomas. *Hematology* **2005**, *2005*, 260–266. [CrossRef] [PubMed]
49. Byrd, A.L.; Belkaid, Y.; Segre, J.A. The Human Skin Microbiome. *Nat. Rev. Microbiol.* **2018**, *16*, 143–155. [CrossRef]
50. Andrews, S.; Babraham, I. FastQC: A Quality Control Tool for High Throughput Sequence Data. Available online: https://www.bioinformatics.babraham.ac.uk/projects/fastqc/ (accessed on 8 October 2019).
51. Dobin, A.; Davis, C.A.; Schlesinger, F.; Drenkow, J.; Zaleski, C.; Jha, S.; Batut, P.; Chaisson, M.; Gingeras, T.R. STAR: Ultrafast Universal RNA-Seq Aligner. *Bioinformatics* **2013**, *29*, 15–21. [CrossRef]
52. Love, M.I.; Huber, W.; Anders, S. Moderated Estimation of Fold Change and Dispersion for RNA-Seq Data with DESeq2. *Genome Biol.* **2014**, *15*, 550. [CrossRef] [PubMed]
53. Blighe, K.; Rana, S.; Lewis, M. EnhancedVolcano: Publication-Ready Volcano Plots with Enhanced Colouring and Labeling. Available online: https://github.com/kevinblighe/EnhancedVolcano (accessed on 8 October 2019).
54. Wickham, H. *Ggplot2: Elegant Graphics for Data Analysis*; Springer: New York, NY, USA, 2016; ISBN 978-3-319-24277-4.
55. Ulgen, E.; Ozisik, O.; Sezerman, O.U. PathfindR: An R Package for Comprehensive Identification of Enriched Pathways in Omics Data Through Active Subnetworks. *Front. Genet.* **2019**, *10*, 858. [CrossRef] [PubMed]
56. Jassal, B.; Matthews, L.; Viteri, G.; Gong, C.; Lorente, P.; Fabregat, A.; Sidiropoulos, K.; Cook, J.; Gillespie, M.; Haw, R.; et al. The Reactome Pathway Knowledgebase. *Nucleic Acids Res.* **2019**, *48*, D498–D503. [CrossRef] [PubMed]
57. Smyth, G.K.; Ritchie, M.; Thorne, N.; Wettenhall, J.; Shi, W.; Hu, Y. Limma: Linear Models for Microarray and RNA-Seq Data User's Guide. Available online: https://www.bioconductor.org/packages/release/bioc/vignettes/limma/inst/doc/usersguide.pdf (accessed on 12 November 2024).
58. Argelaguet, R.; Velten, B.; Arnol, D.; Dietrich, S.; Zenz, T.; Marioni, J.C.; Buettner, F.; Huber, W.; Stegle, O. Multi-Omics Factor Analysis—A Framework for Unsupervised Integration of Multi-omics Data Sets. *Mol. Syst. Biol.* **2018**, *14*, e8124. [CrossRef] [PubMed]
59. Truong, D.T.; Franzosa, E.A.; Tickle, T.L.; Scholz, M.; Weingart, G.; Pasolli, E.; Tett, A.; Huttenhower, C.; Segata, N. MetaPhlAn2 for Enhanced Metagenomic Taxonomic Profiling. *Nat. Methods* **2015**, *12*, 902–903. [CrossRef]
60. Beghini, F.; McIver, L.J.; Blanco-Míguez, A.; Dubois, L.; Asnicar, F.; Maharjan, S.; Mailyan, A.; Manghi, P.; Scholz, M.; Thomas, A.M.; et al. Integrating Taxonomic, Functional, and Strain-Level Profiling of Diverse Microbial Communities with BioBakery 3. *Elife* **2021**, *10*, e65088. [CrossRef]
61. Kumar, M.S.; Slud, E.V.; Okrah, K.; Hicks, S.C.; Hannenhalli, S.; Corrada Bravo, H. Analysis and Correction of Compositional Bias in Sparse Sequencing Count Data. *BMC Genom.* **2018**, *19*, 799. [CrossRef]
62. Frost, H.R.; Li, Z.; Moore, J.H. Principal Component Gene Set Enrichment (PCGSE). *BioData Min.* **2015**, *8*, 25. [CrossRef]
63. Yasumizu, Y.; Hara, A.; Sakaguchi, S.; Ohkura, N. VIRTUS: A Pipeline for Comprehensive Virus Analysis from Conventional RNA-Seq Data. *Bioinformatics* **2021**, *37*, 1465–1467. [CrossRef]
64. Kolde, R. Pheatmap: Pretty Heatmaps. Available online: https://cran.r-project.org/package=pheatmap (accessed on 5 October 2018).
65. Vander Heiden, J.A.; Yaari, G.; UdumanSegre, M.; Stern, J.N.H.; O'Connor, K.C.; Hafler, D.A.; Vigneault, F.; Kleinstein, S.H. PRESTO: A Toolkit for Processing High-Throughput Sequencing Raw Reads of Lymphocyte Receptor Repertoires. *Bioinformatics* **2014**, *30*, 1930–1932. [CrossRef]
66. ImmunoMind Team Immunarch: An R Package for Painless Bioinformatics Analysis of T-Cell and B-Cell Immune Repertoires 2019. Available online: https://zenodo.org/records/10840553 (accessed on 20 November 2024).
67. Vita, R.; Mahajan, S.; Overton, J.A.; Dhanda, S.K.; Martini, S.; Cantrell, J.R.; Wheeler, D.K.; Sette, A.; Peters, B. The Immune Epitope Database (IEDB): 2018 Update. *Nucleic Acids Res.* **2019**, *47*, D339–D343. [CrossRef] [PubMed]
68. Springer, I.; Tickotsky, N.; Louzoun, Y. Contribution of T Cell Receptor Alpha and Beta CDR3, MHC Typing, V and J Genes to Peptide Binding Prediction. *Front. Immunol.* **2021**, *12*, 664514. [CrossRef]

69. Gaydosik, A.M.; Tabib, T.; Geskin, L.J.; Bayan, C.-A.; Conway, J.F.; Lafyatis, R.; Fuschiotti, P. Single-Cell Lymphocyte Heterogeneity in Advanced Cutaneous T-Cell Lymphoma Skin Tumors. *Clin. Cancer Res.* **2019**, *25*, 4443–4454. [CrossRef]
70. Buus, T.B.; Willerslev-Olsen, A.; Fredholm, S.; Blümel, E.; Nastasi, C.; Gluud, M.; Hu, T.; Lindahl, L.M.; Iversen, L.; Fogh, H.; et al. Single-Cell Heterogeneity in Sézary Syndrome. *Blood Adv.* **2018**, *2*, 2115–2126. [CrossRef]
71. Borcherding, N.; Voigt, A.P.; Liu, V.; Link, B.K.; Zhang, W.; Jabbari, A. Single-Cell Profiling of Cutaneous T-Cell Lymphoma Reveals Underlying Heterogeneity Associated with Disease Progression. *Clin. Cancer Res.* **2019**, *25*, 2996–3005. [CrossRef]
72. Herrera, A.; Cheng, A.; Mimitou, E.P.; Seffens, A.; George, D.D.; Bar-Natan, M.; Heguy, A.; Ruggles, K.V.; Scher, J.U.; Hymes, K.; et al. Multimodal Single-Cell Analysis of Cutaneous T Cell Lymphoma Reveals Distinct Sub-Clonal Tissue-Dependent Signatures. *Blood* **2021**, *138*, 1456–1464. [CrossRef] [PubMed]
73. Litvinov, I.V.; Tetzlaff, M.T.; Thibault, P.; Gangar, P.; Moreau, L.; Watters, A.K.; Netchiporouk, E.; Pehr, K.; Prieto, V.G.; Rahme, E.; et al. Gene Expression Analysis in Cutaneous T-Cell Lymphomas (CTCL) Highlights Disease Heterogeneity and Potential Diagnostic and Prognostic Indicators. *Oncoimmunology* **2017**, *6*, e1306618. [CrossRef] [PubMed]
74. Stolearenco, V.; Namini, M.R.J.; Hasselager, S.S.; Gluud, M.; Buus, T.B.; Willerslev-Olsen, A.; Ødum, N.; Krejsgaard, T. Cellular Interactions and Inflammation in the Pathogenesis of Cutaneous T-Cell Lymphoma. *Front. Cell Dev. Biol.* **2020**, *8*, 851. [CrossRef]
75. Hruz, P.; Zinkernagel, A.S.; Jenikova, G.; Botwin, G.J.; Hugot, J.-P.; Karin, M.; Nizet, V.; Eckmann, L. NOD2 Contributes to Cutaneous Defense against Staphylococcus Aureus through α-Toxin-Dependent Innate Immune Activation. *Proc. Natl. Acad. Sci. USA* **2009**, *106*, 12873–12878. [CrossRef]
76. Deshmukh, H.S.; Hamburger, J.B.; Ahn, S.H.; McCafferty, D.G.; Yang, S.R.; Fowler, V.G. Critical Role of NOD2 in Regulating the Immune Response to Staphylococcus Aureus. *Infect. Immun.* **2009**, *77*, 1376–1382. [CrossRef]
77. Soong, G.; Martin, F.J.; Chun, J.; Cohen, T.S.; Ahn, D.S.; Prince, A. Staphylococcus Aureus Protein A Mediates Invasion across Airway Epithelial Cells through Activation of RhoA GTPase Signaling and Proteolytic Activity. *J. Biol. Chem.* **2011**, *286*, 35891–35898. [CrossRef] [PubMed]
78. Nakatsuji, T.; Chen, T.H.; Two, A.M.; Chun, K.A.; Narala, S.; Geha, R.S.; Hata, T.R.; Gallo, R.L. Staphylococcus Aureus Exploits Epidermal Barrier Defects in Atopic Dermatitis to Trigger Cytokine Expression. *J. Investig. Dermatol.* **2016**, *136*, 2192–2200. [CrossRef] [PubMed]
79. Byrd, A.L.; Deming, C.; Cassidy, S.K.B.; Harrison, O.J.; Ng, W.-I.; Conlan, S.; Belkaid, Y.; Segre, J.A.; Kong, H.H. Staphylococcus Aureus and Staphylococcus Epidermidis Strain Diversity Underlying Pediatric Atopic Dermatitis. *Sci. Transl. Med.* **2017**, *9*, eaal4651. [CrossRef] [PubMed]
80. Bergsbaken, T.; Fink, S.L.; Cookson, B.T. Pyroptosis: Host Cell Death and Inflammation. *Nat. Rev. Microbiol.* **2009**, *7*, 99–109. [CrossRef] [PubMed]
81. Vaillant, F.; Blyth, K.; Andrew, L.; Neil, J.C.; Cameron, E.R. Enforced Expression of Runx2 Perturbs T Cell Development at a Stage Coincident with β-Selection. *J. Immunol.* **2002**, *169*, 2866–2874. [CrossRef]
82. Egawa, T.; Tillman, R.E.; Naoe, Y.; Taniuchi, I.; Littman, D.R. The Role of the Runx Transcription Factors in Thymocyte Differentiation and in Homeostasis of Naive T Cells. *J. Exp. Med.* **2007**, *204*, 1945–1957. [CrossRef]
83. Ichikawa, M.; Asai, T.; Saito, T.; Yamamoto, G.; Seo, S.; Yamazaki, I.; Yamagata, T.; Mitani, K.; Chiba, S.; Hirai, H.; et al. AML-1 Is Required for Megakaryocytic Maturation and Lymphocytic Differentiation, but Not for Maintenance of Hematopoietic Stem Cells in Adult Hematopoiesis. *Nat. Med.* **2004**, *10*, 299–304. [CrossRef]
84. Growney, J.D.; Shigematsu, H.; Li, Z.; Lee, B.H.; Adelsperger, J.; Rowan, R.; Curley, D.P.; Kutok, J.L.; Akashi, K.; Williams, I.R.; et al. Loss of Runx1 Perturbs Adult Hematopoiesis and Is Associated with a Myeloproliferative Phenotype. *Blood* **2005**, *106*, 494–504. [CrossRef]
85. Cogen, A.L.; Yamasaki, K.; Sanchez, K.M.; Dorschner, R.A.; Lai, Y.; MacLeod, D.T.; Torpey, J.W.; Otto, M.; Nizet, V.; Kim, J.E.; et al. Selective Antimicrobial Action Is Provided by Phenol-Soluble Modulins Derived from Staphylococcus Epidermidis, a Normal Resident of the Skin. *J. Investig. Dermatol.* **2010**, *130*, 192–200. [CrossRef]
86. Nakatsuji, T.; Chen, T.H.; Narala, S.; Chun, K.A.; Two, A.M.; Yun, T.; Shafiq, F.; Kotol, P.F.; Bouslimani, A.; Melnik, A.V.; et al. Antimicrobials from Human Skin Commensal Bacteria Protect against Staphylococcus Aureus and Are Deficient in Atopic Dermatitis. *Sci. Transl. Med.* **2017**, *9*, eaah4680. [CrossRef]
87. Williams, M.R.; Costa, S.K.; Zaramela, L.S.; Khalil, S.; Todd, D.A.; Winter, H.L.; Sanford, J.A.; O'Neill, A.M.; Liggins, M.C.; Nakatsuji, T.; et al. Quorum Sensing between Bacterial Species on the Skin Protects against Epidermal Injury in Atopic Dermatitis. *Sci. Transl. Med.* **2019**, *11*, eaat8329. [CrossRef] [PubMed]
88. Sun, S.-C. The Non-Canonical NF-KB Pathway in Immunity and Inflammation. *Nat. Rev. Immunol.* **2017**, *17*, 545–558. [CrossRef] [PubMed]
89. Faustman, D.; Davis, M. TNF Receptor 2 Pathway: Drug Target for Autoimmune Diseases. *Nat. Rev. Drug Discov.* **2010**, *9*, 482–493. [CrossRef]
90. Chng, K.R.; Tay, A.S.L.; Li, C.; Ng, A.H.Q.; Wang, J.; Suri, B.K.; Matta, S.A.; McGovern, N.; Janela, B.; Wong, X.F.C.C.; et al. Whole Metagenome Profiling Reveals Skin Microbiome-Dependent Susceptibility to Atopic Dermatitis Flare. *Nat. Microbiol.* **2016**, *1*, 16106. [CrossRef]
91. Wang, X.; Lin, Y. Tumor Necrosis Factor and Cancer, Buddies or Foes? *Acta Pharmacol. Sin.* **2008**, *29*, 1275–1288. [CrossRef]
92. Katze, M.G.; He, Y.; Gale, M. Viruses and Interferon: A Fight for Supremacy. *Nat. Rev. Immunol.* **2002**, *2*, 675–687. [CrossRef]

93. Liu, X.-Y.; Chen, W.; Wei, B.; Shan, Y.-F.; Wang, C. IFN-Induced TPR Protein IFIT3 Potentiates Antiviral Signaling by Bridging MAVS and TBK1. *J. Immunol.* **2011**, *187*, 2559–2568. [CrossRef] [PubMed]
94. Roy, C.R.; Salcedo, S.P.; Gorvel, J.-P.E. Pathogen–Endoplasmic-Reticulum Interactions: In through the out Door. *Nat. Rev. Immunol.* **2006**, *6*, 136–147. [CrossRef]
95. Murray, P.G.; Constandinou, C.M.; Crocker, J.; Young, L.S.; Ambinder, R.F. Analysis of Major Histocompatibility Complex Class I, TAP Expression, and LMP2 Epitope Sequence in Epstein-Barr Virus–Positive Hodgkin's Disease. *Blood* **1998**, *92*, 2477–2483. [CrossRef]
96. Wang, Y.; Finan, J.E.; Middeldorp, J.M.; Hayward, S.D. P32/TAP, a Cellular Protein That Interacts with EBNA-1 of Epstein–Barr Virus. *Virology* **1997**, *236*, 18–29. [CrossRef]
97. Zhao, B.; Zou, J.; Wang, H.; Johannsen, E.; Peng, C.; Quackenbush, J.; Mar, J.C.; Morton, C.C.; Freedman, M.L.; Blacklow, S.C.; et al. Epstein-Barr Virus Exploits Intrinsic B-Lymphocyte Transcription Programs to Achieve Immortal Cell Growth. *Proc. Natl. Acad. Sci. USA* **2011**, *108*, 14902–14907. [CrossRef] [PubMed]
98. Gunnell, A.; Webb, H.M.; Wood, C.D.; McClellan, M.J.; Wichaidit, B.; Kempkes, B.; Jenner, R.G.; Osborne, C.; Farrell, P.J.; West, M.J. RUNX Super-Enhancer Control through the Notch Pathway by Epstein-Barr Virus Transcription Factors Regulates B Cell Growth. *Nucleic Acids Res.* **2016**, *44*, 4636–4650. [CrossRef] [PubMed]
99. Stewart, M.; Terry, A.; Hu, M.; O'Hara, M.; Blyth, K.; Baxter, E.; Cameron, E.; Onions, D.E.; Neil, J.C. Proviral Insertions Induce the Expression of Bone-Specific Isoforms of PEBP2αA (CBFA1): Evidence for a New Myc Collaborating Oncogene. *Proc. Natl. Acad. Sci. USA* **1997**, *94*, 8646–8651. [CrossRef]
100. Suzuki, T.; Shen, H.; Akagi, K.; Morse, H.C.; Malley, J.D.; Naiman, D.Q.; Jenkins, N.A.; Copeland, N.G. New Genes Involved in Cancer Identified by Retroviral Tagging. *Nat. Genet.* **2002**, *32*, 166–174. [CrossRef] [PubMed]
101. Wotton, S.; Stewart, M.; Blyth, K.; Vaillant, F.; Kilbey, A.; Neil, J.C.; Cameron, E.R. Proviral Insertion Indicates a Dominant Oncogenic Role for Runx1/AML-1 in T-Cell Lymphoma. *Cancer Res.* **2002**, *62*, 7181–7185.
102. Blyth, K.; Cameron, E.R.; Neil, J.C. The Runx Genes: Gain or Loss of Function in Cancer. *Nat. Rev. Cancer* **2005**, *5*, 376–387. [CrossRef]
103. Dutta, A.; Zhao, B.; Love, P.E. New Insights into TCR β-Selection. *Trends Immunol.* **2021**, *42*, 735–750. [CrossRef]
104. Blyth, K.; Vaillant, F.; Hanlon, L.; Mackay, N.; Bell, M.; Jenkins, A.; Neil, J.C.; Cameron, E.R. Runx2 and MYC Collaborate in Lymphoma Development by Suppressing Apoptotic and Growth Arrest Pathways in Vivo. *Cancer Res.* **2006**, *66*, 2195–2201. [CrossRef]
105. Liang, J.; Zhou, W.; Sakre, N.; DeVecchio, J.; Ferrandon, S.; Ting, A.H.; Bao, S.; Bissett, I.; Church, J.; Kalady, M.F. Epigenetically Regulated MiR-1247 Functions as a Novel Tumour Suppressor via MYCBP2 in Methylator Colon Cancers. *Br. J. Cancer* **2018**, *119*, 1267–1277. [CrossRef]
106. Lee, S.; Kim, J.-Y.; Kim, Y.-J.; Seok, K.-O.; Kim, J.-H.; Chang, Y.-J.; Kang, H.-Y.; Park, J.-H. Nucleolar Protein GLTSCR2 Stabilizes P53 in Response to Ribosomal Stresses. *Cell Death Differ.* **2012**, *19*, 1613–1622. [CrossRef]
107. Oda, K.; Arakawa, H.; Tanaka, T.; Matsuda, K.; Tanikawa, C.; Mori, T.; Nishimori, H.; Tamai, K.; Tokino, T.; Nakamura, Y.; et al. P53AIP1, a Potential Mediator of P53-Dependent Apoptosis, and Its Regulation by Ser-46-Phosphorylated P53. *Cell* **2000**, *102*, 849–862. [CrossRef] [PubMed]
108. Hwang, S.T.; Janik, J.E.; Jaffe, E.S.; Wilson, W.H. Mycosis Fungoides and Sézary Syndrome. *Lancet* **2008**, *371*, 945–957. [CrossRef] [PubMed]
109. Shannon-Lowe, C.; Rickinson, A.B.; Bell, A.I. Epstein-Barr Virus-Associated Lymphomas. *Philos. Trans. R. Soc. B Biol. Sci.* **2017**, *372*, 20160271. [CrossRef]
110. Rollison, D.E.; Engels, E.A.; Halsey, N.A.; Shah, K.V.; Viscidi, R.P.; Helzlsouer, K.J. Prediagnostic Circulating Antibodies to JC and BK Human Polyomaviruses and Risk of Non-Hodgkin Lymphoma. *Cancer Epidemiol. Biomark. Prev.* **2006**, *15*, 543–550. [CrossRef] [PubMed]
111. Du-Thanh, A.; Foulongne, V.; Guillot, B.; Dereure, O. Recently Discovered Human Polyomaviruses in Lesional and Non-Lesional Skin of Patients with Primary Cutaneous T-Cell Lymphomas. *J. Dermatol. Sci.* **2013**, *71*, 140–142. [CrossRef]
112. Ryan, J.L.; Morgan, D.R.; Dominguez, R.L.; Thorne, L.B.; Elmore, S.H.; Mino-Kenudson, M.; Lauwers, G.Y.; Booker, J.K.; Gulley, M.L. High Levels of Epstein–Barr Virus DNA in Latently Infected Gastric Adenocarcinoma. *Lab. Investig.* **2009**, *89*, 80–90. [CrossRef]
113. Kutok, J.L.; Wang, F. Spectrum of Epstein-Barr Virus-Associated Diseases. *Annu. Rev. Pathol.* **2006**, *1*, 375–404. [CrossRef]
114. Bi, X.; Wang, H.; Zhang, W.; Wang, J.; Liu, W.; Xia, Z.; Huang, H.; Jiang, W.; Zhang, Y.; Wang, L. PD-L1 Is Upregulated by EBV-Driven LMP1 through NF-KB Pathway and Correlates with Poor Prognosis in Natural Killer/T-Cell Lymphoma. *J. Hematol. Oncol.* **2016**, *9*, 109. [CrossRef]
115. Kim, Y.H.; Liu, H.L.; Mraz-Gernhard, S.; Varghese, A.; Hoppe, R.T. Long-Term Outcome of 525 Patients with Mycosis Fungoides and Sézary Syndrome. *Arch. Dermatol.* **2003**, *139*, 857–866. [CrossRef]
116. Wang, L.; Ni, X.; Covington, K.R.; Yang, B.Y.; Shiu, J.; Zhang, X.; Xi, L.; Meng, Q.; Langridge, T.; Drummond, J.; et al. Genomic Profiling of Sézary Syndrome Identifies Alterations of Key T Cell Signaling and Differentiation Genes. *Nat. Genet.* **2015**, *47*, 1426–1434. [CrossRef]
117. Horna, P.; Moscinski, L.C.; Sokol, L.; Shao, H. Naïve/Memory T-cell Phenotypes in Leukemic Cutaneous T-cell Lymphoma: Putative Cell of Origin Overlaps Disease Classification. *Cytom. Part B Clin. Cytom.* **2019**, *96*, 234–241. [CrossRef] [PubMed]

118. Kim, E.Y.; Priatel, J.J.; Teh, S.-J.; Teh, H. TNF Receptor Type 2 (P75) Functions as a Costimulator for Antigen-Driven T Cell Responsesa In Vivo. *J. Immunol.* **2006**, *176*, 1026–1035. [CrossRef] [PubMed]
119. Mukai, Y.; Nakamura, T.; Yoshikawa, M.; Yoshioka, Y.; Tsunoda, S.; Nakagawa, S.; Yamagata, Y.; Tsutsumi, Y. Solution of the Structure of the TNF-TNFR2 Complex. *Sci. Signal.* **2010**, *3*, ra83. [CrossRef] [PubMed]
120. Nicolay, J.P.; Müller-Decker, K.; Schroeder, A.; Brechmann, M.; Möbs, M.; Géraud, C.; Assaf, C.; Goerdt, S.; Krammer, P.H.; Gülow, K. Dimethyl Fumarate Restores Apoptosis Sensitivity and Inhibits Tumor Growth and Metastasis in CTCL by Targeting NF-KB. *Blood* **2016**, *128*, 805–815. [CrossRef]
121. Nicolay, J.P.; Albrecht, J.D.; Assaf, C.; Dippel, E.; Stadler, R.; Wehkamp, U.; Wobser, M.; Guelow, K.; Goerdt, S.; Krammer, P.H. Dimethyl Fumarate (DMF) Therapy in CTCL: Results from a Clinical Phase II Study. *Eur. J. Cancer* **2021**, *156*, S21–S22. [CrossRef]
122. Nicolay, J.P.; Melchers, S.; Albrecht, J.D.; Assaf, C.; Dippel, E.; Stadler, R.; Wehkamp, U.; Wobser, M.; Zhao, J.; Burghaus, I.; et al. Dimethyl Fumarate Treatment in Relapsed and Refractory Cutaneous T Cell Lymphoma—A Multicenter Phase II Study. *Blood J.* **2023**, *142*, 794–805. [CrossRef]
123. Hosoki, K.; Nakamura, A.; Nagao, M.; Hiraguchi, Y.; Tanida, H.; Tokuda, R.; Wada, H.; Nobori, T.; Suga, S.; Fujisawa, T. Staphylococcus Aureus Directly Activates Eosinophils via Platelet-Activating Factor Receptor. *J. Leukoc. Biol.* **2012**, *92*, 333–341. [CrossRef]
124. Fredholm, S.; Gjerdrum, L.M.R.; Willerslev-Olsen, A.; Petersen, D.L.; Nielsen, I.Ø.; Kauczok, C.-S.; Wobser, M.; Ralfkiaer, U.; Bonefeld, C.M.; Wasik, M.A.; et al. STAT3 Activation and Infiltration of Eosinophil Granulocytes in Mycosis Fungoides. *Anticancer Res.* **2014**, *34*, 5277–5286.
125. Aufiero, B.; Guo, M.; Young, C.; Duanmu, Z.; Talwar, H.; Lee, H.K.; Murakawa, G.J. Staphylococcus Aureus Induces the Expression of Tumor Necrosis factor-alpha in Primary Human Keratinocytes. *Int. J. Dermatol.* **2007**, *46*, 687–694. [CrossRef]
126. Tufano, M.A.; Cipollaro de l'Ero, G.; Ianniello, R.; Galdiero, M.; Galdiero, F. Protein A and Other Surface Components of Staphylococcus Aureus Stimulate Production of IL-1 Alpha, IL-4, IL-6, TNF and IFN-Gamma. *Eur. Cytokine Netw.* **1991**, *2*, 361–366.
127. Matthijssens, F.; Sharma, N.D.; Nysus, M.; Nickl, C.K.; Kang, H.; Perez, D.R.; Lintermans, B.; Van Loocke, W.; Roels, J.; Peirs, S.; et al. RUNX2 Regulates Leukemic Cell Metabolism and Chemotaxis in High-Risk T Cell Acute Lymphoblastic Leukemia. *J. Clin. Investig.* **2021**, *131*, e141566. [CrossRef] [PubMed]
128. Fu, L.; Van Doorslaer, K.; Chen, Z.; Ristriani, T.; Masson, M.; Travé, G.; Burk, R.D. Degradation of P53 by Human Alphapapillomavirus E6 Proteins Shows a Stronger Correlation with Phylogeny than Oncogenicity. *PLoS ONE* **2010**, *5*, e12816. [CrossRef]
129. Martinez-Zapien, D.; Ruiz, F.X.; Poirson, J.; Mitschler, A.; Ramirez, J.; Forster, A.; Cousido-Siah, A.; Masson, M.; Pol, S.V.; Podjarny, A.; et al. Structure of the E6/E6AP/P53 Complex Required for HPV-Mediated Degradation of P53. *Nature* **2016**, *529*, 541–545. [CrossRef] [PubMed]
130. Egawa, N.; Egawa, K.; Griffin, H.; Doorbar, J. Human Papillomaviruses; Epithelial Tropisms, and the Development of Neoplasia. *Viruses* **2015**, *7*, 3863–3890. [CrossRef] [PubMed]
131. Intaraphet, S.; Farkas, D.K.; Johannesdottir Schmidt, S.A.; Cronin-Fenton, D.; Søgaard, M. Human Papillomavirus Infection and Lymphoma Incidence Using Cervical Conization as a Surrogate Marker: A Danish Nationwide Cohort Study. *Hematol. Oncol.* **2017**, *35*, 172–176. [CrossRef]
132. Van Doorslaer, K.; Burk, R.D. Evolution of Human Papillomavirus Carcinogenicity. *Adv. Virus Res.* **2010**, *77*, 41–62.
133. Farrell, P.J. Epstein–Barr Virus and Cancer. *Annu. Rev. Pathol. Mech. Dis.* **2019**, *14*, 29–53. [CrossRef]
134. Faulkner, G.C.; Krajewski, A.S.; Crawford, D.H. The Ins and Outs of EBV Infection. *Trends Microbiol.* **2000**, *8*, 185–189. [CrossRef]
135. Gandhi, M.K.; Tellam, J.T.; Khanna, R. Epstein-Barr Virus-Associated Hodgkin's Lymphoma. *Br. J. Haematol.* **2004**, *125*, 267–281. [CrossRef]
136. Luebberding, S.; Krueger, N.; Kerscher, M. Age-related Changes in Skin Barrier Function—Quantitative Evaluation of 150 Female Subjects. *Int. J. Cosmet. Sci.* **2013**, *35*, 183–190. [CrossRef]
137. Choi, E.H. Aging of the Skin Barrier. *Clin. Dermatol.* **2019**, *37*, 336–345. [CrossRef] [PubMed]
138. Suga, H.; Sugaya, M.; Miyagaki, T.; Ohmatsu, H.; Kawaguchi, M.; Takahashi, N.; Fujita, H.; Asano, Y.; Tada, Y.; Kadono, T.; et al. Skin Barrier Dysfunction and Low Antimicrobial Peptide Expression in Cutaneous T-Cell Lymphoma. *Clin. Cancer Res.* **2014**, *20*, 4339–4348. [CrossRef] [PubMed]
139. Nakajima, R.; Miyagaki, T.; Kamijo, H.; Oka, T.; Shishido-Takahashi, N.; Suga, H.; Sugaya, M.; Sato, S. Decreased Progranulin Expression in Mycosis Fungoides: A Possible Association with the High Frequency of Skin Infections. *Eur. J. Dermatol.* **2018**, *28*, 790–794. [CrossRef]
140. Wolk, K.; Mitsui, H.; Witte, K.; Gellrich, S.; Gulati, N.; Humme, D.; Witte, E.; Gonsior, M.; Beyer, M.; Kadin, M.E.; et al. Deficient Cutaneous Antibacterial Competence in Cutaneous T-Cell Lymphomas: Role of Th2-Mediated Biased Th17 Function. *Clin. Cancer Res.* **2014**, *20*, 5507–5516. [CrossRef] [PubMed]

Publication 3: Multi-Omic Data Integration Suggests Putative Microbial Drivers of Aetiopathogenesis in Mycosis Fungoides

4.1 Supplementals of Publication 3

As the supplementary materials of Publication 3 contain non-text files, including Excel spreadsheets and multi-page PDF documents in non-standard formats, they are not included in the print version of this thesis. Readers are referred to the online distribution of the supplementary materials, which can be accessed at:

https://www.mdpi.com/article/10.3390/cancers16233947/s1

5 Overall Discussion

This thesis set out to investigate the contribution of the skin microbiome to the pathogenesis and clinical course of Mycosis fungoides, a malignancy marked by substantial clinical and molecular heterogeneity [1]. Although the microbiome has long been suspected to influence MF progression, microbial dysbiosis had not been firmly established, and its mechanistic relevance remained poorly defined [2]. Together with my co-authors, I performed a holistic in-depth analysis of the MF skin microbiome. Through an integrative multi-omic approach, complemented by molecular and culture-based microbiology techniques, the studies presented in this thesis provide novel evidence for microbial dysbiosis as a clinically relevant, disease-modifying factor in MF, with implications for prognosis, pathogenic signalling, and potential therapeutic targeting.

5.1 Microbiome Dysbiosis in MF Skin

One of the most striking outcomes of this thesis is the identification of a taxonomically altered skin microbiome in MF patients, marking the first conclusive demonstration of dysbiosis in MF skin. This finding not only corroborates the hypothesis that microbial dysbiosis associates with disease progression in MF [3], but also addresses a critical gap in the current literature [2]. Previous sequencing-based studies had failed to detect such differences, likely due to limitations such as small sample sizes [4,5], insufficient patient stratification [6], the absence of intrapatient nonlesional controls [4], restriction to early-stage patients [5], or methodological constraints such as low-resolution 16S sequencing [5,7,8].

In contrast, this work employed whole metagenome shotgun sequencing, enabling species- and strain-level resolution and allowing for a more nuanced characterization of microbial community structure. Given the high interindividual variability of skin microbiome profiles [9,10], this work used non-lesional samples as intrapatient control. Notably, according to a case-report even non-lesional, unaffected-appearing MF skin may harbour malignant T cells and early pathologic changes, even in the absence of visible lesions [11]. Therefore, inclusion of healthy controls would have provided a more

definitive baseline to distinguish MF-specific dysbiosis from background variation. Moreover, sampling was performed during clinically active disease (i.e., reddish patches or plaques), which may have enhanced signal detection. These factors, along with rigorous stratification and deeper sequencing resolution, may explain why this work was able to detect dysbiosis where previous studies did not.

Another possible reason for the disparate findings regarding cutaneous *S. aureus* shifts between this work and other studies may lie in the geographic origin of patient recruitment: while patients in this work were recruited in Central Europe, other investigations enrolled participants in Northern Europe and various regions of the United States (i.e., east coast, Florida, Great Lakes area). Phylogeographic analysis have shown that Methicillin-resistant *Staphylococcus aureus* (MRSA) strains display distinct geographic lineages, including North America and Europe, with highest diversity observed within the European clade [12]. Future studies across broader geographic and clinical cohorts will be needed to validate the generalizability of the finding of microbiome shifts observed in this thesis.

5.2 Microbiome-based Stratification and Potential Prognostic Utility

Building on the demonstration of microbial dysbiosis, a central advancement of this thesis is the stratification of MF patients into prognostically distinct subgroups based solely on skin microbial composition. The identification of two microbiome-defined subtypes — termed ΔSA-positive and ΔSA-neutral — demonstrates that microbial profiles hold clinical relevance beyond merely reflecting disease stage or lesional morphology. Notably, some patients with clinical and/or lesional advanced stage were classified as ΔSA-neutral and presented with a more favourable course. This suggests that the microbiome profile does not simply mirror disease severity, but rather acts as an independent prognostic biomarker, capable of stratifying patients by risk of disease progression irrespective of lesional or clinical stage. This represents the first microbiome-based stratification approach in MF and provides the first evidence that the skin microbiome can adversely influence clinical outcomes, beyond previously hypothesized clinical correlations and anecdotal case reports [13–17], as well as experimental *in vitro* [17–19] and murine studies [20,21].

Interestingly, the findings of this thesis align with observations from Hooper et al. [8], who investigated microbiome shifts associated with narrowband UVB therapy, which is a standard-of-care treatment particularly effective in early-stage MF [22]. Patients who responded to UVB therapy displayed distinct skin microbiome profiles compared to non-responders. At baseline, responders exhibited higher colonization with *S. capitis* and *S. warneri* [8], two coagulase-negative staphylococci (CoNS) known to suppress *S. aureus* virulence via quorum sensing interference [23]. Post-treatment, *S. lugdunensis* colonization increased in responders [8], another CoNS species that competitively inhibits *S. aureus* colonization [24], coinciding with a decline in *S. aureus* abundance [8].

Although we did not perform treatment stratification in the observational setting of this thesis, my findings closely parallel those of Hooper et al.: Higher CoNS levels were negatively correlated with *S. aureus* abundance, and improved clinical outcomes were observed in patients with reduced *S. aureus* colonization (see chapter 3; Publication 2). The consistent association between microbial profiles and clinical course suggests that the microbiome may also hold predictive value, supporting its potential use in guiding therapeutic decisions. Interventional studies are warranted to validate these observations.

5.3 Potential Drivers of Microbiome Shifts: A Role for AMPs and Opportunistic Colonization

A key question arising from this work is what drives the observed shifts in microbial community structure, particularly the depletion of commensals and the overgrowth of *S. aureus* in ΔSA-positive patients. One plausible contributing factor is the upregulation of AMPs in lesional MF skin, which was demonstrated by qPCR. Functional culture-based experiments further supported this mechanism: control isolates from healthy skin failed to thrive under elevated AMP conditions, whereas plaque-derived *S. aureus* isolate exhibited markedly higher resistance. These findings suggest that AMP-mediated disruption of the physiological skin flora may create a niche environment that favours colonization by more resistant, potentially pathogenic strains.

However, since AMP levels did not differ significantly between ΔSA-positive and ΔSA-neutral patients, the question remains why only some patients experience pathogenic *S.*

aureus overgrowth. A critical insight provided by this thesis is that the *S. aureus* strains isolated from plaque lesions in ΔSA-positive patients were genetically distinct from those on non-lesional or healthy skin and exhibited higher virulence potential. This points to a two-step model: first, AMP-induced eradication of commensals, and second, opportunistic replacement by a more virulent *S. aureus* strain in susceptible individuals (see chapter 3; Publication 2).

This model is further supported by external clinical evidence. A study by Ødum et al. [25] reported that severe bacterial infections in MF patients typically occur only after diagnosis has been established. Considering that MF diagnosis takes a median of three years from symptom onset [26], it is conceivable that the overgrowth by virulent *S. aureus* strains in the ΔSA-positive group may result from nosocomial transmission during the course of clinical management. In contrast, ΔSA-neutral patients may not experience this unfortunate event, providing skin commensals the required time to adopt to elevated AMP levels and re-colonize the lesions, resulting in microbial balance preventing pathogenic outgrowth.

5.4 Functional Microbiome–Host Interactions Driving Disease Signalling in MF

Beyond the discovery of taxonomic shifts and its relationship with clinical stratification, this thesis also investigated the functional properties of the skin microbiome and its influence on host transcriptome dynamics. One of the key findings was the identification of *Staphylococcus aureus* protein A (SpA) as a highly enriched virulence factor on MF lesions, corroborated by bioinformatic and culture-based virulence typing. Interestingly, genetic analysis indicated that the SpA variant present on MF lesions may even carry a gain-of-function mutation, potentially enhancing its pathogenic activity (see chapter 3; Publication 2). SpA is a multifunctional factor known to activate NF-κB signalling via several means, including activation of TNFR1 and stimulation of keratinocytes to release TNF-α, thereby inducing inflammation [27–31]. Notably, aberrant activation of the NF-κB axis has previously been associated with poor clinical outcomes in MF patients [32,33]. This convergence of molecular findings raised the hypothesis SpA may be a driving factor in disease signalling. Moreover, given the widely observed transcriptional heterogeneity

in MF [34], it seemed plausible that differential microbial colonization might account for at least part of this variability.

To test this, I applied integrative multi-omic analysis of both the microbiome and host transcriptome using MOFA (Multi-Omics Factor Analysis), an unsupervised statistical framework that identifies shared sources of variation across multi-omics layers [35]. These analyses revealed that the skin microbiome exerts a strong influence on host transcriptional programmes, indicating that differences in microbial colonization account for a substantial proportion of the observed transcriptional heterogeneity. Moreover, MOFA enabled mechanistic inference that *S. aureus* — and likely SpA — drives non-canonical NF-κB activation in lesional skin of ΔSA-positive patients. These findings support a model in which microbial constituents modulate oncogenic signalling pathways and local immune dynamics, contributing to the clinical and molecular heterogeneity of MF (see chapter 4; Publication 3).

Importantly, non-canonical NF-κB is typically activated via TNFR2 and it remains unknown whether SpA can directly engage this receptor, as it does with TNFR1, the receptor for canonical NF-κB signalling. Nonetheless, known crosstalk between the two forms of NF-κB signalling [36,37] may activate non-canonical NF-κB through TNFR1, and high structural similarity between TNFR1 and TNFR2 [38] could enable dual activation by SpA. On the other hand, however, it cannot be precluded the MOFA-derived association may reflect correlation rather than causality, as studies found that the TNFR2-non-canonical NF-κB axis is recurrently mutated in CTCL, leading to enhanced activity [39,40]. Mechanistic studies such as *in vitro* or in mice are needed to validate these findings.

In addition to the previously discussed findings, further clinical and molecular evidence supports a pathogenic role of staphylococcal protein A (SpA) in MF. Beyond its capacity to activate the NF-κB, SpA has been shown to stimulate ADAM17 (also known as TACE) via EGFR signalling, resulting in the proteolytic shedding of TNFR1 and TNFR2 from the cell surface into the circulation [28,41,42]. In line, RNAseq analysis in this thesis revealed upregulation of *ADAM17* expression alongside increased EGFR signalling in plaque-stage MF lesions, albeit statistical significance was narrowly missed for *ADAM17* (see chapter 4; Publication 3, Fig. 1D and Suppl. Material 1).

Notably. circulating levels of TNFR2 have been identified as prognostic markers in patients with peripheral T cell lymphoma (PTCL) [43], a group of non-Hodgkin T cell lymphoma involving peripheral organs such as the skin and gut. In case of skin involvement, PTCL shares some characteristics with MF and is classified as an entity of CTCL (primary cutaneous PTCL) [44–46]. Strikingly, PTCL patients with mucocutaneous involvement are at increased risk compared to those without barrier organ infiltration — a pattern that may be attributable to chronic microbial exposure, such as *S. aureus* [47–50].

The findings of this thesis — namely, the overgrowth of SpA-expressing *S. aureus* strains and the concomitant upregulation of *ADAM17* and EGFR signalling in MF patients with an aggravated disease course — suggest the existence of a shared, microbiome-dependent pathogenic mechanism in both MF and epidermal barrier-involving forms of PTCL, potentially mediated via the SpA/NF-κB axis. Further studies are warranted to elucidate whether disease severity is fuelled by shared microbiome-dependent pathomechanisms across different CTCL entities.

5.5 Aetiopathogenesis: A Proposed Two-Hit Model

In addition to the inferred SpA-mediated fuelling of MF pathogenesis, the integrative analysis of microbiome and host transcriptome uncovered traces of viral sequences and transcriptomic signatures potentially associated with early oncogenic events. Although of correlative and speculative nature, these findings together with the results from chapter 3; Publication 2 led me to propose a potential two-hit model of MF aetiopathogenesis. While this conceptual model has already been outlined in chapter 4; Publication 3, it is briefly recapitulated here, as it synthesizes and contextualizes key observations made throughout this thesis:

In this model (see Figure 5), the first hit represents an oncogenic priming during early thymopoiesis, potentially driven by aberrant *RUNX* expression, which may be triggered by viral infections such as Eppstein-Barr Virus (EBV). Malignant T cells subsequently infiltrate the skin, where the epithelial microenvironment responds by releasing antimicrobial peptides (AMPs), leading to microbial eradication and barrier disruption. The resulting dysbiosis facilitates a “second hit” — re-colonization by AMP-resistant, virulent *S. aureus* strains expressing SpA, which acts as an inflammatory amplifier by

activating non-canonical NF-κB and IL-1B signalling in already primed T cells, promoting the generation of mature effector memory T cells and fuelling disease progression. This model integrates both the early progenitor [51–55] and mature T cell [56,57] hypotheses of MF origin into a coherent, sequential framework.

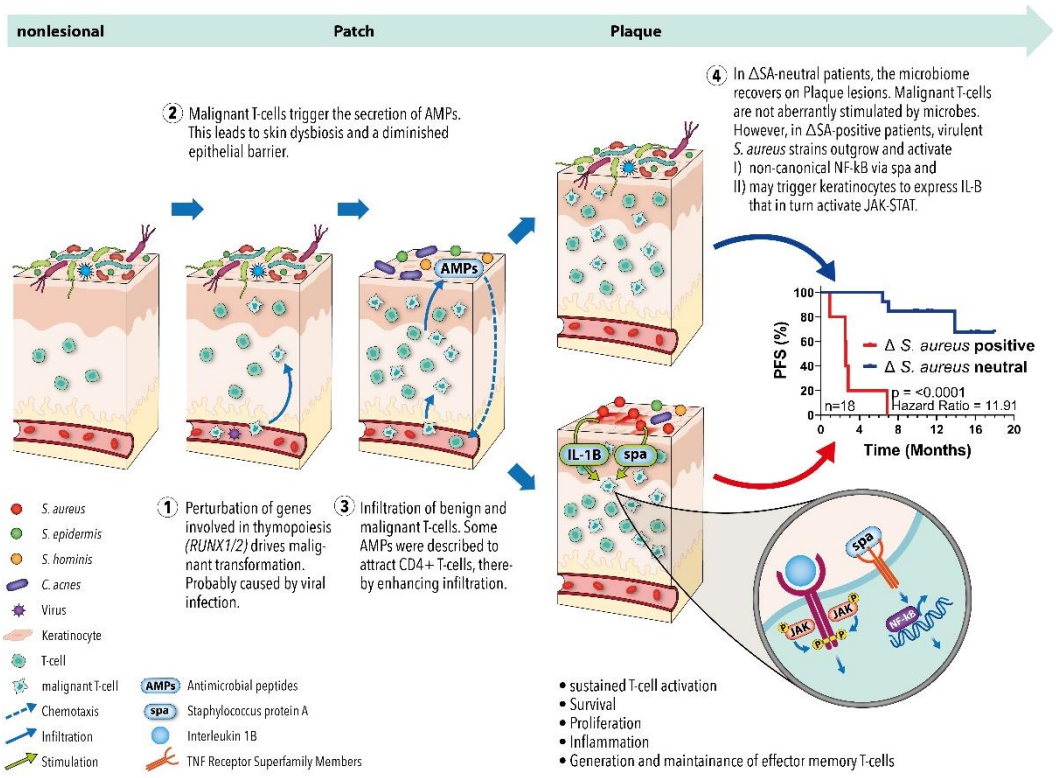

Figure 5: Proposed two-hit model of MF pathogenesis.
Oncogenic transformation during thymic T cell development is triggered by aberrant *RUNX1/2* expression, possibly induced by viral infections (e.g., EBV). Upon skin infiltration, malignant T cells provoke AMP secretion, leading to dysbiosis and barrier disruption. While some patients develop a balanced microbiome (ΔSA-neutral), others (ΔSA-positive) are overgrown by virulent *S. aureus* strains expressing SpA, which activate non-canonical NF-κB and IL-1B signalling, driving inflammation, T cell survival, and effector memory differentiation, which are hallmarks of MF progression [1].
PFS: Progression Free Survival

In support of the proposed two-hit model, the integrative MOFA analysis from chapter 4; Publication 3 assigned high weight to the chemokine receptor *CXCR4*, a molecule known to be overexpressed in MF [58,59], where it promotes skin tropism [60] and is implicated in malignant T-cell proliferation and survival [59]. Notably, *CXCR4* has been shown to be transcriptionally regulated by *RUNX2* in T-cell acute lymphoblastic leukaemia (T-ALL), where it mediates chemotaxis, adhesion, and tissue homing of malignant T cells. [61]. T-ALL is an aggressive haematologic malignancy arising from early T-cell precursors [62]. Given that *RUNX2* is a central regulator of early T cell lymphopoiesis [63,64], and this thesis identified *RUNX2* overexpression alongside antiviral signatures in MF lesions, it is

tempting to speculate that viral perturbations could dysregulate *RUNX2* and *CXCR4* during early T cell development, potentially seeding the initial oncogenic events that later manifest as MF [55]. While correlative, these findings fit within the proposed model of an early developmental "first hit" that predisposes cells to later disease progression.

5.5.1 *Possible Routes of Viral Perturbation*

If the hypothesis of a viral-initiated oncogenic first hit in MF holds true, it remains uncertain in which anatomical compartment this event may occur.

One plausible site for a potential viral-initiated oncogenic event in MF is the thymus, where early T cell development and lineage commitment occur [65,66]. Under physiological conditions, B cells transiently populate the thymus to present self-antigens and support central tolerance, including co-stimulatory signalling to developing thymocytes [67–69]. In angioimmunoblastic T cell lymphoma (AITL), this mechanism is thought to be hijacked by EBV-infected B cells, which chronically present viral antigens such as EBNA1 and provide persistent stimulation, potentially triggering neoplastic T cell transformation [70]. Similar mechanisms have been implicated more broadly in T cell lymphomas, where EBV-driven disruption of thymocyte development either indirectly via chronic activation or directly via infection has been described [71,72]. In support of a related process in MF, this thesis identified high counts of TCRs targeting EBV-associated antigens including EBNA1 in patient-derived blood, nonlesional, and lesional skin samples (chapter 4; Publication 3), suggesting that EBV-infected B cells may chronically overstimulate developing T cells, possibly within the thymic microenvironment.

Another plausible site is the blood compartment. After differentiating from hematopoietic stem cells (HSCs) in the bone marrow, T cell progenitors enter the circulation as so-called circulating T cell progenitors (CTPs) in order to home to the thymus, where they proceed their development into mature and functional T cells of multiple lineages [73–75]. Interestingly, EBV-DNA detected in blood plasma was found to be a well correlating biomarker with EBV-initiated diseases, including peripheral T cell lymphoma [76]. Thus, circulating T cell progenitors may be exposed to EBV in the blood stream, possibly creating a vulnerable window for viral entry and immune manipulation.

Altogether, literature evidence and findings of this thesis support a model in which EBV and/or other viruses may contribute to early oncogenic priming during thymopoiesis, either through direct infection of progenitor cells or via infected B cells in the thymic niche, ultimately predisposing cells to transformation in MF.

5.5.2 *Limitations and Alternative Explanations for a Viral Role in MF*

While this thesis presents multi-omic evidence suggestive of viral involvement in the aetiopathogenesis of MF (see chapters 4; Publication 3, and 5.5.1), several limitations and alternative explanations must be considered. Most importantly, all findings are correlative in nature, and no causal link between viral infection and the initiation or progression of MF has been established.

First, increased antiviral interferon signalling in MF lesions may not reflect active viral infection but could instead represent an antiviral-like immune response directed against malignant T cells. Interferons play a central role in cancer immunosurveillance by enhancing antigen presentation, activating dendritic cells, and promoting cytotoxic T cell responses [77].

Second, EBV is a ubiquitous virus, with over 90% global seroprevalence [78,79]. Thus, detection of EBV antigens or EBV-reactive TCRs in MF skin or circulation does not, in itself, imply pathogenic relevance. These signals could derive from memory T cells, bystander B-cell infection, or general immune activation [80–82].

Third, *RUNX2* overexpression may be an intrinsic feature of the malignant T-cell programme in MF [83], unrelated to external viral triggers. As a key regulator of early T cell development and oncogenic reprogramming [63,84–86], *RUNX2* could become aberrantly activated through virus-independent mechanisms.

Finally, previous studies have yielded inconsistent or negative findings regarding viral nucleic acid or antigen detection in MF skin lesions, weakening the argument for a unifying viral aetiology [3,87]. If viral oncogenesis were a central feature of MF, one would expect broader reproducibility across independent cohorts and methodological platforms. However, it was speculated that existing virus profiling studies may have missed “hit-and-run” agents, i.e., transient infections that trigger neoplastic

transformation but later disappear [88]. This hypothesis would support the presented two-hit-model in this thesis (Figure 5).

Together, although a viral component remains a plausible hypothesis particularly within a multi-step model of MF pathogenesis and given the convergence of several individual findings, current evidence remains speculative. Further research will be required to determine whether viruses contribute directly to malignant transformation in MF, simply modulate the immune landscape of an already transformed lesion, or instead host anti-viral signalling rather represents an anti-tumoral response.

5.6 Technical Considerations and Limitations

As outlined in sections *1.5 Workflow of Microbiome Research* and *1.5.1 Challenges of Human Skin Microbiome Research*, skin microbiome profiling comes with several considerations that stem from inherent complexities and technical limitations. Therefore, a key step of this thesis was to ensure integrity through diligent and precise experimental design and execution, including choice of proper controls, quality checks of workflow steps, and precluding or minimizing contamination.

As the field of microbiome research was entirely new to the Department of Dermatology and the working group of Prof. Mailänder, I independently established a complete end-to-end workflow for skin microbiome profiling — encompassing sample collection, DNA extraction, library preparation, and bioinformatic processing — and initiated external collaborations where needed. As a starting point, I screened the literature for common and possible pitfalls, best-practice workflows, and optimization strategies for skin microbiome analysis.

For the sampling workflow, I adapted and modified a protocol [89] which performs a procedure of swabbing, followed by scraping with a scalpel, and swabbing again to maximize microbial yield. DNA extraction followed the same source protocol with modifications to accommodate available resources and to enhance DNA yield. This included the mechanical disruption step using a Qiagen TissueLyser II at the Institute for Translational Immunology at the University Medical Centre Mainz. Finally, library preparation protocols were optimized to accommodate ultra-low DNA inputs, and extensive quality control steps were implemented prior to sequencing.

The following subsections outline key technical challenges encountered during this journey, the rationale behind specific methodological choices (e.g., WMS vs. 16S), and potential directions for methodological refinement in future research.

5.6.1 *Analysis and Interpretation of Control Samples*

As recommended by Eisenhofer et al. [90], particularly for low-biomass WMS studies, I implemented both negative and positive controls at multiple critical stages of the microbiome wet-lab workflow to monitor contamination and ensure methodological integrity. During sampling, a negative swab-sampling control was included. Each batch of DNA extraction was accompanied by a negative extraction control as well as a positive control consisting of mock bacterial cells. Similarly, each library preparation batch included a positive control using DNA extracted from the same mock community.

For negative controls, this thesis quantified DNA concentration using the highly precise fluorescence-based Qubit assay by ThermoFisher Scientific. All negative controls yielded readings of 0 ng/µl and were thus interpreted as negative. Nonetheless, despite Qubit's ultra-low detection threshold of 0.0005 ng/µl (as specified by the manufacturer), undetected low-level contamination cannot be entirely ruled out. To address this possibility, future studies could leverage declining sequencing costs to also process and sequence negative controls. If microbial signals are detected, researchers may take a conservative approach by removing overlapping taxa from case samples, or apply nuanced contaminant filtering strategies [90]. For the latter, the R package *decontam* provides a statistical framework to identify contaminants by testing whether taxa appear more frequently in negative controls than in true samples using Fisher's exact test [91].

For positive controls, this thesis performed sequencing and taxonomic profiling alongside the case samples. The resulting profiles aligned well with the expected species composition of the mock community (see Supplementary 6 of chapter 3; publication 2), thereby validating the performance and reproducibility of the sequencing pipeline. Nonetheless, controls starting at the microbial cell lysis step deviated more from the ground truth than those starting at the DNA level. Moreover, certain taxa consistently diverged from the expected abundances across batches. These discrepancies may reflect day-to-day variability in sample processing or subtle fluctuations in laboratory conditions

and equipment performance.

It is also important to acknowledge that the precision of WMS taxonomic assignment can vary by microbial feature [92]. MetaPhlAn, the tool used in this thesis, infers taxonomic composition based on a set of clade-specific marker genes [93,94]. Its accuracy thus depends on the quality and representativeness of those markers for the taxa present. As such, the choice of metagenomic profilers should be guided by their suitability for the biological and technical context of the study.

Currently, no consensus exists on how to best handle discrepancies between observed and expected results in positive controls. Future improvements may include the use of mock communities that better reflect the microbial complexity and biomass of human skin samples, as opposed to the commercially available ZymoBIOMICS standard used here.

5.6.2 *Advantages of WMS over 16S in the Context of MF Skin Microbiome Profiling*

This thesis employed WMS over 16S due to several reasons: As outlined in section 1.5 Workflow of Microbiome Research, WMS provides superior taxonomic resolution and enables functional profiling of microbial communities, including the identification of virulence factors and antibiotic resistance genes [95]. These advantages are particularly relevant in the context of MF, where fine-scale taxonomic discrimination is critical. Notably, 16S sequencing has been shown to inadequately distinguish *Staphylococcus* and *Propionibacterium* species in skin microbiome studies [96], two of the key genera associated with MF lesions in this thesis. Furthermore, functional predictions using PICRUSt, a commonly applied inference tool for 16S data [97], have produced incomplete results in skin microbiome applications, omitting key microbial functions [96]. Odds are that functional interference with 16S would have missed out on the identification of the *staphylococcus* gene *spa*, which potentially serves as a highly exacerbating factor in MF.

5.6.3 *Impact of Sequencing Depth on Diversity Estimates in Low Microbial Biomass Samples*

While WMS offers significant advantages over 16S sequencing, it also comes with notable trade-offs. Unlike 16S, which selectively amplifies microbial DNA (albeit with amplification-induced bias [98]), resulting in high sequencing depths, WMS captures all

DNA in a sample, including the host genome [99]. In skin microbiome research, this poses a particular challenge, as skin samples are characterized by low microbial biomass and a disproportionately high fraction of host DNA, exceeding 90–95%. Consequently, even with high total read counts, microbial sequencing depth may be limited, potentially underestimating microbial diversity [50,100,101].

Nonetheless, several studies have demonstrated that WMS, even at shallow sequencing depths, provides results comparable to those of ultra-deep WMS [102–104]. However, also shallow WMS depends on achieving sufficient microbial DNA coverage, which is inherently challenging in low- or ultra-low-biomass samples such as those from the skin or water [105]. Two studies provide practical guidance on thresholds: one recommends ≥50 million raw reads per sample when host DNA comprises ~90% of total content [101], while another suggests that ≥500,000 final microbial reads are adequate to capture overall diversity, though low-abundance taxa may still be underrepresented [102].

In this thesis, the skin microbiome samples largely met these thresholds. On average, 47.2 million raw reads were generated per sample (see chapter 3; publication 2), closely approximating the 50 million raw read benchmark. Regarding the 500,000 final microbial read benchmark, results varied by sample type. Roughly one half of nonlesional samples exceeded this threshold, while only 4 patch and 5 plaque samples met it. As shown in Figure 6, nonlesional samples yielded significantly more microbial reads than lesional samples (Wilcoxon test, $p < 0.05$).

As discussed in chapter 3; publication 2, this pattern mirrors findings from a psoriasis skin microbiome study, where lesional samples similarly contained more human DNA, likely due to the scaly nature of affected skin. This increases the likelihood of sampling human cells such as keratinocytes over microbes during swab collection [100]. However, despite lower final microbial read counts in lesional samples, rarefaction curves indicate that sequencing depth was largely sufficient to capture the true microbial diversity in these samples. In contrast, microbial diversity in nonlesional samples was likely underestimated due to insufficient sequencing depth (see Supplementary 7 of chapter 3; publication 2). Since microbial dysbiosis was assessed by comparing nonlesional skin to lesional samples using PERMANOVA and linear modelling, the underestimation of

diversity in nonlesional skin may have led to a conservative estimate of the dysbiosis on lesional skin.

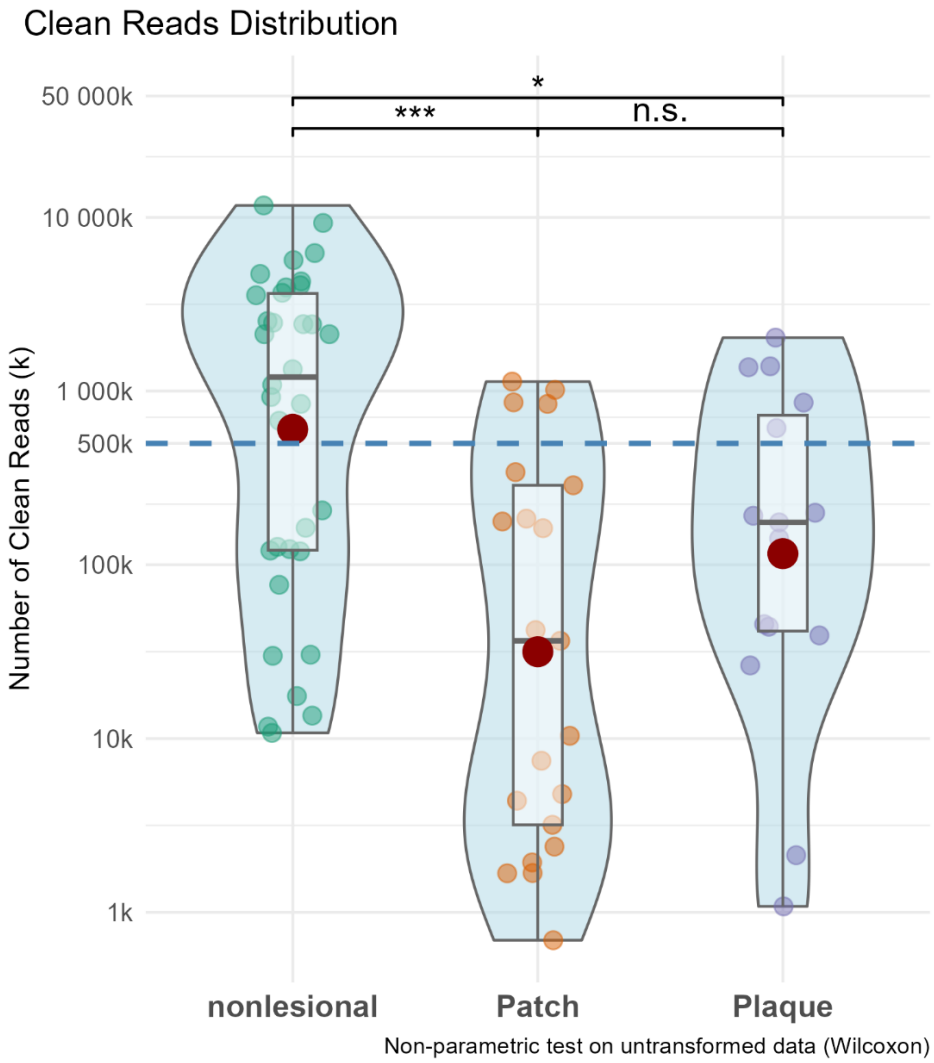

Figure 6: Number of final and clean microbial sequencing per stage.
Violin and Box plots showing the distribution of microbial sequencing reads per stage. Box plots show 1st and 3rd quantiles and median. Dark Red points show mean. Blue dotted line represents the threshold defined by Hillmann et al. [102] at which shallow WMS largely recapitulates ultra-deep WMS taxonomic profiling results. For better visualization, y-scale is log10 transformed. Wilcoxon-test was carried out on untransformed data. *** $p \leq 0.001$, * $p \leq 0.05$, n.s.not significant. Plot and statistical test were generated using R 4.3.1 with packages ggplot2, scales, ggsignif, and rstatix.

5.6.4 *Room for Improvement: Statistical Modelling of Differential Abundance Analysis*

To identify microorganisms that are differentially abundant in Patch and Plaque lesions compared to nonlesional skin, this thesis employed MaAslin2, a generalized linear modelling framework [106,107]. In accordance with the authors' recommendations and a landmark paper on microbial rarefaction [108], samples were analysed at their

individual full sequencing depth. To adjust for variability in sequencing depth across samples, the final microbial read count per sample was included as a covariate in the model. However, as discussed above, required sequencing depth to sufficiently capture microbial diversity may differ systematically between lesional and nonlesional skin, potentially leading to overcorrection when using a single global adjustment term. A more nuanced approach could have incorporated a nested or interaction-based adjustment. Specifically, including an interaction term between lesion status and sequencing depth would enable differential correction depending on whether the sample originated from lesional or nonlesional skin. Such a model could be specified as follows:

```
~ stage + sequencing_depth + lesion:sequencing_depth + (1 |PatientID)
```

Where `stage` refers to the type of skin lesion (nonlesional, patch, plaque), `sequencing_depth` denotes the final microbial read count, `lesion` is a binary indicator for lesional vs. nonlesional samples, and `(1 | PatientID)` specifies a random intercept to account for repeated measures within patients.

5.6.5 *Room for Improvement: Wet-Lab Handling*

On the wet-lab side, future skin microbiome studies in MF using WMS may benefit from optimized sampling strategies. This thesis employed a three-step swab–scrape–swab procedure, where a surgical scalpel is used to gently scrape the skin surface between two swabbing steps to increase biomass yield. However, the force applied during scraping was not standardized prior to study initiation. Additionally, skin from different individuals—and even different sites or lesion types—responded variably depending on factors such as lesion status, skin integrity, and patient age. As consequence, it was already visible that some skin samples yielded more human cells, others less.

To minimize the collection of excessive host DNA, future studies could aim to standardize scraping force, adjust pressure based on skin condition, or explore alternative approaches such as tape stripping. In this technique, an adhesive tape is pressed onto the skin and then removed, capturing the outermost layer(s) of the stratum corneum along with associated microbial cells [109]. Taxonomic profiles obtained via tape stripping have shown high concordance with those obtained from swab-based sampling [110–112]. Notably, one study reported that tape stripping yielded 13.5% microbial DNA

[112], which exceeds the typical 5%-10% microbial DNA content of swabs [100]. It is worth noting, however, that tape stripping tends to remove more of the superficial skin layers than swabbing, allowing it to access slightly deeper layers of the stratum corneum. As different layers of the skin are known to harbour distinct microbial communities [113–115], the choice of sampling method may influence the observed microbiome composition and should therefore be aligned with the specific aims of the study.

Another approach is to optimize microbial DNA extraction and host DNA depletion. Serghiou et al. [116] developed an optimized protocol for extracting highly intact microbial DNA, specifically for the use of swab-sampling from skin. Nonetheless, they used an automated nucleic acid purification platform which is likely not available in most molecular biology laboratories in academia. Further, in a real-world assessment 37.5% of skin samples did not yield detectable amounts of DNA [116], questioning the applicability of this protocol.

Other approaches aim to increase the proportion of microbial DNA through either host DNA depletion or microbial DNA enrichment strategies [117]. Protocols targeting deplete host DNA employ enzymatic and chemical lysis steps that selectively degrade human cells and extracellular DNA from both host and dead microbial sources [117–119]. Several commercially available kits apply such combinations of chemical and enzymatic treatments [120,121]. In addition, Duarte and Porcellato [122] described a protocol that combines host DNA depletion with microbial DNA amplification. While this approach can compensate for low DNA concentrations in challenging samples, it is also prone to amplification bias [122].

Benchmarking studies yielded conflicting results which protocol or commercially available kit performs best. While Qiagen's QIAamp DNA Microbiome Kit and Zymo Biomic's Zymo HostZERO Microbial DNA Kit consistently ranked among the top performers [120,121,123], only Heravi at al. reported that these kits did not introduce community distortion [121], whereas others reported skewing towards gram-positive bacteria [120,123]. This is particularly relevant in the context of MF skin microbiome research, as *S. aureus* is Gram-positive and could be disproportionately enriched.

Nonetheless, all studies and consistently demonstrated that host DNA depletion substantially increases microbial the DNA proportion, resulting in higher detection

sensitivity, improved taxonomic and functional resolution, and significantly reduced sequencing costs [120–123]. Researchers in the field of MF skin microbiome should carefully follow the development of depletion strategies and probably try out one or the other protocol prior to future studies.

5.6.6 *Challenges of Skin Virome Profiling*

While this thesis primarily focused on bacterial and fungal components of the skin microbiome, it also aimed to characterize viral constituents following the identification of antiviral immune signatures in host transcriptomic data. To this end, shotgun whole-genome sequencing reads and mRNA-seq data were utilized to profile superficial and deeper skin layers, respectively (chapter 4; publication 3). However, virome profiling via shotgun sequencing presents several challenges beyond those encountered in bacterial or fungal profiling.

First, the issue of low viral abundance relative to high host background is particularly pronounced. Viruses contain orders of magnitude less DNA than bacterial cells and are vastly outnumbered by host cells, resulting in reduced sensitivity of viral detection [124–126]. Moreover, the absence of a universal marker gene such as the bacterial 16S rRNA gene precludes the use of targeted amplicon sequencing for viruses [125,127]. As a result, enrichment of the viral fraction is commonly applied, and a variety of methods have been developed for this purpose [128,129]. While such approaches can substantially reduce host-derived background, they also introduce method-specific biases and may lead to the loss of certain viral taxa [124]. Since this thesis did not employ virus-specific enrichment protocols, it is likely that the viral diversity in the analyzed samples has been underestimated.

Second, current databases are biased towards double-stranded DNA viruses, as these are easiest to sequence and annotate with available technologies [124]. As a consequence, more than half of reads in typical virome studies fall into the so-called viral “dark matter”; sequences with no known homologs or taxonomic assignment [127]. For instance, while version 2 of MetaPhlAn, a state of the art metagenomic taxonomic classification tool also used in this thesis, can distinguish approximately 13,000 bacterial taxa, it includes only around 3,500 viral species [94]. Likewise, VIRTUS, the mRNA-based

virome profiling pipeline employed in this study to analyze RNA-seq data, is limited to 765 viruses [130].

Next, DNA-based metagenomic approaches are inherently unable to distinguish between transcriptionally active viruses in the lytic phase and dormant viruses in the lysogenic state [131,132]. Thus, DNA-based detection should be interpreted with caution, since the mere presence of viral DNA does not necessarily imply biological activity or relevance to the host condition under investigation.

Finally, there is currently a lack of standardized computational pipelines for viral profiling [133]. The field of viral taxonomic classification remains highly fragmented, and no single approach has yet emerged as a gold standard for either shotgun metagenomics or RNA-seq–based virome studies [133,134]. While recent updates to MetaPhlAn have substantially expanded its viral database, this extension is largely focused on the human gut virome and may offer limited coverage for other body sites, such as the skin [135,136].

Despite these hurdles, preliminary viral signals in MF observed in this thesis invite deeper investigation, particularly with optimized wet-lab protocols for viral enrichment and depletion of host background. Until a consensus on bioinformatic processing is established, a pragmatic strategy may involve running multiple classification pipelines in parallel and comparing the overlap of detected viral taxa to increase confidence in the results.

5.7 Conclusions and Outlook

This thesis presents a comprehensive, multi-layered investigation into the role of the skin microbiome in the pathogenesis and clinical progression of Mycosis fungoides, the most common entity of cutaneous T-cell lymphoma [1]. Through end-to-end generation, analysis, and integration of multiple molecular layers from clinical specimens, this work provides additional evidence that the skin microbiome shapes the clinical outcome of patients, beyond previous clinical observations [87,137], therapeutic responses to antibiotics [19], associations between TCR oligoclonality and *S. aureus* [138,139], or findings from mechanistic *in vitro* [140–142] and murine models [20].

Specifically, this thesis was the first to identify microbial shifts in MF lesions among patients with an inferior clinical course. Using high-resolution metagenomic sequencing and well-matched controls, it overcomes limitations of earlier studies [4–8]. Notably, *S. aureus* strains carrying SpA – an activator of NF-κB – were enriched in the microbiome of aggressive cases, positioning SpA as a previously unrecognized immunomodulatory virulence factor. These findings suggest that the skin microbiome actively modulates disease signalling, with implications for diagnostic stratification and therapeutic intervention.

Several questions remain, including how the ΔSA-positive group acquires virulent *S. aureus* strains and why others are left unaffected. Nosocomial exposure during a vulnerable window of skin flora eradication is speculated in this work, but this hypothesis requires further investigation. At the same time, additional mechanistic insight is needed to determine whether *S. aureus* and SpA actively drive non-canonical NF-κB signalling in MF. It also remains to be clarified whether SpA acts via TNFR2 or through TNFR1. Given that TNFR2 is recurrently mutated in MF [39], it is essential to establish whether the MOFA-identified associations reflect true mechanistic convergence or mere statistical co-variation without causal underpinning.

Although this thesis analysed several molecular levels, but, however, did not use one potentially informative dimension: the microbial transcriptome. Although the necessary RNAseq data had been generated, the analysis focused on host gene expression. Since the biopsies were taken from the same sites as the metagenomic swabs,

metatranscriptomic analysis would have been feasible and could have provided complementary insight into microbial activity. Unlike metagenomics, which reveals functional potential, metatranscriptomics captures actual gene expression. Several promising tools have been developed [151–155], including one that supports joint analysis of host and microbiome transcriptome and their interaction [154]. Exploring this layer could be the focus of a future small-scale retrospective study.

Nevertheless, the findings of this thesis highlight the potential of microbiome-modulating interventions. Given the pathogenic role of *S. aureus* in MF, targeted antimicrobial interventions could represent novel adjunctive therapies. While *S. aureus* eradication has shown benefit in other inflammatory skin diseases such as AD [143], MF-associated strains may be more virulent, potentially necessitating tailored approaches. Future studies may explore *S. aureus*-targeted therapeutic options including phage-derived lysins [144,145], bacteriotherapy [23,146,147], and probiotic approaches [148,149], to restore microbial balance in MF patients [150].

Looking beyond MF, it would be interesting to investigate whether microbiome-dependent pathomechanisms, particularly through SpA, are generalizable to other T-cell lymphoma entities that arise at mucocutaneous barriers. Notably, PTCL patients with mucocutaneous involvement are at increased risk [47–50], possibly due to close contact between neoplastic T cells and microbial communities that may drive similar immune-modulatory interactions.

Methodologically, while this thesis applied state-of-the-art techniques and yielded impactful findings, the data remain observational. As such, the associations identified cannot establish causality [156]. This limitation is a common challenge in microbiome research [99,157,158], where studies often confront the “chicken-or-egg” dilemma: it remains unresolved whether microbial shifts are a cause or consequence of disease.

In summary, this thesis makes a significant contribution to the understanding of MF pathogenesis by establishing a clinically relevant link between microbial dysbiosis and host signalling. It provides compelling evidence that the skin microbiome is not merely a bystander but an active modulator of disease biology, with implications for diagnosis, prognosis, and therapeutic innovation. These insights pave the way for microbiome-informed precision medicine strategies in Mycosis fungoides.

5.8 References of Discussion

1. Dummer, R.; Vermeer, M.H.; Scarisbrick, J.J.; Kim, Y.H.; Stonesifer, C.; Tensen, C.P.; Geskin, L.J.; Quaglino, P.; Ramelyte, E. Cutaneous T Cell Lymphoma. *Nat. Rev. Dis. Prim.* **2021**, *7*, 61, doi:10.1038/s41572-021-00296-9.

2. Jost, M.; Wehkamp, U. The Skin Microbiome and Influencing Elements in Cutaneous T-Cell Lymphomas. *Cancers (Basel).* **2022**, *14*, 1324, doi:10.3390/cancers14051324.

3. Mirvish, J.J.; Pomerantz, R.G.; Falo, L.D.; Geskin, L.J. Role of Infectious Agents in Cutaneous T-Cell Lymphoma: Facts and Controversies. *Clin. Dermatol.* **2013**, *31*, 423–431, doi:10.1016/j.clindermatol.2013.01.009.

4. Harkins, C.P.; MacGibeny, M.A.; Thompson, K.; Bubic, B.; Huang, X.; Brown, I.; Park, J.; Jo, J.-H.; Segre, J.A.; Kong, H.H.; et al. Cutaneous T-Cell Lymphoma Skin Microbiome Is Characterized by Shifts in Certain Commensal Bacteria but Not Viruses When Compared with Healthy Controls. *J. Invest. Dermatol.* **2021**, *141*, 1604–1608, doi:10.1016/j.jid.2020.10.021.

5. Dehner, C.A.; Ruff, W.E.; Greiling, T.; Pereira, M.S.; Redanz, S.; McNiff, J.; Girardi, M.; Kriegel, M.A. Malignant T Cell Activation by a Bacillus Species Isolated from Cutaneous T-Cell Lymphoma Lesions. *JID Innov.* **2022**, *2*, 100084, doi:10.1016/j.xjidi.2021.100084.

6. Salava, A.; Deptula, P.; Lyyski, A.; Laine, P.; Paulin, L.; Väkevä, L.; Ranki, A.; Auvinen, P.; Lauerma, A. Skin Microbiome in Cutaneous T-Cell Lymphoma by 16S and Whole-Genome Shotgun Sequencing. *J. Invest. Dermatol.* **2020**, *140*, 2304-2308.e7, doi:10.1016/j.jid.2020.03.951.

7. Zhang, Y.; Seminario-Vidal, L.; Cohen, L.; Hussaini, M.; Yao, J.; Rutenberg, D.; Kim, Y.; Giualiano, A.; Robinson, L.A.; Sokol, L. "Alterations in the Skin Microbiota Are Associated With Symptom Severity in Mycosis Fungoides." *Front. Cell. Infect. Microbiol.* **2022**, *12*, 1–10, doi:10.3389/fcimb.2022.850509.

8. Hooper, M.J.; Enriquez, G.L.; Veon, F.L.; LeWitt, T.M.; Sweeney, D.; Green, S.J.; Seed, P.C.; Choi, J.; Guitart, J.; Burns, M.B.; et al. Narrowband Ultraviolet B Response in Cutaneous T-Cell Lymphoma Is Characterized by Increased Bacterial Diversity and

Reduced Staphylococcus Aureus and Staphylococcus Lugdunensis. *Front. Immunol.* **2022**, *13*, 1–14, doi:10.3389/fimmu.2022.1022093.

9. Grice, E.A.; Kong, H.H.; Conlan, S.; Deming, C.B.; Davis, J.; Young, A.C.; Bouffard, G.G.; Blakesley, R.W.; Murray, P.R.; Green, E.D.; et al. Topographical and Temporal Diversity of the Human Skin Microbiome. *Science (80-.).* **2009**, *324*, 1190–1192, doi:10.1126/science.1171700.

10. Oh, J.; Byrd, A.L.; Deming, C.; Conlan, S.; Kong, H.H.; Segre, J.A. Biogeography and Individuality Shape Function in the Human Skin Metagenome. *Nature* **2014**, *514*, 59–64, doi:10.1038/nature13786.

11. Pujol, R.M.; Gallardo, F.; Llistosella, E.; Blanco, A.; Bernadc, L.; Bordes, R.; Nomdedeu, J.F.; Servitje, O. Invisible Mycosis Fungoides: A Diagnostic Challenge. *J. Am. Acad. Dermatol.* **2002**, *47*, S168–S171, doi:10.1067/mjd.2002.107231.

12. Nübel, U.; Roumagnac, P.; Feldkamp, M.; Song, J.-H.; Ko, K.S.; Huang, Y.-C.; Coombs, G.; Ip, M.; Westh, H.; Skov, R.; et al. Frequent Emergence and Limited Geographic Dispersal of Methicillin-Resistant Staphylococcus Aureus. *Proc. Natl. Acad. Sci.* **2008**, *105*, 14130–14135, doi:10.1073/pnas.0804178105.

13. SHELLEY, W.B. Demethylchlortetracycline and Griseofulvin as Examples of Specific Treatment for Mycosis Fungoides. *Br. J. Dermatol.* **1981**, *104*, 477–480, doi:10.1111/j.1365-2133.1981.tb15321.x.

14. Lindahl, L.M.; Willerslev-Olsen, A.; Gjerdrum, L.M.R.; Nielsen, P.R.; Blümel, E.; Rittig, A.H.; Celis, P.; Herpers, B.; Becker, J.C.; Stausbøl-Grøn, B.; et al. Antibiotics Inhibit Tumor and Disease Activity in Cutaneous T-Cell Lymphoma. *Blood* **2019**, *134*, 1072–1083, doi:10.1182/blood.2018888107.

15. Jackow, C.M.; Cather, J.C.; Hearne, V.; Asano, A.T.; Musser, J.M.; Duvic, M. Association of Erythrodermic Cutaneous T-Cell Lymphoma, Superantigen-Positive Staphylococcus Aureus, and Oligoclonal T-Cell Receptor Vβ Gene Expansion. *Blood* **1997**, *89*, 32–40, doi:10.1182/blood.V89.1.32.

16. Talpur, R.; Bassett, R.; Duvic, M. Prevalence and Treatment of Staphylococcus Aureus Colonization in Patients with Mycosis Fungoides and Sézary Syndrome. *Br. J. Dermatol.* **2008**, *159*, 105–112, doi:10.1111/j.1365-2133.2008.08612.x.

17. Łyko, M.; Jankowska-Konsur, A. The Skin Microbiome in Cutaneous T-Cell Lymphomas (CTCL)—A Narrative Review. *Pathogens* **2022**, *11*, 935, doi:10.3390/pathogens11080935.

18. Willerslev-Olsen, A.; Krejsgaard, T.; Lindahl, L.; Bonefeld, C.; Wasik, M.; Koralov, S.; Geisler, C.; Kilian, M.; Iversen, L.; Woetmann, A.; et al. Bacterial Toxins Fuel Disease Progression in Cutaneous T-Cell Lymphoma. *Toxins (Basel).* **2013**, *5*, 1402–1421, doi:10.3390/toxins5081402.

19. Fujii, K. Pathogenesis of Cutaneous T Cell Lymphoma: Involvement of Staphylococcus Aureus. *J. Dermatol.* **2022**, *49*, 202–209, doi:10.1111/1346-8138.16288.

20. Fanok, M.H.; Sun, A.; Fogli, L.K.; Narendran, V.; Eckstein, M.; Kannan, K.; Dolgalev, I.; Lazaris, C.; Heguy, A.; Laird, M.E.; et al. Role of Dysregulated Cytokine Signaling and Bacterial Triggers in the Pathogenesis of Cutaneous T-Cell Lymphoma. *J. Invest. Dermatol.* **2018**, *138*, 1116–1125, doi:10.1016/j.jid.2017.10.028.

21. Dey, S.; Vieyra-Garcia, P.A.; Joshi, A.A.; Trajanoski, S.; Wolf, P. Modulation of the Skin Microbiome in Cutaneous T-Cell Lymphoma Delays Tumour Growth and Increases Survival in the Murine EL4 Model. *Front. Immunol.* **2024**, *15*, 1–15, doi:10.3389/fimmu.2024.1255859.

22. Trautinger, F.; Knobler, R.; Willemze, R.; Peris, K.; Stadler, R.; Laroche, L.; D'Incan, M.; Ranki, A.; Pimpinelli, N.; Ortiz-Romero, P.; et al. EORTC Consensus Recommendations for the Treatment of Mycosis Fungoides/Sézary Syndrome. *Eur. J. Cancer* **2006**, *42*, 1014–1030, doi:10.1016/j.ejca.2006.01.025.

23. Williams, M.R.; Costa, S.K.; Zaramela, L.S.; Khalil, S.; Todd, D.A.; Winter, H.L.; Sanford, J.A.; O'Neill, A.M.; Liggins, M.C.; Nakatsuji, T.; et al. Quorum Sensing between Bacterial Species on the Skin Protects against Epidermal Injury in Atopic Dermatitis. *Sci. Transl. Med.* **2019**, *11*, eaat8329, doi:10.1126/scitranslmed.aat8329.

24. Zipperer, A.; Konnerth, M.C.; Laux, C.; Berscheid, A.; Janek, D.; Weidenmaier, C.; Burian, M.; Schilling, N.A.; Slavetinsky, C.; Marschal, M.; et al. Human Commensals Producing a Novel Antibiotic Impair Pathogen Colonization. *Nature* **2016**, *535*, 511–516, doi:10.1038/nature18634.

25. Odum, N.; Lindahl, L.M.; Wod, M.; Krejsgaard, T.; Skytthe, A.; Woetmann, A.; Iversen, L.; Christensen, K. Investigating Heredity in Cutaneous T-Cell Lymphoma in a Unique Cohort of Danish Twins. *Blood Cancer J.* **2017**, *7*, e517–e517, doi:10.1038/bcj.2016.128.

26. Scarisbrick, J.J.; Quaglino, P.; Prince, H.M.; Papadavid, E.; Hodak, E.; Bagot, M.; Servitje, O.; Berti, E.; Ortiz-Romero, P.; Stadler, R.; et al. The PROCLIPI International Registry of Early-stage Mycosis Fungoides Identifies Substantial Diagnostic Delay in Most Patients. *Br. J. Dermatol.* **2019**, *181*, 350–357, doi:10.1111/bjd.17258.

27. Gómez, M.I.; Lee, A.; Reddy, B.; Muir, A.; Soong, G.; Pitt, A.; Cheung, A.; Prince, A. Staphylococcus Aureus Protein A Induces Airway Epithelial Inflammatory Responses by Activating TNFR1. *Nat. Med.* **2004**, *10*, 842–848, doi:10.1038/nm1079.

28. Gómez, M.I.; O'Seaghdha, M.; Magargee, M.; Foster, T.J.; Prince, A.S. Staphylococcus Aureus Protein A Activates TNFR1 Signaling through Conserved IgG Binding Domains. *J. Biol. Chem.* **2006**, *281*, 20190–20196, doi:10.1074/jbc.M601956200.

29. Ledo, C.; Gonzalez, C.D.; Garofalo, A.; Sabbione, F.; Keitelman, I.A.; Giai, C.; Stella, I.; Trevani, A.S.; Gómez, M.I. Protein A Modulates Neutrophil and Keratinocyte Signaling and Survival in Response to Staphylococcus Aureus. *Front. Immunol.* **2021**, *11*, 1–15, doi:10.3389/fimmu.2020.524180.

30. Claßen, A.; Kalali, B.N.; Schnopp, C.; Andres, C.; Aguilar-Pimentel, J.A.; Ring, J.; Ollert, M.; Mempel, M. TNF Receptor I on Human Keratinocytes Is a Binding Partner for Staphylococcal Protein A Resulting in the Activation of NF Kappa B, AP-1, and Downstream Gene Transcription. *Exp. Dermatol.* **2011**, *20*, 48–52, doi:10.1111/j.1600-0625.2010.01174.x.

31. Aufiero, B.; Guo, M.; Young, C.; Duanmu, Z.; Talwar, H.; Lee, H.K.; Murakawa, G.J. Staphylococcus Aureus Induces the Expression of Tumor Necrosis Factor-α in Primary Human Keratinocytes. *Int. J. Dermatol.* **2007**, *46*, 687–694, doi:10.1111/j.1365-4632.2007.03161.x.

32. Tracey, L.; Villuendas, R.; Dotor, A.M.; Spiteri, I.; Ortiz, P.; García, J.F.; Rodríguez Peralto, J.L.; Lawler, M.; Piris, M.A. Mycosis Fungoides Shows Concurrent

Deregulation of Multiple Genes Involved in the TNF Signaling Pathway: An Expression Profile Study. *Blood* **2003**, *102*, 1042–1050, doi:10.1182/blood-2002-11-3574.

33. Shin, J.; Monti, S.; Aires, D.J.; Duvic, M.; Golub, T.; Jones, D.A.; Kupper, T.S. Lesional Gene Expression Profiling in Cutaneous T-Cell Lymphoma Reveals Natural Clusters Associated with Disease Outcome. *Blood* **2007**, *110*, 3015–3027, doi:10.1182/blood-2006-12-061507.

34. Dulmage, B.O.; Geskin, L.J. Lessons Learned from Gene Expression Profiling of Cutaneous T-Cell Lymphoma. *Br. J. Dermatol.* **2013**, *169*, 1188–1197, doi:10.1111/bjd.12578.

35. Argelaguet, R.; Velten, B.; Arnol, D.; Dietrich, S.; Zenz, T.; Marioni, J.C.; Buettner, F.; Huber, W.; Stegle, O. Multi-Omics Factor Analysis—a Framework for Unsupervised Integration of Multi-omics Data Sets. *Mol. Syst. Biol.* **2018**, *14*, 1–13, doi:10.15252/msb.20178124.

36. Sun, S.-C. The Non-Canonical NF-KB Pathway in Immunity and Inflammation. *Nat. Rev. Immunol.* **2017**, *17*, 545–558, doi:10.1038/nri.2017.52.

37. Faustman, D.; Davis, M. TNF Receptor 2 Pathway: Drug Target for Autoimmune Diseases. *Nat. Rev. Drug Discov.* **2010**, *9*, 482–493, doi:10.1038/nrd3030.

38. Mukai, Y.; Nakamura, T.; Yoshikawa, M.; Yoshioka, Y.; Tsunoda, S.; Nakagawa, S.; Yamagata, Y.; Tsutsumi, Y. Solution of the Structure of the TNF-TNFR2 Complex. *Sci. Signal.* **2010**, *3*, doi:10.1126/scisignal.2000954.

39. Ungewickell, A.; Bhaduri, A.; Rios, E.; Reuter, J.; Lee, C.S.; Mah, A.; Zehnder, A.; Ohgami, R.; Kulkarni, S.; Armstrong, R.; et al. Genomic Analysis of Mycosis Fungoides and Sézary Syndrome Identifies Recurrent Alterations in TNFR2. *Nat. Genet.* **2015**, *47*, 1056–1060, doi:10.1038/ng.3370.

40. Park, J.; Yang, J.; Wenzel, A.T.; Ramachandran, A.; Lee, W.J.; Daniels, J.C.; Kim, J.; Martinez-Escala, E.; Amankulor, N.; Pro, B.; et al. Genomic Analysis of 220 CTCLs Identifies a Novel Recurrent Gain-of-Function Alteration in RLTPR (p.Q575E). *Blood* **2017**, *130*, 1430–1440, doi:10.1182/blood-2017-02-768234.

41. Gómez, M.I.; Seaghdha, M.O.; Prince, A.S. Staphylococcus Aureus Protein A Activates TACE through EGFR-Dependent Signaling. *EMBO J.* **2007**, *26*, 701–709, doi:10.1038/sj.emboj.7601554.

42. Solomon, K.A.; Pesti, N.; Wu, G.; Newton, R.C. Cutting Edge: A Dominant Negative Form of TNF-Alpha Converting Enzyme Inhibits ProTNF and TNFRII Secretion. *J. Immunol.* **1999**, *163*, 4105–4108.

43. Heemann, C.; Kreuz, M.; Stoller, I.; Schoof, N.; von Bonin, F.; Ziepert, M.; Löffler, M.; Jung, W.; Pfreundschuh, M.; Trümper, L.; et al. Circulating Levels of TNF Receptor II Are Prognostic for Patients with Peripheral T-Cell Non–Hodgkin Lymphoma. *Clin. Cancer Res.* **2012**, *18*, 3637–3647, doi:10.1158/1078-0432.CCR-11-3299.

44. Willemze, R.; Cerroni, L.; Kempf, W.; Berti, E.; Facchetti, F.; Swerdlow, S.H.; Jaffe, E.S. The 2018 Update of the WHO-EORTC Classification for Primary Cutaneous Lymphomas. *Blood* **2019**, *133*, 1703–1714, doi:10.1182/blood-2018-11-881268.

45. Aderhold, K.; Carpenter, L.; Brown, K.; Donato, A. Primary Cutaneous Peripheral T-Cell Lymphoma Not Otherwise Specified: A Rapidly Progressive Variant of Cutaneous T-Cell Lymphoma. *Case Rep. Oncol. Med.* **2015**, *2015*, 1–3, doi:10.1155/2015/429068.

46. Kempf, W.; Mitteldorf, C.; Battistella, M.; Willemze, R.; Cerroni, L.; Santucci, M.; Geissinger, E.; Jansen, P.; Vermeer, M.H.; Marschalko, M.; et al. Primary Cutaneous Peripheral T-cell Lymphoma, Not Otherwise Specified: Results of a Multicentre European Organization for Research and Treatment of Cancer (EORTC) Cutaneous Lymphoma Taskforce Study on the Clinico-pathological and Prognostic Features. *J. Eur. Acad. Dermatology Venereol.* **2021**, *35*, 658–668, doi:10.1111/jdv.16969.

47. Bekkenk, M.W.; Vermeer, M.H.; Jansen, P.M.; van Marion, A.M.W.; Canninga-van Dijk, M.R.; Kluin, P.M.; Geerts, M.-L.; Meijer, C.J.L.M.; Willemze, R. Peripheral T-Cell Lymphomas Unspecified Presenting in the Skin: Analysis of Prognostic Factors in a Group of 82 Patients. *Blood* **2003**, *102*, 2213–2219, doi:10.1182/blood-2002-07-1960.

48. Kohri, M.; Tsukasaki, K.; Akuzawa, Y.; Tanae, K.; Takahashi, N.; Saeki, T.; Okamura, D.; Ishikawa, M.; Maeda, T.; Kawai, N.; et al. Peripheral T-Cell Lymphoma with Gastrointestinal Involvement and Indolent T-Lymphoproliferative Disorders of the

Gastrointestinal Tract. *Leuk. Res.* **2020**, *91*, 106336, doi:10.1016/j.leukres.2020.106336.

49. Rooks, M.G.; Garrett, W.S. Gut Microbiota, Metabolites and Host Immunity. *Nat. Rev. Immunol.* **2016**, *16*, 341–352, doi:10.1038/nri.2016.42.

50. Byrd, A.L.; Belkaid, Y.; Segre, J.A. The Human Skin Microbiome. *Nat. Rev. Microbiol.* **2018**, *16*, 143–155, doi:10.1038/nrmicro.2017.157.

51. Iyer, A.; Hennessey, D.; O'Keefe, S.; Patterson, J.; Wang, W.; Salopek, T.; Wong, G.K.-S.; Gniadecki, R. Clonotypic Heterogeneity in Cutaneous T-Cell Lymphoma (Mycosis Fungoides) Revealed by Comprehensive Whole-Exome Sequencing. *Blood Adv.* **2019**, *3*, 1175–1184, doi:10.1182/bloodadvances.2018027482.

52. Hamrouni, A.; Fogh, H.; Zak, Z.; Ødum, N.; Gniadecki, R. Clonotypic Diversity of the T-Cell Receptor Corroborates the Immature Precursor Origin of Cutaneous T-Cell Lymphoma. *Clin. Cancer Res.* **2019**, *25*, 3104–3114, doi:10.1158/1078-0432.CCR-18-4099.

53. Iyer, A.; Hennessey, D.; O'Keefe, S.; Patterson, J.; Wang, W.; Wong, G.K.-S.; Gniadecki, R. Skin Colonization by Circulating Neoplastic Clones in Cutaneous T-Cell Lymphoma. *Blood* **2019**, *134*, 1517–1527, doi:10.1182/blood.2019002516.

54. Iyer, A.; Hennessey, D.; O'Keefe, S.; Patterson, J.; Wang, W.; Wong, G.K.-S.; Gniadecki, R. Branched Evolution and Genomic Intratumor Heterogeneity in the Pathogenesis of Cutaneous T-Cell Lymphoma. *Blood Adv.* **2020**, *4*, 2489–2500, doi:10.1182/bloodadvances.2020001441.

55. Iyer, A.; Hennessey, D.; Gniadecki, R. Clonotype Pattern in T-Cell Lymphomas Map the Cell of Origin to Immature Lymphoid Precursors. *Blood Adv.* **2022**, *6*, 2334–2345, doi:10.1182/bloodadvances.2021005884.

56. Kirsch, I.R.; Watanabe, R.; O'Malley, J.T.; Williamson, D.W.; Scott, L.-L.; Elco, C.P.; Teague, J.E.; Gehad, A.; Lowry, E.L.; LeBoeuf, N.R.; et al. TCR Sequencing Facilitates Diagnosis and Identifies Mature T Cells as the Cell of Origin in CTCL. *Sci. Transl. Med.* **2015**, *7*, 1–14, doi:10.1126/scitranslmed.aaa9122.

57. Campbell, J.J.; Clark, R.A.; Watanabe, R.; Kupper, T.S. Sézary Syndrome and Mycosis

Fungoides Arise from Distinct T-Cell Subsets: A Biologic Rationale for Their Distinct Clinical Behaviors. *Blood* **2010**, *116*, 767–771, doi:10.1182/blood-2009-11-251926.

58. Kallinich, T.; Marcus Muche, J.; Qin, S.; Sterry, W.; Audring, H.; Kroczek, R.A. Chemokine Receptor Expression on Neoplastic and Reactive T Cells in the Skin at Different Stages of Mycosis Fungoides. *J. Invest. Dermatol.* **2003**, *121*, 1045–1052, doi:10.1046/j.1523-1747.2003.12555.x.

59. Daggett, R.N.; Kurata, M.; Abe, S.; Onishi, I.; Miura, K.; Sawada, Y.; Tanizawa, T.; Kitagawa, M. Expression Dynamics of CXCL12 and CXCR4 during the Progression of Mycosis Fungoides. *Br. J. Dermatol.* **2014**, *171*, 722–731, doi:10.1111/bjd.13054.

60. Narducci, M.G.; Scala, E.; Bresin, A.; Caprini, E.; Picchio, M.C.; Remotti, D.; Ragone, G.; Nasorri, F.; Frontani, M.; Arcelli, D.; et al. Skin Homing of Sézary Cells Involves SDF-1-CXCR4 Signaling and down-Regulation of CD26/Dipeptidylpeptidase IV. *Blood* **2006**, *107*, 1108–1115, doi:10.1182/blood-2005-04-1492.

61. Matthijssens, F.; Sharma, N.D.; Nysus, M.; Nickl, C.K.; Kang, H.; Perez, D.R.; Lintermans, B.; Van Loocke, W.; Roels, J.; Peirs, S.; et al. RUNX2 Regulates Leukemic Cell Metabolism and Chemotaxis in High-Risk T Cell Acute Lymphoblastic Leukemia. *J. Clin. Invest.* **2021**, *131*, doi:10.1172/JCI141566.

62. Belver, L.; Ferrando, A. The Genetics and Mechanisms of T Cell Acute Lymphoblastic Leukaemia. *Nat. Rev. Cancer* **2016**, *16*, 494–507, doi:10.1038/nrc.2016.63.

63. Vaillant, F.; Blyth, K.; Andrew, L.; Neil, J.C.; Cameron, E.R. Enforced Expression of Runx2 Perturbs T Cell Development at a Stage Coincident with β-Selection. *J. Immunol.* **2002**, *169*, 2866–2874, doi:10.4049/jimmunol.169.6.2866.

64. Stewart, M.; Terry, A.; Hu, M.; O'Hara, M.; Blyth, K.; Baxter, E.; Cameron, E.; Onions, D.E.; Neil, J.C. Proviral Insertions Induce the Expression of Bone-Specific Isoforms of PEBP2αA (CBFA1): Evidence for a New Myc Collaborating Oncogene. *Proc. Natl. Acad. Sci.* **1997**, *94*, 8646–8651, doi:10.1073/pnas.94.16.8646.

65. Takahama, Y. Journey through the Thymus: Stromal Guides for T-Cell Development and Selection. *Nat. Rev. Immunol.* **2006**, *6*, 127–135, doi:10.1038/nri1781.

66. Dutta, A.; Zhao, B.; Love, P.E. New Insights into TCR β-Selection. *Trends Immunol.*

2021, *42*, 735–750, doi:10.1016/j.it.2021.06.005.

67. Yamano, T.; Nedjic, J.; Hinterberger, M.; Steinert, M.; Koser, S.; Pinto, S.; Gerdes, N.; Lutgens, E.; Ishimaru, N.; Busslinger, M.; et al. Thymic B Cells Are Licensed to Present Self Antigens for Central T Cell Tolerance Induction. *Immunity* **2015**, *42*, 1048–1061, doi:10.1016/j.immuni.2015.05.013.

68. Isaacson, P.G.; Norton, A.J.; Addis, B.J. THE HUMAN THYMUS CONTAINS A NOVEL POPULATION OF B LYMPHOCYTES. *Lancet* **1987**, *330*, 1488–1491, doi:10.1016/S0140-6736(87)92622-5.

69. Castañeda, J.; Hidalgo, Y.; Sauma, D.; Rosemblatt, M.; Bono, M.R.; Núñez, S. The Multifaceted Roles of B Cells in the Thymus: From Immune Tolerance to Autoimmunity. *Front. Immunol.* **2021**, *12*, 1–14, doi:10.3389/fimmu.2021.766698.

70. Dunleavy, K.; Wilson, W.H.; Jaffe, E.S. Angioimmunoblastic T Cell Lymphoma: Pathobiological Insights and Clinical Implications. *Curr. Opin. Hematol.* **2007**, *14*, 348–353, doi:10.1097/MOH.0b013e328186ffbf.

71. Watry, D.; Hedrick, J.A.; Siervo, S.; Rhodes, G.; Lamberti, J.J.; Lambris, J.D.; Tsoukas, C.D. Infection of Human Thymocytes by Epstein-Barr Virus. *J. Exp. Med.* **1991**, *173*, 971–980, doi:10.1084/jem.173.4.971.

72. Paterson, R.L.; Kelleher, C.A.; Streib, J.E.; Amankonah, T.D.; Xu, J.W.; Jones, J.F.; Gelfand, E.W. Activation of Human Thymocytes after Infection by EBV. *J. Immunol.* **1995**, *154*, 1440–1449, doi:10.4049/jimmunol.154.3.1440.

73. Schwarz, B.A.; Bhandoola, A. Circulating Hematopoietic Progenitors with T Lineage Potential. *Nat. Immunol.* **2004**, *5*, 953–960, doi:10.1038/ni1101.

74. Bhandoola, A.; von Boehmer, H.; Petrie, H.T.; Zúñiga-Pflücker, J.C. Commitment and Developmental Potential of Extrathymic and Intrathymic T Cell Precursors: Plenty to Choose From. *Immunity* **2007**, *26*, 678–689, doi:10.1016/j.immuni.2007.05.009.

75. Rothenberg, E. V. Transcriptional Control of Early T and B Cell Developmental Choices. *Annu. Rev. Immunol.* **2014**, *32*, 283–321, doi:10.1146/annurev-immunol-032712-100024.

76. Kanakry, J.A.; Hegde, A.M.; Durand, C.M.; Massie, A.B.; Greer, A.E.; Ambinder, R.F.; Valsamakis, A. The Clinical Significance of EBV DNA in the Plasma and Peripheral Blood Mononuclear Cells of Patients with or without EBV Diseases. *Blood* **2016**, *127*, 2007–2017, doi:10.1182/blood-2015-09-672030.

77. Zitvogel, L.; Galluzzi, L.; Kepp, O.; Smyth, M.J.; Kroemer, G. Type I Interferons in Anticancer Immunity. *Nat. Rev. Immunol.* **2015**, *15*, 405–414, doi:10.1038/nri3845.

78. Faulkner, G.C.; Krajewski, A.S.; Crawford, D.H. The Ins and Outs of EBV Infection. *Trends Microbiol.* 2000, *8*, 185–189.

79. Farrell, P.J. Epstein–Barr Virus and Cancer. *Annu. Rev. Pathol. Mech. Dis.* **2019**, *14*, 29–53, doi:10.1146/annurev-pathmechdis-012418-013023.

80. Long, H.M.; Meckiff, B.J.; Taylor, G.S. The T-Cell Response to Epstein-Barr Virus–New Tricks From an Old Dog. *Front. Immunol.* **2019**, *10*, 1–11, doi:10.3389/fimmu.2019.02193.

81. Maurice, N.J.; Taber, A.K.; Prlic, M. The Ugly Duckling Turned to Swan: A Change in Perception of Bystander-Activated Memory CD8 T Cells. *J. Immunol.* **2021**, *206*, 455–462, doi:10.4049/jimmunol.2000937.

82. Doisne, J.-M.; Urrutia, A.; Lacabaratz-Porret, C.; Goujard, C.; Meyer, L.; Chaix, M.-L.; Sinet, M.; Venet, A. CD8+ T Cells Specific for EBV, Cytomegalovirus, and Influenza Virus Are Activated during Primary HIV Infection. *J. Immunol.* **2004**, *173*, 2410–2418, doi:10.4049/jimmunol.173.4.2410.

83. Danielsen, M.; Emmanuel, T.; Nielsen, M.M.; Lindahl, L.M.; Gluud, M.; Ødum, N.; Raaby, L.; Steiniche, T.; Iversen, L.; Bech, R.; et al. RUNX2 as a Novel Biomarker for Early Identification of Patients Progressing to Advanced-Stage Mycosis Fungoides. *Front. Oncol.* **2024**, *14*, doi:10.3389/fonc.2024.1421443.

84. Blyth, K.; Terry, A.; Mackay, N.; Vaillant, F.; Bell, M.; Cameron, E.R.; Neil, J.C.; Stewart, M. Runx2: A Novel Oncogenic Effector Revealed by in Vivo Complementation and Retroviral Tagging. *Oncogene* **2001**, *20*, 295–302, doi:10.1038/sj.onc.1204090.

85. Blyth, K.; Vaillant, F.; Hanlon, L.; Mackay, N.; Bell, M.; Jenkins, A.; Neil, J.C.; Cameron, E.R. Runx2 and MYC Collaborate in Lymphoma Development by Suppressing

Apoptotic and Growth Arrest Pathways in Vivo. *Cancer Res.* **2006**, *66*, 2195–2201, doi:10.1158/0008-5472.CAN-05-3558.

86. Blyth, K.; Vaillant, F.; Jenkins, A.; McDonald, L.; Pringle, M.A.; Huser, C.; Stein, T.; Neil, J.; Cameron, E.R. Runx2 in Normal Tissues and Cancer Cells: A Developing Story. *Blood Cells, Mol. Dis.* **2010**, *45*, 117–123, doi:10.1016/j.bcmd.2010.05.007.

87. Mirvish, E.D.; Pomerantz, R.G.; Geskin, L.J. Infectious Agents in Cutaneous T-Cell Lymphoma. *J. Am. Acad. Dermatol.* **2011**, *64*, 423–431, doi:10.1016/j.jaad.2009.11.692.

88. Dulmage, B.O.; Feng, H.; Mirvish, E.; Geskin, L. Black Cat in a Dark Room: The Absence of a Directly Oncogenic Virus Does Not Eliminate the Role of an Infectious Agent in Cutaneous T-Cell Lymphoma Pathogenesis. *Br. J. Dermatol.* **2015**, *172*, 1449–1451, doi:10.1111/bjd.13519.

89. Oh, J. Human, Bacterial and Fungal Amplicon Collection and Processing for Sequencing. *BIO-PROTOCOL* **2015**, *5*, doi:10.21769/BioProtoc.1477.

90. Eisenhofer, R.; Minich, J.J.; Marotz, C.; Cooper, A.; Knight, R.; Weyrich, L.S. Contamination in Low Microbial Biomass Microbiome Studies: Issues and Recommendations. *Trends Microbiol.* **2019**, *27*, 105–117, doi:10.1016/j.tim.2018.11.003.

91. Davis, N.M.; Proctor, Di.M.; Holmes, S.P.; Relman, D.A.; Callahan, B.J. Simple Statistical Identification and Removal of Contaminant Sequences in Marker-Gene and Metagenomics Data. *Microbiome* **2018**, *6*, 226, doi:10.1186/s40168-018-0605-2.

92. Sun, Z.; Huang, S.; Zhang, M.; Zhu, Q.; Haiminen, N.; Carrieri, A.P.; Vázquez-Baeza, Y.; Parida, L.; Kim, H.-C.; Knight, R.; et al. Challenges in Benchmarking Metagenomic Profilers. *Nat. Methods* **2021**, *18*, 618–626, doi:10.1038/s41592-021-01141-3.

93. Beghini, F.; McIver, L.J.; Blanco-Míguez, A.; Dubois, L.; Asnicar, F.; Maharjan, S.; Mailyan, A.; Manghi, P.; Scholz, M.; Thomas, A.M.; et al. Integrating Taxonomic, Functional, and Strain-Level Profiling of Diverse Microbial Communities with BioBakery 3. *Elife* **2021**, *10*, 1–42, doi:10.7554/eLife.65088.

94. Truong, D.T.; Franzosa, E.A.; Tickle, T.L.; Scholz, M.; Weingart, G.; Pasolli, E.; Tett, A.; Huttenhower, C.; Segata, N. MetaPhlAn2 for Enhanced Metagenomic Taxonomic Profiling. *Nat. Methods* **2015**, *12*, 902–903, doi:10.1038/nmeth.3589.

95. Knight, R.; Vrbanac, A.; Taylor, B.C.; Aksenov, A.; Callewaert, C.; Debelius, J.; Gonzalez, A.; Kosciolek, T.; McCall, L.I.; McDonald, D.; et al. Best Practices for Analysing Microbiomes. *Nat. Rev. Microbiol.* **2018**, *16*, 410–422, doi:10.1038/s41579-018-0029-9.

96. Meisel, J.S.; Hannigan, G.D.; Tyldsley, A.S.; SanMiguel, A.J.; Hodkinson, B.P.; Zheng, Q.; Grice, E.A. Skin Microbiome Surveys Are Strongly Influenced by Experimental Design. *J. Invest. Dermatol.* **2016**, *136*, 947–956, doi:10.1016/j.jid.2016.01.016.

97. Langille, M.G.I.; Zaneveld, J.; Caporaso, J.G.; McDonald, D.; Knights, D.; Reyes, J.A.; Clemente, J.C.; Burkepile, D.E.; Vega Thurber, R.L.; Knight, R.; et al. Predictive Functional Profiling of Microbial Communities Using 16S RRNA Marker Gene Sequences. *Nat. Biotechnol.* **2013**, *31*, 814–821, doi:10.1038/nbt.2676.

98. Brooks, J.P.; Edwards, D.J.; Harwich, M.D.; Rivera, M.C.; Fettweis, J.M.; Serrano, M.G.; Reris, R.A.; Sheth, N.U.; Huang, B.; Girerd, P.; et al. The Truth about Metagenomics: Quantifying and Counteracting Bias in 16S RRNA Studies Ecological and Evolutionary Microbiology. *BMC Microbiol.* **2015**, *15*, 1–14, doi:10.1186/s12866-015-0351-6.

99. Quince, C.; Walker, A.W.; Simpson, J.T.; Loman, N.J.; Segata, N. Shotgun Metagenomics, from Sampling to Analysis. *Nat. Biotechnol.* **2017**, *35*, 833–844, doi:10.1038/nbt.3935.

100. Tett, A.; Pasolli, E.; Farina, S.; Truong, D.T.; Asnicar, F.; Zolfo, M.; Beghini, F.; Armanini, F.; Jousson, O.; De Sanctis, V.; et al. Unexplored Diversity and Strain-Level Structure of the Skin Microbiome Associated with Psoriasis. *npj Biofilms Microbiomes* **2017**, *3*, 14, doi:10.1038/s41522-017-0022-5.

101. Pereira-Marques, J.; Hout, A.; Ferreira, R.M.; Weber, M.; Pinto-Ribeiro, I.; van Doorn, L.-J.; Knetsch, C.W.; Figueiredo, C. Impact of Host DNA and Sequencing Depth on the Taxonomic Resolution of Whole Metagenome Sequencing for Microbiome Analysis. *Front. Microbiol.* **2019**, *10*, 1–9, doi:10.3389/fmicb.2019.01277.

102. Hillmann, B.; Al-Ghalith, G.A.; Shields-Cutler, R.R.; Zhu, Q.; Gohl, D.M.; Beckman, K.B.; Knight, R.; Knights, D. Evaluating the Information Content of Shallow Shotgun Metagenomics. *mSystems* **2018**, *3*, doi:10.1128/msystems.00069-18.

103. La Reau, A.J.; Strom, N.B.; Filvaroff, E.; Mavrommatis, K.; Ward, T.L.; Knights, D. Shallow Shotgun Sequencing Reduces Technical Variation in Microbiome Analysis. *Sci. Rep.* **2023**, *13*, 7668, doi:10.1038/s41598-023-33489-1.

104. Stothart, M.R.; McLoughlin, P.D.; Poissant, J. Shallow Shotgun Sequencing of the Microbiome Recapitulates 16S Amplicon Results and Provides Functional Insights. *Mol. Ecol. Resour.* **2023**, *23*, 549–564, doi:10.1111/1755-0998.13713.

105. Tessler, M.; Neumann, J.S.; Afshinnekoo, E.; Pineda, M.; Hersch, R.; Velho, L.F.M.; Segovia, B.T.; Lansac-Toha, F.A.; Lemke, M.; DeSalle, R.; et al. Large-Scale Differences in Microbial Biodiversity Discovery between 16S Amplicon and Shotgun Sequencing. *Sci. Rep.* **2017**, *7*, 6589, doi:10.1038/s41598-017-06665-3.

106. Mallick, H.; Rahnavard, A.; McIver, L.J.; Ma, S.; Zhang, Y.; Nguyen, L.H.; Tickle, T.L.; Weingart, G.; Ren, B.; Schwager, E.H.; et al. Multivariable Association Discovery in Population-Scale Meta-Omics Studies. *PLoS Comput. Biol.* **2021**, *17*, e1009442, doi:10.1371/journal.pcbi.1009442.

107. Mallick, H.; Rahnavard, A.; McIver, L. Maaslin2 2020.

108. McMurdie, P.J.; Holmes, S. Waste Not, Want Not: Why Rarefying Microbiome Data Is Inadmissible. *PLoS Comput. Biol.* **2014**, *10*, doi:10.1371/journal.pcbi.1003531.

109. Pinkus, H. Examination of the Epidermis by the Strip Method. *J. Invest. Dermatol.* **1952**, *19*, 431–447, doi:10.1038/jid.1952.119.

110. Chng, K.R.; Tay, A.S.L.; Li, C.; Ng, A.H.Q.; Wang, J.; Suri, B.K.; Matta, S.A.; McGovern, N.; Janela, B.; Wong, X.F.C.C.; et al. Whole Metagenome Profiling Reveals Skin Microbiome-Dependent Susceptibility to Atopic Dermatitis Flare. *Nat. Microbiol.* **2016**, *1*, 16106, doi:10.1038/nmicrobiol.2016.106.

111. Ogai, K.; Nagase, S.; Mukai, K.; Iuchi, T.; Mori, Y.; Matsue, M.; Sugitani, K.; Sugama, J.; Okamoto, S. A Comparison of Techniques for Collecting Skin Microbiome Samples: Swabbing Versus Tape-Stripping. *Front. Microbiol.* **2018**, *9*, 1–10,

doi:10.3389/fmicb.2018.02362.

112. Soga, N.; Nagura, R.; Nakamura, R.; Kohda, K.; Motoyama, Y.; Ito, M.; Nakagawa, I.; Nakajima, S.; Ikeuchi, A. Simple Tape-stripping Method for Highly Reliable and Quantitative Analysis of Skin Microbiome. *Exp. Dermatol.* **2024**, *33*, 1–4, doi:10.1111/exd.15154.

113. Zeeuwen, P.L.J.M.; Boekhorst, J.; van den Bogaard, E.H.; de Koning, H.D.; van de Kerkhof, P.M.C.; Saulnier, D.M.; van Swam, I.I.; van Hijum, S.A.F.T.; Kleerebezem, M.; Schalkwijk, J.; et al. Microbiome Dynamics of Human Epidermis Following Skin Barrier Disruption. *Genome Biol.* **2012**, *13*, R101, doi:10.1186/gb-2012-13-11-r101.

114. Stevens, M.L.; Gonzalez, T.; Schauberger, E.; Baatyrbek kyzy, A.; Andersen, H.; Spagna, D.; Kalra, M.K.; Martin, L.J.; Haslam, D.; Herr, A.B.; et al. Simultaneous Skin Biome and Keratinocyte Genomic Capture Reveals Microbiome Differences by Depth of Sampling. *J. Allergy Clin. Immunol.* **2020**, *146*, 1442–1445, doi:10.1016/j.jaci.2020.04.004.

115. Acosta, E.M.; Little, K.A.; Bratton, B.P.; Lopez, J.G.; Mao, X.; Payne, A.S.; Donia, M.; Devenport, D.; Gitai, Z. Bacterial DNA on the Skin Surface Overrepresents the Viable Skin Microbiome. *Elife* **2023**, *12*, 1–21, doi:10.7554/eLife.87192.2.

116. Serghiou, I.R.; Baker, D.; Evans, R.; Dalby, M.J.; Kiu, R.; Trampari, E.; Phillips, S.; Watt, R.; Atkinson, T.; Murphy, B.; et al. An Efficient Method for High Molecular Weight Bacterial DNA Extraction Suitable for Shotgun Metagenomics from Skin Swabs. *Microb. Genomics* **2023**, *9*, 1–14, doi:10.1099/mgen.0.001058.

117. Shi, Y.; Wang, G.; Lau, H.C.-H.; Yu, J. Metagenomic Sequencing for Microbial DNA in Human Samples: Emerging Technological Advances. *Int. J. Mol. Sci.* **2022**, *23*, 2181, doi:10.3390/ijms23042181.

118. Amar, Y.; Lagkouvardos, I.; Silva, R.L.; Ishola, O.A.; Foesel, B.U.; Kublik, S.; Schöler, A.; Niedermeier, S.; Bleuel, R.; Zink, A.; et al. Pre-Digest of Unprotected DNA by Benzonase Improves the Representation of Living Skin Bacteria and Efficiently Depletes Host DNA. *Microbiome* **2021**, *9*, 123, doi:10.1186/s40168-021-01067-0.

119. Nelson, M.T.; Pope, C.E.; Marsh, R.L.; Wolter, D.J.; Weiss, E.J.; Hager, K.R.; Vo, A.T.; Brittnacher, M.J.; Radey, M.C.; Hayden, H.S.; et al. Human and Extracellular DNA

Depletion for Metagenomic Analysis of Complex Clinical Infection Samples Yields Optimized Viable Microbiome Profiles. *Cell Rep.* **2019**, *26*, 2227-2240.e5, doi:10.1016/j.celrep.2019.01.091.

120. Ahannach, S.; Delanghe, L.; Spacova, I.; Wittouck, S.; Van Beeck, W.; De Boeck, I.; Lebeer, S. Microbial Enrichment and Storage for Metagenomics of Vaginal, Skin, and Saliva Samples. *iScience* **2021**, *24*, 103306, doi:10.1016/j.isci.2021.103306.

121. Heravi, F.S.; Zakrzewski, M.; Vickery, K.; Hu, H. Host DNA Depletion Efficiency of Microbiome DNA Enrichment Methods in Infected Tissue Samples. *J. Microbiol. Methods* **2020**, *170*, 105856, doi:10.1016/j.mimet.2020.105856.

122. Duarte, V. da S.; Porcellato, D. Host DNA Depletion Methods and Genome-Centric Metagenomics of Bovine Hindmilk Microbiome. *mSphere* **2024**, *9*, doi:10.1128/msphere.00470-23.

123. Kim, M.; Parrish, R.C.; Tisza, M.J.; Shah, V.S.; Tran, T.; Ross, M.; Cormier, J.; Baig, A.; Huang, C.-Y.; Brenner, L.; et al. Host DNA Depletion on Frozen Human Respiratory Samples Enables Successful Metagenomic Sequencing for Microbiome Studies. *Commun. Biol.* **2024**, *7*, 1590, doi:10.1038/s42003-024-07290-3.

124. Khan Mirzaei, M.; Xue, J.; Costa, R.; Ru, J.; Schulz, S.; Taranu, Z.E.; Deng, L. Challenges of Studying the Human Virome – Relevant Emerging Technologies. *Trends Microbiol.* **2021**, *29*, 171–181, doi:10.1016/j.tim.2020.05.021.

125. Smith, S.E.; Huang, W.; Tiamani, K.; Unterer, M.; Khan Mirzaei, M.; Deng, L. Emerging Technologies in the Study of the Virome. *Curr. Opin. Virol.* **2022**, *54*, 101231, doi:10.1016/j.coviro.2022.101231.

126. Dulanto Chiang, A.; Dekker, J.P. From the Pipeline to the Bedside: Advances and Challenges in Clinical Metagenomics. *J. Infect. Dis.* **2020**, *221*, S331–S340, doi:10.1093/infdis/jiz151.

127. Wang, D. 5 Challenges in Understanding the Role of the Virome in Health and Disease. *PLOS Pathog.* **2020**, *16*, e1008318, doi:10.1371/journal.ppat.1008318.

128. Castro-Mejía, J.L.; Deng, L.; Vogensen, F.K.; Reyes, A.; Nielsen, D.S. Extraction and Purification of Viruses from Fecal Samples for Metagenome and Morphology

Analyses. In; 2018; pp. 49–57.

129. Kleiner, M.; Hooper, L. V; Duerkop, B.A. Evaluation of Methods to Purify Virus-like Particles for Metagenomic Sequencing of Intestinal Viromes. *BMC Genomics* **2015**, *16*, 7, doi:10.1186/s12864-014-1207-4.

130. Yasumizu, Y.; Hara, A.; Sakaguchi, S.; Ohkura, N. VIRTUS: A Pipeline for Comprehensive Virus Analysis from Conventional RNA-Seq Data. *Bioinformatics* **2021**, *37*, 1465–1467, doi:10.1093/bioinformatics/btaa859.

131. Garmaeva, S.; Sinha, T.; Kurilshikov, A.; Fu, J.; Wijmenga, C.; Zhernakova, A. Studying the Gut Virome in the Metagenomic Era: Challenges and Perspectives. *BMC Biol.* **2019**, *17*, 84, doi:10.1186/s12915-019-0704-y.

132. García-López, R.; Pérez-Brocal, V.; Moya, A. Beyond Cells – The Virome in the Human Holobiont. *Microb. Cell* **2019**, *6*, 373–396, doi:10.15698/mic2019.09.689.

133. Nooij, S.; Schmitz, D.; Vennema, H.; Kroneman, A.; Koopmans, M.P.G. Overview of Virus Metagenomic Classification Methods and Their Biological Applications. *Front. Microbiol.* **2018**, *9*, doi:10.3389/fmicb.2018.00749.

134. Destras, G.; Sabatier, M.; Bal, A.; Simon, B.; Semanas, Q.; Regue, H.; Boyer, T.; Ploin, D.; Gillet, Y.; Lina, B.; et al. Comparison of Metatranscriptomics and Targeted-Sequencing Approaches for Comprehensive Microbiome Profiling 2024.

135. Blanco-Míguez, A.; Beghini, F.; Cumbo, F.; McIver, L.J.; Thompson, K.N.; Zolfo, M.; Manghi, P.; Dubois, L.; Huang, K.D.; Thomas, A.M.; et al. Extending and Improving Metagenomic Taxonomic Profiling with Uncharacterized Species Using MetaPhlAn 4. *Nat. Biotechnol.* **2023**, *41*, 1633–1644, doi:10.1038/s41587-023-01688-w.

136. Zolfo, M.; Silverj, A.; Blanco-Míguez, A.; Manghi, P.; Rota-Stabelli, O.; Heidrich, V.; Jensen, J.; Maharjan, S.; Franzosa, E.; Menni, C.; et al. Discovering and Exploring the Hidden Diversity of Human Gut Viruses Using Highly Enriched Virome Samples. *bioRxiv* **2024**, 2024.02.19.580813, doi:10.1101/2024.02.19.580813.

137. Ravat, F.E.; Spittle, M.F.; Russell-Jones, R. Primary Cutaneous T-Cell Lymphoma Occurring after Organ Transplantation. *J. Am. Acad. Dermatol.* **2006**, *54*, 668–675, doi:10.1016/j.jaad.2005.10.015.

138. Linnemann, T.; Gellrich, S.; Lukowsky, A.; Mielke, A.; Audring, H.; Sterry, W.; Walden, P. Polyclonal Expansion of T Cells with the TCR Vbeta Type of the Tumour Cell in Lesions of Cutaneous T-Cell Lymphoma: Evidence for Possible Superantigen Involvement. *Br. J. Dermatol.* **2004**, *150*, 1013–1017, doi:10.1111/j.1365-2133.2004.05970.x.

139. Vonderheid, E.C.; Boselli, C.M.; Conroy, M.; Casaus, L.; Espinoza, L.C.; Venkataramani, P.; Bigler, R.D.; Steve Hou, J. Evidence for Restricted Vβ Usage in the Leukemic Phase of Cutaneous T Cell Lymphoma. *J. Invest. Dermatol.* **2005**, *124*, 651–661, doi:10.1111/j.0022-202X.2004.23586.x.

140. Willerslev-Olsen, A.; Krejsgaard, T.; Lindahl, L.M.; Litvinov, I. V.; Fredholm, S.; Petersen, D.L.; Nastasi, C.; Gniadecki, R.; Mongan, N.P.; Sasseville, D.; et al. Staphylococcal Enterotoxin A (SEA) Stimulates STAT3 Activation and IL-17 Expression in Cutaneous T-Cell Lymphoma. *Blood* **2016**, *127*, 1287–1296, doi:10.1182/blood-2015-08-662353.

141. Willerslev-Olsen, A.; Buus, T.B.; Nastasi, C.; Blümel, E.; Gluud, M.; Bonefeld, C.M.; Geisler, C.; Lindahl, L.M.; Vermeer, M.; Wasik, M.A.; et al. Staphylococcus Aureus Enterotoxins Induce FOXP3 in Neoplastic T Cells in Sézary Syndrome. *Blood Cancer J.* **2020**, *10*, 57, doi:10.1038/s41408-020-0324-3.

142. Blümel, E.; Willerslev-Olsen, A.; Gluud, M.; Lindahl, L.M.; Fredholm, S.; Nastasi, C.; Krejsgaard, T.; Surewaard, B.G.J.; Koralov, S.B.; Hu, T.; et al. Staphylococcal Alpha-Toxin Tilts the Balance between Malignant and Non-Malignant CD4 + T Cells in Cutaneous T-Cell Lymphoma. *Oncoimmunology* **2019**, *8*, e1641387, doi:10.1080/2162402X.2019.1641387.

143. Breuer, K.; HAussler, S.; Kapp, A.; Werfel, T. Staphylococcus Aureus: Colonizing Features and Influence of an Antibacterial Treatment in Adults with Atopic Dermatitis. *Br. J. Dermatol.* **2002**, *147*, 55–61, doi:10.1046/j.1365-2133.2002.04872.x.

144. Jayakumar, J.; Kumar, V.A.; Biswas, L.; Biswas, R. Therapeutic Applications of Lysostaphin against Staphylococcus Aureus. *J. Appl. Microbiol.* **2021**, *131*, 1072–1082, doi:10.1111/jam.14985.

145. Haddad Kashani, H.; Schmelcher, M.; Sabzalipoor, H.; Seyed Hosseini, E.; Moniri, R.

Recombinant Endolysins as Potential Therapeutics against Antibiotic-Resistant Staphylococcus Aureus: Current Status of Research and Novel Delivery Strategies. *Clin. Microbiol. Rev.* **2018**, *31*, doi:10.1128/CMR.00071-17.

146. Nakatsuji, T.; Hata, T.R.; Tong, Y.; Cheng, J.Y.; Shafiq, F.; Butcher, A.M.; Salem, S.S.; Brinton, S.L.; Rudman Spergel, A.K.; Johnson, K.; et al. Development of a Human Skin Commensal Microbe for Bacteriotherapy of Atopic Dermatitis and Use in a Phase 1 Randomized Clinical Trial. *Nat. Med.* **2021**, doi:10.1038/s41591-021-01256-2.

147. Nakatsuji, T.; Chen, T.H.; Butcher, A.M.; Trzoss, L.L.; Nam, S.-J.; Shirakawa, K.T.; Zhou, W.; Oh, J.; Otto, M.; Fenical, W.; et al. A Commensal Strain of Staphylococcus Epidermidis Protects against Skin Neoplasia. *Sci. Adv.* **2018**, *4*, doi:10.1126/sciadv.aao4502.

148. Piewngam, P.; Otto, M. Probiotics to Prevent Staphylococcus Aureus Disease? *Gut Microbes* **2020**, *11*, 94–101, doi:10.1080/19490976.2019.1591137.

149. Piewngam, P.; Khongthong, S.; Roekngam, N.; Theapparat, Y.; Sunpaweravong, S.; Faroongsarng, D.; Otto, M. Probiotic for Pathogen-Specific Staphylococcus Aureus Decolonisation in Thailand: A Phase 2, Double-Blind, Randomised, Placebo-Controlled Trial. *The Lancet Microbe* **2023**, *4*, e75–e83, doi:10.1016/S2666-5247(22)00322-6.

150. Piewngam, P.; Otto, M. Staphylococcus Aureus Colonisation and Strategies for Decolonisation. *The Lancet Microbe* **2024**, *5*, e606–e618, doi:10.1016/S2666-5247(24)00040-5.

151. Terrón-Camero, L.C.; Gordillo-González, F.; Salas-Espejo, E.; Andrés-León, E. Comparison of Metagenomics and Metatranscriptomics Tools: A Guide to Making the Right Choice. *Genes (Basel).* **2022**, *13*, 2280, doi:10.3390/genes13122280.

152. Martinez, X.; Pozuelo, M.; Pascal, V.; Campos, D.; Gut, I.; Gut, M.; Azpiroz, F.; Guarner, F.; Manichanh, C. MetaTrans: An Open-Source Pipeline for Metatranscriptomics. *Sci. Rep.* **2016**, *6*, 26447, doi:10.1038/srep26447.

153. Westreich, S.T.; Treiber, M.L.; Mills, D.A.; Korf, I.; Lemay, D.G. SAMSA2: A Standalone Metatranscriptome Analysis Pipeline. *BMC Bioinformatics* **2018**, *19*, 175,

doi:10.1186/s12859-018-2189-z.

154. Wu, F.; Liu, Y.-Z.; Ling, B. MTD: A Unique Pipeline for Host and Meta-Transcriptome Joint and Integrative Analyses of RNA-Seq Data. *Brief. Bioinform.* **2022**, *23*, 1–11, doi:10.1093/bib/bbac111.

155. Taj, B.; Adeolu, M.; Xiong, X.; Ang, J.; Nursimulu, N.; Parkinson, J. MetaPro: A Scalable and Reproducible Data Processing and Analysis Pipeline for Metatranscriptomic Investigation of Microbial Communities. *Microbiome* **2023**, *11*, 143, doi:10.1186/s40168-023-01562-6.

156. Rohrer, J.M. Thinking Clearly About Correlations and Causation: Graphical Causal Models for Observational Data. *Adv. Methods Pract. Psychol. Sci.* **2018**, *1*, 27–42, doi:10.1177/2515245917745629.

157. Schwabe, R.F.; Jobin, C. The Microbiome and Cancer. *Nat. Rev. Cancer* **2013**, *13*, 800–812, doi:10.1038/nrc3610.

158. De Pessemier, B.; Grine, L.; Debaere, M.; Maes, A.; Paetzold, B.; Callewaert, C. Gut–Skin Axis: Current Knowledge of the Interrelationship between Microbial Dysbiosis and Skin Conditions. *Microorganisms* **2021**, *9*, 353, doi:10.3390/microorganisms9020353.

6 Addendum

During the course of my doctoral studies, I additionally contributed as a coauthor to the following publication. However, as it does not pertain to the subject matter of this dissertation, it will not be discussed further. For the sake of completeness, the publication is included in the addendum.

Zimmer, N*., Trzeciak, E. R.*, Müller, A., **Licht, P**., Sprang, B., Leukel, P., Mailänder, V., Sommer, C., Ringel, F., Tuettenberg, J., Kim, E. & Tuettenberg, A. Nuclear Glycoprotein A Repetitions Predominant (GARP) Is a Common Trait of Glioblastoma Stem-like Cells and Correlates with Poor Survival in Glioblastoma Patients. *Cancers (Basel)*. **15**, 5711 (2023).

* denotes shared first authorship

Full-text link: https://www.mdpi.com/2072-6694/15/24/5711

Supplementals: https://www.mdpi.com/article/10.3390/cancers15245711/s1

cancers

MDPI

Article

Nuclear Glycoprotein A Repetitions Predominant (GARP) Is a Common Trait of Glioblastoma Stem-like Cells and Correlates with Poor Survival in Glioblastoma Patients

Niklas Zimmer [1,†], Emily R. Trzeciak [1,†], Andreas Müller [2,3], Philipp Licht [1], Bettina Sprang [2,3], Petra Leukel [4], Volker Mailänder [1,5], Clemens Sommer [4], Florian Ringel [2], Jochen Tuettenberg [6], Ella Kim [2,3,‡] and Andrea Tuettenberg [1,5,*,‡]

1 Department of Dermatology, University Medical Center Mainz, 55131 Mainz, Germany; plicht@uni-mainz.de (P.L.)
2 Department of Neurosurgery, University Medical Center Mainz, 55131 Mainz, Germany
3 Laboratory of Experimental Neurooncology, University Medical Center Mainz, 55131 Mainz, Germany
4 Institute of Neuropathology, University Medical Center Mainz, 55131 Mainz, Germany
5 Research Center for Immunotherapy, University Medical Center Mainz, 55131 Mainz, Germany
6 Department of Neurosurgery, SHG-Klinikum Idar-Oberstein, 55743 Idar-Oberstein, Germany; j.tuettenberg@io.shg-kliniken.de
* Correspondence: antuette@uni-mainz.de
† These authors contributed equally to this work.
‡ Joint Senior Authors.

Simple Summary: Glioblastoma (GB) is the most common primary brain tumor in adults, but it remains incurable due to its high degree of therapy resistance. Glioblastoma stem-like cells (GSCs) are believed to drive the initiation, progression, and therapy resistance of GB, making them an ideal therapeutic target to improve patient outcomes. However, due to their heterogeneity, there are no universal markers to identify GSCs. We evaluated GARP as a novel marker for GSCs and found that GARP is more stably and uniformly expressed by human GSCs, across cellular states and disease stages, than the commonly used GSC marker, CD133. Additionally, we showed that GARP is intranuclearly localized in GSCs, and we are the first to show that nuclear GARP levels ($GARP^{NU+}$) are associated with poor patient survival. Our findings indicate that GARP/$GARP^{NU+}$ expression is an improved marker for GSCs and suggest a potential application of GARP as a prognostic biomarker for GB.

Abstract: Glioblastoma (GB) is notoriously resistant to therapy. GB genesis and progression are driven by glioblastoma stem-like cells (GSCs). One goal for improving treatment efficacy and patient outcomes is targeting GSCs. Currently, there are no universal markers for GSCs. Glycoprotein A repetitions predominant (GARP), an anti-inflammatory protein expressed by activated regulatory T cells, was identified as a possible marker for GSCs. This study evaluated GARP for the detection of human GSCs utilizing a multidimensional experimental design that replicated several features of GB: (1) intratumoral heterogeneity, (2) cellular hierarchy (GSCs with varied degrees of self-renewal and differentiation), and (3) longitudinal GSC evolution during GB recurrence (GSCs from patient-matched newly diagnosed and recurrent GB). Our results indicate that GARP is expressed by GSCs across various cellular states and disease stages. GSCs with an increased GARP expression had reduced self-renewal but no alterations in proliferative capacity or differentiation commitment. Rather, GARP correlated inversely with the expression of GFAP and PDGFR-α, markers of astrocyte or oligodendrocyte differentiation. GARP had an abnormal nuclear localization ($GARP^{NU+}$) in GSCs and was negatively associated with patient survival. The uniformity of GARP/$GARP^{NU+}$ expression across different types of GSCs suggests a potential use of GARP as a marker to identify GSCs.

Keywords: GARP; nuclear GARP; $GARP^{NU+}$; LRRC32; glioblastoma; glioblastoma stem-like cells

Citation: Zimmer, N.; Trzeciak, E.R.; Müller, A.; Licht, P.; Sprang, B.; Leukel, P.; Mailänder, V.; Sommer, C.; Ringel, F.; Tuettenberg, J.; et al. Nuclear Glycoprotein A Repetitions Predominant (GARP) Is a Common Trait of Glioblastoma Stem-like Cells and Correlates with Poor Survival in Glioblastoma Patients. *Cancers* **2023**, *15*, 5711. https://doi.org/10.3390/cancers15245711

Academic Editors: Martine L. M. Lamfers, Ander Matheu and Benedikt Linder

Received: 20 October 2023
Revised: 17 November 2023
Accepted: 1 December 2023
Published: 5 December 2023

1. Introduction

Glioblastoma (GB) is one of the most aggressive tumors, with an overall survival rate of approximately 15 months [1,2]. The current standard therapy consists of surgical removal of the primary tumor, radiation, and treatment with the chemotherapeutic agent, temozolomide (TMZ) [3]. A high degree of tumor infiltration into the surrounding tissue is a characteristic feature of GB, limiting the clinical efficacy of neurosurgical resection. Despite multi-modal therapy, GB recurrence after initial treatment is almost inevitable [4–6]. Besides the immunosuppressive properties of tumor cells, which suppress anti-tumor immune responses through microglial cells or regulatory T cells, poor prognosis is also attributed to a high degree of therapeutic resistance, either inherent or acquired by therapy, and the extraordinary intratumoral heterogeneity of GB, manifesting via the diversity of molecular and cellular subtypes/cellular states associated with GSCs [7–10].

The notorious therapeutic resistance of GB has been attributed to glioblastoma stem-like cells (GSCs), which comprise a subset of tumor cells that possess some fundamental properties of cancer stem cells, including unlimited self-renewal, aberrant differentiation response, and inherent plasticity. These characteristics enable GSCs to undergo reversible transitions between distinct cellular states in response to environmental signals [11,12].

These unique properties render GSCs capable of adapting to and surviving cytotoxic treatments that are otherwise lethal to non-stem glioma cells, thereby endowing them with the potential to reconstitute the tumor during or after therapy. GSCs are currently considered the main determinants of therapy resistance and drivers of tumor recurrence in GB. Therefore, they are arguably the most clinically relevant cellular target in gliomas. Assessments of GSCs in tumor specimens face several methodological challenges. These include: (I) the relatively low percentage of GSCs compared to the rest of the tumor cells, which are thought to be comprised primarily of non-stem glioma cells or differentiated progenies of GSCs [13,14], (II) an inhomogeneous distribution of GSCs within the tumor, which are located in specialized niches that provide a proper environment for maintaining their undifferentiated state [14], and (III) the phenotypic diversity and inherent high plasticity of GSCs, enabling dynamic transitions between different cell states accompanied by morphological alterations and changes in their phenotypic make-up [15,16]. Furthermore, GSCs possess a high degree of plasticity, which renders them capable of switching between different cellular states and distinct morphological phenotypes. Lack of definitive markers that are stably expressed on GSCs poses a further challenge to the diagnostic stratification of GB based on the evaluation of GSC content in tumor specimens [17].

Although a range of molecules like CD15, L1CAM, SOX2, and Prominin1/CD133 have been implicated as identification markers of GSCs, their diagnostic utility has been limited due to the phenotypic heterogeneity within the GSC compartment, constituted by cells in hierarchically distinct states [18–23]. For example, expression of Prominin1/CD133, historically one of the most investigated and arguably the best validated GSC marker, is sample specific, being restricted to only a subset of GSCs [24–27], and fluctuates significantly during cell cycle [28]. Furthermore, a reversible loss of CD133 expression in $CD133^+$ GSCs was shown to accompany tumor propagation, as revealed in an experimental in vivo model of GB [24]. Considering that the tumor-propagating capacity of $CD133^-$ GSCs is comparable to that of $CD133^+$ GSCs [24], the diagnostic utility of CD133 remains uncertain [29]. Phenotypic diversity and plasticity of GSCs as a means of adaptation to the tumor microenvironment have important implications for the continuing search for GSCs markers that would be universally applicable for different subsets of GSCs and would be expressed unambiguously, regardless of cellular state.

In this regard, Glycoprotein A repetitions predominant (GARP) has recently emerged as a potential marker of human GSCs [7,30]. GARP is a type I transmembrane protein normally expressed on the surface of activated regulatory T cells, where it mediates tolerogenic functions in the tumor microenvironment of GB [7]. GARP consists of 662 amino acids and is composed of an extracellular domain with 20 leucine rich repeats, a hydrophobic transmembrane domain, and a 15 amino acid intracellular part. Recently, we have found

that GARP is also expressed by different types of GB cells, including GSCs, where it shows an atypical pattern of subcellular distribution characterized by GARP localization on both the cell surface and within the nucleus ($GARP^{NU+}$) [7]. Up until now, GARP expression in GSCs has only been shown in vitro, with several open-ended questions remaining. Namely, is GARP/$GARP^{NU+}$ expression associated with a particular cellular state (self-renewal or differentiation) or a particular subtype of GSCs? Does the associated expression of GARP/$GARP^{NU+}$ in GSCs persist during GB progression after therapy?

In the present study, these questions were addressed in vitro and in vivo by analyzing the expression of GARP/$GARP^{NU+}$ in different subtypes of patient-derived GSCs with consideration of intratumoral heterogeneity and the longitudinal changes accompanying GB recurrence. For the first time, the present study examined the potential link of nuclear GARP expression with patient outcomes.

2. Materials and Methods

2.1. Cell Culture

The human glioblastoma cell line T98G was purchased from the ATCC (CRL-1690) and was cultured in Minimum Essential Medium Eagle supplemented with 10% FCS, 1% Glutamine, and 0.1% Primocin. The human melanoma cell lines, Mewo and Ma-Mel-19, were obtained from Dr. Daniela Kramer (Mewo, RRID:CVCL_0445, Cellosaurus) in Mainz, Germany, in 2021 and from Dr. Annette Paschen (Ma-Mel-19, RRID:CVCL_A156, Cellosaurus) in Essen, Germany, in 2014. Mewo cells were cultured in Dulbecco's Modified Eagle Medium supplemented with 10% FCS and 0.1% Primocin. Ma-Mel-19 cells were grown in RPMI 1640 supplemented with 10% FCS, 1% Glutamine, and 0.1% Primocin. T98G, Mewo, and Ma-Mel-19 cells were passed every 2 to 3 days by using Trypsin-EDTA. The cell lines T98G and Ma-Mel-19 were authenticated in August 2022 by PCR single locus technology. The results were compared to the online databases of the DSMZ and Cellosaurus (Eurofins Genomics Europe). Patient-derived GSC lines used in this study were established as previously described and have been well characterized in previous studies, in terms of their stem cell frequency (SCF) and expression of various GSC markers [28,31–33]. Additional information regarding their origin, SCF, predominant phenotype ($Nestin^{+/-}$, $GFAP^{+/-}$), and percentage of CD133-positive cells, as well as an exemplary analysis of the GSC markers, CD133, platelet-derived growth factor receptor alpha (PDGFR-α), and aldehyde dehydrogenase 1 family member A3 (ALDH1A3), can be found in Figure S1 [28,33,34]. In brief, excess glioblastoma tumor tissue was obtained from patients operated on at the Department of Neurosurgery of the Johannes Gutenberg University Medical Center Mainz (JG-UMC), with informed consent. The use of tumor tissue for research purposes was approved by the JG-UMC Institutional Review Board (permission 08.06.2017 #837.211.12(8312-F). For GSC isolation, a combined enzymatic and mechanical titration procedure was used as previously described [28]. To promote self-renewal, glioma cells were cultured in serum-free NeuroBasal (NB) medium supplemented with the following factors: B27 supplement (Invitrogen, Darmstadt, Germany) and the recombinant human cytokines, basic fibroblast growth factor 2 (bFGF) (10 ng/mL) and epidermal growth factor (EGF), (20 ng/mL) (Biochrom GmbH, Merck KGaA, Darmstadt, Germany). For in vitro differentiation, cells were subjected to EGF and bFGF withdrawal and assessed for the expression of neural lineage specific markers after 7 days. Self-renewal promoting conditions are hence referred to as "NB+bFGF/+EGF" whereas differentiation is indicated by "NB-bFGF/-EGF" in the manuscript.

2.2. Western Blot

Protein preparation and Western blotting were performed as previously described in Müller et al., 2023 [35]. Membranes were probed with the following antibodies: anti-CD133/1 (clone: W6B3C1), anti-PDFGR-α (D13C6) (Cell Signaling, #5241T, Danvers, MA, USA), anti-ALDH1A3 (Thermo Fischer Scientific, MA5-25528, Waltham, MA, USA), anti-p53 (DO-1) (Cell Signaling, #18032), anti-actin (C4) (Santa Cruz Biotechnology, sc-47778,

Dallas, TX, USA), anti-glial fibrillary acidic protein (GFAP) (DAKO, Z0334, Santa Clara, CA, USA), anti-p21 (Cell Signaling, #2947), anti-phosphorylated-histone H3 (Ser28) (Cell Signaling, #9713S), anti-HSP70 (Enzo Life Sciences Inc., Farmingdale, NY, USA), anti-mouse IgGκ light chain-binding protein horseradish peroxidase (Santa Cruz Biotechnology, sc-516102), goat anti-rabbit IgG H&L horseradish peroxidase (Abcam, ab205718, Cambridge, UK), goat anti-mouse IgG horseradish peroxidase (Santa Cruz Biotechnology, sc-2055), and goat anti-rabbit horseradish peroxidase (Santa Cruz Biotechnology, sc-2054). Signal intensity was analyzed via densitometry (https://imagej.nih.gov, accessed on 17 October 2023) [36].

2.3. Flow Cytometry

For flow cytometric analysis, the following fixable viability dye and antibodies were used: FVD506 (eBioscience #65-0866-14, San Diego, CA, USA), anti-GARP (Miltenyi #130-103-820 and 130-103-890, updated ordering numbers: 130-125-511 and 130-125-532, Bergisch Gladbach, Germany), anti-CD133 (epitope AC133, Miltenyi # 130-113-111), and their respective isotype controls (Miltenyi #130-113-434 and Miltenyi #130-113-200). Cells were stained with fixable viability dye prior to surface antibody staining of anti-GARP and anti-CD133. Cells were not fixed for the analysis.

Extensive validation of the anti-GARP antibodies mentioned above and a demonstration of their specificity can be found in Figures S2 and S3 as well as in previous work by Zimmer et al., 2019 [7]. In more detail, the anti-GARP antibodies from Miltenyi were validated against two other flow cytometry certified antibodies (Biolegend, 352506, San Diego, CA, USA; Origene, TA337028, Rockland, MD, USA) (Figure S3) and against the polyclonal anti-GARP antibody used in this study (Origene, AP17415PU-N) (Figure S2). Antibody specificity was demonstrated using GARP-overexpressing Mewo cells, resulting from transient transfection using the LOX-IMVI Cell Avalanche Transfection Reagent (EZ Biosystems, EZT-LOXI-1, College Park, MD, USA) as well as a LRRC32 overexpression plasmid (Origene, SC116699) and an empty vector control plasmid (Origene, PS100001) (Figure S3). Transfection was performed in accordance with the manufacturer's recommendations. Cells were stained with fixable viability dye and for surface GARP as described above 48 h post-transfection.

Flow cytometry was performed on a BD LSRII flow cytometer (Heidelberg, Germany) and was analyzed using Cytobank [37]. Doublets, debris, and dead cells were excluded from analysis (Figure S4).

2.4. Confocal Microscopy

Confocal imaging was performed on a Leica SP8 with HyD detector (Wetzlar, Germany) at the Imaging Core Facility (ICF) of the Forschungszentrum für Immuntherapie (FZI) of the University Medical Center Mainz as described before [7]. The following antibodies were used in the study: anti-nestin (Abcam, ab22035), anti-GARP (Origene, AP17415PU-N), and secondary antibodies goat anti-mouse Alexa Fluor 488 or goat anti-rabbit Alexa Fluor 555 (both Thermo Fisher Scientific, Waltham, MA, USA). Validation and specificity of the anti-GARP antibody (Origene AP17415PU-N) for its use in confocal microscopy can be found in Figure S5 and in previous work by Zimmer et al., 2019 [7].

2.5. Animal Experiments

Animal experiments were performed at the Translational Animal Research Facility (TARC) of the JG-UMC, Germany, in accordance with the guidelines of the European Convention for the Protection of Vertebrates Used for Scientific Purposes and under the approval of the State Office of Chemical Investigations of Rhineland-Palatinate (permission #23 177-07/G12-1-020). Immunodeficient mice (strain NMRI) were purchased from a commercial supplier (Charles River Laboratories Germany). After an adaptation period of one to two weeks, mice were subjected to intracerebral injection of GSCs using a standardized procedure as described previously [34,38]. In brief, single-cell suspensions were prepared

from glioma sphere cultures by using a combined trypsin/mechanical titration procedure. Cells were washed twice in PBS and re-suspended in PBS at 2 × 10^4 cells/µL. Cell viability was determined by trypan blue staining. Single-cell suspensions were injected at 5 µL into the caudato-putamen of the right hemisphere using a stereotactic frame (TSE Systems, Bad Homburg, Germany) and the following stereotactic coordinates in reference to the bregma: 1 mm (anteroposterior axis), 3 mm (lateromedial axis), 2.5 mm (vertical axis). Mice were sacrificed at the first manifestation of tumor-associated neurological symptoms.

2.6. GARP Immunohistochemistry and Immunofluorescence

Tumor-bearing mouse brains were extracted and fixed in 4% paraformaldehyde in PBS for at least 24 h at 4 °C as described previously [38]. Briefly, after fixation, brains were paraffin-embedded, dissected into 1–3 µm thick coronal sections and analyzed by immunohistochemical or immunofluorescence staining using antibodies specific to human nestin (R&D Systems GmbH, Wiesbaden-Nordenstadt, Germany), GFAP (DAKO, Z0334), or GARP (Origene, AP17415PU-N). Previous work has demonstrated the specificity of the anti-GARP antibody (Origene, AP17415PU-N) for its use in immunohistochemistry and immunofluorescence [7,39]. For analysis, ImageJ2 (Available online: https://imagej.net/ImageJ2, accessed on 16 August 2021) was used [40].

A GB patient cohort from Zimmer et al., 2019 [7], was reanalyzed to correlate the frequency of $GARP^{NU+}$ cells in tumor tissue to patient overall survival regardless of IDH status. Patient characteristics are described in detail in Figure 1 of Zimmer et al., 2019 [7]. In brief, the patient cohort consisted of 35 newly diagnosed (WHO stage IV) GB patients from the Department of Neurosurgery in Idar-Oberstein, Germany, between January 2009 and May 2015. The median high and low survival times were 12 and 4 months. Primary tumor tissue was resected and stained for GARP via immunohistochemistry. Description of the immunohistochemical staining process can be found in Zimmer et al., 2019 [7]. The frequency of $GARP^{NU+}$ was semi-quantified in tumor tissue with regions of labeled nuclei (categorized as >90%, >50%, >10% $GARP^{NU+}$ cells) at the Institute of Neuropathology, University Medical Center Mainz, Germany [7].

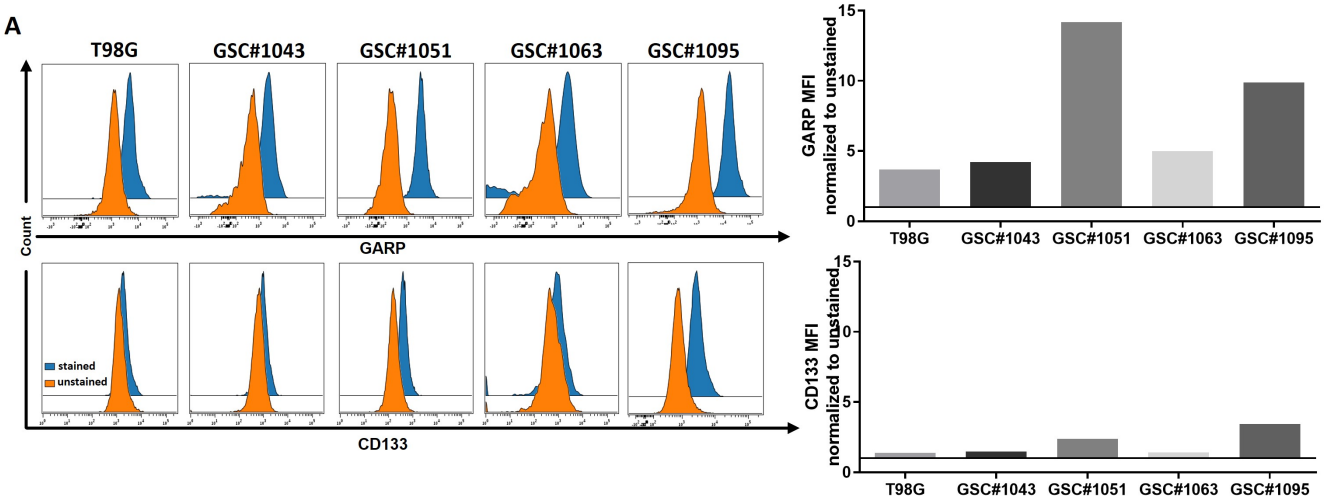

Figure 1. *Cont.*

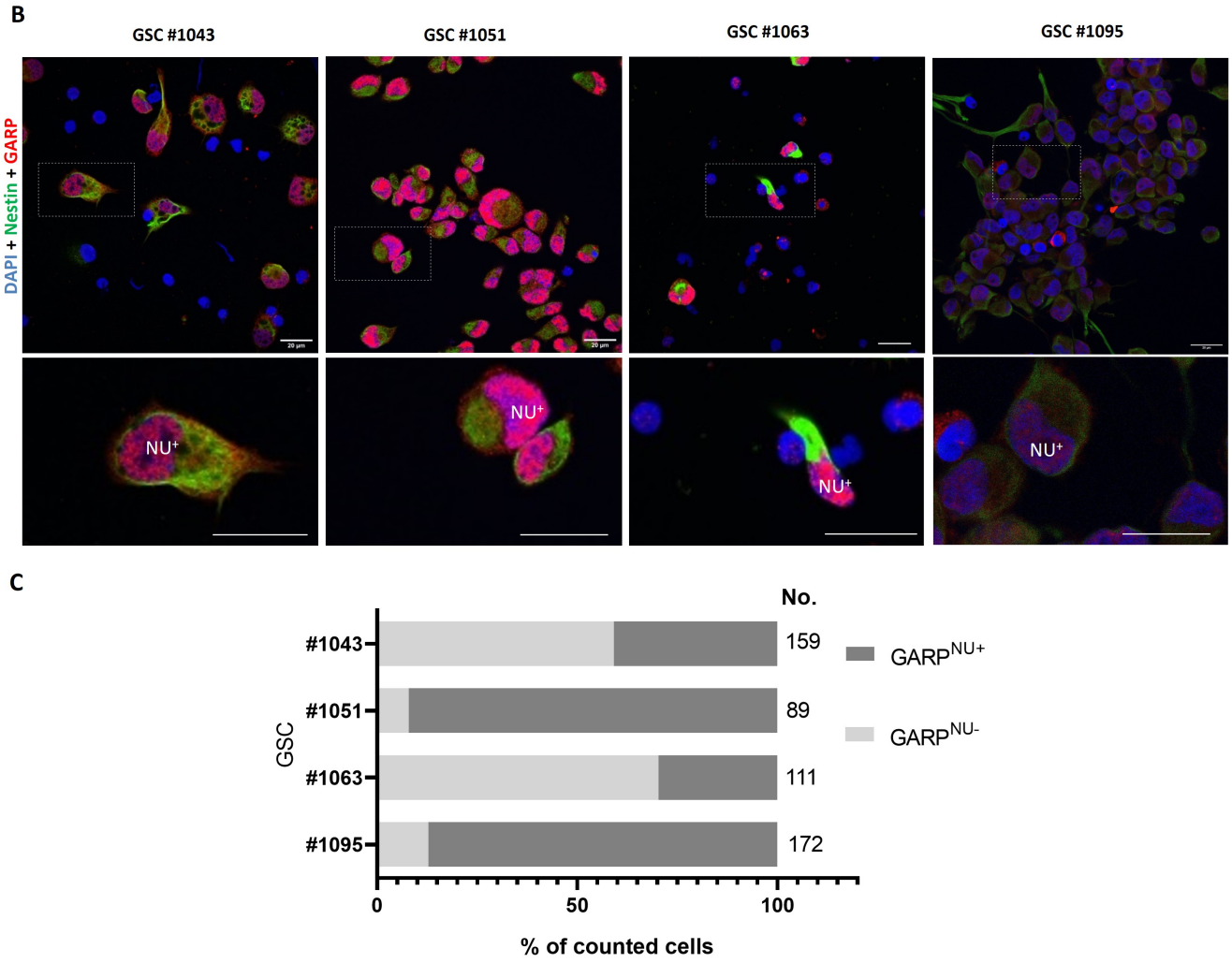

Figure 1. (**A**) Flow cytometric analysis of surface GARP and CD133 on different GSCs and the control, non-stem, GB cell line, T98G. Doublets, debris, and dead cells were excluded from the analysis. Mean fluorescence intensity (MFI) was normalized to the MFI of the respective unstained control. (**B**) Confocal images of GARP- and nestin-expressing GSCs and T98G. Cells were stained for GARP (red) and nestin (green). Cells were counterstained for their nuclei with Hoechst (blue). Note the intranuclear localization of GARP (NU^+). Scale bar corresponds to 20 µm. (**C**) Percentage of $GARP^{NU+}$ cells were determined by counting GARP stained nuclei. "No." indicates the number of counted cells for the analysis.

2.7. Cell Sorting

Single-cell suspensions of the GSC line, #1095, were stained sequentially with the following: fixable viability dye FVD780 (eBioscience #65-0865-14), unconjugated anti-GARP antibody (Origene, AP17415PU-N) or a control unconjugated IgG rabbit isotype antibody (R&D Systems, AB-105-C), followed by a PE-conjugated goat anti-rabbit secondary antibody (Invitrogen, P2771MP). Cells were sorted into $GARP^{low}$ and $GARP^{high}$ populations. Cell sorting gates were defined as the lower 10th ($GARP^{low}$) and upper 90th percentiles ($GARP^{high}$) of all cells. An example gating strategy and proof of positive GARP staining can be found in Figure S6. Debris, doublets, and dead cells were excluded from analysis. Sorting was performed using BD Aria II and III cell sorters at the Core Facility Flow Cytometry (CFFC) of the Forschungszentrum für Immuntherapie (FZI) of the University Medical Center Mainz.

2.8. Extreme Limiting Dilution Assay

The self-renewal capacity of GSC lines was analyzed by extreme limiting dilution assay (ELDA). In brief, single-cell suspensions were serially diluted in self-renewal promoting medium (NB+bFGF/+EGF) and seeded into 24 well plates. The number of replicates used for each serial dilution are indicated as follows: 12 for 100 cells/well, 18 for 50 cells/well, 24 for 25 cells/well, 58 for 12.5 cells/well, 24 for 6.25 cells/well, 18 for 3.125 cells/well, and 12 for 1.56 cells/well. Cells were incubated for three weeks to develop neurospheres. Wells were assessed for neurosphere formation; a positive result was recorded for each dose (number of seeded cells/well) if the examined well contained at least one neurosphere. Each experiment was repeated independently three times. Stem cell frequency (SCF) was calculated using the ELDA: Extreme Limiting Dilution Analysis webtool from the Walter and Eliza Hall Institute of Medical Research (https://bioinf.wehi.edu.au/software/elda/, accessed on 6 September 2023) [41].

2.9. Bioinformatic Pipeline

In a previous work, Kim et al., 2020, performed Illumina RNA-Sequencing on a total of 155 glioblastoma samples derived from 28 patients [32]. These consisted of primary, recurrent, and secondary recurrent tumors (128 samples) as well as GSC cultures developed from freshly resected tumor tissue (27 samples). We obtained unnormalized gene counts through the Gene Expression Omnibus database (GEO) under the accession number: GSE139533. Gene counts were normalized with DESeq2 and analyzed using the likelihood ratio test to decipher the effect of progressing tumor stages on transcript levels within the same patient [42]. Normalized counts for CD133 and GARP were plotted with GraphPad Prism version 9.3.1 for Windows, GraphPad Software, San Diego, CA, USA, www.graphpad.com.

Survival analysis of CD133 and GARP was performed using OncoLnc (http://www.oncolnc.org/, accessed on 8 July 2023) which is based upon data generated by The Cancer Genome Atlas (TCGA) Research Network (https://www.cancer.gov/tcga, accessed on 8 July 2023) [43–45].

2.10. Statistics

Statistical analysis was performed with Student's *t*-test, the likelihood ratio test, the chi-squared test, or two-way ANOVA as indicated. Data are displayed as mean values ± SEM or ±SD as indicated. Survival curve comparison was analyzed using the log-rank (Mantel–Cox) test using GraphPad Prism. Statistical significance is indicated as follows: * $p < 0.05$, ** $p < 0.01$, *** $p < 0.001$, **** $p < 0.001$, and ns (not significant).

3. Results

3.1. GARP Expression Is Conserved across Different Types of GSCs In Vitro and In Vivo

We have previously shown that GARP is expressed by three human GSC lines and by the conventional human glioblastoma cell line, T98G [7]. The questions that remained were whether GARP expression is restricted to a particular type of GSCs or if it represents a common phenotypic trait shared by different subsets of GSCs. To address these questions, we analyzed the expression of GARP in a panel of heterologous GSC lines, differing in their self-renewal capacity, degree of differentiation, and expression of CD133, a proposed marker for GSCs in the past (Figure S1A). All GSCs used in this study invariably expressed nestin, a neural stem cell marker, but they varied in their expression of the astrocyte differentiation marker, GFAP, and CD133, a putative GSC marker (Figure S1A). A non-stem glioblastoma cell line, T98G, (ATCC CRL-1690) was analyzed in parallel as a control. Flow cytometry revealed that the surface expression of GARP varied across heterologous GSCs (Figure 1A). Notably, variations in GARP expression paralleled variations in CD133 levels indicating that GARP and CD133 are not mutually exclusive markers (Figure 1A). Line-dependent variations in GARP expression were also confirmed by microscopic evaluation of intracellular GARP (Figure 1B,C). Confirming our previous observations, microscopic analysis

revealed that GARP localization in GSCs is not restricted to the cell membrane, a normal localization site for GARP, but it also extends to the nuclear compartment (Figure 1B) [7,30]. The nuclear localization of GARP was evident in confocal microscopy with co-staining for nestin, an established marker of neural stem/progenitor cells expressed in the cytoplasm. The prevalence of cells with nuclear GARP (termed hereafter as "GARP^{NU+}") varied between different GSC lines (Figure 1B,C) and mirrored the levels of surface-expressed GARP (Figure 1A), indicating a possible relationship between the two forms. For example, the GSC lines #1051 and #1095 had the highest levels of surface-membrane-associated GARP (Figure 1A), and they also exhibited a high proportion of cells with GARP^{NU+} (92.1% and 87.2%, Figure 1B,C). Vice versa, GSCs with moderate levels of surface GARP (#1043 and #1063, Figure 1A) had lower proportions of cells with GARP^{NU+} (40.9% and 29.7%, Figure 1C).

Our in vitro findings prompted us to test if GARP/GARP^{NU+} expression is sustained in vivo in GSCs involved in tumor propagation. To this end, we analyzed xenograft tumors grown from two GSC lines that express the lowest (line #1043) and highest (line #1051) levels of GARP in vitro (Figure 1). Both lines gave rise to highly invasive brain tumors as ascertained by immunohistochemical staining with an antibody specific for human nestin (Figure S7) and had comparable rates of tumor growth [34]. Immunofluorescence staining for GARP revealed its expression in both #1051 and #1043 xenografts (Figure S8). Notably, GARP expression in #1043 xenograft (low expressor in vitro, Figure 1) was comparable with that in #1051 xenograft (high expressor in vitro, Figure 1), suggesting that GARP expression in GSCs might be even more profound in the tumor context. Concordant with our in vitro findings, tumor-propagating GSCs also showed GARP localization in both the cytoplasm and nucleus (Figure S8). Additionally, GARP^{NU+} was observed to be co-expressed with nestin (Figure S8). These results further support the conclusion that GARP/GARP^{NU+} expression might be a common trait stably sustained (or even augmented) in GSCs involved in tumor propagation.

3.2. Intratumoral Heterogeneity of Subcellular Distribution Patterns of GARP

GBs are known for their high degree of intratumoral heterogeneity, which is thought to reflect the hierarchical diversity of cellular states generated by GSCs [12,46]. Our observation that heterologous GSCs vary in their levels of GARP/GARP^{NU+} (Figures 1 and S8) prompted us to check if this is a mere reflection of intertumoral diversity, GARP/GARP^{NU+} association with a particular GSC subtype or cellular state, or a hierarchical diversification taking place during tumor growth. To address these questions, we made use of isogenic GSCs (lines IT-726-#1, IT-726-#2, IT-726-#3a, IT-726-#3b, and IT-726-#4) that have been isolated from different regions of the same tumor (Figure S9—Cohort 2"—comparison line 1) and provide a unique model for analyzing the impact of intratumoral heterogeneity in an isogenic background [31,32]. Indeed, despite their identical genetic background, isogenic GSCs from the IT-726 set displayed notable morphological differences, considerable variations in their self-renewal capacity, and expression of GSC-associated markers CD133, ALDH1 A3, and PDGFR-α (Figure S1) [31,32].

Interestingly, we found no apparent correlation between CD133 expression and the degree of self-renewal activity. For example, the lines IT-726-1 and IT-726-3B had comparable degrees of self-renewal activity (Figure S1A), but they differed profoundly in the expression of surface CD133 (glycosylated epitope AC133) (Figure 2). Vice versa, the line IT-726-4 expressed similar levels of surface CD133 as the lines IT-726-2, IT-726-3A, and IT-726-3B, (Figure 2), but it stood out markedly from the other lines in terms of its extremely low self-renewal capacity (Figure S1A). In contrast to CD133, the expression of surface GARP was very similar across isogenic lines, and it did not parallel the striking difference in CD133 expression between the IT-726-1 line and its isogenic counterparts (Figure 2). In comparison to the uniform expression of surface GARP, the patterns of GARP subcellular distribution between IT-726 lines were heterogeneous, with the proportion of GARP^{NU+} cells varying across different isogenic lines (Figure 3A). The highest level of GARP^{NU+}

was found in line IT-726-2, which had a prominent expression of nuclear GARP in nearly every cell (Figure 3B, IT-726-2 upper panel). GARP expression was also examined on IT-726 cell lines grown in self-renewal-promoting (NB+bFGF/+EGF) versus differentiation-promoting (NB-bFGF/-EGF) conditions. Interestingly, IT-726-2 displayed a prominent expression of nuclear GARP in almost every cell regardless of culture condition. In contrast, other isogenic IT-726 lines exhibited a mixed pattern of GARP localization in both nuclear and cytoplasmic compartments in self-renewal-promoting conditions (NB+bFGF/+EGF) (Figure 3B, shown for IT-726-4). Notably, the nuclear localization of GARP appeared to be more profound when cells were grown in differentiation-promoting conditions (NB-bFGF/-EGF), suggesting an inverse correlation between $GARP^{NU+}$ and self-renewal capacity. The IT-726-2 line, in which the $GARP^{NU+}$ pattern was predominant (Figure 3B), had a lower self-renewal capacity when compared to the other isogenic counterparts (Figure S1A), consistent with this interpretation.

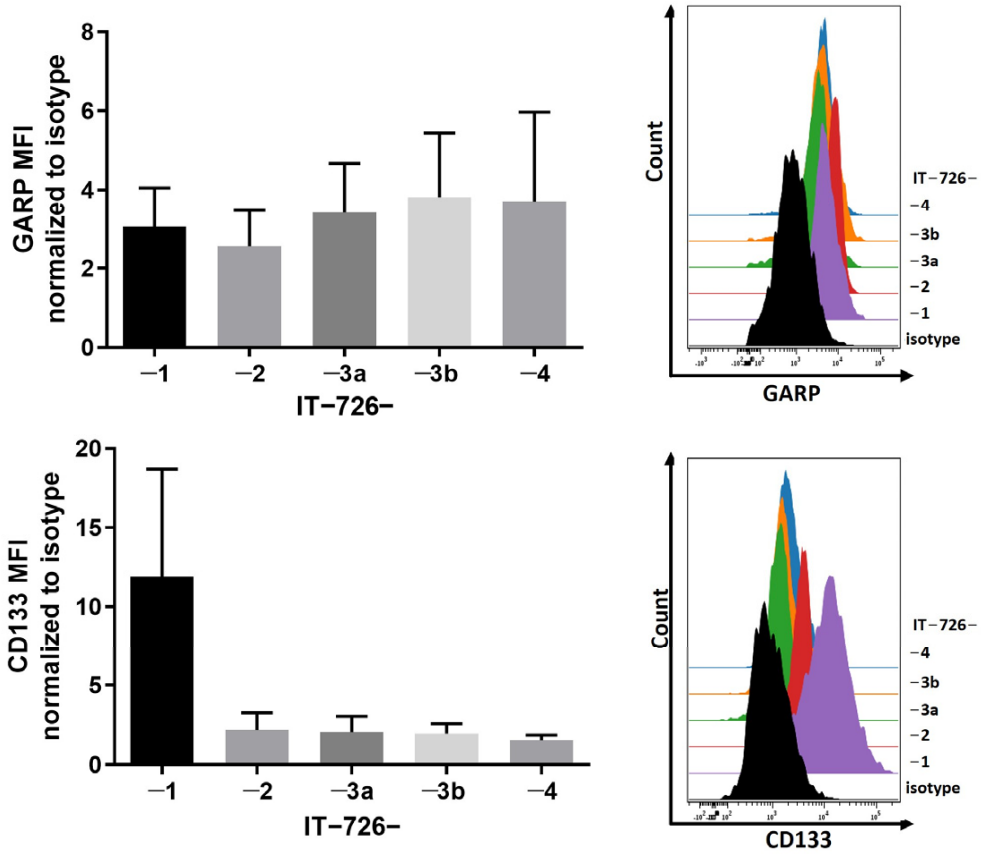

Figure 2. GARP expression in isogenic GSCs derived from newly diagnosed GB IT-726. Flow cytometric analysis of IT-726-1, -2, -3a, -3b, and -4. Doublets, debris, and dead cells were excluded from analysis. Mean fluorescence intensity (MFI) was normalized to the MFI of the unstained control. Histograms display one representative result of three independent measurements. Data are displayed as mean values ± SEM.

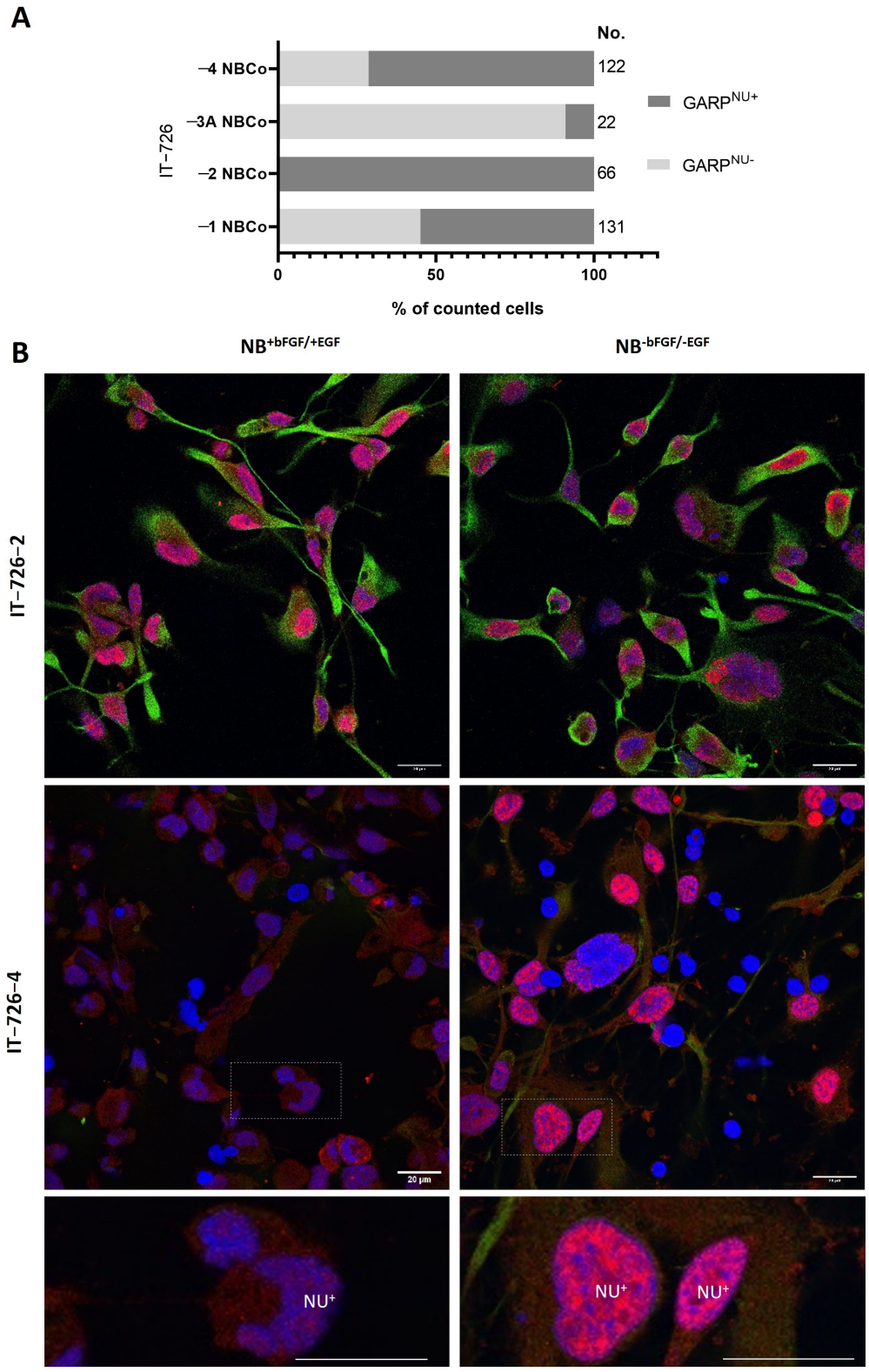

Figure 3. Analysis of expression and localization of GARP in isogenic GSC cell lines, which vary in differentiation states derived from different regions of the same tumor. (**A**) Number of GARP positive nuclei for GSC lines IT-726—1, -2, -3A, and -4 were analyzed by counting double positive (Hoechst and GARP) cell nuclei (NU^+). "No." indicates the number of counted cells for the analysis. (**B**) Confocal images of GARP- and nestin-expressing GSC IT-726 -2 and -4. Cells were stained for their nuclei with Hoechst (blue), GARP (red), and nestin (green). Note the intranuclear localization of GARP. Scale bar corresponds to 20 µm.

3.3. Relationship between GARP Expression and GSCs Stemness

The dual capacity of self-renewal and differentiation are the fundamental and unique properties of stem cells. We therefore sought to determine if there is an association between GARP expression and self-renewal. To this end, cell populations differing in GARP expression ($GARP^{high}$ or $GARP^{low}$) were FACS sorted from the GSC line #1095 and compared with respect to self-renewal activity by ELDA. A demonstration of the sorting efficacy and quantification of surface GARP expression on $GARP^{high}$ vs. $GARP^{low}$ sorted cells via flow cytometry can be found in Figure S6A. The GSC line #1095 was chosen for these investigations because of its well-established stemness attributes as well as molecular and cellular responses to clinically relevant treatments in vitro and in vivo [28,33–35]. The results of ELDA assessments revealed that $GARP^{high}$ and $GARP^{low}$ populations of GSCs differ in their self-renewal propensity, which was significantly ($p = 2.48 \times 10^{-16}$) lower in the $GARP^{high}$ subpopulation compared to $GARP^{low}$ subpopulation (Figure 4).

As loss of self-renewal is a prerequisite for stem cell differentiation, the outcome of the ELDA experiments raised the possibility that GARP expression may be related to differentiation of GSCs. To address this question, $GARP^{high}$ and $GARP^{low}$ GSCs were subjected to comparative assessments for the differentiation-inducing factor p21 and the differentiation-associated markers, GFAP and PDGFRα, activated during astrocyte or oligodendrocyte differentiation. The results showed that $GARP^{high}$ GSCs had considerably higher steady-state levels of p21 compared to $GARP^{low}$ GSCs, which seems consistent with the interpretation that increased expression of GARP is associated with a more differentiated state. However, an elevated level of p21 was unaccompanied by increased expression of GFAP or PDFGRα in $GARP^{high}$ GSCs. Quite the contrary, the expression of either GFAP or PDFGRα was found to be lower in $GARP^{high}$ GSCs than in $GARP^{low}$ GSCs (Figure 5) with the difference in PDGFRα levels being especially profound (Figure 5B). Although the difference in GFAP expression between $GARP^{high}$ and $GARP^{low}$ GSCs was less profound, it was also confirmed by using a different approach, namely the estimation of GFAP-positive differentiating cells by immunofluorescence staining (Figure S10). A decline in proliferative activity is an important functional hallmark of normal stem cell differentiation. Deviating from this rule, $GARP^{high}$ GSCs, which had a reduced self-renewal capacity in comparison to $GARP^{low}$ GSCs (Figure 4), had comparable levels of the proliferation marker PHH3 (Figure 5). Collectively, our data indicate that increased expression of GARP correlates with reduced self-renewal but not with the cessation of proliferation or induction of phenotypic traits of neural differentiation.

3.4. GARP mRNA and Surface Protein Levels Do Not Predict GB Patient Survival

Having established that GARP is expressed in patient-derived GSCs, we sought to determine whether a correlation exists between GARP expression and GB patient survival. To address this question, gene expression and survival data from the TCGA database were analyzed for GARP and CD133 by using OncoLnc.org (Figure S9—Cohort 1) [43–45]. Based on the TCGA dataset, consisting of 152 patients with newly diagnosed glioblastomas, all patients analyzed were stratified by their expression levels of GARP into either "GARP-high" (upper 50%) or "GARP-low" (lower 50%) groups and were analyzed for their survival rates via the online tool OncoLnc [43]. We could not find any significant difference in survival between GARP-high and GARP-low groups (Figure 6A). Similarly, no significant correlation was found between survival and CD133 expression (Figure 6A). In a second approach, GARP and CD133 transcript levels were compared between newly diagnosed glioblastomas (ndGB) and progressed recurrent glioblastomas (recGB) as depicted in Figure S9—Cohort 2—comparison line 2. To this end, we retroactively analyzed RNAseq data from a database that compiles RNAseq data for ndGBs (23 patients) or recGBs (21 patients) as well as 27 primary cultures derived from either ndGB (ndGB-GSCs, 17 cultures) or recGB (recGB-GSCs, 10 cultures) [34]. GARP and CD133 mRNA expression were compared between ndGB samples (ndGB tissues and ndGB-GSC cultures) and recGB samples (recGB tissues and recGB-GSCs). The results showed that expression levels of GARP do not differ

significantly between ndGB and recGB samples whereas CD133 levels were found to be significantly reduced in recGB samples compared to ndGB samples (Figure 6B). In a third approach, surface GARP expression was compared between isogenic ndGB-GSCs and recGB-GSCs isolated from ndGB and recGB tumors of the same patient (Figure S9—Cohort 2—comparison line 3). Both ndGB-GSCs and recGB-GSCs showed virtually the same levels of surface GARP expression, whereas the level of CD133 was significantly lower in recGB-GSCs in comparison to ndGB-GSCs (Figure 6C). This agreed with the results of the RNAseq analysis (Figure 6B) as both GARP transcript and surface GARP (Figure 6C) levels were consistently expressed regardless of disease progression. Interestingly, in contrast to GARP transcript and surface GARP levels, it was found that the percentage of $GARP^{NU+}$ cells were elevated in the recurrent GSC line, IT-654 (Figure 6D).

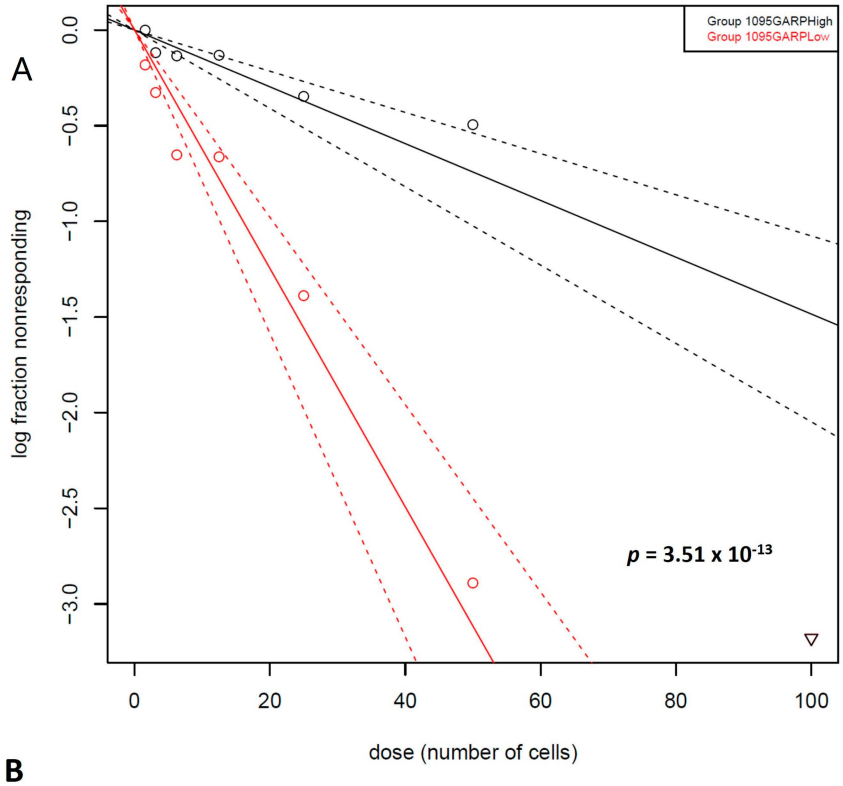

B

1095 subline	Stem cell frequency (1/SCF)			*p* value
	Lower	Estimated	Upper	
$GARP^{High}$	18.75	16.30	14.16	2.48×10^{-16}
$GARP^{Low}$	8.58	7.49	6.53	

Figure 4. Quantitative assessments of self-renewal capacity by extreme limiting dilution assay (ELDA). (**A**) Representative results. (**B**) The pooled results from three independent experiments are indicated in the table. $GARP^{high}$ and $GARP^{low}$ correspond to isogenic GSCs differing in their GARP expression, which were FACs sorted from the GSC line #1095. Estimates of the stem cell frequency (SCF) are framed in red, while lower and upper indicate the confidence intervals for 1/SCF. Statistical significance between groups was calculated by chi-squared tests.

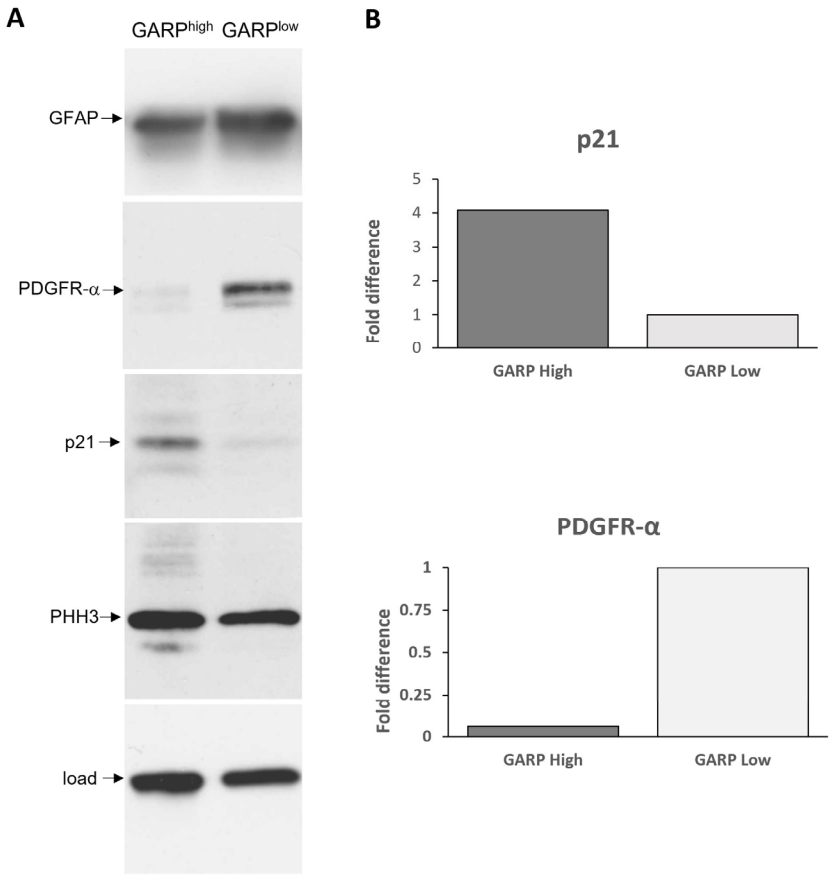

Figure 5. Comparative assessments of glial fibrillary acidic protein (GFAP), platelet-derived growth factor receptor alpha (PDGFR-α), p21, and phosphorylated histone H3 (PHH3) in FACs-sorted $GARP^{high}$ and $GARP^{low}$ isogenic GSCs (#1095) by Western blot. (**A**) Representative results. HSP70 was used as a loading control. The following antibodies were used to probe the membranes: anti-GFAP (DAKO, Z0334), anti-PDFGR-α (D13C6) (Cell Signaling, #5241T), anti-p21 (Cell Signaling, #2947), anti-phospho-histone H3 (Ser28) (Cell Signaling, #9713S), anti-HSP70 (Enzo Life Sciences Inc.), anti-mouse IgGκ light chain-binding protein horseradish peroxidase (Santa Cruz Biotechnology, sc-516102), and goat anti-rabbit IgG H&L horseradish peroxidase (Abcam, ab205718). (**B**) PDGFR-α and p21 bands were quantified by densitometry.

Collectively, these results obtained via different experimental approaches indicate that expression of GARP mRNA and surface protein remain at a constant level throughout GB progression and after therapy—in contrast to the fluctuating expression of CD133. This sustained expression of surface GARP and GARP transcript levels in ndGBs and recGBs suggests the potential utility of GARP as a reliable GSC biomarker, which persists at different tumor stages, possibly allowing for the detection of potential residual disease of a remarkably invasive cancer type.

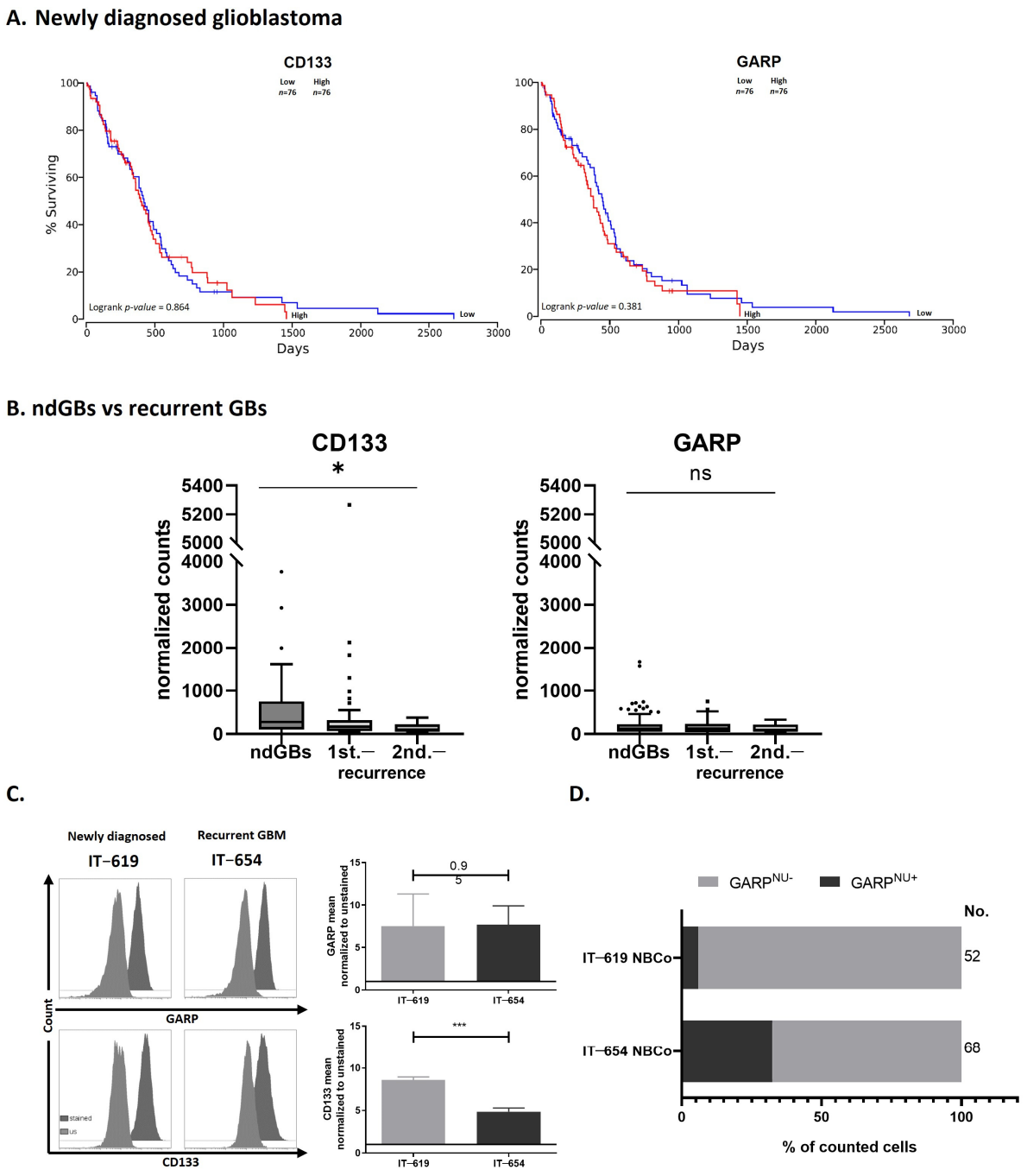

Figure 6. GARP expression in GB is unaffected throughout therapy. (**A**) Survival analysis of GARP and CD133 based on data available through The Cancer Genome Atlas (TCGA). GARP and CD133 mRNA expression data of 152 primary glioblastomas were divided 50/50 into either "low" expression or "high" expression and were analyzed for patient survival. (**B**) Retrospective analysis of transcriptomic data of 155 GB samples from 28 patients of Kim et al., 2020 [32]. ndGBs, first, and second recurrent tumors were analyzed for their GARP and CD133 mRNA levels across tumor stages. (**C**) Flow cytometric analysis of IT-619 and IT-654. Doublets, debris, and dead cells were excluded from analysis. Recurrent IT-654 GSCs exhibited stable surface GARP levels after TMZ and radiotherapy, whereas expression of CD133 decreased after treatment. The MFIs were normalized to the unstained control. $n = 3$. Significance was calculated by Student´s t-test and is indicated as follows: * $p < 0.05$, *** $p < 0.001$, and ns (not significant). (**D**) Number of GARP-positive nuclei for GSC IT-619 and IT-654 were analyzed by counting double-positive (Hoechst and GARP) cell nuclei. "No." indicates the number of counted cells for the analysis.

3.5. Nuclear Localization of GARP Correlates with Poor Survival in Patients with GB

As we observed an upregulation of the percentage of GARP^{NU+} cells in the recurrent GSC line, IT-654 (Figure 6D), we wanted to explore a possible link between GARP^{NU+} and the survival rate of GB patients (Figure S9—Cohort 3). Therefore, we retroactively assessed GARP^{NU+} levels in tumor tissue from a cohort of 35 newly diagnosed GB patients (WHO stage IV) and correlated them to patient overall survival (Figure 7, representative images) [7].

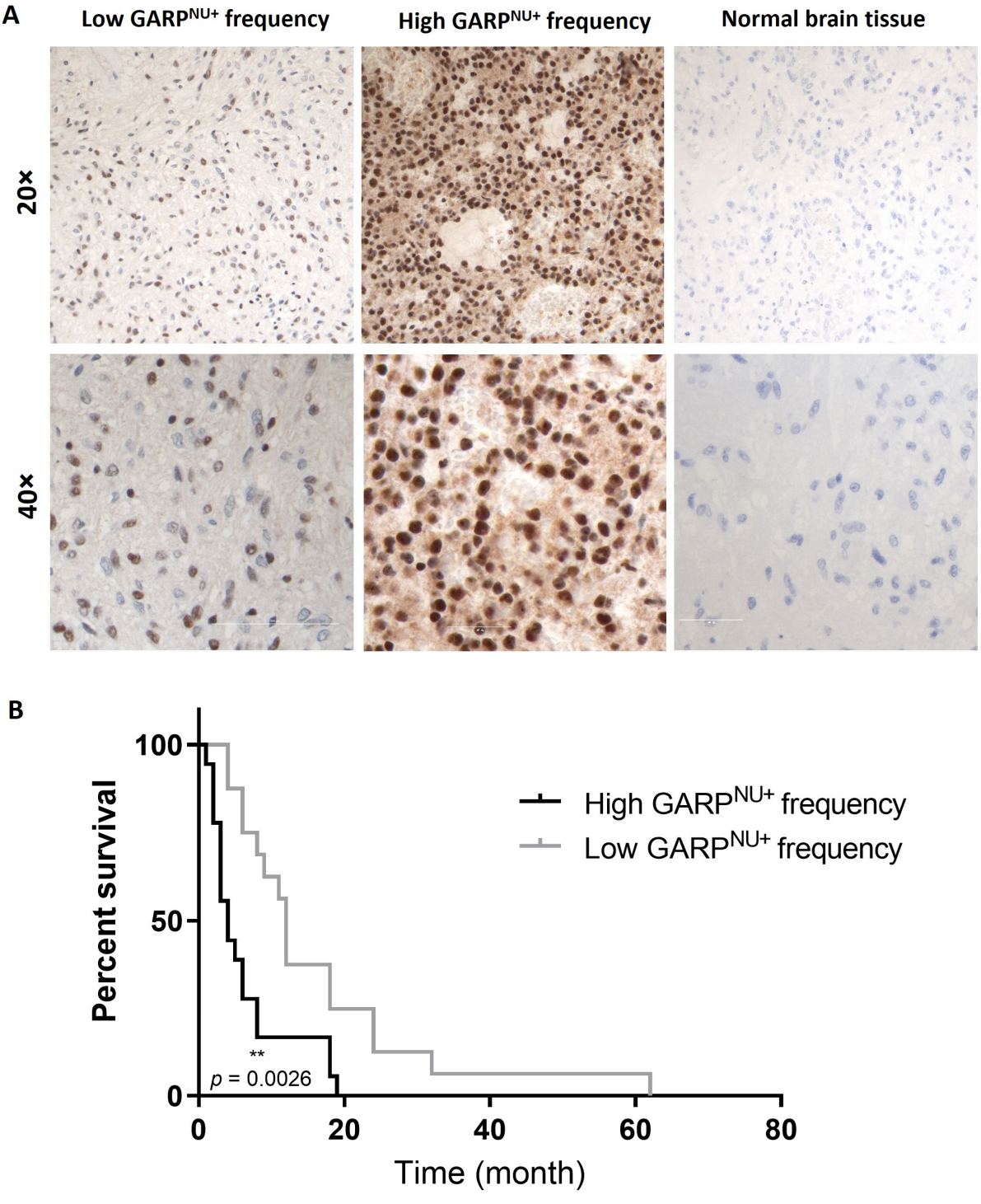

Figure 7. Nuclear GARP is a potential new prognostic biomarker for GB patient survival. (**A**) Immunohistochemistry of GARP in glioblastoma. GB (WHO grade IV) with low frequency of labeled

nuclei (magnification ×20 and ×40) and GB with palisading necroses and a high frequency of stained nuclei (magnification ×20 and ×40). Normal brain tissue had no detectable GARP expression. Bar corresponds to 50 µm (40×) and 200 µm (20×), respectively. (**B**) Survival analysis of 35 GB patients based on their GARP-positive nuclei counts (1: high frequency, $n = 16$ and 2: low frequency, $n = 19$). Comparison of survival curves was performed by log-rank (Mantel–Cox) test (** $p < 0.01$).

Notably, all GB patients in the cohort were found to express $GARP^{NU+}$ but varied in their frequency of $GARP^{NU+}$ cells. Therefore, we divided the cohort into two groups based on their frequency of $GARP^{NU+}$ expression. The first group encompassed 19 GB patients with tumors having a low frequency (~50%) of $GARP^{NU+}$ cells. The other group included 16 patients with a high frequency (>90%) of $GARP^{NU+}$ cells. In striking contrast with the transcriptomic analysis, which showed a consistent lack of correlation between GARP mRNA levels and patient survival (Figure 6A), stratification by $GARP^{NU+}$ revealed a significant correlation between $GARP^{NU+}$ and GB patient survival (Figure 7B). The results showed that patients with a low frequency of $GARP^{NU+}$ had a significantly longer overall survival in comparison to patients with a high frequency of $GARP^{NU+}$ (medians low: 12 months, high: 4 months; $p = 0.0026$, Figure 7B). These results indicate that the abundance of the GARP protein in the nuclear compartment—not GARP transcript levels—is associated with survival in patients with GB.

4. Discussion

GSCs comprise a heterogenous and highly volatile group of cells, which can switch between different phenotypes and molecular programs in response to environmental changes. The high degree of phenotypic plasticity displayed by GSCs poses a challenge in the development of GSC-based diagnostic and GSC-targeting therapeutic strategies. The continuing search for GSC-associated markers has led to the identification of several molecules expressed in some but not all subtypes of human GSCs or associated with some but not all cellular states [11,12]. One approach to counterbalance the phenotypic diversity of GSCs is to simultaneously target multiple markers associated with different types of GSCs, in order to increase the diagnostic coverage of the GSC content in a highly heterogeneous milieu of GBs [11,28,32,47,48]. An alternative possibility is that some phenotypic traits may be conserved across heterogeneous GSCs. Our data indicate that expression of GARP/ $GARP^{NU+}$ may be one such trait. We provide several lines of evidence that GARP/$GARP^{NU+}$ is expressed in otherwise phenotypically distinct GSCs (Figures 1 and 3) and persists invariably across different cellular states (Figure 3). In the past, several groups have tried to identify universal GSC markers. One challenge is that most of the previously identified putative markers of GSCs, e.g., CD133, are not universally expressed in all types of GSCs, which limits the diagnostic utility of such markers for estimating GSC content in tumors [26]. In this regard, both surface GARP and $GARP^{NU+}$ expression appear to be invariably expressed in phenotypically distinct GSCs including $CD133^{+}$ and $CD133^{-}$ subtypes, under in vitro and in vivo experimental conditions (Figures 1, 3 and S8) and in different stages of GB progression (ndGBs or recGBs) (Figure 6).

Our data indicate that GSC-associated expression of GARP persists in different cellular states. However, the degree of GARP expression varies between different cellular states. Interestingly, we find that expression of GARP is elevated in the state associated with a reduced self-renewal but not proliferative capacity and in conjunction with loss of differentiation-associated traits (Figures 4, 5 and S10). Such a pattern is reminiscent of the transit-amplifying state during neurogenesis whereby slow-cycling neural stem cells must first exit from the state of self-renewal and convert into more differentiated but uncommitted and fast-proliferating transit-amplifying progenitors, prior to entering the lineage-commitment stage and differentiation [49]. The simultaneous reduction in self-renewal and differentiation-associated traits without loss of the proliferation activity seen in $GARP^{high}$ GSCs suggests that GARP may have a role in GSCs' transition from the

slow-cycling self-renewal state to a more differentiated and proliferation-competent state similar to that of transit-amplifying progenitors. It should be noted that even the complete loss of self-renewal does not lead to a loss of the tumor-propagating capacity of GSCs, and recent evidence indicates that GB propagation is driven primarily not by self-renewing GSCs but their non-self-renewing progenies [50].

It is important to note that GARP expression is not limited to GSCs alone. Cancer cells, including glioblastoma (as shown in this work with T98G in Figure 1A), activated regulatory T cells and B cells, and platelets are all known to express GARP on their surfaces [28]. Therefore, GARP alone cannot be used to identify GSCs but rather in combination with a panel of other markers to better distinguish between GSCs and other GARP-positive cells in the tumor microenvironment. In this regard, our finding that elevated GARP expression coincides with a significant increase in p21 expression suggests that dual assessments for GARP and p21 may enable a distinguishment between GSC and non-GSC cells. Considering that p21 plays important roles in the maintenance of neural stem cells and is one of the factors implicated in GB radioresistance, the concomitant elevation of p21 and GARP in GSCs further supports the potential merits of GARP as a predictive and prognostic biomarker for GB [51,52]. A limitation of this exploratory work is that it mainly analyzed the expression of GARP in comparison to one GSC reference marker, CD133. Future studies are needed to analyze in depth the association of GARP expression with an expanded panel of putative GSC markers to further evaluate how universally and stably expressed GARP is on GSCs, and on different cellular components of the tumor microenvironment, especially those that are known to express GARP, like activated regulatory T cells and platelets.

Intriguingly, whereas GARP mRNA levels are comparable between ndGBs and recGBs, the level of $GARP^{NU+}$ protein correlated with poor survival in patients with GB (Figure 7). Notably, the critical cutoff for $GARP^{NU+}$ was >90% (Figure 7), which is significantly higher than the 10% cutoff for CD133 expression implicated as a predictive marker for GB recurrence [53].

Although the link between a high frequency of nuclear GARP and poor outcomes of GB patients provides a novel and intriguing insight into the previously unsuspected role of $GARP^{NU}$ in GB, it is important to also acknowledge the limitations of this exploratory study. One is the small patient cohort size (n = 35). The relationship between $GARP^{NU+}$ and clinical outcome from GB must be validated in future studies using larger datasets. A further confirmation in larger follow-up studies is a prerequisite for the conclusion on the diagnostic value of $GARP^{NU+}$ as a prognostic biomarker for GB.

Cancer stem cells are related to reduced survival in glioblastoma patients [11,12]. Therefore, it was surprising to see that a high frequency of $GARP^{NU+}$ tumor cells was linked to reduced overall survival, despite the observed upregulation of $GARP^{NU+}$ in differentiation-promoting conditions (NB-bFGF/-EGF) (Figure 3B). One possible explanation for this is that elevated GARP levels are linked to enhanced immunosuppression in the tumor microenvironment [7,39]. In more detail, previously, we demonstrated both in melanoma [39] and in glioblastoma [7] that tumor cells upregulate the expression of GARP and thus gain tolerogenic potential. This in turn aids in the suppression of effector $CD4^+$ and $CD8^+$ T cell function, required for anti-tumor immune responses, and correspondingly induces suppressive regulatory T cells, which further contribute to the suppression of effective anti-tumor immune responses. Furthermore, the upregulation of GARP, an inhibitory protein, upon the differentiation process of cancer stem cells is consistent with previous reports by Ullah et al., 2020, who similarly demonstrated that the immune checkpoints PD-L1 and HLA-G are upregulated by cancer stem cells upon differentiation [54]. The principal binding partner of GARP, TGF-β, has been shown to induce the expression of PD-L1, but it remains unclear if GARP expression can as well [55,56]. It is worth noting that the simultaneous targeting of GARP, TGF-β1, and PD-1 has been shown to be an effective combination therapy, capable of restoring T effector cell function and overcoming resistance to PD-1/PD-L1 blockade [57,58]. Future studies are planned to clarify the relationship

between GARP, PD-L1, and differentiation to determine if their contribution to immune suppression is responsible for the observed reduction in patient survival.

Interestingly, we found a discrepancy between RNAseq data from primary tumor tissue samples (Figure 6A) and our histological analysis of the frequency of GARP^{NU+}-positive cells in GB patient samples (Figure 7). Whereas no relationship between GARP transcript levels and patient survival was detectable in the TCGA data (Figure 6A), the frequency of GARP^{NU+} GB cells seems to be a suitable prognostic marker for patient survival. It should be considered that the tissue samples used for TCGA RNAseq analysis (Figure 6A) presumably consisted of tumor lysates, which contain a multitude of cell types, ranging from tumor cells to immune cells, up to healthy tissue. As information on the cellular origin of the transcripts is missing due to the bulk sequencing, otherwise significant differences between donors can be diluted into insignificant results based on the individual composition and frequencies of cell types included in the analysis. In addition, GARP mRNA can be detected in many tissues, e.g., heart, kidney, liver, and lung, whereas surface expression of the GARP protein itself seems to be limited to only a number of cell types, e.g., activated regulatory T cells [59], platelets [60], various cancers like GB and malignant melanoma [7,39], and mesenchymal stem cells [61], further contributing to a decreasing validity. Therefore, the identification of the cell type analyzed in RNAseq is key to interpreting and understanding future datasets.

More advanced methods like spatial transcriptomics, multiplex immunofluorescence, and spatial multi-omics single-cell imaging are more fitting to further enhance our understanding of GARP transcript and protein levels in glioblastoma cells and their surrounding microenvironment, as well as their distribution within subcellular compartments [62]. The additional information gained by these techniques would enable the identification of different cell types, their localization within the tumor and relation to other cells of the tumor microenvironment, and the determination of whether a surface or intranuclear localization of the GARP protein is present in these cells. Furthermore, the exclusion of certain cell types (e.g., regulatory T cells or platelets) from the analysis would enable a better understanding of GARP and its subcellular localization on patient outcomes.

Our data suggest that nuclear localization of the GARP protein—rather than abundance of the GARP transcript—is a factor associated with GB progression after therapy. Our finding that GARP is localized to the nucleus is novel and intriguing, as GARP has previously been characterized only as a surface and secreted protein, which currently has no annotated nuclear localization signal (NLS). Interestingly, the use of nuclear localization of an otherwise surface-associated protein as a prognostic marker has been described before [63–65]. One such example is the protein Src, which plays a key role in cell morphology, motility, proliferation, and survival [66]. Urciuoli et al., 2017, was able to show in human osteosarcoma that nuclear localization of Src correlates with overall survival and therefore has relevance as a prognostic marker for osteosarcoma patients [64]. Likewise, it has also been described that PD-L1, a T cell inhibitory molecule in cancer, shows a nuclear localization as a reaction to therapy. In more detail, PD-L1 is translocated from the cell surface into the nucleus as a reaction to high-dose doxorubicin therapy regimens. The nuclear localization of PD-L1 was described as a prognostic biomarker, as patients with low PD-L1 nuclear expression had significantly fewer circulating cancer cells and exhibited a longer overall survival [63,65]. While the mechanisms of GARP nuclear localization in GSCs still have to be elucidated, the potential clinical implications of this previously unknown phenomenon are clear given the critical role of GARP in the activation of TGF-β, one of the key factors [67] contributing to GB progression particularly via the maintenance of GSCs via the induction of, e.g., Sox2 and LIF expression [68,69]. Considering that targeting TGF-β-activating ligands in GB has been intensively explored as a promising therapeutic strategy [67,70], the clarification of GARP^{NU+} activities in GSCs may provide novel insights into the interaction of GARP and TGF-β, as TGF-β activation is known to trigger the nuclear localization of proteins like Smad and Smad4 [71]. Further pointing to the potential merit of GARP as a diagnostic and therapeutic target is the dual impact of GARP on cancer

progression—via the modulation of regulatory T cells and through the direct activities of GARP exerted on cancer (stem) cells themselves.

5. Conclusions

The scope of the present study was to evaluate GARP as a biomarker for heterogeneous GSCs and to determine the effects of GARP on GB patient outcomes. Based on our data, we propose that GARP^{NU+} could potentially serve, in combination with existing GSC markers, as a universal and stably expressed marker for different subsets and cellular states of GSCs as well as a possible prognostic marker for patient outcomes in GB. We propose that GARP assessments may provide the means to identify not only self-renewing GSCs but also their progenies that exit from self-renewal but retain proliferative activity. Further validation of this hypothesis in future studies will require analyses of larger patient cohorts using an extended panel of markers associated with GSCs and GB progression. Future investigations should focus on addressing mechanistic questions, such as the functional significance of GARP in regulating GSC-specific functions, by employing knockdown and/or overexpressing lines, as well as further investigating the role of nuclear GARP, its nuclear retention, and functional relevance.

Supplementary Materials: The following supporting information can be downloaded at: https://www.mdpi.com/article/10.3390/cancers15245711/s1, Figure S1: Heterologous GSC lines differing in their self-renewal capacity, Figure S2: Anti-GARP antibody validation for flow cytometry, Figure S3: Specificity demonstration and validation of anti-GARP antibodies, Figure S4: Flow cytometric gating strategy for GSCs, Figure S5: Anti-GARP antibody validation for confocal microscopy, Figure S6: Flow cytometric gating strategy for GARP^{high} and GARP^{low} sorted GSCs, Figure S7: Invasive xenograft tumors arisen from GSC lines, #1051 and #1043, Figure S8: GARP is expressed in xenograft tumors arisen from GSC lines, #1051 and #1043, Figure S9: Study design and models used for the assessment of GARP, Figure S10: Frequency of GFAP^{+} GARP^{high} and GARP^{low} GSCs.

Author Contributions: Conceptualization: N.Z., A.T., E.K., J.T., F.R., V.M. and C.S.; methodology: N.Z., E.R.T., A.M., P.L. (Philipp Licht), P.L. (Petra Leukel) and B.S.; validation: N.Z. and E.R.T.; formal analysis: N.Z., E.R.T., A.M. and P.L. (Philipp Licht); resources: A.T. and E.K.; writing—original draft: N.Z., E.R.T., A.T. and E.K.; writing—review and editing: all authors; visualization, N.Z.; project administration: N.Z.; supervision: A.T. and E.K.; funding acquisition: A.T. and E.K. All authors have read and agreed to the published version of the manuscript.

Funding: This research was funded by CRC1066, TP-B14 to A.T., Wilhelm-Sander-Foundation (2020.132.2) to A.T., and Hiege-Stiftung against skin cancer (200504) to A.T., a DAAD One-Year Research Grant for Doctoral Candidates (57552339) to E.R.T., and a FAZIT PhD Fellowship (090892021) to A.M.

Institutional Review Board Statement: The use of tumor tissue for research purposes was approved by the JG-UMC Institutional Review Board (permission 08.06.2017 #837.211.12(8312-F) and patients' informed consent. Animal experiments were performed in the Translational Animal Research Facility (TARC) of the JG-UMC, Germany, in accordance with the guidelines of the European Convention for the Protection of Vertebrates Used for Scientific Purposes and under the approval from the State Office of Chemical Investigations of Rhineland-Palatinate (permission #23 177-07/G12-1-020).

Informed Consent Statement: Written informed consent of all patients was obtained for "scientific use of tumor tissue not needed for histopathological diagnosis" in the admission contract of Idar-Oberstein hospital.

Data Availability Statement: Data are available in a publicly accessible repository that does not issue DOIs. Publicly available datasets were analyzed in this study. This data can be found here: https://www.ncbi.nlm.nih.gov/geo/query/acc.cgi?acc=GSE139533 and here: http://www.oncolnc.org/ (accessed on 9 April 2021).

Acknowledgments: We thank the Imaging Core Facility of the Cell Biology Unit (CBU) of Krishnaraj Rajalingam in the PKZI Mainz for providing the Leica SP8 microscope. We thank Kristian Schuetze, manager of the Flow Cytometry Core Facility (CFFC) of the PKZI Mainz, for his technical assistance in cell sorting. We thank the CFFC for providing the BD Aria II and III cell sorters.

Conflicts of Interest: The authors declare no conflict of interest.

References

1. Wen, P.Y.; Weller, M.; Lee, E.Q.; Alexander, B.M.; Barnholtz-Sloan, J.S.; Barthel, F.P.; Batchelor, T.T.; Bindra, R.S.; Chang, S.M.; Chiocca, E.A.; et al. Glioblastoma in adults: A Society for Neuro-Oncology (SNO) and European Society of Neuro-Oncology (EANO) consensus review on current management and future directions. *Neuro Oncol.* **2020**, *22*, 1073–1113. [CrossRef] [PubMed]
2. Louis, D.N.; Perry, A.; Reifenberger, G.; von Deimling, A.; Figarella-Branger, D.; Cavenee, W.K.; Ohgaki, H.; Wiestler, O.D.; Kleihues, P.; Ellison, D.W. The 2016 World Health Organization Classification of Tumors of the Central Nervous System: A summary. *Acta Neuropathol.* **2016**, *131*, 803–820. [CrossRef] [PubMed]
3. Stupp, R.; Mason, W.P.; van den Bent, M.J.; Weller, M.; Fisher, B.; Taphoorn, M.J.B.; Belanger, K.; Brandes, A.A.; Marosi, C.; Bogdahn, U.; et al. Radiotherapy plus concomitant and adjuvant temozolomide for glioblastoma. *N. Engl. J. Med.* **2005**, *352*, 987–996. [CrossRef] [PubMed]
4. Campos, B.; Olsen, L.R.; Urup, T.; Poulsen, H.S. A comprehensive profile of recurrent glioblastoma. *Oncogene* **2016**, *35*, 5819–5825. [CrossRef] [PubMed]
5. Gallego, O. Nonsurgical treatment of recurrent glioblastoma. *Curr. Oncol.* **2015**, *22*, e273–e281. [CrossRef] [PubMed]
6. Lim, M.; Xia, Y.; Bettegowda, C.; Weller, M. Current state of immunotherapy for glioblastoma. *Nat. Rev. Clin. Oncol.* **2018**, *15*, 422–442. [CrossRef] [PubMed]
7. Zimmer, N.; Kim, E.; Sprang, B.; Leukel, P.; Khafaji, F.; Ringel, F.; Sommer, C.; Tuettenberg, J.; Tuettenberg, A. GARP as an Immune Regulatory Molecule in the Tumor Microenvironment of Glioblastoma Multiforme. *Int. J. Mol. Sci.* **2019**, *20*, 3676. [CrossRef]
8. Cai, X.; Sughrue, M.E. Glioblastoma: New therapeutic strategies to address cellular and genomic complexity. *Oncotarget* **2018**, *9*, 9540–9554. [CrossRef]
9. Ghosh, D.; Nandi, S.; Bhattacharjee, S. Combination therapy to checkmate Glioblastoma: Clinical challenges and advances. *Clin. Transl. Med.* **2018**, *7*, 33. [CrossRef]
10. Bonavia, R.; Inda, M.-M.; Cavenee, W.K.; Furnari, F.B. Heterogeneity maintenance in glioblastoma: A social network. *Cancer Res.* **2011**, *71*, 4055–4060. [CrossRef]
11. Dirkse, A.; Golebiewska, A.; Buder, T.; Nazarov, P.V.; Muller, A.; Poovathingal, S.; Brons, N.H.C.; Leite, S.; Sauvageot, N.; Sarkisjan, D.; et al. Stem cell-associated heterogeneity in Glioblastoma results from intrinsic tumor plasticity shaped by the microenvironment. *Nat. Commun.* **2019**, *10*, 1787. [CrossRef] [PubMed]
12. Gimple, R.C.; Bhargava, S.; Dixit, D.; Rich, J.N. Glioblastoma stem cells: Lessons from the tumor hierarchy in a lethal cancer. *Genes Dev.* **2019**, *33*, 591–609. [CrossRef] [PubMed]
13. Kolenda, J.; Jensen, S.S.; Aaberg-Jessen, C.; Christensen, K.; Andersen, C.; Brünner, N.; Kristensen, B.W. Effects of hypoxia on expression of a panel of stem cell and chemoresistance markers in glioblastoma-derived spheroids. *J. Neurooncol.* **2011**, *103*, 43–58. [CrossRef] [PubMed]
14. Schiffer, D.; Mellai, M.; Annovazzi, L.; Caldera, V.; Piazzi, A.; Denysenko, T.; Melcarne, A. Stem cell niches in glioblastoma: A neuropathological view. *Biomed Res. Int.* **2014**, *2014*, 725921. [CrossRef] [PubMed]
15. Ivanov, V.N.; Hei, T.K. Induction of apoptotic death and retardation of neuronal differentiation of human neural stem cells by sodium arsenite treatment. *Exp. Cell Res.* **2013**, *319*, 875–887. [CrossRef] [PubMed]
16. Natsume, A.; Ito, M.; Katsushima, K.; Ohka, F.; Hatanaka, A.; Shinjo, K.; Sato, S.; Takahashi, S.; Ishikawa, Y.; Takeuchi, I.; et al. Chromatin regulator PRC2 is a key regulator of epigenetic plasticity in glioblastoma. *Cancer Res.* **2013**, *73*, 4559–4570. [CrossRef] [PubMed]
17. Lathia, J.D.; Mack, S.C.; Mulkearns-Hubert, E.E.; Valentim, C.L.L.; Rich, J.N. Cancer stem cells in glioblastoma. *Genes Dev.* **2015**, *29*, 1203–1217. [CrossRef] [PubMed]
18. Günther, H.S.; Schmidt, N.O.; Phillips, H.S.; Kemming, D.; Kharbanda, S.; Soriano, R.; Modrusan, Z.; Meissner, H.; Westphal, M.; Lamszus, K. Glioblastoma-derived stem cell-enriched cultures form distinct subgroups according to molecular and phenotypic criteria. *Oncogene* **2008**, *27*, 2897–2909. [CrossRef]
19. Chen, R.; Nishimura, M.C.; Bumbaca, S.M.; Kharbanda, S.; Forrest, W.F.; Kasman, I.M.; Greve, J.M.; Soriano, R.H.; Gilmour, L.L.; Rivers, C.S.; et al. A hierarchy of self-renewing tumor-initiating cell types in glioblastoma. *Cancer Cell* **2010**, *17*, 362–375. [CrossRef]
20. Singh, S.K.; Hawkins, C.; Clarke, I.D.; Squire, J.A.; Bayani, J.; Hide, T.; Henkelman, R.M.; Cusimano, M.D.; Dirks, P.B. Identification of human brain tumour initiating cells. *Nature* **2004**, *432*, 396–401. [CrossRef]
21. Lee, J.; Kotliarova, S.; Kotliarov, Y.; Li, A.; Su, Q.; Donin, N.M.; Pastorino, S.; Purow, B.W.; Christopher, N.; Zhang, W.; et al. Tumor stem cells derived from glioblastomas cultured in bFGF and EGF more closely mirror the phenotype and genotype of primary tumors than do serum-cultured cell lines. *Cancer Cell* **2006**, *9*, 391–403. [CrossRef] [PubMed]
22. Son, M.J.; Woolard, K.; Nam, D.-H.; Lee, J.; Fine, H.A. SSEA-1 is an enrichment marker for tumor-initiating cells in human glioblastoma. *Cell Stem Cell* **2009**, *4*, 440–452. [CrossRef]
23. Ludwig, K.; Kornblum, H.I. Molecular markers in glioma. *J. Neurooncol.* **2017**, *134*, 505–512. [CrossRef] [PubMed]
24. Beier, D.; Hau, P.; Proescholdt, M.; Lohmeier, A.; Wischhusen, J.; Oefner, P.J.; Aigner, L.; Brawanski, A.; Bogdahn, U.; Beier, C.P. CD133(+) and CD133(-) glioblastoma-derived cancer stem cells show differential growth characteristics and molecular profiles. *Cancer Res.* **2007**, *67*, 4010–4015. [CrossRef] [PubMed]

25. Ogden, A.T.; Waziri, A.E.; Lochhead, R.A.; Fusco, D.; Lopez, K.; Ellis, J.A.; Kang, J.; Assanah, M.; McKhann, G.M.; Sisti, M.B.; et al. Identification of A2B5+CD133- tumor-initiating cells in adult human gliomas. *Neurosurgery* **2008**, *62*, 505–514. [CrossRef]
26. Bao, S.; Wu, Q.; McLendon, R.E.; Hao, Y.; Shi, Q.; Hjelmeland, A.B.; Dewhirst, M.W.; Bigner, D.D.; Rich, J.N. Glioma stem cells promote radioresistance by preferential activation of the DNA damage response. *Nature* **2006**, *444*, 756–760. [CrossRef]
27. Tang, X.; Zuo, C.; Fang, P.; Liu, G.; Qiu, Y.; Huang, Y.; Tang, R. Targeting Glioblastoma Stem Cells: A Review on Biomarkers, Signal Pathways and Targeted Therapy. *Front. Oncol.* **2021**, *11*, 701291. [CrossRef]
28. Barrantes-Freer, A.; Renovanz, M.; Eich, M.; Braukmann, A.; Sprang, B.; Spirin, P.; Pardo, L.A.; Giese, A.; Kim, E.L. CD133 Expression Is Not Synonymous to Immunoreactivity for AC133 and Fluctuates throughout the Cell Cycle in Glioma Stem-Like Cells. *PLoS ONE* **2015**, *10*, e0130519. [CrossRef]
29. Bidlingmaier, S.; Zhu, X.; Liu, B. The utility and limitations of glycosylated human CD133 epitopes in defining cancer stem cells. *J. Mol. Med.* **2008**, *86*, 1025–1032. [CrossRef]
30. Zimmer, N.; Trzeciak, E.R.; Graefen, B.; Satoh, K.; Tuettenberg, A. GARP as a Therapeutic Target for the Modulation of Regulatory T Cells in Cancer and Autoimmunity. *Front. Immunol.* **2022**, *13*, 928450. [CrossRef]
31. Faußˇ, J.; Sprang, B.; Leukel, P.; Sommer, C.; Nikolova, T.; Ringel, F.; Kim, E.L. ALDH1A3 Segregated Expression and Nucleus-Associated Proteasomal Degradation Are Common Traits of Glioblastoma Stem Cells. *Biomedicines* **2021**, *10*, 7. [CrossRef] [PubMed]
32. Kim, E.L.; Sorokin, M.; Kantelhardt, S.R.; Kalasauskas, D.; Sprang, B.; Fauss, J.; Ringel, F.; Garazha, A.; Albert, E.; Gaifullin, N.; et al. Intratumoral Heterogeneity and Longitudinal Changes in Gene Expression Predict Differential Drug Sensitivity in Newly Diagnosed and Recurrent Glioblastoma. *Cancers* **2020**, *12*, 520. [CrossRef] [PubMed]
33. Barrantes-Freer, A.; Kim, E.; Bielanska, J.; Giese, A.; Mortensen, L.S.; Schulz-Schaeffer, W.J.; Stadelmann, C.; Brück, W.; Pardo, L.A. Human glioma-initiating cells show a distinct immature phenotype resembling but not identical to NG2 glia. *J. Neuropathol. Exp. Neurol.* **2013**, *72*, 307–324. [CrossRef] [PubMed]
34. Kalasauskas, D.; Sorokin, M.; Sprang, B.; Elmasri, A.; Viehweg, S.; Salinas, G.; Opitz, L.; Rave-Fraenk, M.; Schulz-Schaeffer, W.; Kantelhardt, S.R.; et al. Diversity of Clinically Relevant Outcomes Resulting from Hypofractionated Radiation in Human Glioma Stem Cells Mirrors Distinct Patterns of Transcriptomic Changes. *Cancers* **2020**, *12*, 570. [CrossRef]
35. Müller, A.; Weyerhäuser, P.; Berte, N.; Jonin, F.; Lyubarskyy, B.; Sprang, B.; Kantelhardt, S.R.; Salinas, G.; Opitz, L.; Schulz-Schaeffer, W.; et al. Concurrent Activation of Both Survival-Promoting and Death-Inducing Signaling by Chloroquine in Glioblastoma Stem Cells: Implications for Potential Risks and Benefits of Using Chloroquine as Radiosensitizer. *Cells* **2023**, *12*, 1290. [CrossRef] [PubMed]
36. Schneider, C.A.; Rasband, W.S.; Eliceiri, K.W. NIH Image to ImageJ: 25 years of image analysis. *Nat. Methods* **2012**, *9*, 671–675. [CrossRef] [PubMed]
37. Kotecha, N.; Krutzik, P.O.; Irish, J.M. Web-based analysis and publication of flow cytometry experiments. *Curr. Protoc. Cytom.* **2010**, *53*, 10–17. [CrossRef]
38. Kim, E.L.; Wüstenberg, R.; Rübsam, A.; Schmitz-Salue, C.; Warnecke, G.; Bücker, E.-M.; Pettkus, N.; Speidel, D.; Rohde, V.; Schulz-Schaeffer, W.; et al. Chloroquine activates the p53 pathway and induces apoptosis in human glioma cells. *Neuro Oncol.* **2010**, *12*, 389–400. [CrossRef]
39. Hahn, S.A.; Neuhoff, A.; Landsberg, J.; Schupp, J.; Eberts, D.; Leukel, P.; Bros, M.; Weilbaecher, M.; Schuppan, D.; Grabbe, S.; et al. A key role of GARP in the immune suppressive tumor microenvironment. *Oncotarget* **2016**, *7*, 42996–43009. [CrossRef]
40. Schindelin, J.; Arganda-Carreras, I.; Frise, E.; Kaynig, V.; Longair, M.; Pietzsch, T.; Preibisch, S.; Rueden, C.; Saalfeld, S.; Schmid, B.; et al. Fiji: An open-source platform for biological-image analysis. *Nat. Methods* **2012**, *9*, 676–682. [CrossRef]
41. Hu, Y.; Smyth, G.K. ELDA: Extreme limiting dilution analysis for comparing depleted and enriched populations in stem cell and other assays. *J. Immunol. Methods* **2009**, *347*, 70–78. [CrossRef]
42. Love, M.I.; Huber, W.; Anders, S. Moderated estimation of fold change and dispersion for RNA-seq data with DESeq2. *Genome Biol.* **2014**, *15*, 550. [CrossRef] [PubMed]
43. Anaya, J. OncoLnc: Linking TCGA survival data to mRNAs, miRNAs, and lncRNAs. *PeerJ Comput. Sci.* **2016**, *2*, e67. [CrossRef]
44. Brat, D.J.; Verhaak, R.G.W.; Aldape, K.D.; Yung, W.K.A.; Salama, S.R.; Cooper, L.A.D.; Rheinbay, E.; Miller, C.R.; Vitucci, M.; Morozova, O.; et al. Comprehensive, Integrative Genomic Analysis of Diffuse Lower-Grade Gliomas. *N. Engl. J. Med.* **2015**, *372*, 2481–2498. [CrossRef] [PubMed]
45. Ciriello, G.; Miller, M.L.; Aksoy, B.A.; Senbabaoglu, Y.; Schultz, N.; Sander, C. Emerging landscape of oncogenic signatures across human cancers. *Nat. Genet.* **2013**, *45*, 1127–1133. [CrossRef] [PubMed]
46. Bradshaw, A.; Wickremsekera, A.; Tan, S.T.; Peng, L.; Davis, P.F.; Itinteang, T. Cancer Stem Cell Hierarchy in Glioblastoma Multiforme. *Front. Surg.* **2016**, *3*, 21. [CrossRef] [PubMed]
47. Lan, X.; Jörg, D.J.; Cavalli, F.M.G.; Richards, L.M.; Nguyen, L.V.; Vanner, R.J.; Guilhamon, P.; Lee, L.; Kushida, M.M.; Pellacani, D.; et al. Fate mapping of human glioblastoma reveals an invariant stem cell hierarchy. *Nature* **2017**, *549*, 227–232. [CrossRef] [PubMed]
48. Silver, A.; Feier, D.; Ghosh, T.; Rahman, M.; Huang, J.; Sarkisian, M.R.; Deleyrolle, L.P. Heterogeneity of glioblastoma stem cells in the context of the immune microenvironment and geospatial organization. *Front. Oncol.* **2022**, *12*, 1022716. [CrossRef]
49. Miyashita, S.; Hoshino, M. Transit Amplifying Progenitors in the Cerebellum: Similarities to and Differences from Transit Amplifying Cells in Other Brain Regions and between Species. *Cells* **2022**, *11*, 726. [CrossRef]

50. Barrett, L.E.; Granot, Z.; Coker, C.; Iavarone, A.; Hambardzumyan, D.; Holland, E.C.; Nam, H.; Benezra, R. Self-renewal does not predict tumor growth potential in mouse models of high-grade glioma. *Cancer Cell* **2012**, *21*, 11–24. [CrossRef]
51. Jin, X.; Kuang, Y.; Li, L.; Li, H.; Zhao, T.; He, Y.; Di, C.; Kang, J.; Yuan, L.; Yu, B.; et al. A positive feedback circuit comprising p21 and HIF-1α aggravates hypoxia-induced radioresistance of glioblastoma by promoting Glut1/LDHA-mediated glycolysis. *FASEB J.* **2022**, *36*, e22229. [CrossRef] [PubMed]
52. Marqués-Torrejón, M.Á.; Porlan, E.; Banito, A.; Gómez-Ibarlucea, E.; Lopez-Contreras, A.J.; Fernández-Capetillo, O.; Vidal, A.; Gil, J.; Torres, J.; Fariñas, I. Cyclin-dependent kinase inhibitor p21 controls adult neural stem cell expansion by regulating Sox2 gene expression. *Cell Stem Cell* **2013**, *12*, 88–100. [CrossRef] [PubMed]
53. Abdoli Shadbad, M.; Hosseinkhani, N.; Asadzadeh, Z.; Brunetti, O.; Silvestris, N.; Baradaran, B. The Prognostic Value of CD133 in Predicting the Relapse and Recurrence Pattern of High-Grade Gliomas on MRI: A Meta-Analysis. *Front. Oncol.* **2021**, *11*, 722833. [CrossRef] [PubMed]
54. Ullah, M.; Meziani, S.; Shah, S.; Kaci, R.; Pimpie, C.; Pocard, M.; Mirshahi, M. Differentiation of cancer cells upregulates HLA-G and PD-L1. *Oncol. Rep.* **2020**, *43*, 1797–1804. [CrossRef] [PubMed]
55. Ni, X.Y.; Sui, H.X.; Liu, Y.; Ke, S.Z.; Wang, Y.N.; Gao, F.G. TGF-β of lung cancer microenvironment upregulates B7H1 and GITRL expression in dendritic cells and is associated with regulatory T cell generation. *Oncol. Rep.* **2012**, *28*, 615–621. [CrossRef] [PubMed]
56. Song, S.; Yuan, P.; Wu, H.; Chen, J.; Fu, J.; Li, P.; Lu, J.; Wei, W. Dendritic cells with an increased PD-L1 by TGF-β induce T cell anergy for the cytotoxicity of hepatocellular carcinoma cells. *Int. Immunopharmacol.* **2014**, *20*, 117–123. [CrossRef] [PubMed]
57. De Streel, G.; Bertrand, C.; Chalon, N.; Liénart, S.; Bricard, O.; Lecomte, S.; Devreux, J.; Gaignage, M.; de Boeck, G.; Mariën, L.; et al. Selective inhibition of TGF-β1 produced by GARP-expressing Tregs overcomes resistance to PD-1/PD-L1 blockade in cancer. *Nat. Commun.* **2020**, *11*, 4545. [CrossRef]
58. Bertrand, C.; van Meerbeeck, P.; de Streel, G.; Vaherto-Bleeckx, N.; Benhaddi, F.; Rouaud, L.; Noël, A.; Coulie, P.G.; van Baren, N.; Lucas, S. Combined Blockade of GARP:TGF-β1 and PD-1 Increases Infiltration of T Cells and Density of Pericyte-Covered GARP+ Blood Vessels in Mouse MC38 Tumors. *Front. Immunol.* **2021**, *12*, 704050. [CrossRef]
59. Hahn, S.A.; Stahl, H.F.; Becker, C.; Correll, A.; Schneider, F.-J.; Tuettenberg, A.; Jonuleit, H. Soluble GARP has potent antiinflammatory and immunomodulatory impact on human $CD4^+$ T cells. *Blood* **2013**, *122*, 1182–1191. [CrossRef]
60. Zimmer, N.; Krebs, F.K.; Zimmer, S.; Mitzel-Rink, H.; Kumm, E.J.; Jurk, K.; Grabbe, S.; Loquai, C.; Tuettenberg, A. Platelet-Derived GARP Induces Peripheral Regulatory T Cells-Potential Impact on T Cell Suppression in Patients with Melanoma-Associated Thrombocytosis. *Cancers* **2020**, *12*, 3653. [CrossRef]
61. Xing, H.; Liang, C.; Xu, X.; Sun, H.; Ma, X.; Jiang, Z. Mesenchymal stroma/stem-like cells of GARP knockdown inhibits cell proliferation and invasion of mouse colon cancer cells (MC38) through exosomes. *J. Cell. Mol. Med.* **2020**, *24*, 13984–13990. [CrossRef]
62. Asp, M.; Bergenstråhle, J.; Lundeberg, J. Spatially Resolved Transcriptomes-Next Generation Tools for Tissue Exploration. *Bioessays* **2020**, *42*, e1900221. [CrossRef] [PubMed]
63. Ghebeh, H.; Lehe, C.; Barhoush, E.; Al-Romaih, K.; Tulbah, A.; Al-Alwan, M.; Hendrayani, S.-F.; Manogaran, P.; Alaiya, A.; Al-Tweigeri, T.; et al. Doxorubicin downregulates cell surface B7-H1 expression and upregulates its nuclear expression in breast cancer cells: Role of B7-H1 as an anti-apoptotic molecule. *Breast Cancer Res.* **2010**, *12*, R48. [CrossRef]
64. Urciuoli, E.; Coletta, I.; Rizzuto, E.; de Vito, R.; Petrini, S.; D'Oria, V.; Pezzullo, M.; Milano, G.M.; Cozza, R.; Locatelli, F.; et al. Src nuclear localization and its prognostic relevance in human osteosarcoma. *J. Cell. Physiol.* **2018**, *233*, 1658–1670. [CrossRef] [PubMed]
65. Satelli, A.; Batth, I.S.; Brownlee, Z.; Rojas, C.; Meng, Q.H.; Kopetz, S.; Li, S. Potential role of nuclear PD-L1 expression in cell-surface vimentin positive circulating tumor cells as a prognostic marker in cancer patients. *Sci. Rep.* **2016**, *6*, 28910. [CrossRef] [PubMed]
66. Roskoski, R. Src protein-tyrosine kinase structure and regulation. *Biochem. Biophys. Res. Commun.* **2004**, *324*, 1155–1164. [CrossRef] [PubMed]
67. Han, J.; Alvarez-Breckenridge, C.A.; Wang, Q.-E.; Yu, J. TGF-β signaling and its targeting for glioma treatment. *Am. J. Cancer Res.* **2015**, *5*, 945–955. [PubMed]
68. Ikushima, H.; Todo, T.; Ino, Y.; Takahashi, M.; Miyazawa, K.; Miyazono, K. Autocrine TGF-beta signaling maintains tumorigenicity of glioma-initiating cells through Sry-related HMG-box factors. *Cell Stem Cell* **2009**, *5*, 504–514. [CrossRef]
69. Peñuelas, S.; Anido, J.; Prieto-Sánchez, R.M.; Folch, G.; Barba, I.; Cuartas, I.; García-Dorado, D.; Poca, M.A.; Sahuquillo, J.; Baselga, J.; et al. TGF-beta increases glioma-initiating cell self-renewal through the induction of LIF in human glioblastoma. *Cancer Cell* **2009**, *15*, 315–327. [CrossRef]
70. Shaim, H.; Shanley, M.; Basar, R.; Daher, M.; Gumin, J.; Zamler, D.B.; Uprety, N.; Wang, F.; Huang, Y.; Gabrusiewicz, K.; et al. Targeting the αv integrin/TGF-β axis improves natural killer cell function against glioblastoma stem cells. *J. Clin. Investig.* **2021**, *131*, e142116. [CrossRef]
71. Golestaneh, N.; Mishra, B. TGF-beta, neuronal stem cells and glioblastoma. *Oncogene* **2005**, *24*, 5722–5730. [CrossRef]

7 Danksagung

Am Ende dieser Arbeit möchte ich all jenen danken, die mich auf der Reise meiner Dissertation begleitet, ermutigt und unterstützt haben. Ohne Eure vielfätige Hilfe – sei es wissenschaftich, organisatorisch, freundschaftlich oder emotional – wäre dieses Projekt und damit meine Promotion in dieser Form nicht möglich gewesen.

An erster Stelle möchte ich meinem Doktorvater [redacted] danken, der mich als seinen Doktoranden aufgenommen hat, nachdem ich ihn unvermittelt in seiner Sprechstunde an der Hautklinik der Universitätsmedizin Mainz aufgesucht hatte. Es ist alles andere als selbstverständlich, einem jungen Absolventen des Lehramts-Masterstudiengangs so viel Vertrauen entgegenzubringen – und mir während der gesamten Promotionszeit so große wissenschaftliche Freiheit zu gewähren.

Mein besonderer Dank gilt auch unserem Laborleiter [redacted], der stets ein offenes Ohr für fachliche Fragen hatte und mir jederzeit mit Rat sowie auch spaßigen Konversationen zur Seite stand.

Danken möchte ich auch unserem Direktor der Hautklinik Mainz, [redacted], der meinem Projekt stets mit Wohlwollen begegnete und es auf vielfältige Weise unterstützte.

Ebenfalls danken möchte ich den (damaligen) Assistenzärzten der Hautklinik Mainz, [redacted] und [redacted], die mich bei der klinischen Probennahme unterstützt und den Kontakt zu meinem Kooperationspartner, der Hautklinik des Universitätsklinikums Frankfurt a. M., hergestellt haben.

Ein großer Dank gilt meinen Kooperationspartnern der Mikrobiologie und Biotechnologie an der JGU Mainz, [redacted] und [redacted], die sich direkt offen und begeistert von meinem Projekt zeigten. Durch ihre kreativen Ideen und tatkräftige Unterstützung hat dieses Projekt erheblich an Tiefe und Qualität gewonnen. Besonders freut mich, dass die Erforschung des Hautmikrobioms bei CTCL in ihrer Arbeitsgruppe fortgeführt wird.

Mein herzlicher Dank gilt auch meinen lieben Doktoranden-Kollegen und Freunden aus dem Labor der Hautklinik am PKZI der Universitätsmedizin Mainz: [redacted]

Danksagung

[redacted]. Mit Euch habe ich eine super schön Zeit während meiner Promotion verbracht, an die ich mich gerne zurückerinnern werde.

Darüber hinaus danke ich den tollen Menschen in meinem privaten Umfeld, meiner Familie, meinen Freunden sowie meiner Freundin, die mich bei meinem Promotionsvorhaben stets unterstützt haben, und die zusammen mit mir durch Erfolge wie auch Rückschläge gehen.

Zu guter Letzt möchte ich auch dem Hotel sowie dem Team des True Beach Resorts in Marsa Alam, Ägypten, danken, wohin ich im Januar entflohen bin, um einen Großteil dieser Arbeit zu verfassen. Das angenehme Klima, der schöne Strand, die entspannte Atmosphäre der Hotelanlage sowie das fürsorgliche All-Inclusive-Paket aus Speisen und (nicht-)alkoholischen Getränken haben mir den Einstieg ins Schreiben erheblich erleichtert.

8 Curriculum Vitae